NOTICE

The quality of this microform is heavily dependent upon the quality of the original thesis submitted for microfilming. Every effort has been made to ensure the highest quality of reproduction possible.

If pages are missing, contact the university which granted the degree.

Some pages may have indistinct print especially if the original pages were typed with a poor typewriter ribbon or if the university sent us an inferior photocopy.

Previously copyrighted materials (journal articles, published tests, etc.) are not filmed.

Reproduction in full or in part of this microform is governed by the Canadian Copyright Act, R.S.C. 1970, c. C-30.

AVIS

La qualité de cette microforme dépend grandement de la qualité de la thèse soumise au microfilmage. Nous avons tout fait pour assurer une qualité supérieure de reproduction.

S'il manque des pages, veuillez communiquer avec l'université qui a conféré le grade.

La qualité d'impression de certaines pages peut laisser à désirer, surtout si les pages originales ont été dactylographiées à l'aide d'un ruban usé ou si l'université nous a fait parvenir une photocopie de qualité inférieure.

Les documents qui font déjà l'objet d'un droit d'auteur (articles de revue, tests publiés, etc.) ne sont pas microfilmés.

La reproduction, même partielle, de cette microforme est soumise à la Loi canadienne sur le droit d'auteur, SRC 1970, c. C-30.

QUANTITATIVE BIOSTRATIGRAPHIC ANALYSIS OF THE CENOZOIC OF THE LABRADOR SHELF AND GRAND BANKS

by

Marc A. D'Iorio

A dissertation submitted to the School of Graduate Studies and Research in partial fulfillment of the requirements for the degree of Ph.D. in Geology

UNIVERSITY OF OTTAWA

OTTAWA, CANADA, 1988

ISBN 0-315-46752-5

UNIVERSITÉ D'OTTAWA
UNIVERSITY OF OTTAWA

A Lyne,

pour son aide, ses encouragements et sa patience.

Résumé

Un modèle à haute résolution des biozonations du Cénozoïque est dévelopé en utilisant un ensemble de données intégré comprenant les dernières apparitions de foraminifères et de palynomorphes. Les biozonations sont établies en utilisant les algorithmes informatiques d'un modèle d'ordination et d'échelonement appelé RASC (Ranking And SCaling). La séquence des évènements, telle que publiée dans la littérature, et la séquence d'échelonement de RASC indiquent un coefficient de correlation de rang qui est statistiquement significatif. La séquence d'échelonement de RASC est convertie en échelle chronologique numérique en utilisant l'age postulé d'un sous-ensemble des évènements. Les ages des marqueurs lithologiques, tel que mesurés que cette échelle, correspondent à ceux publiés dans la littérature.

Une analyse de correspondance de cet ensemble de données révèle que la latitude des puits de forage est la source principale de tendance. L'interprétation des scores de l'analyse de correspondance, dans le contexte des biozonations RASC, fournit de précieux indices au sujet de la paléocirculation. En se basant sur les scores d'analyse de correspondance, le commencement du courrant du Labrador est

établit au début de la zone RASC X (fin Miocène). De manière semblable, les scores et la distribution des évènements de la zone RASC II (début Eocène) suggèrent le début de la période du réchaufement climatique et d'un courant de l'équateur.

L'analyse des distributions des fréquences montre que les évènements n'ont pas des variances égales et fournit des estimés pour ces dernières. Dans une première application de RASC, pour cette analyse, les variances des évènements ont été supposées égales puisqu'il n'est pas possible d'évaluer les variances et la distance entre les évènements simultanément. Après la première application de RASC, les distributions des fréquences sont estimées en calculant la différence entre les positions attendues et observées des évènements dans un graphique de la séquence RASC versus le rang des évènements dans les puits de forage. Cette méthode fournit de bons estimés des distributions des fréquences puisque la variance conjointe est de $\sigma^2 = 0.48$ comparée à $\sigma^2 = 0.50$ tel qu'assigné dans le modèle RASC. Ces estimés de variances sont réintroduits dans RASC puis recalculés. Les solutions stabilisent après la quatrième application de RASC. Des déviations systématiques sont observées au début et à la fin de la séquence d'échelonement. Elles sont probablement reliées à des problèmes d'échantillonage dans ces sections de quelques puits. Les distributions des fréquences servent

d'indiquateurs de la valeur des évènements comme marqueurs biostratigraphiques et de leur synchronéité.

La variation du paramètre de la valeur z maximale (AAA) n'a aucun effet significatif sur le rang des évènements dans la séquence d'échelonement. Généralement, la longueur de la séquence augmente avec une augmentation de AAA. La variation de ce paramètre produit de plus grandes fluctuations dans l'échelonement du début et de la fin de la séquence et dans les zones constraintes par des discordances, où quelques microfossiles peuvent être retravaillés. Ces résultats sont consistents avec les déviations observées dans l'analyse des distributions des fréquences.

Les techniques de correlations objectives du modèle CASC (Correlation And SCaling in time) fournissent des correlations de biozones et d'isochrones à travers la région étudiée. CASC est une méthode efficace de reconnaître les profils d'accumulation des sédiments. Les profondeurs des époques Cénozoïques, ainsi que déterminées par des méthodes biostratigraphiques, montrent un haut degré de correspondence avec celles déterminées par CASC. Des déviations mineures systématiques près du haut et du bas de la séquence sont semblables à celle décèlées par l'analyse des distributions des fréquences.

Abstract

A high-resolution Cenozoic biozonation model is developed using an integrated data set of last occurrences of foraminifers and palynomorphs. The biozonation is erected using the RASC (Ranking And SCaling) computer algorithms. The sequential order of the events as published in the literature and the RASC optimum sequence show a statistically significant rank-correlation coefficient. The RASC scaled sequence is converted into a numerical time scale using the postulated ages of a subset of events. The position of lithological markers in the RASC sequence and in the numerical time scale corresponds to their assigned literature age.

The correspondence analysis (CA) technique exposes the latitudes of the wells as being the major source of trend in the data set. The interpretation of CA scores in the context of RASC biozones provides valuable insight into paleo-circulation patterns. Based on CA event scores, the onset of the Labrador current is suggested at the start of RASC zone X (Late Miocene). Similarly, the scores and distribution of events of zone II (Early Eocene) indicate the beginning of warming period and of a northward current from the equator.

The analysis of frequency distributions shows that events do not have equal variances and provide an estimate of their

variance. In the first application of the RASC model for this analysis, it is not possible to evaluate both the variance of events and the distance between them and the event variances are assumed to be equal. After the first RASC run, the frequency distributions of events were measured by collecting the differences in observed and expected position of events from spline-fitted plots of event sequences in wells against the RASC scaled optimum sequence. These measures provide a good estimate of frequency distributions as indicated by a pooled variance of $\sigma^2 = 0.48$ compared to the value of $\sigma^2 = 0.50$ assigned by the initial RASC model. An iterative procedure of calculating standard deviation and inputing them into RASC shows stabilization of estimates after the fourth RASC run. The frequency distributions show a systematic departure near the top and bottom of the scaled optimum sequence. These deviations are probably related to lack of data in these sections of some wells. The frequency distributions also provide an indicator of the value of events as markers and highlight reworked and diachronous events.

The variation of the maximum probit parameter (AAA) in the RASC model has no significant effect on the rank of events in the optimum sequence. The length of the scaled sequence generally increases with an increasing value of AAA. Varying this parameter produces greater fluctuations in scaling near the top and bottom of scaled sequences and in zones bounded by

marked unconformities or disconformities where a few microfossils may have been reworked or caved-in. These results are consistent with the deviations observed in the frequency distribution study.

The objective correlation technique of the CASC model (Correlation And SCaling in time) provides correlations of biozones and isochrons through the wells of the study area. It is an effective method of identifying patterns of sediment accumulations. Biostratigraphically determined Cenozoic epoch boundaries show good agreement with the corresponding CASC estimated depths. Minor deviations between the two estimates reflect the systematic deviations near the top and bottom of the scaled optimum sequence similar to those observed in frequency distribution results.

Table of content

LIST OF TABLES

LIST OF FIGURES

FIGURE 5.2: Plot of the average event deviation against the RASC distance of the corresponding event. The squares represent palynomorph events whereas the circles represent foraminifers. Systematic deviations from zero are exhibited at either end of the scale. In the middle portion of the RASC sequence, palynomorphs seem to have average values closer to zero than the foraminifers.

FIGURE 5.3 (a): Geographical distribution of the deviations between observed and expected positions of event G. yeguaensis. All occurrences of this species are below their RASC position.

FIGURE 5.3 (b): Histogram of the frequency distribution of event G. yeguaensis.

FIGURE 5.4 (a): Geographical distribution of the deviations between observed and expected positions of event T. alsatica. It has a broad geographic extent as it was identified in 14 wells throughout the study area.

FIGURE 5.4 (b): Histogram of the frequency distribution of event T. alsatica. The shape of the histogram indicates a normal distribution. The low variance makes this event a good marker.

FIGURE 5.5 (a): Geographic distribution of the deviations between observed and expected position of event #264 K. conversa.

FIGURE 5.5 (b): Geographic distribution of the deviations between observed and expected position of event #41 P. aff. paucicostata.

FIGURE 5.5 (c): Geographic distribution of the deviations between observed and expected position of event #316 Xenikoon DA.

FIGURE 6.1: Plot of the length of the scaled optimum sequence against the corresponding critical probit value

FIGURE 6.2: Plot of the deviation in normalized RASC position between sequence of varying critical probit values. All sequences are compared to the scaled optimum sequence of Figure 3.5.

1. Introduction

1.1 Quantitative biostratigraphic analysis.

Purpose of the study

The first objective of this study is to apply the ranking and scaling (RASC) model to an integrated biostratigraphic data set of palynomorphs and foraminifers. Throughout this experiment, the effects of data integration on the resolution of RASC biozonations can be evaluated and a higher resolution Cenozoic biostratigraphic model should result.

The second step of this study is to build a chronostratigraphic numerical time scale from the integrated biozonation scheme. Both foraminiferal and palynomorph index species are used to calibrate the RASC sequence into a numerical time scale.

The chronostratigraphic scheme in conjunction with the well data allows objective correlation of zones and of isochrons, from well to well. These correlations are built using a model named CASC (Correlation And SCaling in time). Isochrons and RASC biozones are traced between the wells of the study area and general patterns in the sediment accumulation rates are determined.

The integrated data set is studied by correspondence analysis to identify paleoceanographic patterns in different zones. Results are interpreted in the context of the RASC biozonations.

The normality of the distribution of species extinctions (events) constitutes a basic premise of the RASC model. This assumption is tested by estimating the frequency distributions of events. These measures allow the calculation of the standard deviations of events and provide a way to refine the RASC model.

The robustness of the RASC model, with respect to the critical probit value, is tested. The value of this input parameter is varied and the ranked and scaled positions of event in the resulting sequences are evaluated. The differential scaling of segments of these sequences also is examined.

1.2 Previous work

The ranking and scaling model was developed by Gradstein and Agterberg (1982) (also see Agterberg and Nel 1982a, 1982b and Heller et al. 1983, 1985). The RASC model was applied to Cenozoic foraminifers of the Northwest Atlantic by Gradstein

and Agterberg (1982), Gradstein (1985), Gradstein et al. (1988a,1988b, in press); it also was applied to Mesozoic foraminifers of the same area by Williamson (1987) and to dinoflagellates and foraminifers of the Canadian Atlantic Margin by D'Iorio (1986, 1987).

The CASC model was developed by Agterberg and Gradstein (1983) (also see Agterberg 1983, Gradstein and Agterberg 1985, Agterberg et al. 1985, and Agterberg and Gradstein 1988). Published applications of CASC are restricted to the Northwest Atlantic; more specifically: the Late Jurassic and Early Cretaceous, (Williamson and Agterberg, 1988) and the Cenozoic (Gradstein and Agterberg 1985, D'Iorio 1987 and Gradstein et al. 1988a, 1988b, in press).

The correspondence analysis computer programme used in this study was published by Gauch (1982). Specific applications of correspondence analysis in the context of RASC biozonations were published by Bonham-Carter et al. (1986) and, in part, by D'Iorio (1987).

Finally, the technique to evaluate frequency distributions was developed and published by Agterberg and D'Iorio (1988) in an application on Cenozoic foraminifers of the Labrador Shelf and Grand Banks.

1.3 Geological history of the Labrador sea

The Labrador Sea is an embayment of the Atlantic ocean bounded to the west by Labrador and Baffin Island and to the east by Greenland. The Labrador Sea evolved from the separation of Greenland and Eurasia by sea-floor spreading, from Late Campanian to mid-Eocene time (Srivastava and Tapscott, 1986). The opening of the Labrador Sea is discussed by van der Linden et al. (1976), Sclater et al. (1977), Srivastava (1978), Umpleby (1979), Gradstein and Srivastava (1980), Grant (1980), Mc Whae (1981), Srivastava (1986) and many others. The following is a summary of the review by Srivastava (1978).

The opening of the Labrador Sea is dated according to magnetic Anomalies 20 to 32 on either side of the now inactive Labrador Sea ridge. Two distinct trends are apparent in these Anomalies and reflect the major phases of the opening of the North Atlantic. The first trend is represented by Anomalies 25 to 32. They preceded the onset of tectonic activities on the Reykjanes ridge. According to the geochronological scale of Berggren et al. (1985), Anomaly 32 began at 74.0 Ma B.P. and Anomaly 25 terminated at 58.6 Ma B.P.. This interval of time represents the first phase of the opening of the Labrador Sea at which time the Labrador Sea ridge was the mid-Atlantic

ridge. The second and final phase of the opening of the Labrador Sea is recorded by Anomalies 20 to 24. These are characterized by a sharp angle that changes the direction of the magnetic lineation from west northwest - east southeast in the Labrador Sea to north-south off the coast of Labrador. This bending of Anomalies was first described by Vogt et al. (1969). It represents simultaneous sea-floor spreading in the Labrador and Norwegian Seas.

1.4 Cenozoic paleoceanographic circulation

An early seaway, favouring polarward circulation, probably caused an incursion of Atlantic water as far north as Baffin Bay from Danian time (Berggren and Hollister, 1977). Other authors (cf. Sclater et al., 1977) favour a later onset of the Atlantic-Arctic passage. The widening of the Labrador Sea in Early to Middle Eocene time had made possible a strong incursion of relatively warm Atlantic waters in the southern Labrador Sea (Gradstein and Srivastava, 1980). This influence tapered off from the Late Eocene on due to the presence of cooler Atlantic waters (Gradstein and Srivastava, 1980).

The onset of the Labrador current is postulated in Late Miocene time (Gradstein and Srivastava, 1980).

1.5 Labrador Shelf Cenozoic lithostratigraphy

Throughout the Cenozoic, the Labrador Shelf and Grand Banks were passive margins. Changes in depositional environments can be accounted for by relative sea-level changes. These include subsidence history and related effects such as variation in terrigenous sediment influx.

The Cenozoic sedimentological conditions throughout the Labrador Shelf were similar as there is no large disparity in new sediment availability (van der Linden et al., 1976) and a shelf-wide current has existed in that area since the Cretaceous (Gradstein and Srivastava 1980).

A complete lithostratigraphical scheme for the lithology of the Labrador Shelf was put forth by Umpleby in 1979; it was reviewed by McWhae et al. in 1980. Their revision is based on the presence of traceable unconformities or seismic markers on the Labrador Shelf revealed by more seismic data and more well control. The revisions affect mostly the nomenclature of the formations and members and not their boundaries (see Figure 1.1). Balkwill (1987) provided the most updated description of the Labrador Shelf lithostratigraphy.

Figure 1.1: Summary of the stratigraphic units on the Labrador Shelf (from Srivastava, 1986).

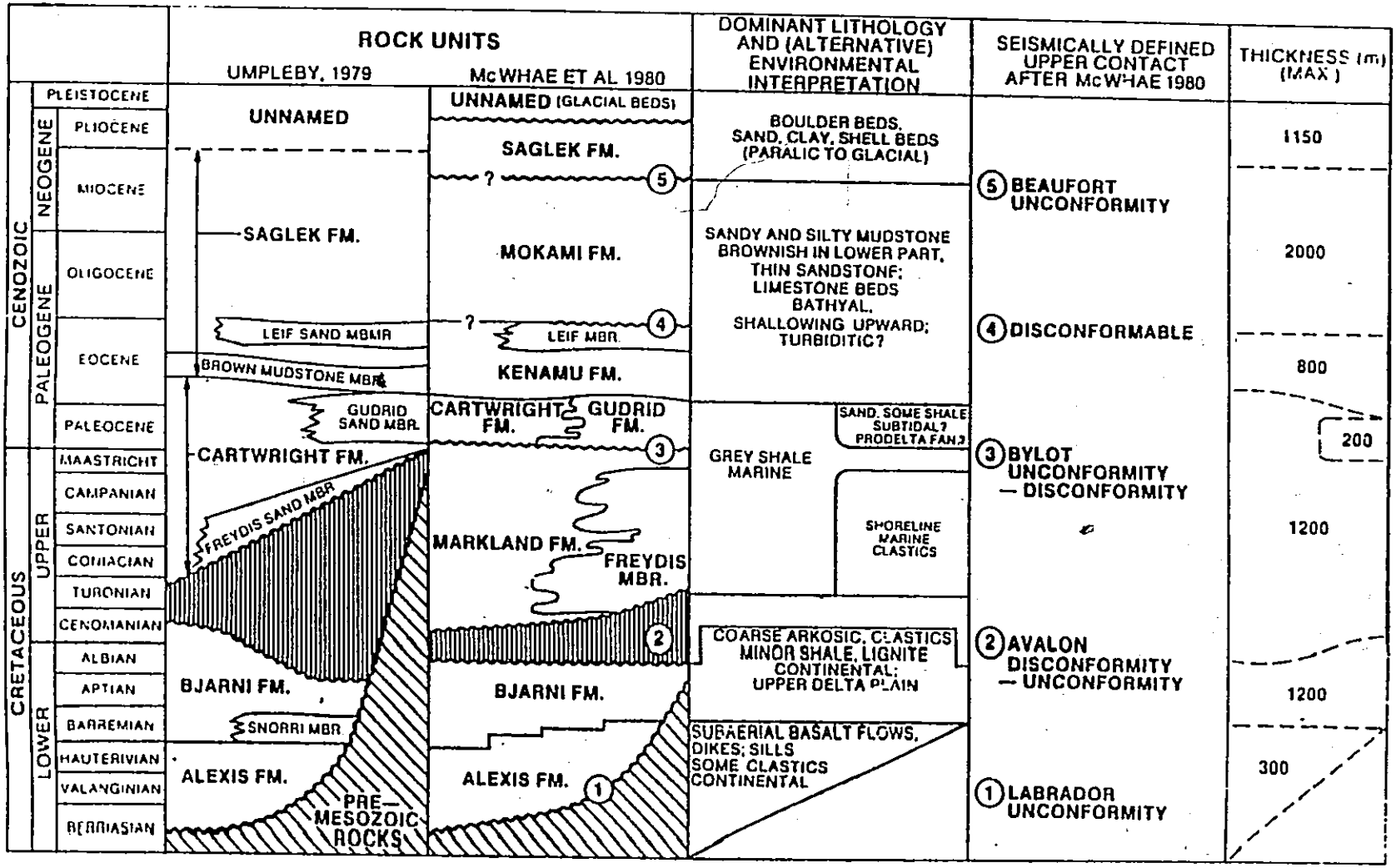
ROCK UNITS
UMPLEBY, 1979
McWHAE ET AL 1980
DOMINANT LITHOLOGY AND (ALTERNATIVE) ENVIRONMENTAL INTERPRETATION
SEISMICALLY DEFINED UPPER CONTACT AFTER McWHAE 1980
THICKNESS (m) (MAX.)
CENOZOIC
CRETACEOUS
PLEISTOCENE
NEOGENE
PLIOCENE
MIOCENE
PALEOGENE
OLIGOCENE
EOCENE
PALEOCENE
UPPER
LOWER
MAASTRICHTIAN
CAMPANIAN
SANTONIAN
CONIACIAN
TURONIAN
CENOMANIAN
ALBIAN
APTIAN
BARREMIAN
HAUTERIVIAN
VALANGINIAN
BERRIASIAN
UNNAMED
SAGLEK FM.
LEIF SAND MBR.
BROWN MUDSTONE MBR.
GUDRID SAND MBR.
CARTWRIGHT FM.
FREYDIS SAND MBR.
BJARNI FM.
SNORRI MBR.
ALEXIS FM.
PRE-MESOZOIC ROCKS
UNNAMED (GLACIAL BEDS)
SAGLEK FM.
MOKAMI FM.
LEIF MBR.
KENAMU FM.
CARTWRIGHT FM.
GUDRID FM.
MARKLAND FM.
FREYDIS MBR.
BJARNI FM.
ALEXIS FM.
BOULDER BEDS, SAND, CLAY, SHELL BEDS (PARALIC TO GLACIAL)
SANDY AND SILTY MUDSTONE BROWNISH IN LOWER PART, THIN SANDSTONE; LIMESTONE BEDS BATHYAL, SHALLOWING UPWARD; TURBIDITIC?
SAND, SOME SHALE SUBTIDAL? PRODELTA FAN?
GREY SHALE MARINE
SHORELINE MARINE CLASTICS
COARSE ARKOSIC CLASTICS MINOR SHALE, LIGNITE CONTINENTAL; UPPER DELTA PLAIN
SUBAERIAL BASALT FLOWS, DIKES; SILLS SOME CLASTICS CONTINENTAL
5 BEAUFORT UNCONFORMITY
4 DISCONFORMABLE
3 BYLOT UNCONFORMITY — DISCONFORMITY
2 AVALON DISCONFORMITY — UNCONFORMITY
1 LABRADOR UNCONFORMITY
1150
2000
800
200
1200
1200
300

Four formations are identified in the Cenozoic by McWhae et al. 1980. This subdivision represented a refinement of the two formations described by Umpleby (1979).

1.5.1 Cartwright Formation

At the Cretaceous-Tertiary boundary, the Bylot unconformity is used to divide Umpleby's Cartwright Formation into the Markland (Cretaceous) and the restricted Cartwright (Cenozoic) Formations. The restricted Cartwright Formation ranges from Paleocene to Early Eocene time and parallels the Labrador-southern Baffin shelves as an elongated seaward-dipping prism (Balkwill, 1987). This formation consists of medium to dark-grey mudstone grading to light-grey splintery, siliceous shale. The lower part of the formation includes thin intervals of light-grey silt, very fine sand and grey-brown to dark-brown micrite. The contacts with the underlying Carboniferous dolomite and overlying sand member are sharp (Umpleby, 1979). Umpleby suggested that two sand members were developed locally within the Cartwright Formation: the Freydis Sand Member at the base and the Gudrid Sand Member at the top. Mcwhae et al. (1980), upgraded the status of the Gudrid Sand Member to a formation.

1.5.2 Gudrid Formation

The Gudrid Formation consists of arkosic sand with an abundant clay matrix. Clasts of rounded and frosted quartz and nearly fresh feldspar occur in approximately equal amounts. The upper part of this formation is interpreted as a distal turbidite with the characteristic Bouma sequence. The lower part of this formation has a continental character. Poor sorting and its arkosic nature suggest a lower delta plain deposition. The sand is devoid of marine fossils, but palynomorphs suggest a Paleocene to earliest Eocene age (Umpleby, 1979). The Foraminifera of the overlying mudstone support this hypothesis.

1.5.3 Kenamu Formation

This formation corresponds to the lower part of Umpleby's (1979) Saglek Formation. The Kenamu Formation is shale dominated and oversteps older Cenozoic strata landward, resting up-dip from the cratonic monocline on Precambrian basement (Balkwill, 1987). It disconformably overlies the

Cartwright Formation and is bounded above by the Mokami Formation. It ranges from early Middle Eocene to Late Eocene. Balkwill (1987) recognizes three informal members in the Kenamu Formation.

The "lower Kenamu" is upward-fining and is made up of slightly silty grey shales, containing early Eocene marine fossils.

The "middle Kenamu" consists of lower and middle Eocene marine shales, which coarsen upward to siltstone.

The "upper Kenamu" is mainly made up of marine siltstone that coarsen upwards, in parts of some basins, to coastal sandstones.

Leif Sand Member

This formal member was described by Umpleby (1979). It consists of light brown-grey to white, fine-grained quartzose sand. Intervals show a mixed lithology where the sand is scattered through the matrix. A visual estimate reveals the composition to be approximately 40% sand, 30% silt and 30% mud. Palynology and foraminifers indicate a Late Eocene age for this member. Its upper contact is sharp and corresponds to a major log marker (Umpleby, 1979).

1.5.4 Mokami Formation

This formation is the middle subdivision of Umpleby's Saglek Formation. It disconformably overlies the Kenamu Formation and is bounded above by the Beaufort unconformity. It ranges from Oligocene to Late Miocene.

Across the superior boundary, the lithology changes from a partly consolidated, brownish, neritic claystone and soft shale (Mokami Formation) to an unconsolidated, porous, white brown to grey feldspathic to cherty sandstone (restricted Saglek Formation) (McWhae et al., 1980).

1.5.5 Saglek Formation

A late Eocene disconformity divides Saglek Formation into the Mokami and Kenamu Formations. The Kenamu Formation comprises the Brown Mudstone and Leif Sand Members. The Beaufort unconformity defines the top of the Mokami Formation and the lower boundary of the Saglek Formation.

The lower part of the Saglek Formation is defined as a proximal, coarse-grained facies of an upper Oligocene-Miocene

sequence. The upper Saglek sandstones are proximal facies of an upper Miocene-Pliocene sequence (Balkwill, 1987).

1.6 Cenozoic lithostratigraphy of the Grand Banks

The lithostratigraphy Cenozoic of the Grand Banks is simple as only the Banquerau Formation is defined. It is characteristically composed of marine shales which were deposited as the continuation of a major transgression which extended from the Late Cretaceous to late Tertiary time (Arthur et al. 1982). Deep-water conditions prevailed throughout this time interval (Arthur et al. 1982).

1.7 Acknowledgements

I am very grateful to Frits Agterberg for his support, his patience, and his invaluable advice throughout the course of this study. I also want to thank Felix Gradstein for providing the foraminiferal data set, for his stratigraphic and paleontological insights, and for his enthusiastic support.

Graham Williams and Sedley Barss, of Dartmouth, are thanked for providing the palynomorph data set. Anthony Jenkins, of Calgary, and Martin Head, of Toronto, offered helpful stratigraphical advice on the palynomorph data set.

I also wish to thank Ning Lew for helping me get started in the computing aspect of quantitative stratigraphy and Graeme Bonham-Carter for his collaboration in the correspondence analysis study.

Shell Resources Canada is gratefully acknowledged for financially supporting this project from 1984 to 1987. I thank the Geological Survey of Canada for providing the data used in the study, computing facilities, and technical support.

2. Nature of data and computer-based data management

2.1 Introduction

In this study, data sets of different biological nature are used simultaneously in a quantitative biostratigraphic analysis of the Cenozoic of the Labrador Shelf and Grand Banks. The study is restricted to the Cenozoic section as its emphasis lies in quantitative stratigraphic modeling rather than in a complete geological description of the area.

2.2 Data sets

The data set has two major constituents: the foraminifers and the palynomorphs. The foraminiferal information was provided by F. M. Gradstein of the Atlantic Geoscience Centre in Dartmouth, Nova Scotia. The data were published as part of the Gradstein-Thomas database (Gradstein et al., 1985, p.517-520); this material was available in a format compatible with the Ranking And SCaling (RASC) model input. The palynomorph information was provided by G. M. Williams and S. Barss, both of the Atlantic Geoscience Centre. These data have been used

in previous studies of the area (Barss et al. 1979) but have not been published in their entirety. A third, minor part of the data set contains seismic and lithological markers.

The study area, depicted in Figure 2.1, consists of the Labrador Shelf and Grand Banks of the Canadian Atlantic Margin. Twenty three well sections were studied. Foraminiferal data were provided for all wells but palynomorph data were only available for 16 sections; Table 2.1 identifies the wells and the type of stratigraphic information they contain.

2.2.1 Nature of the foraminifers

The foraminifers (from the Latin foramen=hole and ferre= to bear) are single-celled marine microorganisms that live either on the bottom or float in the water column of oceans (Boersma, 1978, p.19). The following discussion of the foraminifers is based on Boersma (1978, p.19-78) and on Brazier (1980, p.90-121).

Foraminifers belong to the phylum Protozoa. Unicellular or acellular organization is the single feature common to the various members of this phylum which is divided further into classes on the basis of the locomotor apparati. Because

Figure 2.1: Location map of the wells of the Labrador Shelf and Grand Banks used in this study.

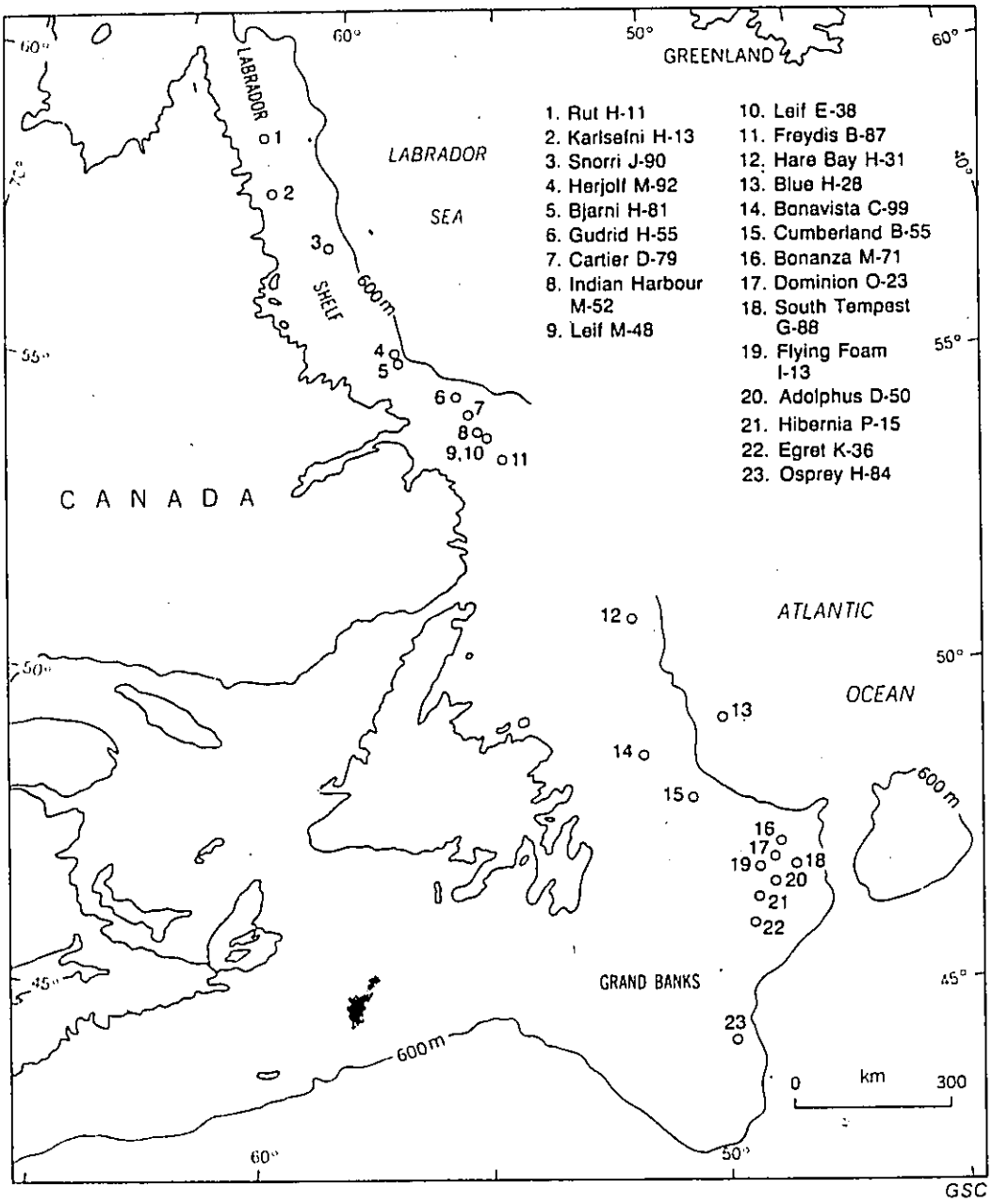
GREENLAND
LABRADOR
SEA
LABRADOR SHELF
600m
CANADA
ATLANTIC
OCEAN
GRAND BANKS
600m
600m
1. Rut H-11
2. Karlsefni H-13
3. Snorri J-90
4. Herjolf M-92
5. Bjarni H-81
6. Gudrid H-55
7. Cartier D-79
8. Indian Harbour M-52
9. Leif M-48
10. Leif E-38
11. Freydis B-87
12. Hare Bay H-31
13. Blue H-28
14. Bonavista C-99
15. Cumberland B-55
16. Bonanza M-71
17. Dominion O-23
18. South Tempest G-88
19. Flying Foam I-13
20. Adolphus D-50
21. Hibernia P-15
22. Egret K-36
23. Osprey H-84
0 km 300
GSC

Wells	Foramini-fers	Palyno-morphs	Seismic markers	Litho-logical markers
Rut H-11	YES	NO	NO	NO
Karlsefni H-13	YES	YES	NO	YES
Snorri J-90	YES	YES	NO	YES
Herjolf M-92	YES	YES	NO	YES
Bjarni H-81	YES	YES	NO	YES
Gudrid H-55	YES	YES	NO	YES
Cartier D-70	YES	YES	NO	YES
Indian Harbour M-52	YES	YES	NO	NO
Leif M-48	YES	YES	NO	YES
Leif E-38	YES	YES	NO	NO
Freydis B-87	YES	YES	NO	YES
Hare Bay E-21	YES	NO	NO	NO
Blue H-28	YES	NO	NO	NO
Bonavista C-99	YES	YES	NO	NO
Cumberland B-55	YES	YES	NO	NO
Bonanza M-71	YES	NO	NO	NO
Dominion O-23	YES	YES	YES	NO
South Tempest G-88	YES	NO	NO	NO
Flying Foam I-13	YES	YES	YES	NO
Adolphus D-50	YES	NO	YES	NO
Hibernia P-15	YES	NO	YES	NO
Egret K-36	YES	YES	YES	NO
Osprey H-84	YES	YES	NO	NO

TABLE 2.1: Type of data available in the wells of the study area

Foraminifera possess pseudopods and are non-flagellate, they are placed in the class Sarcodina. Most Foraminifera are distinguishable from other Sarcodina by the possession of mineralized shells. Table 2.2 shows the classification scheme of foraminifers.

A living foraminiferid is a single-celled organism differentiated into an outer layer of clear ectoplasm and an inner layer of darker endoplasm. The ectoplasm surrounds the test and gives rise to filose or reticulose pseudopodia responsible for the food intake and expulsion of debris. The endoplasm occurs within the test and contains food vacuoles and the nucleus.

The foraminifers are characterized by an alternation of a gamont generation which reproduces sexually, and of a schizont generation which reproduces asexually. This cycle may take from one to two or more years to complete; asexual reproduction prevails.

It is the composition and structure of the test that usually determines the classification of the groups of foraminifers. The organic-walled forms belong to the Suborder Allogromiina. The Suborder Textulariina comprises the forms that have agglutinated tests. Finally, the Suborders Miliolina, Fusulinina, and Rotaliina encompass the forms with calcareous tests. The Miliolina have porcelaneous tests, the

FORAMINIFERA

Kingdom Protista
Phylum Sarcodina
Class Rhizopoda
Order Foraminiferida

Suborders : Allogromiina (encompasses 1 superfamily)
Textulariina (encompasses 2 superfamilies)
Fusulinina (encompasses 3 superfamilies)
Miliolina (encompasses 1 superfamily)
Rotaliina (encompasses 12 superfamilies)

DINOFLAGELLATES

Kingdom Protista
Division Pyrrhophyta

Classes: Desmophyceae
Orders: Desmocapsales
Prorocentrales
Dinophyceae
Orders: Gymnodiniales
Peridiniales
Dinophysiales
Ebriophyceae
Ellobiophyceae

SPORES AND POLLEN

Kingdom Plantae
Division Tracheophyta

Subdivisions: Psilopsida
Lycopsida
Sphenopsida
Pteropsida

TABLE 2.2: Classification of foraminifers and palynomorphs

Fusulinina have tests of microgranular calcite whereas the Rotaliina have perforated walls of radial or granular hyaline calcite.

Foraminiferal tests may possess one or more chambers. The spatial arrangement of the chambers is the determining factor for the classification of the Super Families of foraminifers. Further subdivision into genera and species can be based on characteristics of the apertures and openings, pores or ornamentations, and other characteristics.

Physical variables

The principal physical factor to affect the diversity and abundance of both planktonic and benthic foraminifers is water temperature. Benthic forms are more vulnerable to physical variables. They are strongly influenced by watermass and substrate properties that are, to a considerable extent, controlled by water depth, salinity, and temperature, but also are affected by the factors that influence their food supply. Such factors include upwelling current systems and light intensity; the latter controls the rate of photosynthesis of symbiotic algae; light intensity also is affected by turbidity). Below the carbonate compensation depth (CCD) andin basins with corrosive bottom water, agglutinated benthic forms prevail, resistant to carbonate dissolution that affects the calcareous benthics.

Chemical variables

Foraminifers inhabit environments that have salinities ranging from as low as 0.05 % to as high as 5.7 %. The greatest diversity of species occurs for the more typical open-ocean salinity values of approximately 3.5 %. Other chemical variables include alkalinity and presence of trace elements and nutrients.

2.2.2 Foraminifers of the Cenozoic of the Labrador Shelf and Grand Banks.

Both benthic and planktonic foraminifers are used in this study. Because most of the well sections studied use well cuttings, the last occurrence (LO) of the species is the only reliable information on the stratigraphic range. This study uses LO events.

The editing of the foraminiferal data was minor as it was available in RASC input format. There are 171 foraminiferal events occurring 816 times in 23 different well sections.

The cumulative frequency of event occurrences in well sections, for both foraminifers and palynomorphs, is depicted in Figure 2.2. This diagram was constructed so that the

Figure 2.2: Cumulative number of event occurrences as a function of the number of wells in which events occur. The cumulative number of events increases with the decrease in number of wells in which events occur.

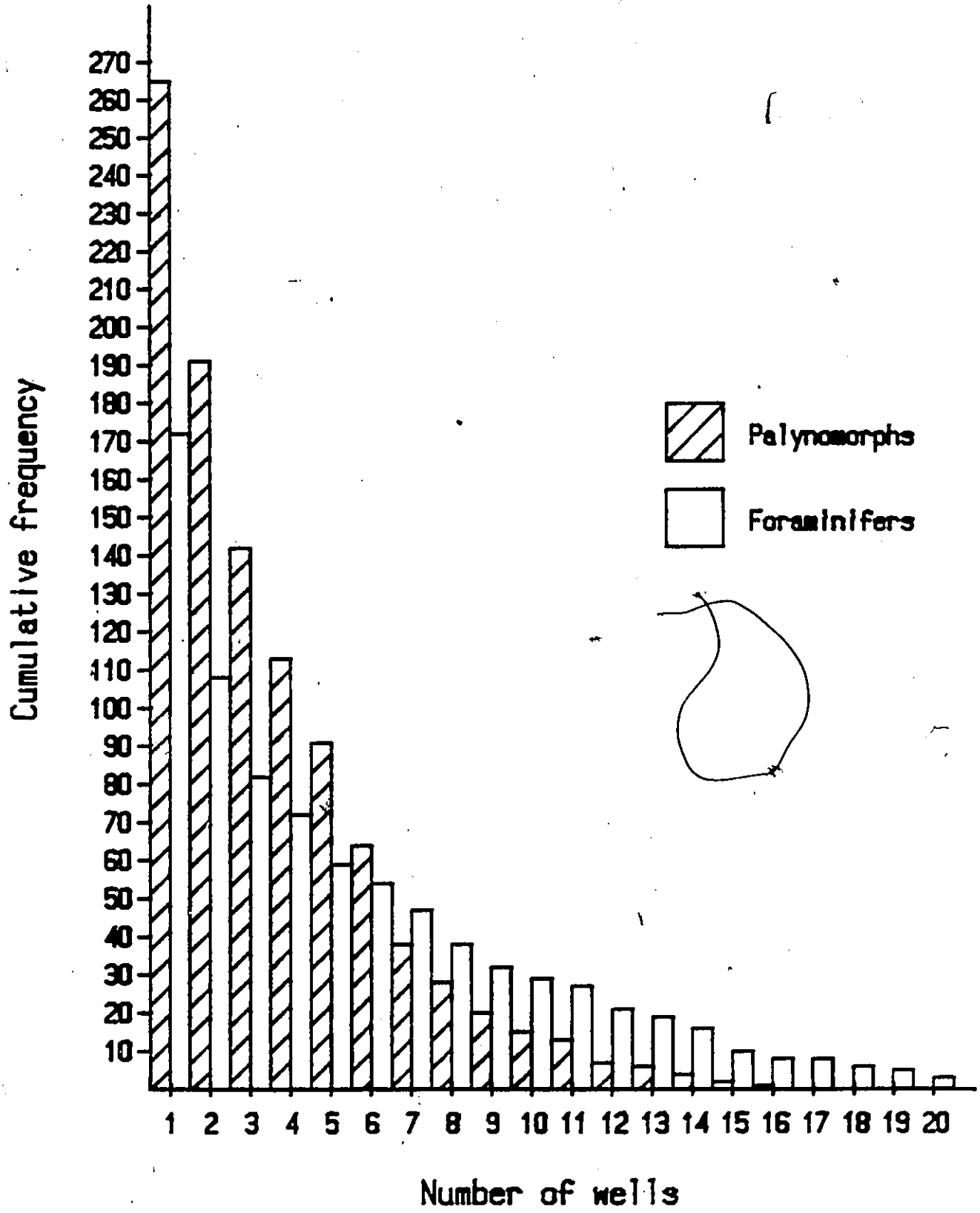
Cumulative frequency
270
260
250
240
230
220
210
200
190
180
170
160
150
140
130
120
110
100
90
80
70
60
50
40
30
20
10
1 2 3 4 5 6 7 8 9 10 11 12 13 14 15 16 17 18 19 20
Number of wells
Palynomorphs
Foraminifers

cumulative number of occurrences increases while the number of sections in which events occur decreases (see Figure 2.2). The foraminifers are more diversified than the palynomorphs for species occurring in 7 or more sections. Their greater horizontal distribution makes the foraminifers well suited for a probabilistic study such as the present one.

There are several marker events in the data set that will be used to convert arbitrary zonation scales to numerical time scales. These will be examined in Chapter 3.

2.2.3 Nature of the dinoflagellates, spores and pollens

The following discussion of the palynomorphs is based on Williams (1978, p. 293-326), Heuser (1978, p.327-340), and on Brazier (1980, p.21-29 and 58-77).

Dinoflagellates

The dinoflagellates are unicellular biflagellate algae that range in size from 5 µm to 2mm. They constitute the Division Pyrrhophyta (from the Greek **pyrrhos**=flame-coloured,

and phyta=plants) of the Algae. Most forms are planktonic and occur in both marine and freshwater environments. A few forms are marine sand-dwelling. Most dinoflagellates are autotrophic (contain chromatophores and carry out photosynthesis) though some are heterotrophic and feed by ingesting their food.

The dinoflagellates are classified further into four classes: the Ebriophyceae, the Ellobiophyceae, the Desmophyceae, and the Dinophyceae. The last two classes encompass 2 and 3 orders respectively. The three orders of the Class Dinophyceae are the only known dinoflagellates of the fossil record. Table 2.2 shows the classification scheme of dinoflagellates.

Dinoflagellates are unicellular organisms in which the protoplast consists of a denser outer region that harbours the chromatophores and of an inner region that, where present, contains the nucleus and vacuoles. There are two parts to the dinoflagellate life cycle including a vegetative stage and an endocysted one. They form a major part of the ocean plankton and play an predominant role in the food chain of the marine realm. The dinoflagellates use flagellar locomotion to move to the surface at night and to greater depths during the day when they must avoid the harmful ultra-violet rays.

Physical and chemical variables

The dinoflagellates as a group, have a wide temperature tolerance (1° to 35°C) with an optimum diversity in the 18° to 25 °C range. Many dinoflagellates have distributions that parallel the ocean temperature zones and may be used as climatic indicators. Certain genera occur in both fresh and salt water although most dinoflagellates are marine.

Spores and pollen

In contrast to the other microfossils used in this study, spores and pollen are an allochthonous group, that is they are not a marine group but the product of terrestrial vegetation. They are incorporated in the marine geological record as biogenic components of fine-grained detrital or terrigenous marine sediments.

Spores and pollen belong to the Kingdom Plantae, to the Division Tracheophyta and to one the 4 subdivisions: Psilopsida, Lycopsida, Sphenopsida, and Pteropsida (see Table 2.2).

Pollen grains constitute the male reproductive bodies in seed plants whereas spores are some of the earliest preserved

remains of plants. Pollen grains range in size from 20 µm to 80 µm, with rare forms less than 10 µm and more than 200 µm. Physical variables include shape, number and type of apertures, sculpture, and wall structure.

The size of late Cenozoic spores compares to that of pollen grains; older spores may be as large as 2 mm. The physical characteristics of spores include the same variables as those of pollen.

Despite the lengthy and complex transport process, marine pollen assemblages seem to reflect the vegetation of the provenance area. The nature of the assemblages will depend on the extent of area of permanent drainage.

2.2.4 Palynomorphs of the Cenozoic of the Labrador Shelf and Grand Banks.

The palynomorph data were provided as a listing of all occurrences in 16 Labrador Shelf / Grand Banks wells. These occurrences were coded using the Unique Taxon Number (UTN) system (five digit numbers). The data have to be recoded to accommodate the more compact, three digit, RASC format. In order to recode the data, a listing of all possible palynomorph event names was first compiled. This listing was

numbered to sequentially follow the foraminiferal listing. Once merged, the foraminiferal and palynomorph listings constitute the RASC dictionary; it is listed in Appendix A starting at page 300. Only the top (youngest) occurrences of palynomorphs were included in the data set. Two data files were prepared for each group of data. The first is an occurrence file and the second a corresponding depth file. The recoding and the compilation of the palynomorph data files were performed manually. There are 265 different palynomorph events occurring 1001 times in the 16 offshore wells.

The cumulative frequency of event occurrences in well sections, for both foraminifers and palynomorphs is depicted in Figure 2.2. The distribution of palynomorphs indicates that there is a large number of species that occur in few wells and that the diversity falls rapidly with an increasing number of sections. The palynomorphs are more diverse than the foraminifers when considering events that occur in 6 sections or less.

2.2.5 Other stratigraphic information of the Cenozoic on the Labrador Shelf and Grand Banks

Several of the Labrador Shelf wells contain useful lithological information on the following units: Main Sand Member, Brown Mudstone Member, Gudrid Sand Member, Leif Sand Member and Cartwright Formation. The boundaries of these units correspond to Umpleby's (1979) lithological description of the Labrador Shelf. This information is valuable because it provides a lithological control of the biozonation scheme derived in this study.

Four distinct seismic events are identified in several wells. These events are termed Seismic events #1 to #4.

2.2.6 Integrated data set

A computer programme was written to integrate the 1817 microfossil occurrences and create the RASC data and depth files. This programme is listed in Appendix B at page 307. It was written in BASIC on a Victor 9000 microcomputer at the Bedford Institute of Oceanography, in Dartmouth. The data files were later transferred to the CYBER 730 mainframe

computer at the ministry of Energy, Mines and Resources in Ottawa.

A comprehensive list of data was compiled where the events, their depths, and dictionary numbers were listed for each well section. Because of the size of the data set, a BASIC program was written to compile this list. The data are listed in Appendix A. The computer programme DATALIST is listed in Appendix B. This programme was first written for operation on the Victor 9000 computer but later was adapted to run on IBM PC/XT machines.

2.3 Hardware

2.3.1 Computers

From the onset of the study, it was obvious that most of the computing would require a mainframe computer because of the voluminous data set and of the myriads of matrix operations required for the application of the RASC model. The CYBER 730 computer at the department of Energy, Mines and Resources was used because several quantitative stratigraphic models were operational on that system. However, most file

manipulation was carried out on a microcomputer because of greater flexibility of its editing system. Because the foraminiferal data set was available on the Victor 9000 microcomputer in use at the Bedford Institute of Oceanography, it was convenient to use this machine for the data integration. All files and programmes later were transferred to the IBM microcomputer system.

2.3.2 Output devices

The plotter used in this study is a Roland DXY-960. It was interfaced with either an IBM PC/AT or an AT&T (IBM PC/XT clone). It has a resolution of 2800 X 3600 pixels on 11 inch by 17 inch paper.

DECORANA plots were sent to a laser printer connected to the Energy, Mines and Resources VAX computer. All other printers used in this study were dot-matrix printers linked to microcomputers.

3. Ranking and scaling of biostratigraphic events

3.1 Introduction

The ranking and scaling model used in this study was developed by Agterberg and Nel (1982a, 1982b) and Gradstein and Agterberg (1982) in the framework of the International Geological Correlation Programme (IGCP) Project 148. This project undertook to develop and test the mathematical theory necessary for quantitative biostratigraphical analysis. The organisation of this project was funded by the United Nation Educational, Scientific and Cultural Organization (UNESCO). Project 148 spanned ten years from 1976 to 1985 and, from 1979, was directed by Dr. F. Agterberg of the Geological Survey of Canada.

3.2 The philosophy of the Ranking And SCaling model(RASC)

The purpose of the model is to use biostratigraphic occurrences from well sections to produce a regional

biozonation scheme. The data used in this model are termed events. They can be highest, lowest or peak occurrences of fossil species. Events also can represent lithological or seismic markers. These events are extracted from selected well sections from the study area. A list of all possible events is compiled and sequentially numbered from 1. This list is termed the dictionary. It is used to numerically code the data from the well sections. For the purpose of RASC, wells are coded from their stratigraphic top downwards. After a preliminary phase of filtering to remove noisy data, the model proceeds in two distinct steps. The first is the ranking of events. There are two methods for ranking. Both result in the placing of events in their average positions relative to one another, producing a ranked sequence. The second step in the model is the scaling of the sequence. By using frequencies of crossovers between events from one well to another, the scaling process assigns a statistical scale to the ranked sequence producing the scaled optimum sequence. Events that are close statistically to one another cluster together; these are interpretable as fossil assemblage zones. The scaled optimum sequence is plotted as a dendrogram; the distance between an event and its neighbour is plotted horizontally so that clusters become more apparent. This dendrogram is the regional biozonation model produced by RASC. RASC also provides several tests to assess the normality of

individual well sequences vis-a-vis the scaled optimum sequence.

3.2.1 Preliminary filtering

The raw data consist of an ordered list of events for each well sequence. The events are arranged in order of increasing depth. At the raw data stage, there are many events that occur in only a few sections. These occurrences are of little or no value in the compilation of the scaled sequence because RASC is a probabilistic model. A cut-off value allows the events that do not occur in a given number of well sections to be removed from the data set before the calculations. Events that do not meet the filtering value but that are of stratigraphic significance can be reinserted in the final scaled optimum sequence by considering their positions relative to their neighbours in the wells where they occur.

3.2.2 Ranking of events

The ranking of events can be accomplished by the modified Hay method or by the presorting technique. Both methods yield equally acceptable results but presorting considerably abbreviates the procedure.

After the filtering of events, RASC places the remaining events in a cumulative order matrix. Each column and associated row correspond to an event. To simplify further discussion, the event represented by row and column i will be referred to as event i. By analyzing individual well sequences, a score of 1 is added to the value s_{ij} each time event i occurs stratigraphically above event j. When events i and j co-occur, a score of 0.5 is added to both s_{ij} and s_{ji}. A critical value CRIT1 sets the threshold number of comparison for pairs of events to be considered in ranking. The s_{ij} and s_{ji} values are zeroed when their sum is less than the CRIT1 value; this sum corresponds to the number of times events i and j occur in the same well sections. The ranking can proceed, once the cumulative order matrix is established.

The modified Hay method of ranking

As opposed to Hay's technique (1972), RASC considers simultaneous events in the ranking procedure. The Hay's method consists of matrix permutation to maximize the values in the upper right triangle of the cumulative order matrix. By proceeding sequentially, changing j+1 from 1 to n (where n is the total number of events) for each row (represented by i), the values s_{ij} and s_{ji} are compared. Unless s_{ij} is less than s_{ji} the comparison proceeds by incrementing the value of j or i; otherwise the rows i and j are interchanged, as are the corresponding columns. The comparison of values then is started from the beginning of the row. The biggest time expenditure in this method is the resolution of cycles. A cycle occurs when there is no consistent ranking solution; for example, if event A occurs above event B which occurs above event C which, in turn, occurs above event A. There are two possible causes for cycling problems. The first is that the cycling events occur in close stratigraphic proximity and that their relative position are easily interchanged. The second cause of cycles is that the data may be too patchy or insufficient to give a solution. When cycles occur, the routine cannot progress any further in the ranking of events. To break cycles, the difference in s_{ij} and s_{ji} values for the cycling events is considered. The s_{ij} and s_{ji} values are

zeroed for the pair of events that has the lowest difference. The cycle is thereby broken and the comparison is resumed.

The final result of the modified Hay method is a ranked sequence. This sequence corresponds to the order of events in the permuted cumulative order matrix.

Presorting option

By using the cumulative order matrix, simple scores can evaluate the average position of events compared to others.

A simplified matrix A is derived in the following way:

when $s_{ij} > s_{ji}$ then $a_{ij} = 1$

when $s_{ij} < s_{ji}$ then $a_{ij} = 0$

when $s_{ij} = s_{ji}$ and is different from 0 then $a_{ij} = 0.5$

The values in the A matrix are summed for each row. The Rank Presort Number is determined as follows:

$$RPN_i = \frac{(N-1) \text{ X } (\text{sum of } a_i)}{(N-1) - b_i} \qquad \text{(Eq. 3.1)}$$

where ; N is the number of events

: a_i is the score in the A matrix in the ith column of the row being studied

: b_i is the number of zeros in the ith row that correspond to the situation where $s_{ij} = s_{ji} = 0$

Events are arranged in order of decreasing RPN and constitute the ranked optimum sequence.

Harper (1984) found the results of both ranking techniques to be equally statistically satisfactory. The presorting being much simpler and less expensive in computer time was to be preferred according to Harper.

3.2.3 Scaling

The model scales the ranked optimum sequence by giving statistical estimates of the distances between events using the frequencies of relative position inversions (crossovers) between events in all wells. The scale is statistical but parallel to the chronological scale. The scaled optimum

sequence is plotted as a dendrogram. In this type of diagram, interevent distance estimates are plotted horizontally (see Figure 3.1). These events that occur close to one another form distinct clusters. Clusters are separated from one another by larger interevent distances; these may be referred to as intercluster distances. Clusters are equivalent to fossil assemblage zones and are interpreted as such. In fact, both represent groups of fossils or events that occur in close chronological proximity.

Scaling assumptions

The scaling of the ranked sequence is based on the four following assumptions (cf. Heller et al., 1985 p.12) :

1: The frequencies of the positions x_A (positions of event A in different wells relative to an average position), satisfy a normal random distribution for all events. The mean is denoted as EX_A, and the variance as σ^2 (Figure 3.2).

2: The frequency of the distance between two positions (x_B-x_A or d_{AB}) also satisfies a normal distribution, written as $f(d_{AB})$, which has a mean of $EX_B - EX_A$ or δ_{AB} and a variance of $2\ \sigma^2$. It is δ_{AB}, the mean distance between two events, or

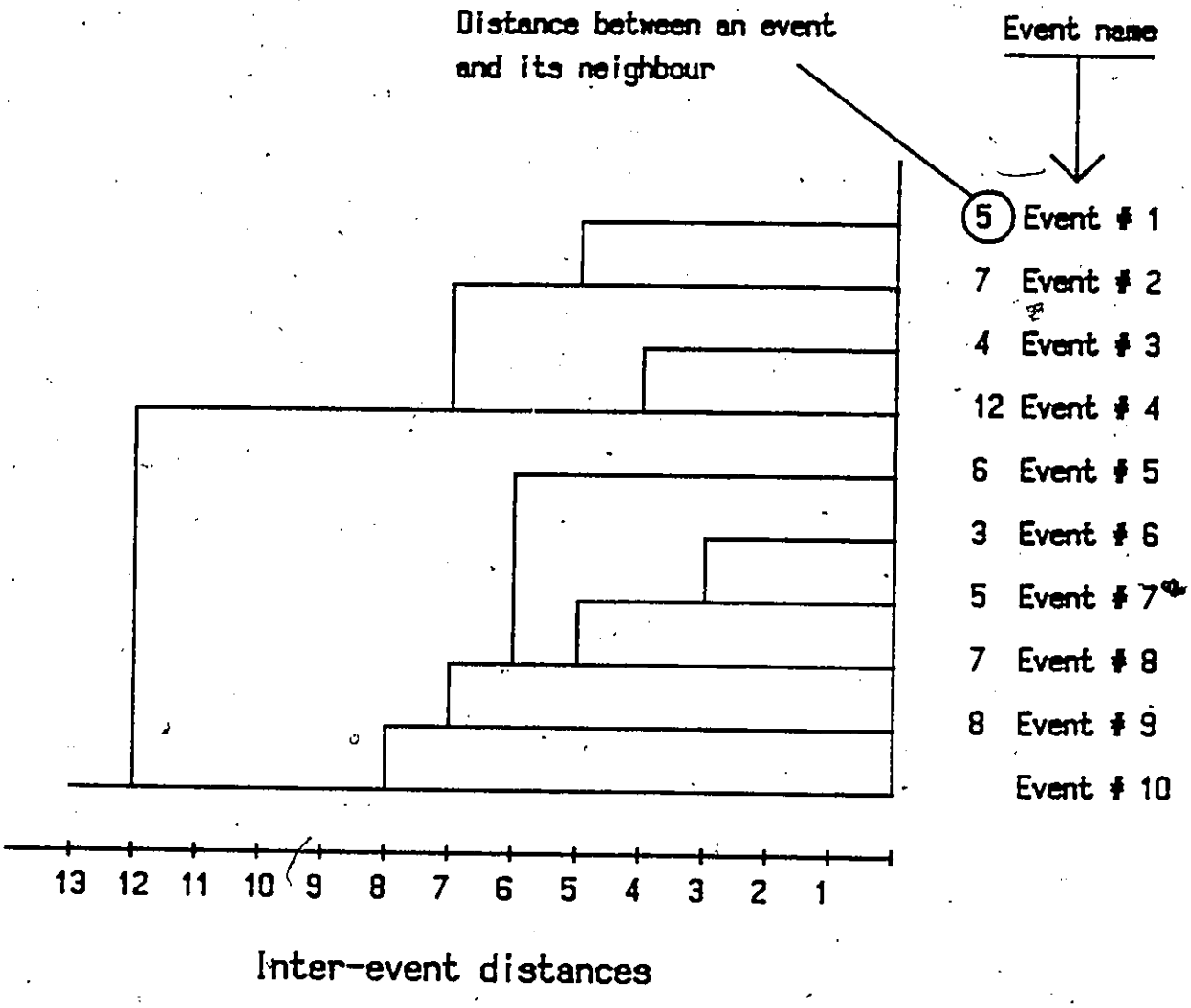

FIGURE 3.1: Example of a dendrogram: the distance between an event and its successor is plotted horizontally. Events that occur close to one another form clusters. Clusters are separated by larger inter-event distances.

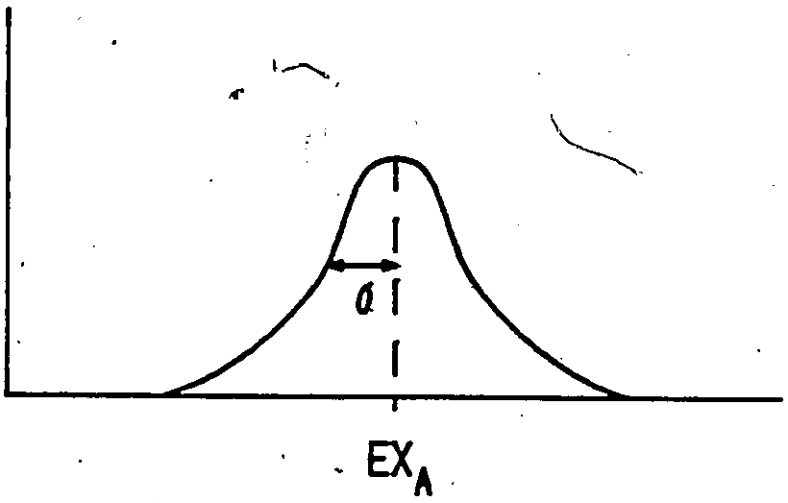

FIGURE 3.2: Distribution of event A, satisfying assumption #1 of scaling. The mean of the distribution is EX_A and its standard deviation σ.

the distance between two events in the average sequence, that RASC will estimate (Figure 3.3).

3: The statistical probability of event A occurring above event B is equal to the observed frequency of that situation ($F_{AB} = P_{AB}$). The probability P_{AB} is consequently also the probability that d_{AB} is greater than or equal to 0. If P_{AB} was the probability that d_{AB} was lesser than or equal to 0, then the parameters δ_{AB} and σ^2 could be directly derived from the z-value:

$$z = \frac{d_{AB} - \delta_{AB}}{\sigma \sqrt{2}} \qquad \text{(Eq. 3.2)}$$

then:

$$z = \frac{0 - \delta_{AB}}{\sigma \sqrt{2}} = \frac{\delta_{AB}}{\sigma \sqrt{2}} \qquad \text{(Eq. 3.3)}$$

Because it is known that $z_{BA} = -z_{AB}$, it follows that:

$$z_{AB} = \frac{\delta_{AB}}{\sigma \sqrt{2}} \quad \text{-->-->} \quad \delta_{AB} = \sigma \sqrt{2}.\ z_{AB} \qquad \text{(Eq. 3.4)}$$

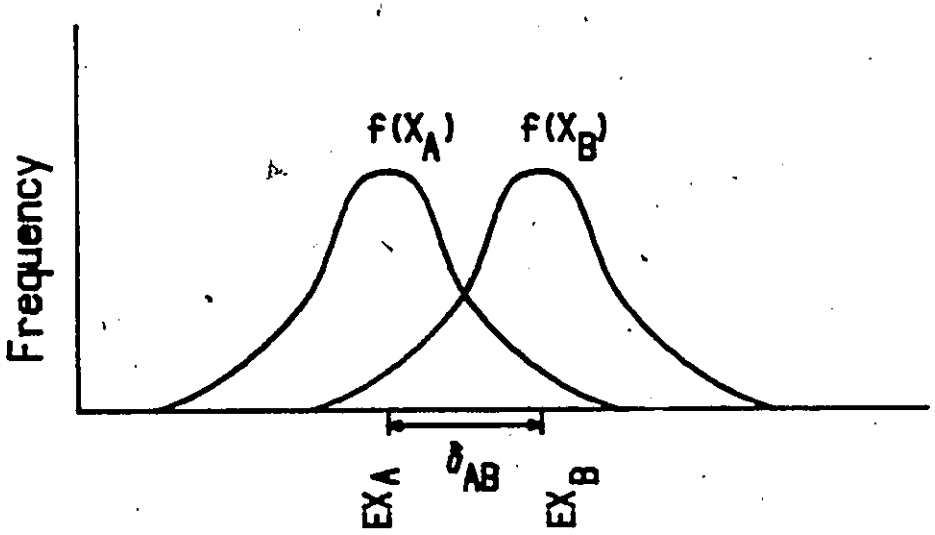

Figure 3.3: Illustration of assumption #2 of scaling: when considering events A and B, the frequency of the distance between two positions (x_B-x_A or d_{AB}) satisfies a normal distribution, written as $f(d_{AB})$, which has a mean of $EX_B - EX_A$ or δ_{AB} and a variance of $2\sigma^2$. It is δ_{AB}, the mean distance between the two events, or the distance between two events in the average sequence, that RASC will estimate.

The z-values are listed in statistical tables for the cumulative standard normal distribution expressed in percentages (in this instance P_{AB}) (see e.g., Hogg and Tanis, 1983).

4: The variance of all events is equal and preset at 0.5. The numerical value of σ^2 is of little importance as the scale is arbitrary. This particular value was selected as it simplifies calculations:

$$\sigma \sqrt{2} = 1 \text{ --> } z_{AB} = \delta_{AB} \quad \text{(Eq. 3.5)}$$

These assumptions are the basis of the scaling process used in RASC.

The first step in the scaling procedure is to build a new matrix (F) where rows and columns represent the ranked sequence. The values in the matrix are the crossover frequencies based on the values of the S matrix:

$$F_{ij} = S_{ij} / (S_{ij} + S_{ji}) \quad \text{(Eq. 3.6)}$$

The value F_{ij} represents the number of times event i occurs above event j divided by the number of times events i and j occur in the same well section. A new critical value is introduced in the model at this time. The CRIT2 value is the threshold number of occurrence in the same well section, two events must meet in order to be considered for scaling. The CRIT2 value must be equal to or greater than to the CRIT1 value because pairs of events not considered for ranking can not be considered for scaling. The new critical value allows the user more control over the scaling procedure.

The following step in RASC is to calculate a Z matrix containing the z values for pairs of events. The z value for the crossover of a pair of events is readily calculated because the probability and standard deviation are known and a normal distribution for that situation is assumed. The calculations in the algorithm are based on Abramowitz and Stegun (1964).

The z value represents a statistical distance between events. When the probability of crossover between events is 50 %, the z value is 0; this stands to reason because it is not known which event occurs above the other. When an event always occurs above another, the z value is infinity. This situation creates problems in calculations. A critical value, AAA, is introduced as a remedy. When the crossover frequency of two events i and j is $F_{ij} = 1.0$ (i.e., event is always

occurs above event j), then the corresponding z-value is set equal to AAA. This value is set by the user, but usually is taken to correspond to a P value of 95 % (i.e., the probability of finding event i above event j is 0.95).

Direct and indirect distance estimates

The z_{AB} value represents the direct distance estimate for events A and B. Such direct estimates can be considered as imprecise because the events A and B do not occur frequently in the same section. Furthermore, the Z matrix contains a wealth of other information that could be used to estimate δ_{AB}. Figure 3.4 illustrates how a third event (C for example) can be used to estimate δ_{AB}. This indirect estimate is noted as $\delta_{AB.C}$ and is equal to $\delta_{AC}-\delta_{BC}$. All pairs of events are considered in the distance estimate for one pair of events. The total number of estimates used in one distance estimate is N^*-1 where N^* represents the number of events that can be used in this estimate. N^* does not necessarily correspond to the total number of events in the Z-matrix as some may have been discarded when the threshold CRIT2 was set. The mean distance δ_{AB} becomes :

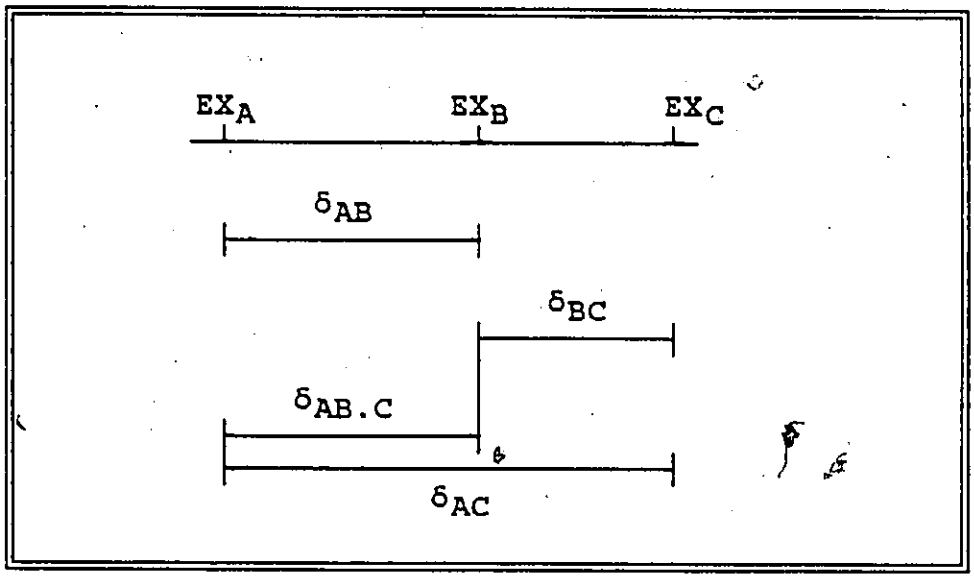

FIGURE 3.4: Illustration of the indirect distance estimate. The distance δ_{AB} can be measured directly between the events A and B, or by using a third event, C, to calculate $\delta_{AB.C}$ which is equal to $\delta_{AC} - \delta_{BC}$

$$\delta_{AB} = \frac{z_{AB} + (z_{AC} - z_{BC}) + (z_{AD} - z_{BD}) + \ldots}{N^{*}-1} \qquad \text{(Eq. 3.7)}$$

Weighted optimum sequence

Weights can be assigned to all estimates so that they will take into account the number of co-occurrences of two events; the distance estimate of events that are found in the same section more frequently, will have a greater weight. The weight, w_{AB}, assigned to z_{AB} is, by definition, inversely proportional to the variance of $f(z_{AB})$, therefore:

$$w_{AB} = \frac{1}{\sigma^2 (z_{AB})} \qquad \text{(Eq. 3.8)}$$

To relate the weight to the number of co-occurrences of events A and B (r_{AB}), Equation 3.8 must be described in terms of this factor. The functional relationship of the variances $\sigma^2 (z_{AB})$ and $\sigma^2 (p_{AB})$ is derived from the binomial frequency distribution $f(p_{AB})$ which has a mean of P_{AB} and a variance $\sigma^2 (p_{AB})$ of:

$$\sigma^2 (p_{AB}) = \frac{P_{AB} (1-P_{AB})}{r_{AB}} \quad \text{(Eq. 3.9)}$$

The relationship between the two variances can be expressed as follows (cf. Brauer Hudson and Agterberg, 1982):

$$\sigma^2 (z_{AB}) = \frac{2\pi}{e^{-ZAB^2}} \cdot \sigma^2 (P_{AB}) \quad \text{(Eq. 3.10)}$$

The value of the weight, w_{AB}, can now be defined as follows:

$$w_{AB} = \frac{r_{AB} \cdot e^{-ZAB^2}}{P_{AB} (1-P_{AB}) . 2\pi} \quad \text{(Eq. 3.11)}$$

where: P_{AB} equals F_{AB} (observed crossover frequency)

r_{AB} is the number of sections that are common to events A and B

z_{AB} is the corresponding z-value

Combined weights $w_{AB.K}$ must be calculated for the indirect distance estimates. They are calculated as follows:

$$w_{AB.K} = \frac{1}{\frac{1}{w_{BK}} + \frac{1}{w_{AK}}} = \frac{w_{BK} \cdot w_{AK}}{w_{BK} + w_{AK}} \quad \text{(Eq. 3.12)}$$

After the calculation of the weights, new weighted indirect distance estimates are computed by the model. These estimates are denoted as $\delta_{AB}w$:

$$\delta_{AB}w = \frac{w_{AB}z_{AB} + w_{AB.C}(z_{AC}-z_{BC}) + w_{AB.D}(z_{AD}-z_{BD}) + \ldots}{w_{AB} + w_{AB.C} + w_{AB.D} + \ldots} \quad \text{(Eq. 3.13)}$$

Standard deviation

In the previous discussion, all computations were based on the variance $2\sigma^2$. After the weighted indirect distance estimates, it is now possible to calculate a variance associated with these calculations:

$$\sigma^2\ (\delta_{AB}w) = \frac{w_{AB}(z_{AB}-\delta_{AB}w)^2 + w_{AB.C}(z_{AC}-z_{BC}+\delta_{AB}w)^2 + \ldots}{w_{AB} + w_{AB.C} + \ldots} \quad \text{(Eq. 3.14)}$$

Final reordering

Because the estimates for successive distances are not independent, the standard deviations cannot be simply listed. For this reason the last processing option in the programme repeats all calculations for the distance estimates with a new z-matrix based on the new sequence of events. The purpose of this procedure is to calculate a new set of standard deviations.

The new results of scaling may differ from the previous ones as indirect distance estimates will have changed where the sequence has changed. As some distances may be negative, reordering can occur and the entire procedure may be repeated up to four times. After four times almost all distances are positive and the final optimum scaled sequence is obtained.

3.2.4 Final scaled optimum sequence

The final result of RASC is a scaled sequence of events, ordered from youngest to oldest. The results are presented in a dendrogram. In this type of diagram, the sequence of events is listed in a column and the distances between successive

events are plotted horizontally. Vertical lines are dropped from each horizontal line until the next horizontal line is met. Events that occur together or close to one another (i.e. with small interevent distances) form clusters in the dendrogram. These clusters are interpretable as interval zones as they represent events in close chronological proximity. The dendrogram provides a biozonation model for the study area.

3.2.5 Well normality testing

After the scaling is completed, the model assesses the normality of individual well sequences compared to the final scaled optimum sequence.

Occurrence table

The occurrence table identifies the sections in which the events of the scaled optimum sequence occur. It is made up of several columns. The first represents the events of the scaled sequence listed from stratigraphic top to bottom. The following columns represent well sections. When an event is

recognized in a well, an X is placed in the corresponding column and row (the column represents the well and the row identifies the events; see Table 3.1). This table allows a preliminary interpretation of the data and results by highlighting missing sections in some wells and the particular distribution of certain events.

Step model

To illustrate which events are out of place compared to their average position, penalty scores are assigned to all events in a well section. These scores are derived by calculating the difference in event position in a well and in the optimum sequence. For each level that an event is out of its relative position (in the optimum sequence) a penalty point is added to the score (see Table 3.2).

A shortcoming of the step model is that it penalizes equally all events that are out of position, irrespective of their proximity (in RASC units) to their expected ranks. Events that belong to a cluster may not be out of position and should not be penalized as such. This scoring system seems to make inefficient use of the scaled sequence but, as a

RASC scaled optimum sequence	Well sequences: 1	2	3	4	5	6
B	X		X	X	X	X
A	X	X		X	X	
C			X			X
E		X	X		X	X
D	X	X	X			X
F	X		X		X	X
G	X	X		X	X	
H	X	X	X		X	
I	X			X	X	
J	X		X	X		

Table 3.1: Example of an occurrence table comparing the RASC scaled optimum sequence to 6 wells numbered from 1 to 6. When an event is present in both a well and in the RASC sequence, an X is placed in the apropriate row and column. This model highlights obvious problems with the data such as a well missing a section of the geological record (e.g.; well #4, events C to F) or wells that are shallower than others (e.g.; well #6, event G and below).

Well section Fictitious1	KASC scaled optimum sequence	Penalty score
A	B	1.0
B	A	1.0
D	D	0.0
F	F	0.0
G	G	0.0
H	I	1.0
I	J	1.0
J	H	2.0

Table 3.2: Step model well normality testing for the Fictitious1 well.

preliminary assessment, it permits recognition of events out of position.

Scattergram

Scattergrams provide visual estimates of the fit of individual wells to the RASC sequence by plotting the level of the events in individual wells against the position of the events in the RASC sequence. The optimum sequence is plotted on the vertical axis, while the well is represented by the horizontal axis. Co-eval events are stacked to be included in the diagram without creating extra levels. Scattergrams indicate the level of deviation in the position of events in the well sections and in the optimum sequence.

Event-position testing in individual wells

The objective of event-position testing is to assign a score to evaluate the similarity between the position of an event in a well section and in the optimum sequence. The drawback of the step model is avoided by using the RASC scale as the measure of event position in the optimum sequence. The

comparison becomes more difficult because the well data only contain relative positions of events (levels). To assign event scores, this testing technique identifies an event and its neighbours (above and below) in a section and the RASC distance of all three. First- and second-order differences are calculated from these positions (see Table 3.3). In the example of Table 3.3, the second-order difference is calculated for event D, of the well section Fictitious1, as follows:

$$2^{nd}\text{-order difference} = (x_F - x_D) - (x_D - x_B) \quad \text{(Eq. 3.15)}$$

or more simply

$$2^{nd}\text{-order difference} = -[\, 2\, x_D - (x_F + x_B)\,] \quad \text{(Eq. 3.16)}$$

where: B is the neighbouring event above event D in the well section.

: F is the neighbouring event below event D in the well section.

: x_{EV} represents the cumulative RASC distance from first position for event EV.

From these calculations it is apparent that no second-order differences can be calculated for the first and last events in a well section because these only have one neighbouring event.

RASC scaled optimum sequence		Well section: Fictitious1			
		Well Order	RASC dist.	1st order diff.	2nd order diff.
B	0.0	A			
A	0.2	B	0.0		
C	0.7			1.1	
E	0.9	D	1.1		-0.9
D	1.1			0.2	
F	1.3	F	1.3		
G	1.7	G			

TABLE 3.3: Example the derivation of the second order differences in event-position well normality testing. The 2nd order difference is calculated for event D in a well sequence called Fictitious1.

During scaling it was assumed that each event position can be regarded as a realization of an independent normal random variable with a variance equal to σ^2. If the successive differences are regarded similarly as realizations of independent normal random variables with variances equal to $2\sigma^2$, then the variance of the second-order differences, σ^2_2, would equal $6\sigma^2$. However, because successive distance estimates are autocorrelated, an autocorrelation coefficient, Ω, must be estimated. This estimate is required in determining the number of independent values involved in the normal distribution curve.

RASC estimates the normal distribution by fitting a doubly truncated normal distribution to the central 60% of the observed second-order differences. The second-order differences are ordered, from all sections, from the smallest value to the largest one. The standard deviation, σ_2 of the central 60% of the ordered values is determined and assumed to represent a truncated normal distribution. From statistical tables, the standard deviation of a truncated normal distribution, σ_2, is approximately 0.463 the standard deviation of the corresponding full normal distribution, ρ_2 (if 20% is truncated from each tail). Division of σ_2 by .463 yields the estimate of ρ_2. This new standard deviation is used by RASC to identify anomalous events at the 95% and 99% confidence levels. The 95% and 99% probability units

(probits) of this estimated normal distribution are given from statistical tables as ± 1.960 σ_2 and ± 2.576 σ_2 respectively. When the second-order difference of events exceed the 95% or 99% probability limits, they are marked on the output with an asterisk or a double asterisk respectively. By using only the central 60% of the distribution, anomalous values ,which are more likely to occur in the tails of the distribution, are avoided.

Because the well data are not scaled chronologically, relatively large second-order differences will be given to events on either side of a hiatus or unconformity as these features will, in general, be marked by large interevent distances.

3.3 Application of RASC to the integrated data set

When RASC was applied to the integrated data set, a minimum threshold of 7 occurrences was used. Of the initial 437 events, 85 remained after filtering. These events represent 913 occurrences in the 23 offshore wells identified in Figure 2.1. There are 47 foraminiferal and 38 palynomorph events in the final scaled optimum sequence (Figure 3.5). This almost equal number of foraminiferal and palynomorph

Figure 3.5: Final scaled optimum sequence, or biozonation model, of the Cenozoic of the Labrador shelf and Grand Banks based on an integrated data set of foraminifers, dinoflagellates and spores and pollen.

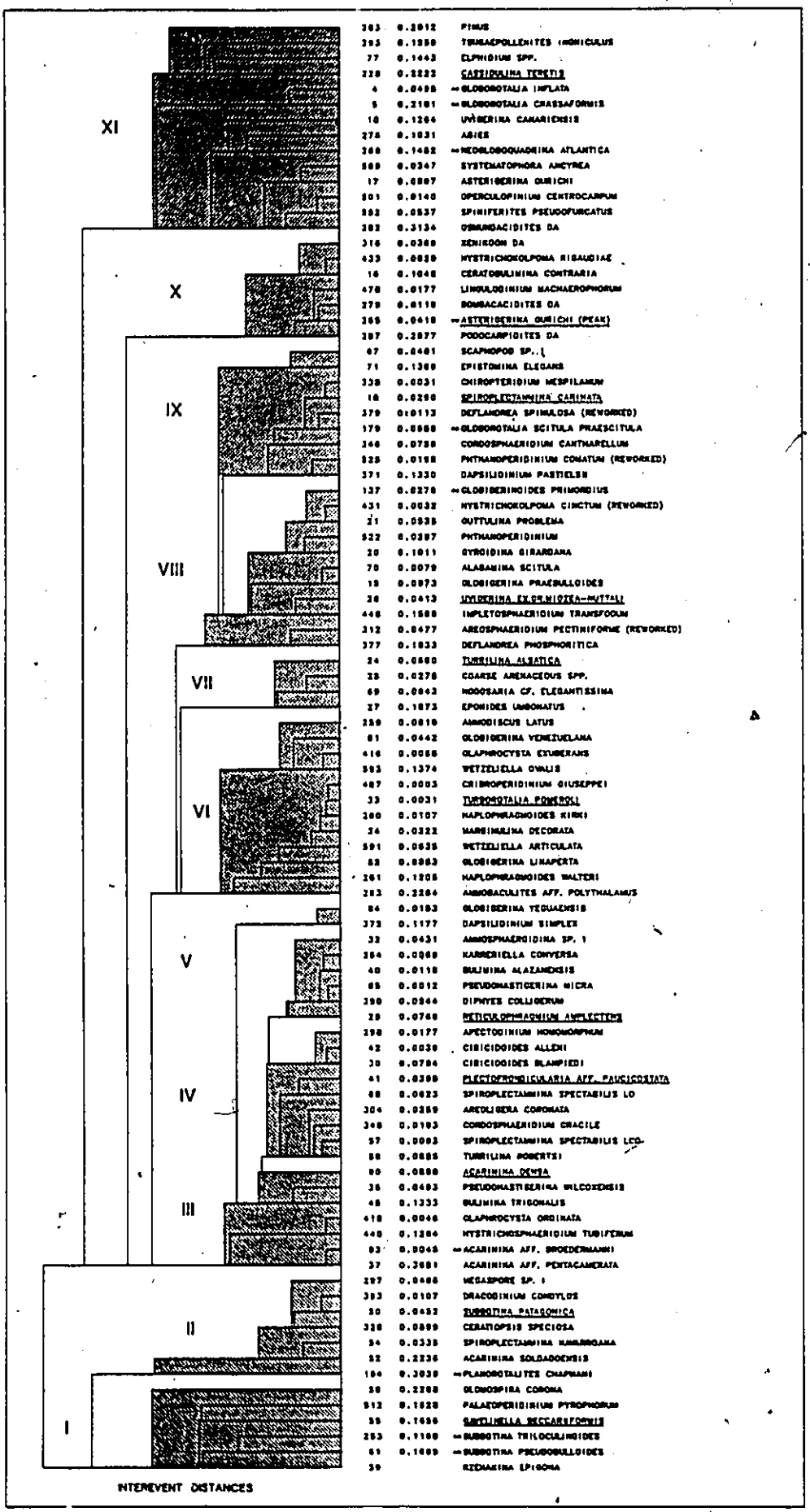
XI
X
IX
VIII
VII
VI
V
IV
III
II
I
INTERVENT DISTANCES
303 0.2812 PINUS
295 0.1358 TRIPAEPOLLENITES (MONICULUS
77 0.1443 ELPHIDIUM SPP.
228 0.2823 CASSIDULINA TEXTILIS
4 0.0495 =GLOBOROTALIA INFLATA
5 0.2101 =GLOBOROTALIA CRASSAFORMIS
18 0.1264 UVIGERINA CANARIENSIS
276 0.1031 ABIES
288 0.1482 =NEOGLOBOQUADRINA ATLANTICA
589 0.0347 SYSTEMATOPHORA ANCYREA
17 0.0807 ASTERIGERINA GURICHI
301 0.0140 OPERCULOPINIUM CENTROCARPUM
282 0.0537 SPINIFERITES PSEUDOFURCATUS
282 0.3134 OSMUNDACIDITES DA
316 0.0388 XENIKOON DA
433 0.0838 HYSTRICHOKOLPOMA RIGAUDIAE
16 0.1648 CERATOBULIMINA CONTRARIA
478 0.0177 LINGULODINIUM MACHAEROPHORUM
279 0.0118 BOMBACACIDITES DA
269 0.0618 =ASTERIGERINA GURICHI (PEAK)
287 0.2877 PODOCARPIDITES DA
67 0.0481 SCAPHOPOD SP..(
71 0.1369 EPISTOMINA ELEGANS
338 0.0031 CHIROPTERIDIUM MESPILANUM
18 0.0298 SPIROPLECTAMMINA CARINATA
379 0:0113 DEFLANDREA SPINULOSA (REWORKED)
179 0.0888 =GLOBOROTALIA SCITULA PRAESCITULA
246 0.0758 CORDOSPHAERIDIUM CANTHARELLUM
325 0.0188 PHTHANOPERIDINIUM CONATUM (REWORKED)
371 0.1330 DAPSILIDINIUM PASTIELSII
137 0.0278 =GLOBIGERINOIDES PRIMORDIUS
431 0.0832 HYSTRICHOKOLPOMA CINCTUM (REWORKED)
21 0.0935 GUTTULINA PROBLEMA
322 0.0387 PHTHANOPERIDINIUM
20 0.1811 GYROIDINA GIRARDANA
70 0.0079 ALABAMINA SCITULA
19 0.0873 GLOBIGERINA PRAEBULLOIDES
28 0.0413 UVIGERINA EXCELLIOZEA-HUTTALI
446 0.1588 IMPLETOSPHAERIDIUM TRANSFODUM
312 0.0477 AREOSPHAERIDIUM PECTINIFORME (REWORKED)
377 0.1833 DEFLANDREA PHOSPHORITICA
24 0.0680 TURRILINA ALBATICA
25 0.0278 COARSE ARENACEOUS SPP.
69 0.0843 NODOSARIA CF. ELEGANTISSIMA
27 0.1873 EPONIDES UMBONATUS
259 0.0819 AMMODISCUS LATUS
81 0.0442 GLOBIGERINA VENEZUELANA
416 0.0068 OLAPHROCYSTA EXUBERANS
593 0.1374 WETZELIELLA OVALIS
487 0.0003 CRIBROPERIDINIUM GIUSEPPEI
33 0.0031 TURBOROTALIA POMEROLI
280 0.0107 HAPLOPHRAGMOIDES KIRKI
34 0.0322 MARGINULINA DECORATA
591 0.0635 WETZELIELLA ARTICULATA
82 0.0883 GLOBIGERINA LINAPERTA
261 0.1205 HAPLOPHRAGMOIDES WALTERI
283 0.3264 AMMOSACULITES AFF. POLYTHALAMUS
84 0.0183 GLOBIGERINA YEGUAENSIS
373 0.1177 DAPSILIDINIUM SIMPLEX
32 0.0431 AMMOSPHAEROIDINA SP. 1
264 0.0068 KARRERIELLA CONVERSA
40 0.0118 BULIMINA ALAZANENSIS
85 0.0812 PSEUDOMASTIGERINA MICRA
290 0.0844 DIPHYES COLLIGERUM
29 0.0748 RETICULOPHRAGMIUM AMPLECTENS
298 0.0177 APECTODINIUM HOMOMORPHUM
42 0.0838 CIBICIDOIDES ALLENI
30 0.0784 CIBICIDOIDES BLAMPIEDI
41 0.0398 PLECTOFROMBICULARIA AFF. PAUCICOSTATA
88 0.0823 SPIROPLECTAMMINA SPECTABILIS LO
304 0.0389 AREOLIGERA CORONATA
348 0.0193 CORDOSPHAERIDIUM GRACILE
57 0.0083 SPIROPLECTAMMINA SPECTABILIS LCO-
88 0.0885 TURRILINA ROBERTSI
90 0.0888 ACARININA DENSA
35 0.0483 PSEUDOMASTIGERINA WILCOXENSIS
45 0.1333 BULIMINA TRIGONALIS
418 0.0046 OLAPHROCYSTA ORDINATA
448 0.1384 HYSTRICHOSPHAERIDIUM TUBIFERUM
83 0.0045 =ACARININA AFF. BROEDERMANNI
37 0.2681 ACARININA AFF. PENTACAMERATA
297 0.0468 MEGASPORE SP. 1
303 0.0107 DRACODINIUM CONDYLOS
30 0.0432 TURBOTINA PATAGONICA
328 0.0899 CERATIOPSIS SPECIOSA
34 0.0335 SPIROPLECTAMMINA NAMIBIANA
32 0.2236 ACARININA SOLDADOENSIS
184 0.3039 =PLANOROTALITES CHAPMANI
38 0.2288 OLOMOSPIRA CORONA
912 0.1528 PALAEOPERIDINIUM PYROPHORUM
35 0.1636 GAUDRINELLA MICCARIFORMIS
253 0.1188 =SUBBOTINA TRILOCULINOIDES
61 0.1489 =SUBBOTINA PSEUDOBULLOIDES
39 RIEDELIELLA EPIGONA

ZONE	AGE OF ZONE	NAME OF MARKER EVENT
I	Paleocene	Gavelinella beccariiformis
II	Early Eocene	Subbotina patagonica
III	early Middle Eocene	Acarinina densa
IV	late Middle Eocene	Plectofrondicularia aff. gaudicostata
V	Late Eocene	Reticulophragmium amplectens
VI	Late Eocene	Turborotalia pomeroli
VII	Oligocene	Turrilina alsatica
VIII	Late Oligocene to Early Miocene	Uvigerina ex. gr. graciliformis
IX	Middle Miocene	Spiroplectamina carinata
X	Middle Late Miocene	Asterigerina gurichi
XI	Pliocene-Pleistocene	Cassidulina peretis

Table 3.4: Names and ages of identified biozones of Figure 3.5.

events is fortuitous but ensures that there is no bias towards one group of fossils.

The dendrogram is a biozonation scheme. The clusters are interpreted as interval zones. The 11 numbered interval zones of Figure 3.5 are referred to by the name of one or more of their most characteristic members (see Table 3.4).

3.4 Biozonation of the Cenozoic of the Labrador Shelf and Grand Banks

The Cenozoic biozonation of the study area (Figure 3.5) are divided into 11 zones. Although the zones are named after one typical member, they all contain several marker and significant events. In the following discussion, the zone boundaries refer to the total RASC distance from first position (top of the optimum sequence) to the first and last events in a particular zone. The chronostratigraphic ages of the foraminiferal events are listed in Gradstein and Agterberg (1985, p.346-348) unless otherwise specified. All geochronologic ages were selected using the Berggren et al. (1985) Cenozoic time scale. The foraminifers to palynomorph ratio include only events that met the threshold value of 7 occurrences.

Zone I, Gavelinella beccariiformis zone

Age of zone: Paleocene

Zone boundaries: 6.97 to 7.80 RASC units.

Foraminifers to palynomorph ratio: 3 to 1

Index events:

63 Ma - **Subbotina triloculinoides** and **S. pseudobulloides** - events 253 and 61; two rare events that mark approximately the end of Danian time.

59 Ma - **Paleoperidinium pyrophorum** - event 512; identified as late Paleocene (NP 8) event by Williams and Bujak (1985).

58 Ma - **Gavelinella beccariiformis** - event 55; occurs up to standard zone P5 (Tjalsma and Lohmann, 1983), which fits in well with its disappearance in the Adolphus section together with **Aragonia velascoensis** (Paleocene) and below the appearance of **Pseudohastigerina** (post P5).

58 Ma - **Glomospira corona** - event 56; corresponds to the Paleocene/Eocene boundary on continental margin wells.

Preliminary paleo-environmental interpretation:

The assemblage reflects an abrupt change from an extensive shelf province in the Early Paleocene to turbiditic

facies and depositional depths in excess of 1000 m from the Late Danian to the Thanetian (Berggren, 1977, p.399).

Zone II, Subbotina patagonica zone

Age of zone: Early Eocene

Zone boundaries: 6.22 to 6.67 RASC units.

Foraminifers to palynomorph ratio: 3 to 2

Index events:

57 Ma - **Planorotalites chapmani** - event 194; disappears in standard zone P6. Specimens are often transitional between **P. chapmani** and **Pseudohastigerina**. The latter is thought to appear at the boundary of P5 and P6.

55 Ma - **Subbotina patagonica** - event 50; The end of the peak of this species occurs at the boundary of NP11/NP12, which coincides with the time of Anomaly 24, just after 55 Ma.

52 Ma - **Dracodinium condylos** - event 393; identified in lower NP14 in the Rockall plateau by Costa and Downie (1979).

Other significant event:

Ceratiopsis speciosa - event 326; late Early Eocene event identified in P8 by Williams and Bujak (1985).

Preliminary paleo-environmental interpretation:

This zone represents a greater distribution of foraminifers that are usually restricted to low or mid-latitude.

Zone III: Acarinina densa zone

Age of zone: early Middle Eocene

Zone boundaries: 5.43 to 5.83 RASC units.

Foraminifers to palynomorph ratio: 4 to 2

Index events:

52 Ma - **Acarinina aff. broedermanni** - event 93 ; this species has its top well below **A. densa**, near the Early-Middle Eocene boundary at 52 Ma.

49 Ma - **Acarinina densa** - event 90; corresponds to the time of optimum climatic warming in the Labrador sea, in the early Middle Eocene. It probably falls near Anomaly 21 from 46 Ma to 52 Ma (averaging 49 Ma).

Preliminary paleo-environmental interpretation:

The nature of the events that make up this zone strongly suggests the correlation with the climatic warming of the

early Middle Eocene. As Zone II, low and mid-latitude forms seem to make northward incursions.

Zone IV, Plectofrondicularia aff. paucicostata zone

Age of zone: late Middle Eocene

Zone boundaries: 5.08 to 5.34 RASC units.

Foraminifers to palynomorph ratio: 6 to 3

Index events:

52 Ma - Spiroplectammina spectabilis LCO (Last Common Occurrence)- event 57; this species also has its top below A. densa, near the Early-Middle Eocene boundary at 52 Ma.

49 Ma - Turrilina robertsi - event 86;

41 Ma - Apectodinium homomorphum - event 298; last occurs in the Middle Eocene (NP14) according to Williams and Bujak (1985).

Zone V, Reticulophragmium amplectens zone

Age of zone: Late Eocene

Zone boundaries: 4.75 to 5.01 RASC units.

Foraminifers to palynomorph ratio: 6 to 2

Index events:

40 Ma - **Reticulophragmium amplectens** - event 29; usually falls below **Turborotalia pomeroli** and above **Acarinina densa** in RASC runs. It is tentatively placed at 40 Ma.

38 Ma - **Pseudohatigerina micra** - event 85; this event occurs in southern wells and corresponds to the Late Eocene. The top is placed immediately below the inferred Eocene/Oligocene boundary.

37 Ma - **Diphyes colligerum** - event 390; most records confine this event to the Eocene (Goodman and Witmer, 1985). Williams and Bujak (1985) find the last occurrence (regional and world) at the Eocene/Oligocene boundary.

Preliminary paleo-environmental interpretation:

Relatively uniform climatic conditions seem to characterize this zone.

Zone VI, Turborotalia pomeroli zone

Age of zone: Late Eocene

Zone boundaries: 3.97 to 4.53 RASC units.

Foraminifers to palynomorph ratio: 8 to 4

Index events:

38 Ma - **Wetzeliella articulata** - event 591; found in the early Late Eocene (NP18) according to Williams and Bujak (1985).

38 Ma - **Turborotalia pomeroli** - event 33; this event co-occurs with **Pseudohatigerina micra** in southern wells and corresponds to the late Late Eocene. The top is placed immediately below the inferred Eocene/Oligocene boundary.

37 Ma - **Ammodiscus latus** - event 259; corresponds to the Eocene/Oligocene boundary.

37 Ma - **Cribroperidinium giuseppei** - event 487; early Late Eocene event (NP19), Williams and Bujak (1985). This event is also recognized as Late Eocene in the Norwegian-Greenland Sea (Manum, 1976).

Other significant event:

Wetzeliella ovalis - event 593; ranges up to the top of the Bartonian (early Late Eocene) (Costa, 1985).

Zone VII. Turrilina alsatica zone

Age of zone: Oligocene

Zone boundaries: 3.63 to 3.79 RASC units.

Foraminifers to palynomorph ratio: 4 to 0

Index events:

30 Ma - **Turrilina alastica** - event 24; the last occurrence of this distinctive Oligocene taxon roughly equates to the top of the Boom Clay of Belgium.

Preliminary paleo-environmental interpretation:

Event 25, Coarse arenaceous spp., characterizes a shallowing paleoecologic event corresponding to the Oligocene eustatic sea-level drop.

Zone VIII, Uvigerina ex. gr. miozea-nuttali zone

Age of zone: Late Oligocene to Early Miocene

Zone boundaries: 2.87 to 3.43 RASC units.

Foraminifers to palynomorph ratio: 5 to 5

Index events:

24 Ma - **Deflandrea phosphoritica** - event 377; found up to the latest Oligocene (NP25) by Williams and Bujak (1985). Only one record in the literature gives a higher range; i.e.,

Jan du Chene (1977) identified "Deflandrea groupe phosphoritica" [illegible] Early Miocene of Spain.

20 Ma - Uvigerina ex. gr. miozea-nuttali - event 26; found below Globigerina praebulloides (see later) in the RASC sequence and is slightly older.

20 Ma - Globigerinoides primordius trilobus - event 137; rare Early Miocene event.

17 Ma - Globigerina praebulloides - event 15; disappears locally at the early Middle Miocene of the Scotian Shelf wells (Gradstein and Agterberg, 1982).

Significant events:

Areosphaeridium pectiniforme - event 312; using the broader concept of the species of Sarjeant (1984), this event could be Late Oligocene.

Hystrichokolpoma cinctum - event 431; this species is found up to the Early Miocene (as "H. cf. cinctum") in the Norwegian-Greenland Sea (Manum, 1976). Stover (1977) identified this species sporadically up into the Early Miocene.

Preliminary paleo-environmental interpretation:

This relatively homogeneous zone reflects a more uniform environment prior to the onset of major cooling.

Zone IX, Spiroplectammina carinata zone

Age of zone: Early to Middle Miocene

Zone boundaries: 2.34 to 2.73 RASC units.

Foraminifers to palynomorph ratio: 3 to 5

Index events:

19 Ma - Cordosphaeridium cantharellum - event 346; identified in the Early Miocene in the Norwegian-Greenland Sea (Manum, 1976) and offshore Carolina (Stover, 1977). Williams and Bujak (1985) assign this event to NN2.

17 Ma - Globorotalia scitula praescitula - event 179; probably occurs in the late Early to early Middle Miocene warming event, as observed from the northern incursion of warmer water planktonic taxa.

Zone X, Astigerina gurichi zone

Age of zone: middle Late Miocene

Zone boundaries: 1.87 to 2.08 RASC units.

Foraminifers to palynomorph ratio: 1 to 5

Preliminary paleo-environmental interpretation:

With the onset of the Labrador current at the boundary of Zones IX and X, the low and mid-latitude species are not found because of the low salinity.

11 Ma - **Asterigerina gurichi** - event 17; corresponds to the Middle-Late Miocene boundary.

11 Ma - **Systematophora ancyrea** - event 569; last occurrence in the Middle to Late Miocene on the Northwest continental Shelf (Harland, 1978) and in the Norwegian-Greenland Sea (Manum, 1976).

9 Ma - **Spiniferites pseudofurcatus** - event 552; identified as Late Miocene by Williams and Bujak (1985).

Zone XI, Cassidulina teretis zone

Age of zone: Pliocene to Pleistocene

Zone boundaries: 0.00 to 1.55 RASC units.

Foraminifers to palynomorph ratio: 3 to 7

Index events:

3.5 Ma - **Globorotalia inflata**, **G. crassiformis** and **Neogloboquadrina atlantica** - events 4, 269 and 5; these

species are thought to disappear with the onset of major glaciation in the Labrador sea, dated at approximately 3.5 Ma.

Preliminary paleo-environmental interpretation:

As in Zone X, the Labrador current excluded low and mid-latitude species from northern wells so that they usually do not often meet the threshold number of occurrences. This Zone is heterogeneous marking the onset of glaciation in the Labrador Sea.

3.4.1 Effect of integration on the optimum sequence

To restate what was mentioned earlier, the integration process was expected to enhance the stratigraphic resolution in two ways. Because RASC is a probabilistic model, the increase in raw data produces results based on a greater population. With an increased number of crossovers to rely on for distance estimates, the optimum sequence is more accurate as indicated by smaller standard deviations of the estimated distances. The second enhancement of the biozonation model stems from the data itself. The foraminiferal data set is relatively complete for deeper marine paleo-environments but less so for relatively shallow conditions. The palynomorph data set is characteristically less representative of the deep

marine environment. The use of the integrated data set should automatically result in the enhancement of the final biozonation because this data set better reflects the geological record. The possibility of constructing mixed biozonations without biasing particular fossil species (or groups of fossils) is a great asset of the RASC model.

To evaluate the effect of integration on the biozonation model, a biozonation based on foraminifers only (Figure 3.6 (b)) was compared to the integrated biozonation. The dinoflagellates and spores and pollen events were removed from the scaled sequence of Figure 3.5 and the remaining interevent distances adjusted accordingly (Figure 3.6 (a)) producing an "integrated" foraminiferal zonation. Visual comparison of the initial and integrated foraminiferal zonation (Figure 3.6 (a) and (b)) highlights the increased stratigraphic resolution resulting from biodata integration. In the initial model, some zones were indistinguishable because of the small number of events they contained. The number of interpretable zones increased from 10 to 11 through integration.

The complementary nature of the foraminiferal and palynomorph data sets is illustrated in many zones, for example, in zones V and X of Figure 3.5. In zone V, the foraminifers to palynomorph ratio is 6 to 2, whereas in zone X it is 1 to 5.

Figure 3.6(a): RASC foraminiferal biozonation based on the integrated data set.

Figure 3.6(b): RASC foraminiferal biozonation based on the foraminifers-only data set.

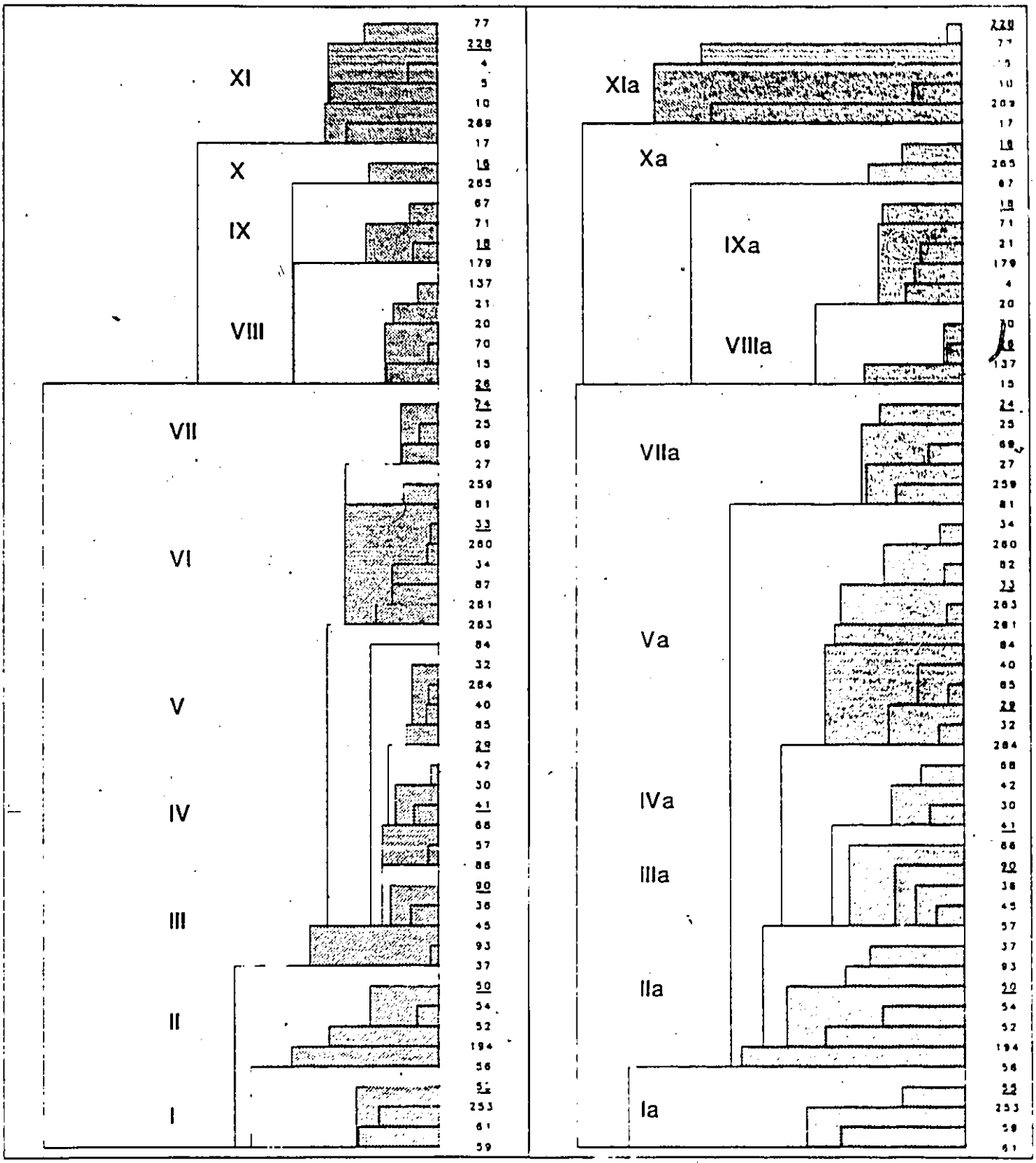
XI
X
IX
VIII
VII
VI
V
IV
III
II
I
XIa
Xa
IXa
VIIIa
VIIa
Va
IVa
IIIa
IIa
Ia

Aside from increasing the number of identifiable zones, the integration process also completes the geological record by filling in artificial gaps in the data sets. Indeed, large distances between clusters may represent unconformities, disconformities, or nondepositional hiatuses. However, they may also represent an artifact of the model because of the particular nature or shortcomings of the data set. Because the two data sets are complementary, unjustifiably large intercluster distances are reduced as, for example, between zones X and XI of Figure 3.6(a) and zones Xa and XIa of Figure 3.6(b). What initially might have been interpreted as a major environmental change, actually corresponds to a minor regional change reflected in the foraminiferal population.

3.4.2 RASC biozonation versus literature sequence of events

To assess the quality of the RASC biozonation, a theoretical sequence of events was prepared using literature ages. This sequence is listed in Table 3.5. The theoretical and RASC sequences are compared by rank correlation techniques. The Kendall Tau rank correlation coefficient between the two rankings is 0.894. This coefficient was calculated as described by Kendall (1970). Its convincingly

Foraminifers			Palynomorphs		
4	# **	Globorotalia inflata	552	*	Spiniferites pseudofurcatus
5	# **	Globorotalia crassaformis	569	##	Systematophora ancyrea
269	# **	Neogloboquadrina atlantica	346	*	Cordosphaeridium cantharellum
17	#	Aaterigerina gurichi	377	*	Deflandrea phosphoritica
265	# **	Asterigerina gurichi (peak)	390	*	Diphyes colligerum
15	#	Globigerina praebulloides	487	*	Cribroperidinium giuseppei
179	# **	Globorotalia scitula praescitula	591	*	Wetzeliella articulata
26	#	Uvigerina ex.gr.miozea-nuttali	298	*	Apectodinium homomorphum
137	# **	Globigerinoides primordius	393	*	Dracodinium condylos
24	#	Turrilina alsatica	326	*	Ceratiopsis speciosa
259	#	Ammodiscus latus	512	*	Palaeoperidinium pyrophorum
32	#	Ammosphaeroidina sp. 1			
82	#	Globigerina linaperta			
85	#	Pseudohastigerina micra			
29	#	Cyclammina amplectens			
86	#	Turrilina robertsi			
90	#	Acarinina densa			
57	#	Spiroplectammina spectabilis LCO			
93	#	Acarinina aff. broedermanni			
50	#	Subbotina patagonica			
194	# **	Planorotalites chapmani			
55	#	Gavelinella beccariiformis			
56	#	Glomospira corona			
61	# **	Subbotina pseudobulloides			
253	# **	Subbotina triloculinoides			

Table 3.5: Chronostratigraphic markers used to calibrate the RASC scaled optimum sequence in to a numerical time scale. The Beggren et al. (1985) time scale is used to obtain numerical ages. The symbols define the following: # from Gradstein and Agterberg (1985); * from Williams and Bujak (1985); ## from Harland (1978); ** events that do not meet the minimum occurrence threshold.

high value ascertains that the RASC sequence parallels a chronological sequence.

3.5 Numerical time scale of RASC biozonation

By using the events identified in Table 3.5, the biozonation scheme can be converted into a biostratigraphic numerical time scale. These events are characteristic and by knowing both their approximate age and RASC position, a best fitting spline can interpolate their observed age in this area and the age of the other events.

3.5.1 Method of numerical time scale calibration

A plot of age versus RASC distance can be prepared using the previously mentioned index events. A cubic spline is fitted to the points of that graph; this best fitting curve will be used to derive the age of all events in the RASC sequence. The spline curve is fitted using a modification of the De Boor's (1978) algorithm. This method was applied with a computer programme named SPLIN which will be described in a later chapter. The spline-fitted RASC sequence (as observed

in Figure 3.7) can be replotted as a biostratigraphic time-scale where the ages of all events are placed on a linear time scale (Figure 3.8).

3.5.2 Chronologically calibrated biozonation

The most noticeable gap in the biostratigraphic record is observed during the Oligocene. It corresponds to the drop in eustatic sea-level mentioned in Chapter 1 and in the discussion of Zone VII of Figure 3.5. A less obvious hiatus can be observed in the Early to Middle Miocene. This disconformity and the sketchiness of the younger biochronology can presumably be associated with the onset of the Labrador current.

The older part of the biochronological record is also sparse and seems to indicate the presence of a hiatus. Two factors contribute to these findings. First, the Paleocene was not sampled in many southern wells, reducing the number of events that meet the minimum number of occurrences threshold. Secondly, there was an abrupt change in paleo-environment as mentioned in the discussion of Zone I. This change would probably have been more emphasized had it not been for the sampling problem previously mentioned.

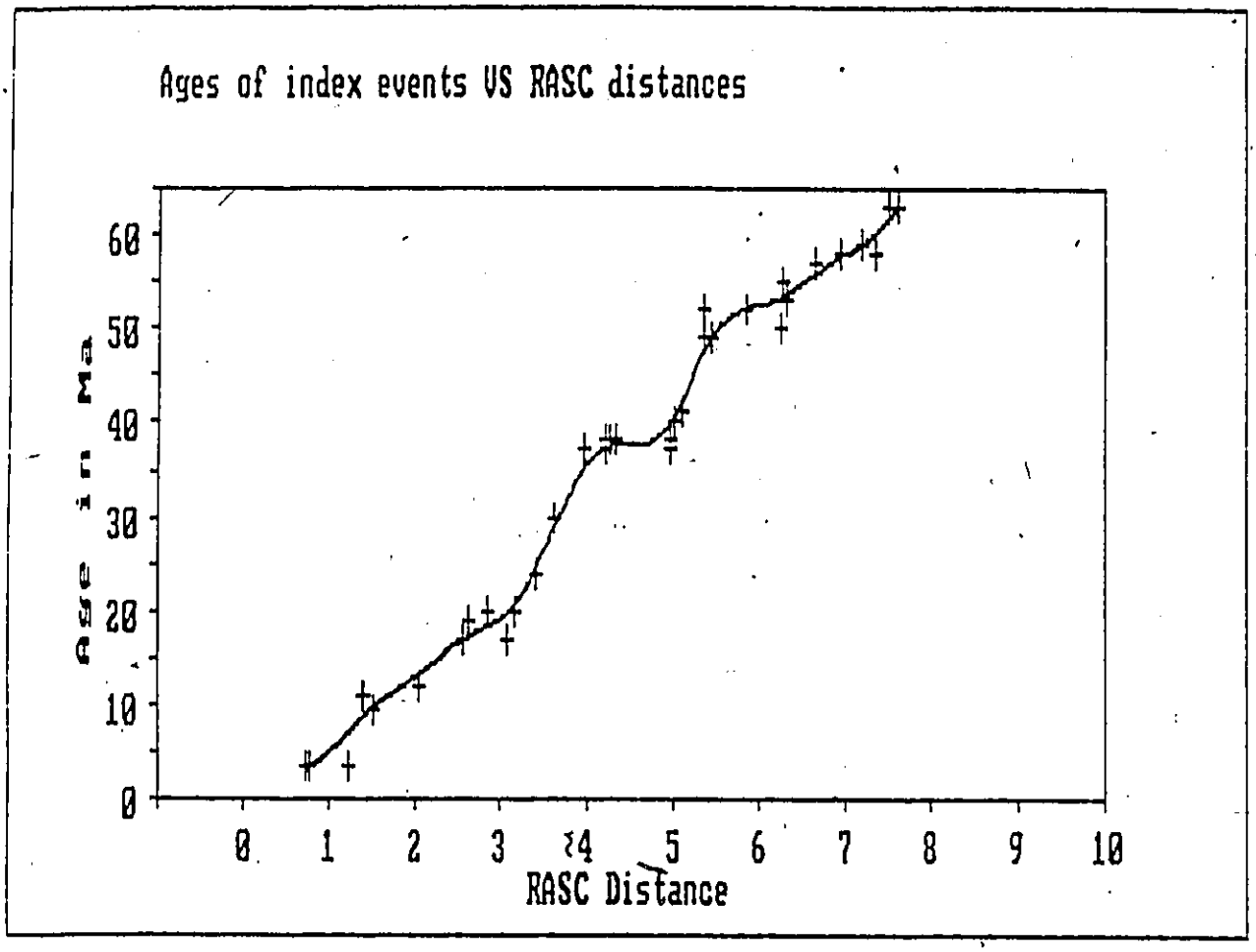

Figure 3.7: Spline-fitted plot of the literature ages of marker events versus their RASC scaled sequence position. The spline curve provides an age estimates for all RASC distances and vice-versa.

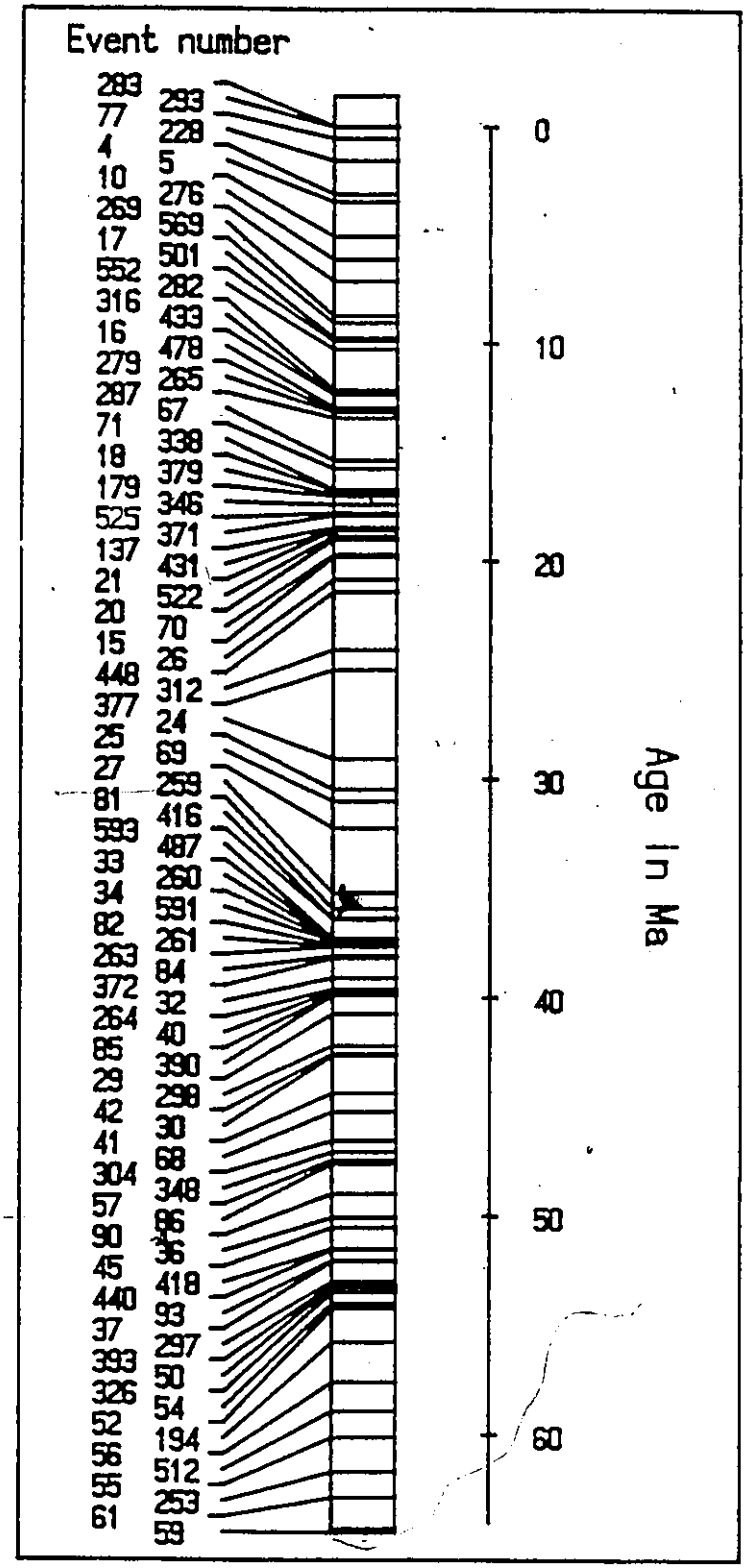

FIGURE 3.8: Numerical biostratigraphic time scale of the converted RASC scaled optimum sequence

3.5.3 Histogram of biochronological scale

A histogram of the numerical scale emphasizes the gaps and peaks in the biostratigraphic record. This histogram, (Figure 3.9) represents the number of events per interval of 1. Ma. It is expected that the event frequency would be higher in periods chronologically preceding an hiatus because most events represent species extinctions. The extinctions that would normally occur in the missing part of the geological record should be observed in the last part of the record preceding this gap.

This type of event diversity peak occurs before the Early Oligocene hiatus. However, no such peak is observed in the Late Oligocene. This is because the low sea-levels of that time did not necessarily favour species diversity. This is compounded by the problem of sampling in periods of low sedimentation rates. Indeed, events that are present may not have been observed so that their last occurrence was placed in Zone VI. Conversely, reworking of certain events would locate them in Zone VIII (after the hiatus). If such were the situation, this would create a distinctive post-hiatus peak. When considering the nature of the events (last occurrences), a peak frequency would certainly not be expected to occur

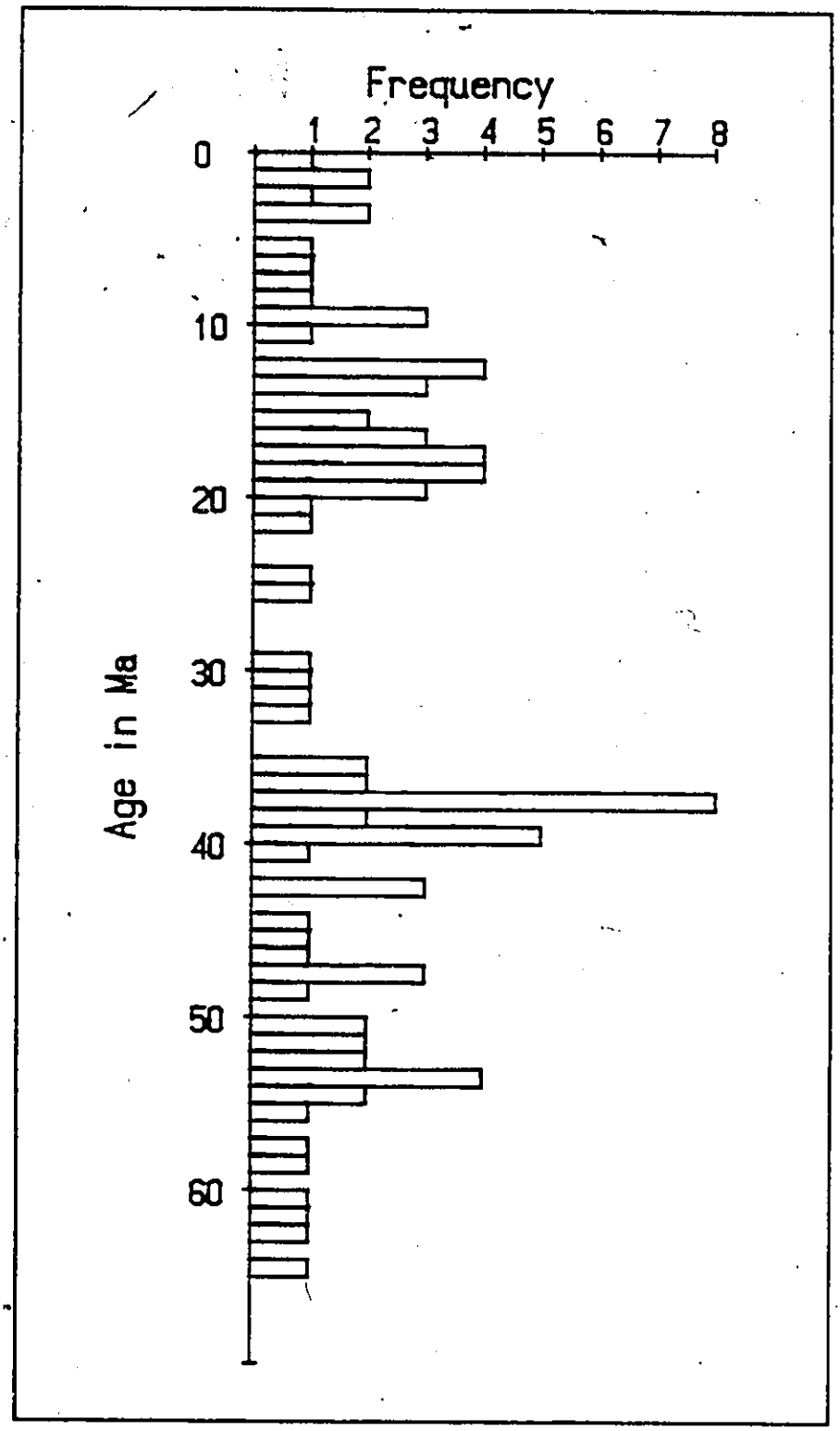

FIGURE 3.9: Histogram of the numerical time scale of Figure 3.8. The time intervals are of 1 Ma.

after a period of about ten million years of low diversity and a hiatus. However, when looking at the period from 16 Ma to 20 Ma in Figure 3.9, high frequencies are observed to occur. This phenomenon strongly supports the hypothesis that the Oligocene dinoflagellate events of Zone VIII are reworked and should not be used to infer the age of the zone.

3.6 Lithostratigraphic control

The RASC positions of lithological boundaries are determined by using the "unique event" option of the RASC programme. Once a distance is assigned to a boundary, its age can be determined using the numerical time scale as derived from Figure 3.7. The RASC inferred ages of the lithological units are listed in Table 3.6. They were published in D'Iorio (1986). Also listed in that table are the age assignments as given by Umpleby (1979) by whose lithological scheme these markers are identified.

The RASC ages correlate very well to the published lithological boundary ages. The only discrepancy is in the age of the Leif sand member. In a previous discussion the problem of Oligocene biochronology was studied. Because of sampling problems and lack of biostratigraphic control, there

Formation or Member	Time-calibrated RASC scale ages (D'Iorio, 1986)	Age assigned by Umpleby (1979)
Leif sand Member	33 Ma to 34 Ma	Upper Eocene
Brown Mudstone Member	39 Ma to 54 Ma	Lower Eocene to Middle Eocene
Top of the Cartwright Formation	54 Ma	Lower Eocene
Gudrid Sand Member	55 Ma to 56 Ma	Paleocene to uppermost Eocene

Table 3.6: Comparison of ages of lithological units of the Labrador shelf. The literature values are those of Umpleby (1979) adapted to the Berggren et al. (1985) time scale, the time-calibrated RASC ages are from D'Iorio (1986).

is a greater uncertainty in this section of the numeric scale. This problem is again amplified by the fact that the positioning of the Leif Sand Member boundaries is based on fewer occurrences than any other lithological unit.

3.7 Conclusions

(3a) Integration of biostratigraphic data has a two-fold effect on the regional biozonation. By using a probabilistic model, the increase in biostratigraphic data directly results in an increased accuracy of the results. Secondly, the different data sets geologically complement each other giving a more realistic portrait of the geological record.

(3b) A literature-based sequence of biostratigraphic events shows a significant correlation with the ranking and scaling final sequence (Kendall Tau rank correlation coefficient = 0.89).

(3c) Using marker events of the RASC sequence and their literature chronological value, the RASC scaled sequence is calibrated with respect to a numerical time scale. This scale is used to assign a regional age to all events in the RASC sequence.

(3d) Using the biochronological scheme developed through RASC scale calibration, further refinements of zone ages can be made. Zone VIII now seems to be restricted to the Miocene but includes several Oligocene reworked events. These events show up as a peak that follows a 10 Ma period of low diversity and nondeposition.

(3e) The calibrated RASC scale can also be used to infer the age of lithological markers in the data set. Comparison to the Umpleby (1979) classification shows high correlation.

4. Correspondence analysis

4.1 Introduction

Correspondence analysis isolates major trends in the data and places them on preferential axes. Although its application does not depend on RASC, the interpretation of the results is easier when compared to the RASC biozones. The analysis is based on the output of the computer programme DECORANA that was developed and published by Hill (1979). The purpose of the analysis is to identify main trends in the data. Each trend is represented by an independent axis. On such an axis, each event and well are given a score. The trend in the events is identified by placing the events scores in order of relative magnitude. The well trends are identified in the same way. Correspondence analysis is based on finding multivariate trends in events X wells matrices (Gauch, 1982). As in reciprocal averaging (Hill, 1973), scores are assigned to both events and wells. Each event score is the average of the scores of the wells in which that event occurs. Similarly, well scores are equal to the average of the scores of the events they contain. Iterative recalculation of the scores is continued until stabilization of the results is reached. The resulting set of scores is the

first axis of correspondence analysis. The second and higher axes are obtained by a similar iterative process followed by detrending to remove quadratic dependence between axes. These procedures, as well as the DECORANA FORTRAN programme used in this study, are published in Hill (1979).

Because of ecological or paleoenvironmental conditions, events may be restricted to a range of wells. Overlapping ranges form an interpretable, progressive sequence. By plotting both event and well scores together, trends are visible on a preferred diagonal axis and consequently easier to interpret.

Unlike RASC, correspondence analysis benefits from using all events that occur in more than one well. Differential paleoenvironmental conditions of biozones will be best illustrated by events that occur in only a few well sections. Anomalous behaviour of certain types of events can also be highlighted by this type of analysis.

This analysis is not meant to be a exhaustive study of oceanographic and ecologic factors controlling the environment, but rather an application of correspondence analysis to emphasize certain environmental factors affecting the distribution of events in the study area.

4.2 Methodology

The following discussion of correspondence analysis is based on Hill (1979).

Detrended correspondence analysis is derived from a simpler method of ordination known as reciprocal averaging (or correspondence analysis). The methods differ in that detrended correspondence analysis systematically removes any correlation between axes of different order.

The algorithm of reciprocal averaging begins with the selection of trial species scores, followed by the calculation of sample (well) scores such that the sample score is the mean score of the species that occur in it; the species scores in turn are recalculated as the means of the scores of the samples in which they occur. As this process is iterated, the scores stabilize to give a solution which is independent of the initial trial scores. The resulting species score vector is the first component axis. A second axis is derived by performing the same iterative procedure, but taking out a regression on the first axis at the end of each iteration cycle, so that the new scores are uncorrelated with those of the first axis. Subsequent axes may be determined in a similar fashion.

Let X be the data matrix with elements x_{ij}, i representing a row index for species and j a column index and let $a = a_i$ be a column vector of the species scores and $b = b_j$ be a row vector of sample scores. Then the iteration algorithm is:

$$b_j = \sum_i x_{ij} a_i / \sum_i x_{ij} \qquad \text{(Eq. 4.1)}$$

$$a_i = \sum_j x_{ij} b_j / \sum_j x_{ij} \qquad \text{(Eq. 4.2)}$$

A trial vector a is used in Equation 4.1 to determine a trial vector b, which, in turn, is used to generate an improved trial vector a in Equation 4.2. This process is continued until a and b stabilize, yielding the species and sample scores for the first axis. Hill (1979) used an eigenvector method to accelerate stabilization of the results. This method is generally used in correspondence analysis whereas reciprocal averaging is based on the iterative procedure. The direct eigenvector method is applicable to smaller data matrices whereas the iterative procedure is preferred when several hundred species are involved (as in this study).

The programme DECORANA was developed by Hill (1979) to perform both reciprocal averaging and detrended correspondence analysis. A subroutine was added by Bonham-Carter et al. (1986) to reorganize and plot the species and samples matrix

in order of increasing score. This step facilitates interpretation as it places the entries along the principal diagonal depicting the range of events (species) in wells (samples) and highlighting their overlap.

DECORANA contains a number of scaling options. In this study, however, no rescaling of axes was performed as the results were not to be interpreted on their own but in the context of the RASC biozonation model.

4.3 Preliminary application of DECORANA

Correspondence analysis was performed on the integrated data set by running the DECORANA programme. Unlike the RASC programme, almost no filtering of data was performed. Events that occur only once were removed from the data set as they cannot contain information pertinent to trends in the data. All other events are retained as these occurrences can provide useful information on differential environmental conditions in specific wells.

In the preliminary analysis, the 23 well sections of Figure 2.1 were studied. The resulting well and species scores are presented in Tables 4.1 and 4.2 respectively. The principal trend that emerges from the results is the strong

WELL NAME (wells ordered from North to South)	WELL SCORES OF THE FIRST AXIS OF CORRESPONDENCE ANALYSIS
RUT H-11	186
KARLSEFNI H-13	14
SNORRI J-90	3
HERJOLF M-92	17
BJARNI H-81	24
GUDRID H-55	67
CARTIER D-70	0
INDIAN HARBOUR M-52	26
LEIF E-38	12
LEIF M-48	17
FREYDIS B-87	0
HARE BAY E-21	157
BLUE H-28	257
BONAVISTA C-99	95
CUMBERLAND B-55	53
BONANZA M-71	197
DOMINION O-23	144
SOUTH TEMPEST G-88	206
FLYING FOAM I-13	94
ADOLPHUS D-50	237
HIBERNIA P-15	214
EGRET K-36	140
OSPREY H-84	158

Table 4.1: Well scores of the first axis of correspondence analysis. All 23 well sections were studied in the preliminary analysis.

Table 4.2: First axis event scores in the preliminary application of correspondence analysis. The events are refered to by their RASC dictionary number; the names of these events are listed in Appendix A.

Event number	First axis score	Event number	First axis score	Event number	First axis score	Event number	First axis score	Event number	First axis score	Event number	First axis score	Event number	First axis score
72	456	33	207	520	112	417	63	305	10	512	-43	393	-91
147	441	96	199	472	109	338	60	358	10	427	-50	284	-92
122	434	53	197	78	106	501	60	325	9	330	-53	309	-92
146	434	27	196	86	106	45	59	570	6	448	-53	326	-92
234	426	77	192	181	106	44	58	591	5	311	-56	531	-92
156	405	40	187	340	106	552	58	433	3	363	-56	577	-92
179	405	230	183	546	106	34	57	293	1	426	-56	354	-93
110	392	263	170	528	105	270	57	576	1	432	-56	323	-94
136	373	452	166	485	103	379	57	471	-1	435	-56	373	-96
79	366	32	164	9	102	304	54	315	-10	540	-56	286	-98
82	365	265	164	39	102	369	52	280	-11	600	-56	434	-98
68	355	15	163	523	102	494	52	59	-15	440	-57	461	-98
187	340	190	163	530	102	348	50	587	-16	467	-57	507	-98
6	335	310	163	118	100	383	50	497	-17	374	-58	342	-99
151	334	24	161	329	100	593	49	367	-19	500	-58	529	-99
37	328	36	157	388	98	377	48	522	-20	364	-60	295	-100
89	326	20	156	318	97	403	46	291	-21	459	-60	344	-101
194	319	492	156	554	97	518	45	287	-22	460	-60	397	-102
93	312	69	152	56	96	575	45	298	-22	74	-61	596	-102
90	311	261	152	565	96	458	42	282	-23	505	-61	314	-103
81	306	260	148	517	91	469	41	474	-23	288	-63	503	-103
164	299	85	145	343	90	502	41	361	-24	316	-68	350	-107
26	296	47	144	76	88	283	39	396	-24	345	-69	322	-108
84	284	29	143	545	88	346	39	535	-24	317	-71	470	-108
162	284	11	141	30	87	41	36	390	-25	487	-72	300	-109
161	283	109	141	384	84	496	35	419	-25	35	-73	533	-110
144	280	117	141	63	82	547	35	428	-25	60	-75	75	-111
2	277	226	141	431	82	339	33	525	-26	337	-75	306	-111
4	277	549	141	319	80	88	32	526	-33	380	-75	566	-111
269	277	57	140	508	80	303	32	568	-34	425	-75	493	-112
71	274	16	136	571	80	320	32	537	-35	328	-76	294	-114
14	263	18	136	279	77	478	32	307	-37	335	-78	415	-114
250	263	25	135	55	75	312	31	372	-37	61	-79	67	-115
94	259	509	133	42	73	539	30	296	-41	62	-79	281	-117
172	240	275	127	228	73	592	30	504	-41	289	-79	299	-117
159	227	264	125	418	73	416	26	524	-41	301	-79	560	-117
1	218	451	124	54	72	399	25	594	-41	292	-85	398	-122
49	215	253	121	457	67	569	23	333	-42	446	-86	206	-124
50	213	527	121	578	66	297	22	447	-42	599	-86	378	-125
52	213	38	118	70	65	515	21	334	-43	543	-87	290	-127
10	210	411	112	391	65	449	20	375	-43	347	-88	173	-134
17	210	424	112	21	64	365	18	376	-43	423	-89		
259	208	511	112	349	63	371	16	479	-43	276	-91		

correlation of the first axis well scores with geographical position of the wells as in the Bonham-Carter et al. (1986) study. When latitude is plotted against well scores, distinct areas of trend emerge (Figure 4.1). With the exception of Rut H-11, the Labrador Shelf wells have low scores and the Grand Banks higher ones (see Table 4.1).

Because these scores are obtained through reciprocal averaging, an anomalous well score must characterize either an environmental trait particular to that well or the nature of the events it contains. It follows that the Rut anomaly can be justified in two ways: (a) this well contains mostly high scoring events not characteristic of other northern wells; or (b) there is a geological abnormality in this section causing the high score.

As noted in Table 2.1, palynomorph data were not available in the Rut H-11 well. From Table 4.3 it can further be noted that the average score of the 108 foraminifers is 178.8, whereas the average score of the palynomorphs is -11.2. The combination of these facts explains the high Rut H-11 score.

Because of the reciprocal averaging technique, the higher foraminiferal average score can also be the result of one of the following two possibilities: (a) foraminifers display an anomalous behaviour reflected in their scores; or (b) 6 of the

Figure 4.1 (a): Plot of well scores against distance along simplified 600 m depth projection line.

Figure 4.1 (b): Plot of foraminifer to palynomorph ratio against distance along the 600 m depth projection line. Most of the wells that exhibit high well scores also have low or zero foraminifer to palynomorph ratios.

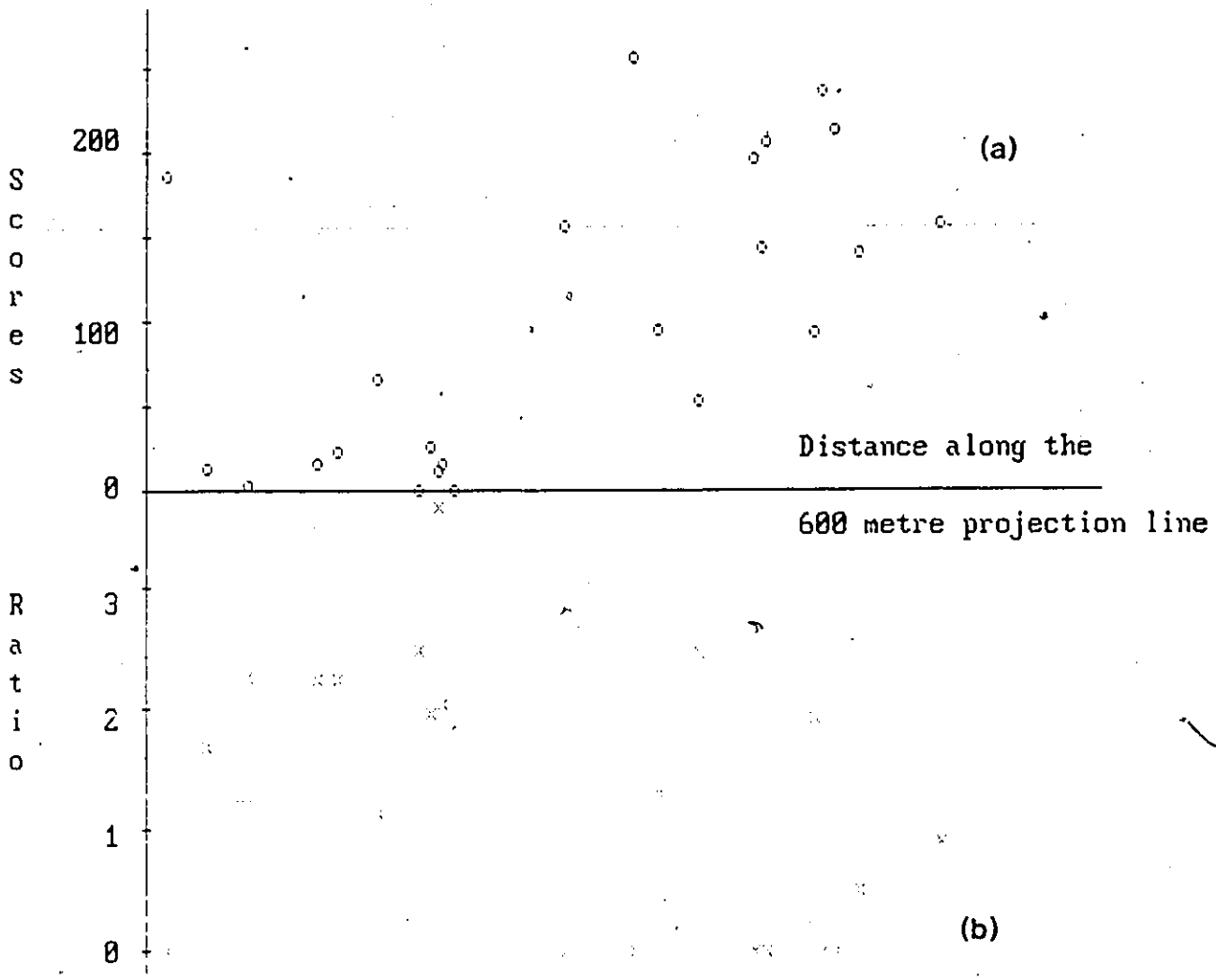
200
100
0
Scores
(a)
Distance along the
600 metre projection line
3
2
1
0
Ratio
(b)

	Preliminary application	Final application
Number of events	299	280
Sample mean	57.4	2.1
Mean foraminiferal score	178.8	48.9
Mean palynomorph score	-11.2	-19.6
Difference in palynomorph and foraminifer scores	190.0	68.5
Difference in palynomorph and foraminifer scores divided by σ	1.40	0.49
Mean dinoflagellate score	-6.9	-10.5
Mean spores and pollen score	-49.7	-102.5
Sample standard deviation.	135.8	139.1
Sample variance	18453	19351

Table 4.3: Comparison of the two applications of correspondence analysis and of the omission of the wells in which no palynomorph data were available.

southernmost wells, which have the higher scores, contain only foraminiferal events (see Table 2.1). The comparison in Table 4.3 shows that this causes these wells to impart higher values to the scores of the foraminiferal events they contain.

Biological explanations for the first axis of correspondence analysis were discarded because the latitude related trend was also recognized when a foraminifers-only data set was used in a similar study by Bonham-Carter et al. (1986). Therefore the lower event scores of the palynomorphs are presumed to be mostly due to their absence in the high scoring lower-latitude wells and the Rut well anomalous high score is due to the foraminiferal events it contains.

As previously mentioned, the average palynomorph score is -11.2. The average scores of the dinoflagellates and the spores and pollen are -6.9 and -49.7, respectively. The mean of all events is 57.4 and the standard deviation, σ, is 135.8. The marked difference in dinoflagellates and spores and pollen average scores will be studied in the final application of correspondence analysis.

4.4 Correspondence analysis of the reduced integrated data set

To verify that latitude explains the first axis of correspondence analysis, DECORANA is applied to a modified integrated data set made up of the 16 wells in which palynomorph and foraminiferal data were available (see Table 2.1). The resulting well scores are presented in Table 4.4 and plotted against the distance from North along the 600 metre depth projection line (see Figure 4.2). The event scores are presented in Figures 4.3 to 4.13.

4.5 Analysis of well scores

A North-South well differentiation is apparent in Figure 4.2. The Labrador Shelf wells show a progressively increasing score to the south but, in general, have scores less than -29. Similarly, Grand Banks wells show scores increasing southward. The Grand Banks scores are characteristically higher than 33.

The partitioning of the wells into two groups represents a natural geographic division that will be better explained by examining time slices based on the eleven RASC biozones.

WELL NAME (wells ordered from North to South)	WELL SCORES OF THE FIRST AXIS OF CORRESPONDENCE ANALYSIS
KARLSEFNI H-13	-76
SNORRI J-90	-66
HERJOLF M-92	-37
BJARNI H-81	-2
GUDRID H-55	5
CARTIER D-70	-60
INDIAN HARBOUR M-52	-41
LEIF E-38	-1
LEIF M-48	-29
FREYDIS B-87	-58
BONAVISTA C-99	50
CUMBERLAND B-55	33
DOMINION O-23	113
FLYING FOAM I-13	65
EGRET K-36	82
OSPREY H-84	150

Table 4.4: Well scores of the first axis of correspondence analysis. Only the 16 well sections with both foraminifers and palymorphs data were used in this application of DECORANA.

Figure 4.2 : Plot of first axis well scores against the distance along the 600 m depth projection line. The Labrador shelf and Grand Banks wells show a distinct partition in scores.

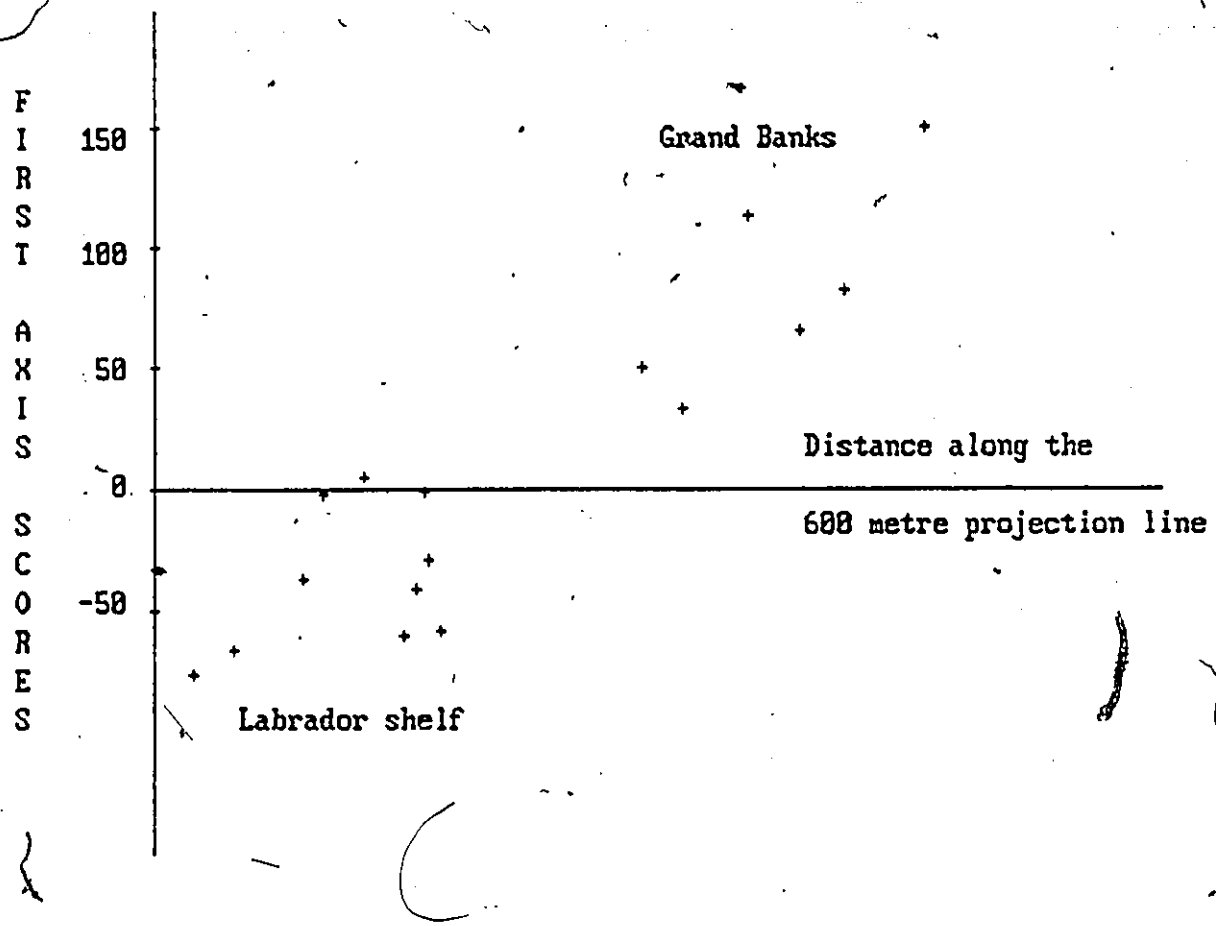
FIRST AXIS SCORES
150
100
50
0
-50
Grand Banks
Distance along the
600 metre projection line
Labrador shelf

4.6 Analysis of event scores

The event scores range from -254 to 469 with a mean of 2.1 and an unbiased standard deviation of σ = 139.1. The average score of the foraminifers is 48.9, whereas the palynomorph average score is -19.6. The average scores of the dinoflagellates and spores and pollen are -10.5 and -102.5, respectively.

In the preliminary application of DECORANA, the difference in the average scores of palynomorphs and foraminifers presented a major bias in the analysis. As can be observed in Table 4.3, the difference between the average scores of these two groups decreases from 190.0 to 68.5 and the standardized difference (difference divided by the standard deviation) from 1.40 to 0.49. This difference can be accounted for in major part by the relatively greater abundance of foraminifers in the southern wells.

4.7 DECORANA-RASC paleoenvironmental interpretation

The RASC position of the events that occur in fewer than 7 sections, must be determined in order to subdivide the

DECORANA output into the 11 RASC zones. By using the RASC unique event option, a RASC distance is given to all events. This was carried out as described in section 3.2.1.

A programme named ZONER (see Appendix B pages 315 to 318) was created to divide the DECORANA output into desired zones, as specified by the user. This routine greatly accelerates the processing of the RASC zones.

All zones are plotted in descending order of well score (left to right) and in descending order of event score (downwards) (Figures 4.3 to 4.13). These zones can now be interpreted environmentally using the DECORANA analysis.

Three distinct groups of events can be recognized. The first and third groups represent events that have an affinity to northern and southern wells respectively, whereas the second group represents either wide ranging events or events with no particular affinity. The score boundary for these groups was selected according to the minimum Grand Banks group well score (33) and to the maximum Labrador Shelf group well score (-29). To translate well scores into event scores, they must be multiplied by 3.58 as this scaling factor was employed in DECORANA to facilitate the analysis. The corresponding event score boundaries for the second group are -104 and 118. There are 65 events in the first group, 157 in the second, and 58 in the third.

4.7.1 Chi-squared test

The events were divided into their respective zones according to their RASC distances and into their respective DECORANA groups according to their first axis scores.

A contingency table was prepared (see Table 4.5). The expected event frequency of group j in zone i , E_{ij}, was calculated as follows:

$$E_{ij} = S_i * S_j / n \qquad \text{(Eq. 4.3)}$$

Where : S_i is the number of events in zone i,

S_j is the number of events in group j, and

n is the total number of events.

The chi-squared value for the contingency table is 25.55 which does not represent a statistically significant departure from the average for a level of significance of α = 0.05 and 20 degrees of freedom. The critical chi-squared value for α =0.05 in each zone (d.f.=2) and each group (d.f.=10) are 5.99 and 16.92, respectively. Again, no significant departure from the average is observed in any group or zone as a whole.

ZONE	Group 1 Northern affinity score ≤ -104			Group 2 Wide distribution -104 < score < 118			Group 3 Southern affinity score ≥ 118			TOTALS	
	O	E	C	O	E	C	O	E	C	O	chi²
I	4	1.86	2.47	4	4.49	0.05	0	1.66	1.66	8	4.18
II	4	2.55	0.82	3	6.17	1.63	4	2.28	1.30	11	3.75
III	13	10.45	0.62	19	25.23	1.54	13	9.32	1.45	45	3.62
IV	12	8.12	1.85	18	19.63	0.13	5	7.25	0.70	35	2.68
V	5	4.41	0.08	13	10.65	0.52	1	3.94	2.19	19	2.79
VI	4	5.80	0.56	17	14.02	0.63	4	5.18	0.27	25	1.46
VII	5	5.34	0.02	13	12.90	0.00	5	4.76	0.01	23	0.03
VIII	8	9.52	0.24	25	22.99	0.18	8	8.49	0.03	41	0.44
IX	5	6.27	0.26	18	15.14	0.54	4	5.59	0.45	27	1.25
X	2	4.88	1.70	13	11.78	0.13	6	4.35	0.63	21	2.45
XI	3	5.80	1.35	14	14.02	0.00	8	5.17	1.54	25	2.89
TOTALS	65		9.97	157		5.55	58		10.47	[illegible]	[illegible]

Table 4.5: Observed and expected event frequencies in each zone. O = observed frequency; E = expected frequency and C = Chi-squared measure ($(O-E)^2 / E$).

However, the chi-squared measures do indicate interesting variations in the distribution of events in the zones.

4.7.2 Environmental interpretation of individual zones

Ten of eleven zones show a three-fold differentiation. A first group of events, usually palynomorphs, is characterized by scores less than -104 and is restricted to northern wells. A second group encompasses most geographically wide ranging events. Finally, the third group contains events occur only in southern wells with scores greater than 118. It is the ratio of the number of events in each of the three groups that reveals most about the prevailing environmental conditions.

Biozone I

Foraminifer to palynomorph ratio: 6 to 2

Event score group ratio: 4 : 4 : 0

Average event score: -133

Sampling problems (missing data) were experienced in many southern wells and the Paleocene was not sampled. These

EVENT NAME	#	SCORE	Well number															
			2	3	7	11	8	4	10	5	9	6	15	14	17	20	16	21
PALAEOPERIDINIUM PYROPHORUM	512	-77	X	X	X	X	X	X		X			X					X
GAVELINELLA BECCARIIFORMIS	55	-90	X			X	X	X		X		X	X					
GLOBOSPIRA CORONA	56	-91	X	X	X	X	X	X	X	X		X	X	X				
ALISOCYSTA CIRCUMTABULATA	334	-99	X				X						X					
PLANOROTALITES COMPRESSUS	60	-140					X	X										
RZEHAKINA EPIGONA	59	-153		X	X	X	X	X				X						
SUBBOTINA PSEUDOBULLOIDES	61	-209	X				X											
GAVELINELLA DANICA	62	-209	X				X											

Figure 4.3: First axis results of correspondence analysis for Zone I of RASC biozonation.

problems are apparent in Figure 4.3 and resulted in the absence of events of group 3 in this zone.

Biozone II

Foraminifer to palynomorph ratio: 6 to 5

Event score group ratio: 4 : 3 : 4

Average event score: 12

This zone marks the onset of climatic warming. It is expressed as the northward migration of species (i.e.; greater diversity in northern wells). From Table 4.5 it is observed that more species than expected are found in group 3. It can be speculated that climatic warming did not homogenize the event distribution in the study area but gave a more equatorial and tropical character to the assemblages while preserving the latitudinal gradient. This differentiation is similar to the one observed by Bonham-Carter et al. (1986) in their "Time 2" and follow the general pattern of three-fold latitudinal differentiation that is observed in most zones.

EVENT NAME	#	SCORE	Well number 2	3	7	11	8	4	10	5	9	6	15	14	17	20	16	21
PLANOROTALITES AUSTRALIFORMIS	161	262											X				X	
PLANOROTALITES CHAPMANI	194	262											X				X	
ACARININA SOLDADOENSIS	52	128	X				X						X				X	X
SUBBOTINA PATAGONICA	50	119	X				X					X	X	X			X	X
PLANOROTALITES PLANOCONICUS	47	75					X	X						X			X	
MEGASPORE SP. 1	297	-28	X	X	X	X	X	X	X	X		X	X	X	X		X	
SPIROPLECTAMMINA NAVARROANA	54	-86	X	X	X	X	X	X	X	X		X	X		X			
DRACODINIUM CONDYLOS	393	-114		X	X	X	X		X	X			X					
CERATIOPSIS SPECIOSA	326	-134	X	X	X	X	X	X	X	X			X					
EISENACKIA CRASSITABULATA	398	-156				X			X									
PALAEOCYSTODINIUM BENJAMINII	507	-192		X			X											

Figure 4.4: First axis results of correspondence analysis for Zone II of RASC biozonation.

Biozone III

Foraminifer to palynomorph ratio: 27 to 16

Event score group ratio: 13 : 19 : 13

Average event score: 6

As in Zone II, more events than expected were found in groups 1 and 3. The second group of events shows a significant northward incursion of low and mid-latitude forms. Examples of this incursion are **Acarinina densa**, **A.** aff. **Broedermanni** and **A.** aff. **pentacamerata**.

As the previous zone, Zone III reflects the Eocene climatic warming.

Biozone IV

Foraminifer to palynomorph ratio: 15 to 21

Event score group ratio: 12 : 18 : 5

Average event score: -33

From Table 4.5, the climatic warming appears terminated as the observed event frequency of group 3 is less than the expected frequency. The northern affinity group is larger than expected due to the numerous palynomorphs it contains.

EVENT NAME	#	SCORE	Well number 2	3	7	11	8	4	10	5	9	6	15	14	17	20	16	21
MOROZOVELLA AEQUA	162	469															X	X
MOROZOVELLA SPINULOSA	89	356												X				X
MOROZOVELLA ARAGONENSIS	159	309											X	X			X	X
ACARININA AFF. BROEDERMANNI	93	277											X	X				X
BULIMINA BRADBURYI	151	262											X				X	
GLOBIGERINA SENNI	226	262											X				X	
ACARININA DENSA	90	251										X	X	X			X	X
FORMA P EVITT	411	197								X							X	
PHELODINIUM MAGNIFICUM	520	197								X							X	
ADNATOSPHAERIDIUM RETICULENSE	329	164						X	X				X				X	X
OSANGULARIA EXPANSA	49	125					X						X				X	
GLAPHROCYSTA ORDINATA	418	122			X	X				X			X		X		X	X
HETERAULACACYSTA LEPTALEA	424	122	X												X		X	
ACARININA AFF. PENTACAMERATA	37	91					X					X					X	
NUTTALIDES TRUMPYI	164	84	X										X				X	
ALISOCYSTA ORNATA	343	83		X													X	
CORDOSPHAERIDIUM GRACILE	348	71	X	X		X					X		X		X		X	X
CORDOSPHAERIDIUM INODES	349	66		X				X							X		X	
PSEUDOHASTIGERINA WILCOXENSIS	36	37	X	X			X					X	X	X	X		X	
BULIMINA OVATA	230	32	X	X											X		X	
ACARININA INTERMEDIA WILCOXENSIS	96	9	X										X	X				
SIPHOGENERQIDES ELEGANTA	88	-3				X						X		X				
CIBICIDOIDES AFF. WESTI	44	-4	X				X										X	
SPIROPLECTAMMINA SPECTABILIS LCO	57	-8		X	X	X	X	X	X	X		X	X	X	X		X	
GLOBIGERINATHEKA KUGLERI	94	-14				X								X				
ADNATOSPHAERIDIUM VITTATUM	333	-43					X		X				X					
KLEITHRIASPHAERIDIUM LOFFRENSE	460	-43				X							X					
AREOSPHAERIDIUM DIKTYOPLOKUS	311	-58		X									X					
HYSTRICHOKOLPOMA CINCTUM TURGIDUM	432	-58		X									X					
BULIMINA TRIGONALIS	45	-82	X	X		X	X	X				X					X	
HOMOTRYBLIUM TENUISPINOSUM	427	-83	X	X	X			X					X		X			
HYSTRICHOSPHAERIDIUM TUBIFERUM	440	-83		X	X	X	X	X					X		X			
AREOLIGERA SENONENSIS	306	-109				X				X								
CERATIOPSIS DIEBELII	323	-122			X		X	X	X	X								
DEFLANDREA DENTICULATA	373	-122	X	X		X		X			X		X					
ACHILLEODINIUM BIFORMOIDES	317	-129	X	X									X					
AREOSPHAERIDIUM	309	-137		X	X	X	X						X					
OPERCULOPINIUM CF HIRSUTUM	500	-155	X		X							X						
RATONICYSTA URSULAE	397	-162	X	X	X	X							X					
PLATYCARYAPOLLENITES DA	286	-169	X					X	X									
APECTODINIUM HYPERACANTHUM	299	-188		X	X	X	X	X										
CERATIOPSIS DARTMOORIA	322	-193	X	X		X	X		X									
APECTODINIUM PARVUM	300	-195	X		X	X	X	X										
APECTODINIUM QUINQUELATUM	301	-209	X				X											
DEFLANDREA CF PHOSPHORITICA	378	-242	X		X													

Figure 4.5: First axis results of correspondence analysis for Zone III of RASC biozonation.

EVENT NAME	#	SCORE	Well number 2	3	7	11	8	4	10	5	9	6	15	14	17	20	16	21
CIBICIDOIDES TRUNCANUS	187	469															X	X
PALEOHYSTRICHOPHORA INFUSORIOIDES	509	193					X											X
LENTINIA WETZELII	472	178			X					X							X	X
POLYSPHAERIDIUM ZOHARYI	530	143				X									X		X	
LENTICULINA SUBPAPILLOSA	38	128					X										X	
ARKOLIGERA CORONATA	304	82		X	X			X			X				X		X	X
SAKLANDIA	539	73						X					X		X			
KISSELOVIA CRASSIRAMOSA	458	69					X						X		X			
SPIROPLECTAMMINA SPECTABILIS LO	68	66	X														X	
DRACODINIUM VARIELONGITUDUM (DR?)	396	55								X			X					
ANOMALINOIDES ACUTA	190	20				X		X									X	
DIPHYES COLLIGERUM	390	-20		X	X			X	X	X			X	X	X			
APECTODINIUM HOMOMORPHUM	298	-26		X	X	X		X	X	X		X	X					X
KISSELOVIA TENUIVIRGULA	459	-31						X	X	X			X					
GLADHROCYSTA PASTIELSII	419	-37	X			X				X			X	X				
CIBICIDOIDES BLANPIEDI	30	-51	X	X		X	X	X	X	X		X		X			X	
CIBICIDOIDES ALLENI	42	-52	X	X	X	X	X		X	X		X	X	X		X		
PALAEOCYSTODINIUM	505	-68		X			X			X			X					
PLECTOFRONDICULARIA AFF. PAUCICOSTATA	41	-72	X	X	X	X	X	X	X	X			X	X	X			
RPONIDES SP. 5	74	-75				X			X	X		X						
DEFLANDREA OBRISPELDENSIS	376	-84	X	X		X	X						X		X			
DEFLANDREA HYALINA	375	-99	X				X						X					
LEJEUNECYSTA HYALINA	467	-100	X				X		X				X					
LENTICULINA ULATISENSIS	75	-109				X				X								
TURRILINA ROBERTSI	86	-136	X	X		X	X	X						X				
CERATIOPSIS WARDENENSIS	328	-136		X	X		X	X	X			X						
SPIROPLECTAMMINA DENTATA	35	-137			X	X	X	X				X						
DEFLANDREA SP. B	380	-140					X	X										
WILSONIDIUM ECHINOSUTURATUM	599	-141	X	X		X	X		X				X					
SCHIZOCYSTIA RUGOSA	540	-147				X	X		X									
AZOLLA	314	-169	X	X	X		X	X		X								
COMASPHAERIDIUM COMETES	344	-178				X	X											
ALABAMINA WILCOXENSIS	39	-209	X				X											
UVIGERINA BATJESI	53	-214	X	X				X										
NODOSARIA CF. POZOENSIS	63	-254	X	X														

Figure 4.6: First axis results of correspondence analysis for Zone IV of RASC biozonation. DR indicates reworking.

Biozone V

Foraminifer to palynomorph ratio: 7 to 11

Event score group ratio: 5 : 13 : 1

Average event score: -67

This zone reflect "equitable" climatic conditions with many wide ranging species and fewer events restricted to the southern wells.

Biozone VI

Foraminifer to palynomorph ratio: 9 to 15

Event score group ratio: 4 : 17 : 4

Average event score: -10

Group 2 events dominate this zone probably indicating uniformity in environmental conditions.

EVENT NAME	#	SCORE	Well number																	
			2	3	7	11	8	4	10	5	9	6	15	14	17	20	16	21		
GLOBIGERINA YEGUAENSIS	84	213										X	X	X				X		
EOCLADOPYXIS PENICULATA (DR)	403	63	X					X	X				X		X			X		
KARRERIELLA CONVERSA	264	23	X	X				X		X				X	X		X			
MARGINULINA DECORATA	34	3	X	X	X	X	X	X	X	X		X		X	X		X	X		
AMMOSPHAEROIDINA SP. 1	32	0		X	X	X	X	X		X		X	X	X	X		X			
WETZELIELLA ARTICULATA	591	-18	X	X	X		X		X	X				X	X		X			
CYCLAMMINA AMPLECTENS	29	-28	X	X	X	X	X	X	X	X		X	X	X	X		X			
ARENOLIGERA SENONENSIS	307	-33				X		X	X		X	X			X					
HAPLOPHRAGMOIDES WALTERI	261	-43	X		X	X	X	X		X		X	X	X	X					
WETZELIELLA SYMMETRICA	594	-53					X	X					X							
IMPLETOSPHAERIDIUM SCALENFURCATUM	447	-63		X	X		X	X					X		X					
DAPSILIDINIUM SIMPLEX	372	-77	X	X	X	X		X					X				X			
IMPAGIDINIUM VICTORIANUM	446	-95		X		X	X				X		X							
HETERAULACACYSTA CAMPANULA	423	-100			X	X							X							
CYCLONEPHELIUM VANNOPHORUM	363	-132	X		X	X	X							X						
PTERODINIUM CINGULATUM	533	-179	X			X		X	X											
SPONGODINIUM DELITIENSE (DR?)	560	-185		X				X												
KRISTOMINA SP. 5	118	-206	X	X	X				X											
ANOMALINA SP. 1	173	-232	X	X	X	X														

FIGURE 4.7: First axis results of correspondence analysis for Zone V of RASC biozonation. DR indicates reworking.

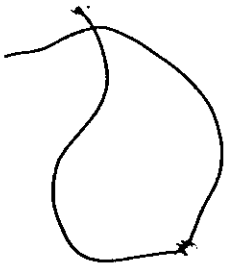

EVENT NAME	#	SCORE	Well number 2	3	7	11	8	4	10	5	9	6	15	14	17	20	16	21
CATAPSYDRAX AFF. DISSIMILIS	147	469															X	X
GLOBIGERINA LINAPERTA	82	352												X		X	X	X
GLOBIGERINA VENEZUELANA	81	228				X								X	X		X	X
ACHOMOSPHAERA ALCICORNU	318	149							X				X	X			X	
METZELIELLA OVALIS	593	76				X	X	X	X	X			X		X		X	X
TURBOROTALIA POMEROLI	33	75				X	X					X		X				X
THALASSIPHORA PELAGICA	578	71					X	X	X					X	X		X	
BULIMINA ALAZANENSIS	40	64					X	X				X		X			X	
AMMODISCUS LATUS	259	57			X		X	X				X	X	X	X		X	
GLAPHROCYSTA EXUBERANS	416	34			X	X		X	X				X	X	X		X	
THALASSIPHORA DELICATA	576	2	X	X							X		X				X	
AMMOBACULITES AFF. POLYTHALAMUS	263	-2		X	X		X	X	X					X	X		X	
TUBIDERMODINIUM SULCATUM	587	-13				X	X			X			X	X				
HAPLOPHRAGMOIDES KIRKI	260	-58	X	X	X	X	X		X			X			X		X	
HOMOTRYBLIUM ACULEATUM	426	-58		X									X					
WILSONIDIUM INTERMEDIUM	600	-58		X									X					
DEFLANDREA EOCENICA	374	-78				X	X						X					
PSEUDOHASTIGERINA MICRA	85	-96			X	X		X	X					X				
ROTTNESTIA BORUSSICA	537	-97			X							X						
CRIBROPERIDINIUM GIUSEPPEI	487	-98		X	X	X	X		X	X					X			
LINGULODINIUM DC	479	-99	X				X						X					
POLYSTEPHANOPHORUS	531	-137		X	X	X	X						X					
THALASSIPHORA PATULA	577	-140	X	X		X			X				X					
GLAPHROCYSTA DIVARICATA	415	-174		X	X	X	X	X	X									
RPONIDES POLYGONUS	206	-239	X			X												

Figure 4.8: First axis results of correspondence analysis for Zone VI of RASC biozonation.

Biozone VII

Foraminifer to palynomorph ratio: 4 to 19

Event score group ratio: 5 : 13 : 5

Average event score:

Observed and expected values are almost identical in this zone. This zone marks the onset of shallowing as indicated by the presence of the Coarse arenaceous spp., a paleoecologic shallowing marker event.

Biozone VIII

Foraminifer to palynomorph ratio: 4 to 36

Event score group ratio: 8 : 25 : 8

Average event score: 14

Palynomorphs largely dominate this zone. From the expected versus observed frequency values of Table 4.5, it can be concluded that the zone displays average behaviour of latitude related trends.

EVENT NAME	#	SCORE	Well number															
			2	3	7	11	8	4	10	5	9	6	15	14	17	20	16	21
PHTHANOPERIDINIUM LEVIMURUM	527	163					X								X		X	
PHTHANOPERIDINIUM ALECTROLOPHUM	523	152					X						X		X		X	
CHIROPTERIDIUM PARTISPINATUM	340	135						X									X	
SPINIDINIUM SVERDRUPIANUM	545	123				X							X	X			X	
KISSELOVIA COLEOTHRYPTA (REWORKED)	457	119			X						X		X	X	X		X	
DINOPTERIGIUM CLADOIDES SENSU MORG.	388	114	X									X	X	X	X		X	
TURRILINA ALSATICA	24	77			X		X		X	X		X	X	X	X	X	X	
EPONIDES UMBONATUS	27	73		X		X	X							X	X	X	X	
GLAPHROCYSTA INTRICATA	417	66		X				X							X		X	
RHOMBOIDINIUM	535	55								X			X					
NODOSARIA CF. ELEGANTISSIMA	69	53	X		X	X			X	X						X	X	X
CYCLONEPHELIUM SP. C	365	20		X									X	X				
SPINIFERITES MEMBRANACEUS	547	10		X				X									X	
LENTINIA SERRATA	471	3			X		X	X		X			X				X	
SYSTEMATOPHORA AREOLATA	570	-15	X				X						X		X			
COARSE ARENACEOUS SPP.	25	-28	X	X	X	X	X	X	X	X		X	X	X	X		X	
XENIKOON	315	-42							X			X						
CYCLONEPHELIUM SP. B	364	-43				X							X					
SURCULOSPHAERIDIUM LONGIFURCATUM	566	-109				X				X								
CORRUDINIUM INCOMPOSITUM	554	-121				X	X			X								
METZELIELLA DA	596	-181			X		X											
PISTILLIPOLLENITES MCGREGORII	284	-182	X	X	X	X						X						
LENTINIA	470	-201	X	X	X		X	X										

Figure 4.9: First axis results of correspondence analysis for Zone VII of RASC biozonation.

EVENT NAME	#	SCORE	Well number																
			2	3	7	11	8	4	10	5	9	6	15	14	17	20	16	21	
ARROSPHAERIDIUM ARCUATUM	310	294											X	X	X		X	X	
ISABELIDINIUM COOKSONIAE (DR)	452	272												X	X		X		
UVIGERINA EX.GR.MIOZRA-NUTTALI	26	231					X						X	X	X	X	X	X	
PALAEOPERIDINIUM CRETACEUM	511	197								X							X		
PENTADINIUM LATICINCTUM	517	188									X		X		X		X		
SYSTEMATOPHORA PLACACANTHA	571	137							X	X			X	X	X		X		
MEMBRANOPHORIDIUM ASPINATUM	485	134					X					X	X	X	X		X		
ACHOMOSPHAERA CRASSIPELUS	319	132						X		X			X	X	X		X		
HYSTRICHOKOLPOMA CINCTUM (DR)	431	110		X			X	X					X		X		X	X	
DISTATODINIUM PARADOXUM	391	105				X				X					X		X		
PHTHANOPERIDINIUM MICROSPINATUM	528	98										X		X					
GYROIDINA GIRARDANA	20	90				X	X	X	X	X	X	X	X	X	X	X	X	X	
DIACROCANTHIDIUM	383	69										X	X						
METZELIELLA LUNARIS (DR)	592	65							X						X				
LEJEUNECYSTA TENELLA	469	64									X	X		X					
CYCLONEPHELIUM MEMBRANIPHORUM	361	55								X			X						
GLOBIGERINA PRAEBULLOIDES	15	52		X	X	X	X	X	X	X		X	X	X	X	X	X	X	
OLIGOSPHAERIDIUM ASTERIGERUM	496	37							X					X					
CYCLONEPHELIUM DY	367	35							X	X	X		X	X					
DEFLANDREA PHOSPHORITICA	377	35	X	X		X		X		X		X	X	X	X	X	X		
AREOSPHAERIDIUM PECTINIFORME (DR)	312	29			X	X	X	X					X	X	X		X		
GUTTULINA PROBLEMA	21	11		X	X	X			X	X	X	X		X		X	X		
CYCLONEPHELIUM DISTINCTUM	358	1	X	X						X			X				X		
ACHOMOSPHAERA RAMULIFERA	325	-1		X											X				
OLIGOSPHAERIDIUM COMPLEX (DR)	497	-3					X				X	X	X						
PHTHANOPERIDINIUM	522	-16		X	X		X		X	X	X	X	X	X	X				
OVOIDINIUM VERRUCOSUM	504	-53					X	X					X						
HYSTRICHOSPHAERIDIUM DIFFICILE	435	-58		X									X						
AREOLIGERA SEMICIRCULATA	305	-64					X					X							
IMPLETOSPHAERIDIUM TRANSFODUM	448	-64			X	X	X	X	X	X			X	X					
ALABAMINA SCITULA	70	-72			X	X		X	X	X					X				
PHTHANOPERIDINIUM ECHINATUM	526	-84			X	X	X	X				X		X					
POLYSPHAERIDIUM	529	-95				X	X		X	X	X								
ALTERBIA (DR)	345	-128	X		X		X						X						
CHATANGIELLA VNIGRI (DR)	337	-140					X	X											
HOMOTRYBLIUM	425	-140					X	X											
ODONTOCHITINA COSTATA (DR)	493	-168			X	X	X		X										
CUPANIEIDITES DA	281	-190			X	X	X												
NYASSAPOLLENITES DB	295	-190	X			X	X	X											
SEQUOIAPOLLENITES DA	290	-193																	
NYSSAPOLLENITES DA	294	-202	X	X	X	X	X	X											

Figure 4.10: First axis results of correspondence analysis for Zone VIII of RASC biozonation. DR indicates reworking.

Biozone IX

Foraminifer to palynomorph ratio: 5 to 22

Event score group ratio: 5 : 18 : 4

Average event score: 1

This zone shows a uniform latitude gradient in its fauna and flora. The correlation between the observed and expected frequency of events (see Table 4.5) in each geographic group testifies to the uniformity of this zone.

Biozone X

Foraminifer to palynomorph ratio: 5 to 22

Event score group ratio: 2 : 13 : 6

Average event score: 29

Several pieces of evidence support the postulated onset of the Labrador current at the beginning of this zone. First, low and mid-latitude planktonic foraminifera are absent from Labrador Shelf wells, presumably because of low salinity associated with the Labrador current. Furthermore, several dinoflagellate warm temperate species show local tops in this zone, such as **Hystrichokolpoma rigaudae**, **Lingulodinium machaerophorum** and **Operculodinium israelianum**. These

EVENT NAME	#	SCORE	Well number 2	3	7	11	8	4	10	5	9	6	15	14	17	20	16	21
SPINIFERITES MONILIS	549	262											X				X	
CYCLOGYRA INVOLVENS	181	156				X			X								X	X
EPISTOMINA ELEGANS	71	151						X		X			X		X	X	X	
PALEOCYSTODINIUM GOLZOWENSE	508	130					X				X		X	X	X		X	
ISABELIDINIUM ACUMINATUM (DR)	449	114									X				X			
ELLIPSOIDICTYUM	399	86									X			X				
DEFLANDREA SPINULOSA (DR)	379	81				X	X			X			X	X	X		X	
CHIROPTERIDIUM MESPILANUM (DR?)	338	64	X		X		X	X		X		X	X	X	X		X	X
CORDOSPHAERIDIUM CANTHARELLUM	346	57			X		X		X	X			X	X	X		X	
TANYOSPHAERIDIUM DA	575	50					X						X	X				
SPIROPLECTAMMINA CARINATA	18	-48		X	X	X	X	X	X	X	X	X	X	X	X	X	X	X
DAPSILIDINIUM PASTIELSII	371	31			X		X	X	X	X	X	X	X	X	X		X	
PARALECANIELLA INDENTATA	515	10	X		X	X							X		X		X	
CYCLOPSIELLA VIETA	369	-8	X				X			X				X		X		
LEPTODINIUM	474	-1			X	X			X		X		X				X	
SVALBARDELLA	568	-6						X					X					
PHTHANOPERIDINIUM COMATUM (DR)	525	-22			X	X	X	X			X		X	X	Y			
HOROLOGINELLA	428	-55			X		X					X	X					
SPINIDINIUM ECHINOIDEUM (DR?)	543	-56							X	X								
CHATANGIELLA TRIPARTITA (DR)	335	-60			X		X		X	X	X		X					
PHTHANOPERIDINIUM AMOENUM (DR?)	524	-81			X	X								X				
CORDOSPHAERIDIUM FIBROSPINOSUM (DR?)	347	-96		X	X			X	X	X			X					
CIBICIDOIDES GROSSA	270	-138	X								X							
SCAPHOPOD SP. 1	67	-148	X	X	X	X		X	X	X	X							
POLYPODIACIDITES DA	288	-154	X	X			X	X				X						
LACINIADINIUM	461	-192		X			X											
SEQUOIAPOLLENITES	289	-209	X				X											

Figure 4.11: First axis results of correspondence analysis for Zone IX of RASC biozonation. DR indicates reworking.

EVENT NAME	#	SCORE	Well number 2	3	7	11	8	4	10	5	9	6	15	14	17	20	16	21
SPHAEROIDINA BULLOIDES	117	262											X				X	
NEMATOSPHAEROPSIS BALCOMBIANA	492	211										X					X	
ISABELIDINIUM BELFASTENSE (DR)	451	180										X	X	X			X	
UVIGERINA PEREGRINA	78	135						X									X	
SPINIFERITES SCABRATUS	554	131					X					X	X					X
ASTERIGERINA GURICHI (PEAK)	265	124										X	X		X			
PERISSEIASPHAERIDIUM	518	84								X				X				
BOMBACACIDITES DA	279	71	X	X	X		X				X	X		X	X	X	X	X
ODONTOCHITINA OPERCULATA (DR)	494	68					X		X				X				X	
OPERCULOPINIUM ISRAELIANUM	502	60		X			X			X			X		X		X	
CERATOBULIMINA CONTRARIA	16	48		X	X	X	X	X	X	X	X	X	X	X	X	X	X	X
CHIROPTERIDIUM LOBOSPINOSUM (DR)	339	32		X				X	X						X		X	
LINGULODINIUM MACHAERROPHORUM	478	28	X	X	X	X	X	X	X	X	X	X	X	X	X	X	X	X
HYSTRICHOKOLPOMA RIGAUDIAE	433	-5	X	X	X		X	X		X	X	X	X	X	X		X	
PODOCARPIDITES DA	287	-56	X	X		X	X	X	X	X	X	X		X		X		
TILIAEPOLLENITES	291	-74			X	X	X					X		X				
OVOIDINIUM	503	-81						X	X		X							
TILIAEPOLLENITES DA	292	-87			X	X			X	X	X	X						
XENIKOON DA	316	-98	X	X	X	X		X	X	X	X	X		X				
HYSTRICHOSPHAERIDIUM	434	-202	X					X										
CHLAMYDOPHORELLA NYEI	342	-218	X	X			X											

Figure 4.12: First axis results of correspondence analysis for Zone X of RASC biozonation. DR indicates reworking.

premature extinctions are also associated with the decreased salinity due to the current.

The event score group ratio shows more species than expected in the geographically wide ranging second group and in the third group. In the first group fewer events than expected are observed. The decreased frequency in the first group can be explained by the current sweeping the fossils southwards. Unlike the situation in the Eocene, more species were not brought into the study area as the current came from an area of low diversity. The increase in the frequency of the second group is a direct result of the decrease in group 1. Finally, group 3 displays higher than expected diversity as all species requiring higher salinity were restricted to southern wells.

Biozone XI

Foraminifer to palynomorph ratio: 9 to 16

Event score group ratio: 3 : 14 : 8

Average event score: 48

Again, planktonic foraminifera are restricted to southern wells due to the low salinity on the Labrador Shelf brought on by the Labrador current . Moreover, few species are found

EVENT NAME	#	SCORE	Well number															
			2	3	7	11	8	4	10	5	9	6	15	14	17	20	16	21
NONIONELLA PIZARRENSE	11	262											X				X	
CASSIDULINA CURVATA	109	262											X				X	
ASTERIGERINA GURICHI	17	181					X				X	X	X	X	X	X	X	X
DICONODINIUM	384	177											X		X			
SUMATRADINIUM	565	173						X					X					X
PURSENKOINA GRACILIS	9	152					X						X		X		X	
CASSIDULINA SP.	76	149											X	X				
SPINIDINIUM CF VESTITUM	546	135						X									X	
UVIGERINA CANARIENSIS	10	100					X		X			X	X	X	X		X	
SPINIFERITES PSEUDOFURCATUS (DR)	552	74	X					X		X			X	X	X		X	
APTEODINIUM SPIRIDOIDES (DR)	303	64							X				X	X				
CANNOSPHAEROPSIS DA	320	64							X				X	X				
OPERCULODINIUM CENTROCARPUM	501	64	X		X		X	X		X		X	X	X	X		X	X
PINUS	283	30	X	X	X	X	X	X	X		X	X	X	X	X	X	X	X
SYSTEMATOPHORA ANCYREA (DR)	569	28	X		X	X	X	X	X	X	X	X	X	X	X		X	X
NEOGLOBOQUADRINA PACHYDERMA	1	-13					X						X					
TSUGAEPOLLENITES INGNICULUS	293	-13	X	X	X	X	X	X	X	X	X	X	X	X		X		X
CHENOPODIUMSPORITES DA	280	-21				X		X	X			X	X	X				
OSMUNDACIDITES DA	282	-36	X	X	X	X	X	X	X	X	X	X	X	X				X
ELPHIDIUM SPP.	77	-42		X					X		X			X				
OSMUNDACIDITES	296	-95	X	X	X		X						X	X				
CASSIDULINA TERETIS	228	-99	X	X					X		X		X					
CHATANGIELLA (DR)	330	-109		X		X	X	X						X				
CORDOSPHAERIDIUM MULTISPINOSUM	350	-122			X		X				X							
ABIES	276	-150	X	X	X	X	X	X			X	X						

Figure 4.13: First axis results of correspondence analysis for Zone XI of RASC biozonation. DR indicates reworked species.

only on the shelf area because of the current. Sampling problems were experienced in southern wells as can be observed from the absence of **Cassidulina teretis** from many southern sections. This species is usually a good regional marker.

Proportionally to other groups, more species than expected occur in the high scoring southern wells, in spite of the sampling problem that was experienced. The environment was probably more favourable to most species in these wells because they are not influenced by the Labrador current.

4.8 Conclusion

(4a) The use of correspondence analysis to complement RASC provides a powerful tool to characterize paleoenvironmental gradients in the biostratigraphic record.

(4b) The onset and decline of paleoceanographic currents differentiated the wells into two groups and imparted gradients in the well scores of both groups.

(4c) The events scores were divided in three groups reflecting either a northern or southern affinity, or a widespread distribution.

(4d) The postulated onset of the Labrador current early in Zone X time is supported by the event scores resulting from correspondence analysis.

5. Frequency Distribution of Biostratigraphic Events

5.1 Introduction

The RASC model assumes that all events display a normal distribution with equal variances. This study attempts to verify these hypotheses and to modify the RASC model accordingly.

Individual well sequences are compared to the scaled optimum sequence using spline fitting techniques to obtain estimates of the variance of the events. The frequency distributions of events can be computed by collecting the differences between the known (observed) RASC event positions and their spline (expected) values.

The variance estimates can be used in a modified RASC routine that does not assume equal variances for all events. The frequency distributions can further be used to study the positions of events in individual wells relative to their average position. This measure is useful in tracing the time transgressiveness of events and to identify good marker events.

5.2 Methodology

The scaling assumptions of the RASC model are listed in section 3.2.3. To recapitulate, it is stipulated that each event has a Gaussian distribution along the RASC scale with a mean position value of EX_{event} and a variance of σ^2. The variances of all events are assumed to be equal, and are given an arbitrary value as they cannot be estimated at the same time as the interevent distances. The interdependence of the variances and of the computation of the RASC scaled optimum sequence prohibits the measurement of the frequency distributions $f(x_{event})$ within RASC.

This study is based on the methodology developed by Agterberg and D'Iorio (1988) in the study of the frequency distribution of foraminiferal events in the Gradstein-Thomas database (cf. Gradstein et al., 1985).

5.2.1 Frequency distribution model

Frequency distributions can be estimated by comparing observed and expected relative positions of events in sequences where the RASC event distances are the observed data

points. To estimate the expected RASC distances of all occurrences of each event, the well sequences are individually plotted against the scaled optimum sequence and spline-fitted. The expected RASC position of an event in a well will be approximated by the spline-curve value corresponding to its level in that well. Once the differences between observed and expected values are calculated, the frequency distributions can be estimated and the RASC assumptions verified.

5.2.2 Spline-fitting technique

A spline-curve of the n^{th} degree is a piece-wise polynomial expressing y as a function of x, whose first (n-1) derivatives are continuous. The abscissae in which the pieces join to form the curve are called knots.

There are two types of spline-curves, ordinary splines and smoothing splines. They differ in that the latter curve does not go through data points and its shape is controlled by the sum of squares of the residuals, as measured in the direction of the axis of the dependent variable. Both types of splines can be solved by the same type of mathematical equations. Smoothing splines are better suited to most

geological applications where data points do not represent error-free measures.

Cubic splines are used in this application because splines of the third degree are computationally simple and have sufficient flexibility for most purposes (Wold, 1974). The following discussion is based on Reinsch (1967, 1971).

Spline functions are fitted to points x_i and y_i, $i = 0, 1, \ldots, n$, assuming that $x_0<x_1<x_2<\ldots<x_n$. This function can be described as:

$$y_i = g(x_i) + e_i \qquad \text{(Eq. 5.1)}$$

where e_i is an error term of known standard deviation σ_i.

A cubic smoothing spline can be fitted with $e_i = 0$ at one or more tie points (Agterberg, 1988); the following condition can thereby be stipulated:

$$y_i = g(x_i) = a_i + b_i(x - x_i) + c_i(x - x_i)^2 + d_i(x - x_i)^3 \qquad \text{(Eq. 5.2)}$$

and

$$g(x_i)_- - g(x_i)_+ = 0 \quad (i = 2,\ldots, n-1) \qquad \text{(Eq. 5.3)}$$

further,

$$g'''(x_i)_- - g'''(x_i)_+ = 2p\frac{e_i}{\sigma_i} \quad (i = 1,\ldots, n) \qquad \text{(Eq. 5.4)}$$

where p is a parameter to be determined later.

Reinsch (1967) expressed the solution of a cubic spline as minimizing:

$$\int_{-\infty}^{\infty} \{g''(x)^2\, dx\} \qquad \text{(Eq. 5.5)}$$

such that:

$$\sum_{i=0}^{n} \left[\frac{g(x_i) - y_i}{\sigma_i} \right]^2 \leq S \qquad \text{(Eq. 5.6)}$$

where S is a constant.

The previously mentioned Lagrangian parameter, p, can be introduced for minimization:

$$\int_{-\infty}^{\infty} \{g''(x)^2\, dx\} + p \left[\sum_{i=1}^{n} \left[\frac{g(x_i) - y_i}{\sigma_i} \right]^2 + z^2 - S \right] \qquad \text{(Eq. 5.7)}$$

where z is an auxiliary variable.

From the Euler-Lagrangian equations it follows that the optimal function f(x) obeys:

$$f'''(x) = 0 \quad x_i < x \leq x_{i+1} \quad (i = 1, \ldots, n-1) \qquad \text{(Eq. 5.8)}$$

The following Reinsch (1967) abbreviations are adopted to simplify the notation:

C: column vector with elements c_i, $i = 2, \ldots, n-1$.

Y: column vector of elements y_i, $i = 1, \ldots, n$.

T: positive definite tridiagonal matrix of order n-2, containing elements $t_{i,i} = 2(h_{i-1} + h_i) / 3$, $t_{i,i-1} = t_{i+1,i} = h_i / 3$, where $h_i = x_{i+1} - x_i$.

Q: tridiagonal matrix with n rows and (n-2) columns containing elements $q_{i-1,i} = 1 / h_{i-1}$, $q_{i,i} = -(1 / h_{i-1}) - (1 / h_i)$, and $q_{i+1,i} = 1 / h_{i+1}$.

A: column vector with n elements a_i.

D: diagonal matrix of order n with $d_{i,i} = \sigma_i$.

The continuity of the first derivative can now be expressed as:

$$T\ C = Q'\ A \qquad \text{(Eq. 5.9)}$$

and the condition of the third derivative becomes:

$$Q\ C = p\ D^{-2}\ (Y - A) \qquad \text{(Eq. 5.10)}$$

From Equations 5.9 and 5.10, it follows that:

$$C = p\ (Q'\ D^2\ Q + p\ T)^{-1}\ Q''\ Y \qquad \text{(Eq. 5.11)}$$

and:

$$A = Y - p^{-1} D^2 Q C \qquad \text{(Eq. 5.12)}$$

To solve for p, Equation 5.7 is minimized with respect to z and p, leading to:

$$p z = 0 \qquad \text{(Eq. 5.13)}$$

Equation 5.7 now becomes:

$$\sum_{i=0}^{n} \left[\frac{g(x_i) - y_i}{\sigma_i}\right]^2 = S - z^2 \qquad \text{(Eq. 5.14)}$$

From Equations 5.11 and 5.12 it follows that:

$$S - z^2 = D Q (D' D^2 Q)^{-1} Q' Y \qquad \text{(Eq. 5.15)}$$

From Equation 5.13 it can be deduced that either $p = 0$ or $z = 0$. As the right-hand side of Equation 5.15 is non-negative, $p \neq 0$ only if $S \geq \sigma^2$ reducing the cubic spline to a best fitting straight line. This least-square fitting line is defined by:

$$a_i = (1 - D^2 Q (D' D^2 Q)^{-1}) y_i \qquad \text{(Eq. 5.16)}$$

$$b_i = (a_{i+1} - a_i) / (x_{i+1} - x_i) \qquad \text{(Eq. 5.17)}$$

$$c_i = d_i = 0 \qquad \text{(Eq. 5.18)}$$

If $z = 0$, the parameter p is obtained by solving Equation 5.14 that now becomes:

$$S = D\,Q\,(Q'\,D^2\,Q + p\,T)^{-1}\,Q'\,Y \qquad \text{(Eq. 5.19)}$$

The solution to Equation 5.19 is solved algorithmically by Reinsch (1967, 1971). The computer algorithms used to solve equations of spline-curves are published by De Boor (1978).

Spline fitting can be applied to plots of relative levels of events in wells against their RASC distances from the top of the scaled optimum sequence. The data points become the knots of the spline-curve. If two or more events were to occur at the same level (coeval events), they are replaced by a point whose coordinates are that level and the average RASC distance of these coeval events.

A smoothing factor (SF) is determined as being the square root of the mean squared deviation of the RASC values, at the knots, from their respective spline values.

5.3 Preliminary results

The 23 well data set was analysed to estimate frequency distributions for separate events. The scaled optimum sequence presented in Chapter 3 was used as the starting point in this study. The "unique" events included in Figure 3.5

were removed from the scaled optimum sequence so as not to bias the results with events that do not occur in at least the threshold number of wells.

A preliminary step is to obtain the spline (expected) values for the events positions for all events in all wells. Spline fitting is carried out according to De Boor's (1978) algorithms, by a FORTRAN 77 programme named SPLIN. For the purposes of this study, the levels of events in the well sequences are used as independent variables and their RASC positions measured from the top of the scaled optimum sequence are used as dependent variables. In order to have a smoothing factor that is representative of the standard deviation of the residuals, coeval events were separated by $1/1000^{th}$ of a unit, and no averaging of values for coeval events was carried out.

Twenty-three input files were prepared for SPLIN, one for each well. Each file contains the dictionary numbers of the events occuring in that well, their RASC positions in the scaled optimum sequence, their respective levels and depths in the well and weights. The average SPLIN weight and the smoothing factor are inversely proportional. In this preliminary step, weights of 1.0 are set with a smoothing factor value of SF = 0.7071 (or $1/\sqrt{2}$). This SF value was chosen because it corresponds to the fixed value of the standard deviation of events as assigned by the RASC model.

It is noted that identical results would be obtained by using weights of 0.7071 and smoothing factor SF = 1.0.

The SPLIN programme returns an output file containing the level of the event in the well and its expected position in the RASC scaled optimum sequence according to the specified smoothing factor.

5.3.1 Statistical behaviour of data

To collect the deviations between observed and expected RASC positions, the 23 input and output files must be compared and reorganized to regroup individual events and to measure their means, standard deviations, and other statistics, and to prepare histograms of their distribution. A BASIC programme named MODULES was prepared to manipulate all files and to compute the pertinant statistics. It is listed in Appendix B (pages 318 to 325). Also listed in this appendix is GRAPHTOT (pages 326 to 331), a routine that uses the MODULES output files to plot histograms of the frequency distributions of events and to graph the geographical position of the deviations from expected positions on a North-South axis. The user may select to view, print and/or save the plots that are produced.

Table 5.1 lists the results of this first measure of the frequency distributions. Two variances are listed; the first corresponds to the computed unbiased variance whereas the second value calculates the unbiased variance if the mean was zero. The term unbiased indicates that the sums of squared deviations were divided by degrees of freedom f_i. The second variance is the most important because a basic premise of RASC is the normality of event distribution. The unbiased variances using a mean of 0 are the ones retained for further discussion and application.

A pooled variance of all species, s^2, can be calculated as follows:

$$s^2 = \frac{\sum_{i=1}^{k} f_i \, s^2_i}{\sum_{i=1}^{k} f_i} \qquad \text{(Eq.5.20)}$$

where: $f_i = n_i - 1$,

n_i is the number of occurrences of event i,

s^2_i is the variance of event i.

The s^2 value is 0.474 for the 85 events in the preliminary step of frequency distribution analysis. This measure was approximately as expected because RASC assigns a variance of $\sigma^2 = 0.5$ to all events. The closeness of these

Table 5.1: Preliminary frequency distribution of RASC events. Events are referred to by their dictionary number as listed in Appendix A. F_i is the number of wells in which the event is identified, σ^2 is the variance and (0 mean) indicates that the mean was assumed to be 0. The value σ is used as weight in the following run of RASC.

Event number	RASC distance	Mean	F_i	σ^2	σ^2 (0 mean)	σ weight
283	0.000	-1.055	15	0.120	1.313	1.146
293	0.201	-0.909	14	0.105	0.995	0.997
77	0.357	-0.802	8	0.152	0.887	0.942
228	0.502	-0.837	7	0.210	1.026	1.013
10	0.991	-0.653	11	0.119	0.589	0.767
276	1.118	-0.154	8	0.500	0.527	0.726
569	1.369	-0.333	14	0.226	0.346	0.588
17	1.404	-0.375	13	0.155	0.307	0.554
501	1.484	-0.283	11	0.198	0.285	0.534
552	1.498	-0.265	7	0.127	0.208	0.457
282	1.552	-0.275	13	0.311	0.393	0.627
316	1.866	-0.312	10	0.335	0.443	0.666
433	1.902	-0.253	12	0.402	0.473	0.6[illegible]
16	1.905	-0.290	20	0.203	0.292	0.5[illegible]0
478	2.010	-0.172	16	0.622	0.654	0.808
279	2.028	-0.067	11	0.473	0.478	0.691
287	2.082	-0.145	11	0.330	0.353	0.594
67	2.339	-0.061	8	0.123	0.128	0.357
71	2.387	-0.305	11	0.437	0.539	0.734
338	2.526	-0.104	11	0.280	0.292	0.540
18	2.530	-0.011	20	0.216	0.216	0.465
379	2.559	0.072	7	0.705	0.711	0.843
346	2.638	0.033	8	0.367	0.368	0.607
525	2.713	0.041	8	0.621	0.623	0.789
371	2.733	0.083	11	0.477	0.484	0.696
431	2.894	-0.226	7	1.253	1.313	1.146
21	2.897	0.181	11	0.157	0.193	0.439
522	2.951	0.056	10	0.316	0.319	0.565
20	2.980	0.208	18	0.165	0.210	0.459
70	3.081	0.183	8	0.112	0.150	0.387
15	3.089	0.187	20	0.271	0.308	0.555
26	3.187	0.255	12	0.249	0.320	0.566
448	3.228	0.028	8	1.044	1.045	1.022
312	3.385	0.044	8	1.563	1.566	1.251
377	3.432	0.007	11	1.045	1.045	1.022
24	3.626	0.153	14	0.154	0.180	0.424
25	3.694	0.149	19	0.283	0.306	0.553
69	3.721	0.072	11	0.430	0.436	0.660
27	3.785	0.031	10	0.405	0.406	0.637
259	3.973	0.139	14	0.082	0.103	0.321
81	4.035	0.087	10	0.321	0.329	0.574
416	4.079	-0.042	8	1.639	1.641	1.281
593	4.085	-0.109	9	0.954	0.967	0.983
487	4.223	-0.046	7	0.791	0.793	0.891

continued...

Event number	RASC distance	Mean	F_i	σ^2	σ^2 (0 mean)	σ weight
33	4.223	-0.034	7	0.724	0.725	0.852
260	4.226	-0.051	14	0.169	0.171	0.414
34	4.237	-0.253	14	0.244	0.313	0.560
591	4.259	-0.084	9	0.318	0.326	0.571
82	4.323	0.014	7	0.092	0.092	0.303
261	4.408	-0.009	15	0.158	0.158	0.397
263	4.529	0.011	13	0.313	0.313	0.560
84	4.755	0.048	7	0.093	0.096	0.310
372	4.770	0.428	7	0.809	1.023	1.011
32	4.888	0.069	17	0.226	0.231	0.480
264	4.931	0.222	9	0.274	0.329	0.574
40	4.938	0.118	7	0.307	0.323	0.569
85	4.950	0.212	8	0.620	0.671	0.819
390	4.951	0.195	8	0.662	0.705	0.840
29	5.005	0.292	19	0.213	0.303	0.551
298	5.082	-0.124	9	0.485	0.502	0.708
42	5.100	0.108	13	0.463	0.476	0.690
30	5.103	0.047	12	0.258	0.261	0.511
41	5.183	0.211	13	0.537	0.585	0.765
68	5.222	0.351	7	0.180	0.323	0.569
304	5.284	0.413	7	1.334	1.532	1.238
348	5.310	0.211	8	1.313	1.364	1.168
57	5.329	-0.052	17	0.367	0.370	0.608
86	5.338	0.169	8	0.164	0.197	0.444
90	5.424	-0.033	9	0.200	0.201	0.449
36	5.514	0.017	11	0.289	0.289	0.538
45	5.560	-0.083	8	0.720	0.728	0.853
418	5.693	0.193	7	0.282	0.326	0.571
440	5.698	0.157	7	0.604	0.633	0.795
93	5.824	0.085	7	0.152	0.161	0.401
37	5.829	0.063	7	0.207	0.211	0.460
297	6.194	0.353	14	0.532	0.666	0.816
393	6.243	0.407	7	0.193	0.386	0.622
50	6.253	0.292	11	0.133	0.226	0.476
326	6.299	0.329	9	0.442	0.563	0.750
54	6.389	0.188	14	0.424	0.461	0.679
52	6.422	0.422	7	0.237	0.445	0.667
56	6.949	0.472	15	0.127	0.366	0.605
512	7.176	0.626	9	0.322	0.762	0.873
55	7.339	0.452	9	0.090	0.320	0.566
59	7.781	0.789	7	0.159	0.885	0.941

two values (0.474 and 0.5) indicates that the frequency distribution estimation method is a good one.

5.3.2 Test for equality of the variances of events

From Table 5.1, it can be observed that the variances of events differ significantly from one another. This can be statistically verified by the Bartlett chi-squared test for equality of variances. Bartlett has shown that the chi-squared value may be estimated as follows (cf. Hald, 1952, p.291):

$$(\text{chi})^2 = -(1/c) \sum_{i=1}^{k} \ln (s^2_i/s^2) \qquad \text{(Eq. 5.21)}$$

where:

$$c = 1 + \frac{1}{3\,(k-1)} + \left(\sum_{i=1}^{k} \frac{1}{f_i} - \frac{1}{f} \right), \qquad \text{(Eq. 5.22)}$$

The chi-squared measure obtained for the data set was 158.5 which exceeds the 99% confidence level of 117.1 for 84 degrees of freedom. This test confirms inequality of the variances s^2_i.

5.3.3 Test for normality of event distribution

One of the first assumptions in the RASC scaling procedure is normality of event distributions. The calculation of z-values is based on this condition. Because it is established that the variances are inequal, all collected deviations between expected and observed positions can be divided by the corresponding standard deviation of their events in order to standardize all values for comparison.

It is not possible to test the normality of the distribution of individual events because of the low frequency of each event. However, it is possible to test the normality of all events as a whole by plotting the 913 standardized deviations in one composite histogram (see Figure 5.1). This figure is approximately symmetrical. Thirteen classes are plotted, each representing intervals of 0.4. To test the normality of this distribution, expected frequencies were calculated for each class using $\sigma = 1.0$. The ensuing chi-squared estimate is equal to 11.63. This value is less than the 90% and 99% confidence intervals chi-squared values of 15.99 and 23.21, respectively, for 10 degrees of freedom. It may, therefore, be concluded that the standardized deviations have approximately a Gaussian distribution.

Figure 5.1: Composite histogram of the standardized deviations of events. For the chi-squared test, each interval ranged 0.4 units except for the first one which amalgamated two classes: a first ranging from -3.0 to -2.6 containing 1 event and a second ranging from -2.6 to -2.2 containing 4 events.

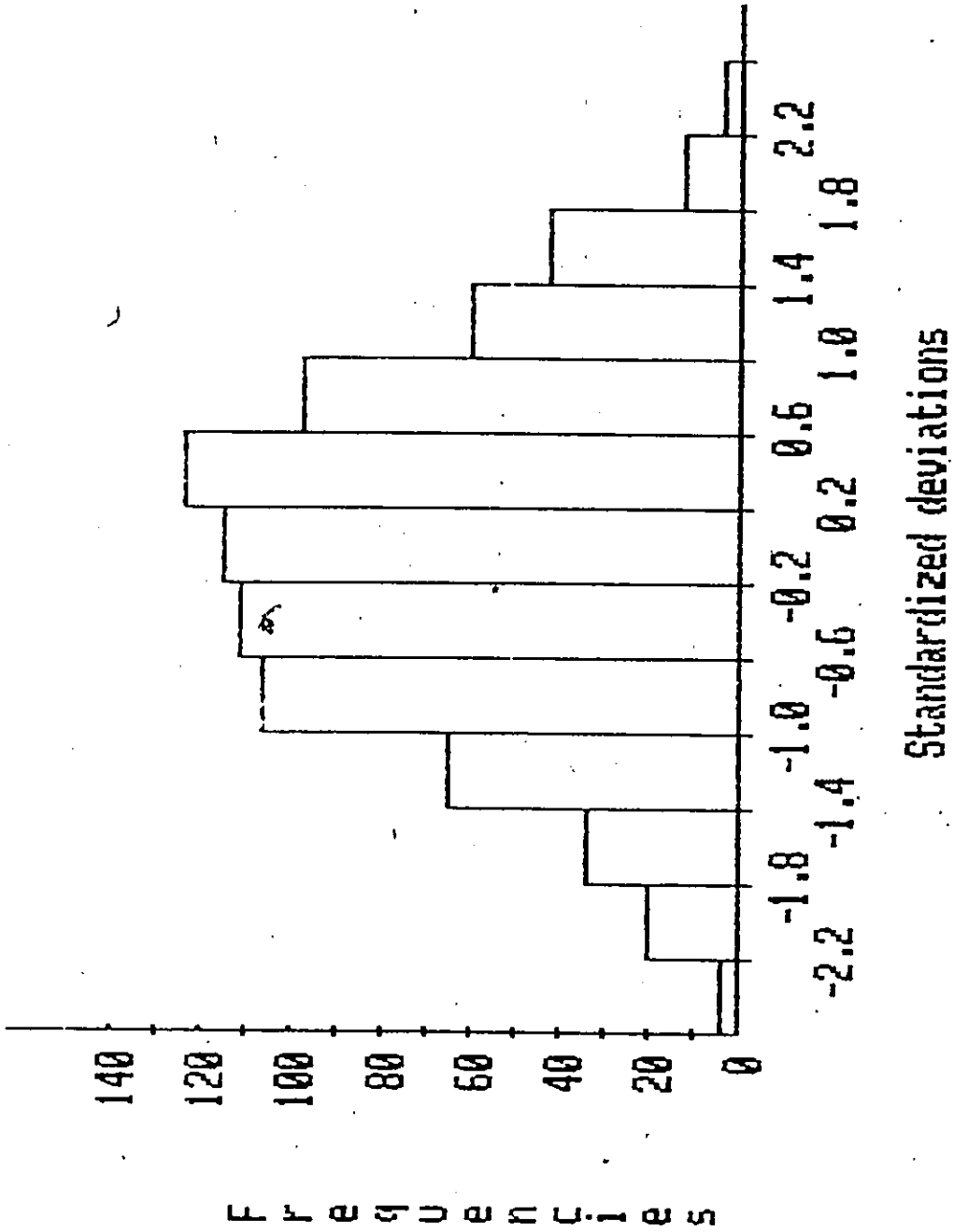
Frequencies
0
20
40
60
80
100
120
140
-2.2
-1.8
-1.4
-1.0
-0.6
-0.2
0.2
0.6
1.0
1.4
1.8
2.2
Standardized deviations

5.4 Calibration of the RASC model

The preceding results suggest that a refinement can be applied to the RASC model. The assumption of equal variances for all events can now be modified as estimates of separate event standard deviations are available.

5.4.1 Refined probit estimates

The scaling process in RASC is based on interevent "distance" estimates (see section 3.2.3) which depend on probit values of event crossover frequencies.

The probability of event A occurring above event B (or $P(D_{AB} > 0)$) is assumed to be equal to the relative frequency of event A occurring above event B. This probability can also be expressed as:

$$P(D_{AB} > 0) = \frac{1}{\sqrt{(2\pi)}} \int_{\delta AB/\sigma\sqrt{2}}^{\infty} e^{-z^2/2} \, dz \qquad \text{(Eq. 5.23)}$$

where: δ_{AB} is the mean interval between events A and B (see section 3.2.3), and

$\sigma\sqrt{2}$ represents the standard deviation of the random variable D_{AB}.

In the RASC model, σ was set equal to an arbitrary value because it was not possible to estimate both σ and δ_{AB} from the same equation. To simplify Equation 5.23, σ was assigned a value of $1/\sqrt{2}$.

The refinement of the RASC model is based on using estimates of variances of D_{AB} based on the measured variances of events A and B where:

$$\sigma^2(D_{AB}) = \sigma^2_A + \sigma^2_B \qquad \text{(Eq. 5.24)}$$

where: σ^2_X is the measured unbiased variance of event X, based on a mean of 0, as estimated in the frequency distribution calculations.

In the new RASC model, Equation 5.23 becomes:

$$P\ (D_{AB} > 0) = \frac{1}{\sqrt{(2\pi)}} \int_{\delta_{AB}/\sqrt{(\sigma^2_A + \sigma^2_B)}}^{\infty} e^{-z^2/2}\, dz \qquad \text{(Eq. 5.25)}$$

The main RASC routine and four subroutines were changed to accommodate this new model of different event variances. The modified routines are listed in Appendix B (pages 333 to 360). The previously mentioned changes in the RASC model resulted in the calculation of new z-values with:

$$z'_{AB} = z_{AB} * \sqrt{(\sigma^2_A + \sigma^2_B)} \qquad \text{(Eq. 5.26)}$$

with all other conditions remaining the same as in the original RASC model.

The final reordering option of RASC is not used in modified RASC to better evaluate the effects of variable event standard deviations. Modified RASC requires an extra input file in 2I6 format containing event numbers and their respective standard deviations multiplied by 10000, a procedure adopted to simplify the programming.

5.4.2 Iterative RASC procedure

After the first step of modified RASC, new frequency distributions were obtained and new estimates of standard deviations of events were used as input for the next run of modified RASC. In the second and subsequent applications of spline fitting, the weights that were previously set equal to one, were assigned the values of the standard deviations of the corresponding events. To compensate for this change, the smoothing factor was increased to SF = 1.0. Because of the inverse proportionality of SF and average weights, the overall result was not affected by these changes.

The iterative procedure of applying RASC and recalculating frequency distributions was continued until the standard deviations were converging. The fourth set of frequency distributions was retained as the refined solution. The decision to retain the fourth solution was based on observed stabilization of the s^2 value and length of the scaled optimum sequence. An equally rapid convergence was obtained by Agterberg and D'Iorio (1988).

5.5 Refined frequency distributions

One effect of using the separate standard deviations of events is the shrinking of the size of the scaled optimum sequence from 7.781 RASC units in the initial run to 6.753 RASC units after the final iteration. This decrease in length of the scaled optimum sequence is linked with a similar decrease in the standard deviations. The pooled variance values, s^2, are: 0.474, 0.406, 0.383, and 0.375 for the first to final iterations, respectively. The length of the RASC sequence decreased by 13.2% whereas the standard deviations diminished 11.1%, on average, between the initial and final estimates.

5.5.1 Behaviour of data set

The results of the final estimates of frequency distributions are listed in Table 5.2 and plotted in Appendix C. The variances remain significantly different as supported by a chi-squared measure of 316, as calculated by Equation 5.21. As previously mentioned, the corresponding 99% confidence limit is 117.1 for 84 degrees of freedom.

The average deviation from mean position for each event is plotted against its respective RASC distance (see Figure 5.2). This plot indicates clear departures from the mean position at the top and bottom of the sequence. These differences were not affected by the modified RASC iteration and are probably the result of spline fitting underestimating values near the top of the sequence and overestimating them near the bottom. This tendency is accentuated by the sampling problems experienced in some wells for the Late Miocene and Paleocene sections (see Chapters 3 and 4). The RASC distance estimates are less accurate as fewer events are present in these zones. Furthermore, the RASC model may overestimate interevent distances at the extremities of the sequence because there are fewer comparisons to be made with adjacent events of other zones (i.e.; events at the top can only be compared to older ones and events at the bottom can only be

Table 5.2: Events, RASC distances and statistics after three runs of the refined RASC. Events are referred to by their dictionary number as listed in Appendix A. F_i represents the number of occurrences of the events whereas σ^2 is the variance based on the measured value of the mean and σ^2 is the variance based on a mean of 0. Both the skewness and the kurtosis are calculated using a mean of 0.

EVENT	RASC dist.	MEAN	F_1	σ^2_1	σ^2_2 (0 mean)	SKEWNESS	KURTOSIS
283	0.000	-0.970	15	0.078	1.086	-1.233	-1.911
77	0.229	-0.834	8	0.084	0.878	-1.396	-2.139
293	0.298	-0.711	14	0.077	0.621	-1.318	-1.664
228	0.380	-0.698	7	0.079	0.646	-1.478	-2.144
10	0.854	-0.523	11	0.080	0.380	-1.555	-0.860
276	0.924	-0.270	8	0.383	0.466	-2.741	6.537
17	1.247	-0.255	13	0.059	0.129	-1.909	0.938
569	1.264	-0.129	14	0.076	0.094	-1.199	-1.075
552	1.283	-0.134	7	0.075	0.096	-0.856	-2.255
501	1.379	-0.098	11	0.143	0.154	-1.413	0.006
282	1.391	-0.099	13	0.114	0.124	-1.070	0.597
316	1.548	-0.233	10	0.200	0.261	-1.688	0.108
433	1.605	-0.118	12	0.382	0.397	-1.477	0.258
16	1.617	-0.201	20	0.173	0.215	-1.321	0.100
279	1.660	-0.011	11	0.240	0.240	0.027	-0.478
287	1.688	-0.091	11	0.160	0.169	-1.287	0.586
478	1.722	-0.096	16	0.472	0.482	-0.482	-1.374
379	1.799	-0.141	7	0.402	0.426	-0.972	-1.165
67	1.847	-0.157	8	0.070	0.099	-1.925	1.062
71	1.937	-0.236	11	0.343	0.405	-1.363	-0.164
18	1.970	-0.135	20	0.181	0.200	-0.994	-0.174
338	1.986	-0.101	11	0.333	0.345	-1.693	3.241
346	2.018	-0.060	8	0.320	0.325	-0.977	0.243
525	2.046	-0.004	8	0.615	0.615	-0.400	-1.397
371	2.081	-0.057	11	0.347	0.351	-1.172	1.015
21	2.153	-0.032	11	0.040	0.041	-0.550	-0.369
20	2.249	-0.050	18	0.098	0.100	-0.811	0.922
522	2.285	-0.062	10	0.362	0.366	-0.279	-1.251
431	2.296	-0.304	7	1.740	1.848	-1.908	3.515
15	2.344	-0.126	20	0.231	0.248	-1.208	0.830
70	2.355	-0.065	8	0.040	0.045	-2.025	2.449
448	2.508	-0.100	8	0.828	0.839	-0.741	-1.483
26	2.602	0.151	12	0.206	0.231	1.597	0.860
312	2.705	-0.014	8	1.371	1.371	-1.302	0.104
377	2.970	0.151	11	0.793	0.818	0.529	-1.499
69	3.110	0.041	11	0.370	0.372	-0.457	-1.558
24	3.113	0.224	14	0.052	0.106	1.550	-0.211
25	3.137	0.178	19	0.123	0.156	1.462	0.062
27	3.338	0.223	10	0.344	0.399	0.964	-0.412
259	3.441	0.174	14	0.062	0.095	1.483	-0.656
416	3.578	0.081	8	1.913	1.920	-0.493	-0.081
82	3.593	-0.081	7	0.050	0.057	-2.129	3.329
81	3.612	0.223	10	0.274	0.330	1.508	0.200
487	3.614	-0.020	7	0.749	0.749	0.074	-0.485
84	3.635	-0.351	7	0.019	0.163	-1.477	-2.146

continued...

EVENT	RASC dist.	MEAN	Fi	σ^2_1	σ^2_2 (0 mean)	SKEWNESS	KURTOSIS
261	3.645	-0.070	15	0.045	0.050	-1.137	0.050
34	3.658	-0.128	14	0.179	0.196	-0.834	-0.746
593	3.675	0.148	9	1.050	1.075	0.911	0.486
591	3.741	0.164	9	0.447	0.477	0.806	-0.948
33	3.768	0.055	7	0.531	0.535	0.703	-1.419
40	3.829	-0.185	7	0.236	0.276	-0.845	-1.681
263	3.840	0.041	13	0.163	0.165	0.268	-1.003
372	3.850	0.162	7	0.825	0.855	0.877	-0.921
85	3.888	-0.056	8	0.424	0.428	0.279	-1.266
390	3.894	-0.045	8	0.662	0.664	-0.389	-1.879
260	3.898	0.246	14	0.083	0.148	1.514	-0.745
29	3.910	-0.050	19	0.102	0.105	-0.847	0.259
68	4.057	-0.008	7	0.054	0.054	1.261	1.37
32	4.063	0.008	17	0.081	0.081	0.345	-0.256
264	4.097	0.099	9	0.134	0.145	1.414	-0.448
42	4.164	0.018	13	0.502	0.502	0.073	-0.198
30	4.216	-0.035	12	0.149	0.150	-0.384	-0.521
41	4.277	0.070	13	0.332	0.337	1.982	4.456
298	4.335	-0.095	9	0.356	0.366	-0.310	-1.361
86	4.509	0.093	8	0.122	0.132	0.993	-0.282
90	4.554	0.017	9	0.053	0.053	1.585	2.379
36	4.637	0.031	11	0.159	0.160	1.342	1.114
304	4.639	0.447	7	1.477	1.711	2.344	4.138
45	4.721	0.065	8	0.676	0.681	0.310	-1.408
57	4.744	0.243	17	0.259	0.322	1.297	0.357
440	4.778	0.094	7	0.324	0.335	1.110	-0.139
37	4.829	0.082	7	0.091	0.099	2.571	6.302
348	4.859	0.535	8	1.648	1.975	2.769	6.286
93	4.972	0.110	7	0.011	0.025	1.809	-0.556
418	5.002	0.255	7	0.144	0.220	2.400	3.954
297	5.057	0.189	14	0.239	0.277	0.610	0.014
50	5.082	0.109	11	0.035	0.048	1.508	-0.087
393	5.186	0.279	7	0.092	0.183	1.760	-0.670
52	5.360	0.382	7	0.071	0.241	1.517	-1.951
326	5.383	0.434	9	0.337	0.549	2.608	5.627
54	5.526	0.335	14	0.319	0.439	1.445	-0.075
56	5.845	0.477	15	0.106	0.350	1.495	-0.998
512	6.082	0.592	9	0.296	0.690	1.830	0.308
55	6.190	0.487	9	0.074	0.341	1.515	-1.394
59	6.753	0.950	7	0.148	1.201	1.526	-1.841

Figure 5.2: Plot of the average event deviation against the RASC distance of the corresponding event. The squares represent palynomorph events while the circles represent foraminifers. Systematic deviations from zero are exhibited at either end of the scale. In the middle portion of the RASC sequence, palynomorphs seem to have average values closer to zero than the foraminifers.

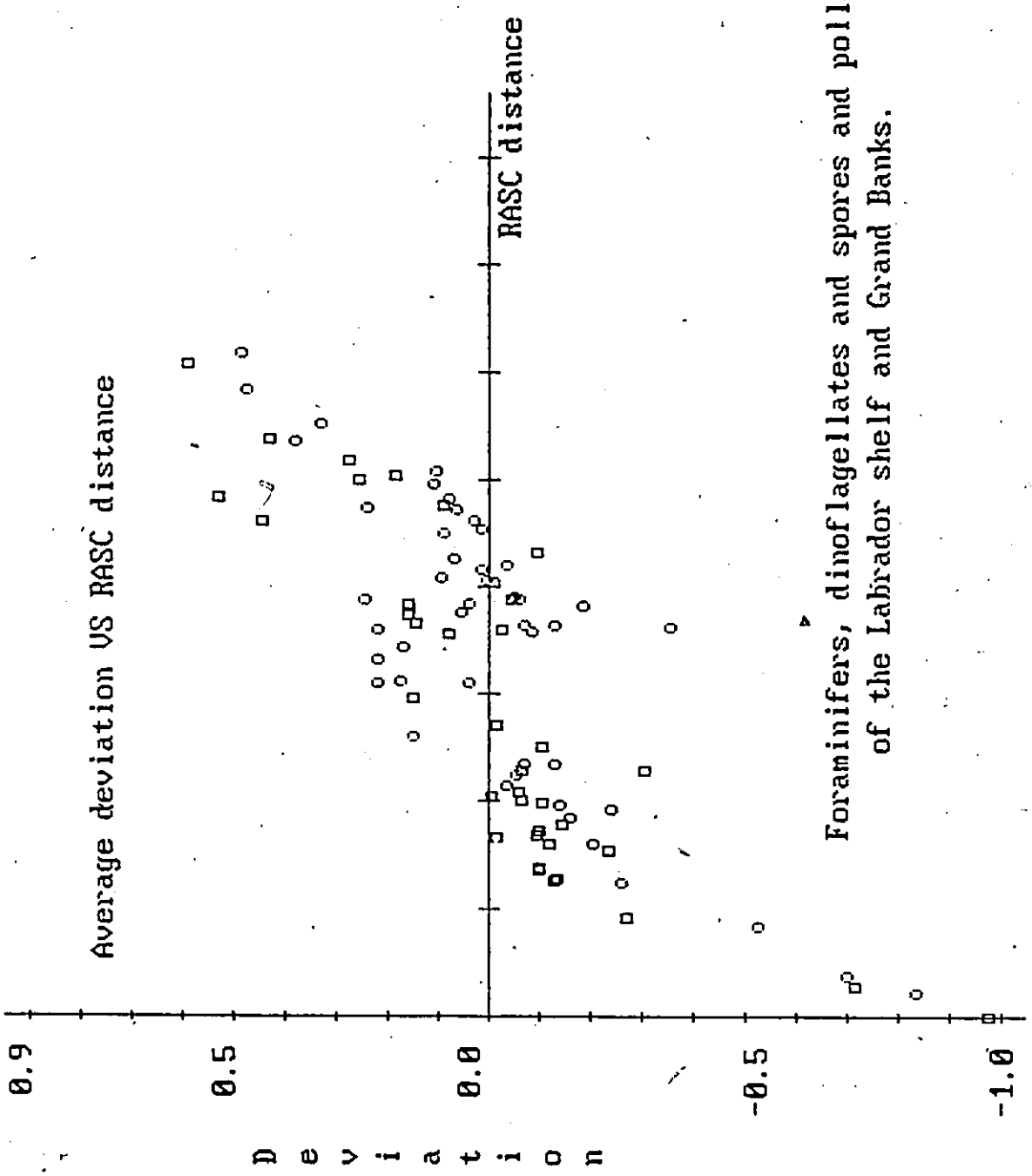

Foraminifers, dinoflagellates and spores and pollen of the Labrador shelf and Grand Banks.

compared to younger ones). The measures of skewness included in Table 5.2 also reflect the observed trend of deviation at either end of the sequence. Large negative and positive skewness values are observed at the top and bottom of the sequence, respectively.

Notwithstanding the systematic departure at both ends of the sequence, Figure 5.2 shows a pattern in average deviations from RASC distances 1 to 5, that could be interpreted as periodicity. This pattern is also apparent in the study by Agterberg and D'Iorio (1988). It can be postulated that positive deviations represent environmentally favourable periods whereas negative deviations represent early extinctions probably the result of environmental changes. A positive average deviation indicates that the RASC position is greater (older) than the expected position in the wells. This implies that the event is, on average, younger than the RASC position indicates (i.e.; the species survived longer). The converse is true for negative distances.

The first and last five events in the sequence are ignored in the following discussion as they are attributed to the previously mentioned systematic departure. Tracing the mean deviations from the bottom of the sequence, large positive deviations are observed from 4.86 to 5.53 RASC units. This approximately corresponds to the Early Eocene warming period (see Chapter 4) that presumably provided favourable

environmental conditions. The ensuing drop in mean deviations correlates with the change in paleocirculation pattern that occurred in the early Middle Eocene which caused the disappearance of tropical and low latitude species from the Grand Banks wells where they had migrated. G. yeguaensis exemplifies this drop in mean deviations (see Figure 5.3 (a) and (b)). This species is restricted to southern wells (Figure 5.3 (a)) and is typically a low-latitude species (F.M. Gradstein, pers. comm. 1988). The stability of the Middle and Late Eocene environments provides a reasonable explanation for the positive deviations observed from RASC distances 4.0 to 2.5. All younger events exhibit negative deviations. The succession of the Oligocene eustatic sea-level drop and the onset of the Labrador current in the Miocene provide probable causes for these slightly negative values. It must be noted that Figure 5.2 amplifies the vertical scale five-fold to show these deviations.

5.5.2 Marker events identification

Table 3.5 lists the events most likely to be used as chronological markers in this study. Their frequency and geographical distributions are plotted before those of other events in Appendix C from page 361 to 405.

Figure 5.3 (a): Geographical distribution of the deviations between observed and expected positions of event G. yeguaensis. All occurrences of this species are below their RASC position.

Figure 5.3 (b): Histogram of the frequency distribution of event G. yeguaensis.

EVENT NUMBER 84 :GLOBIGERINA YEGUAENSIS

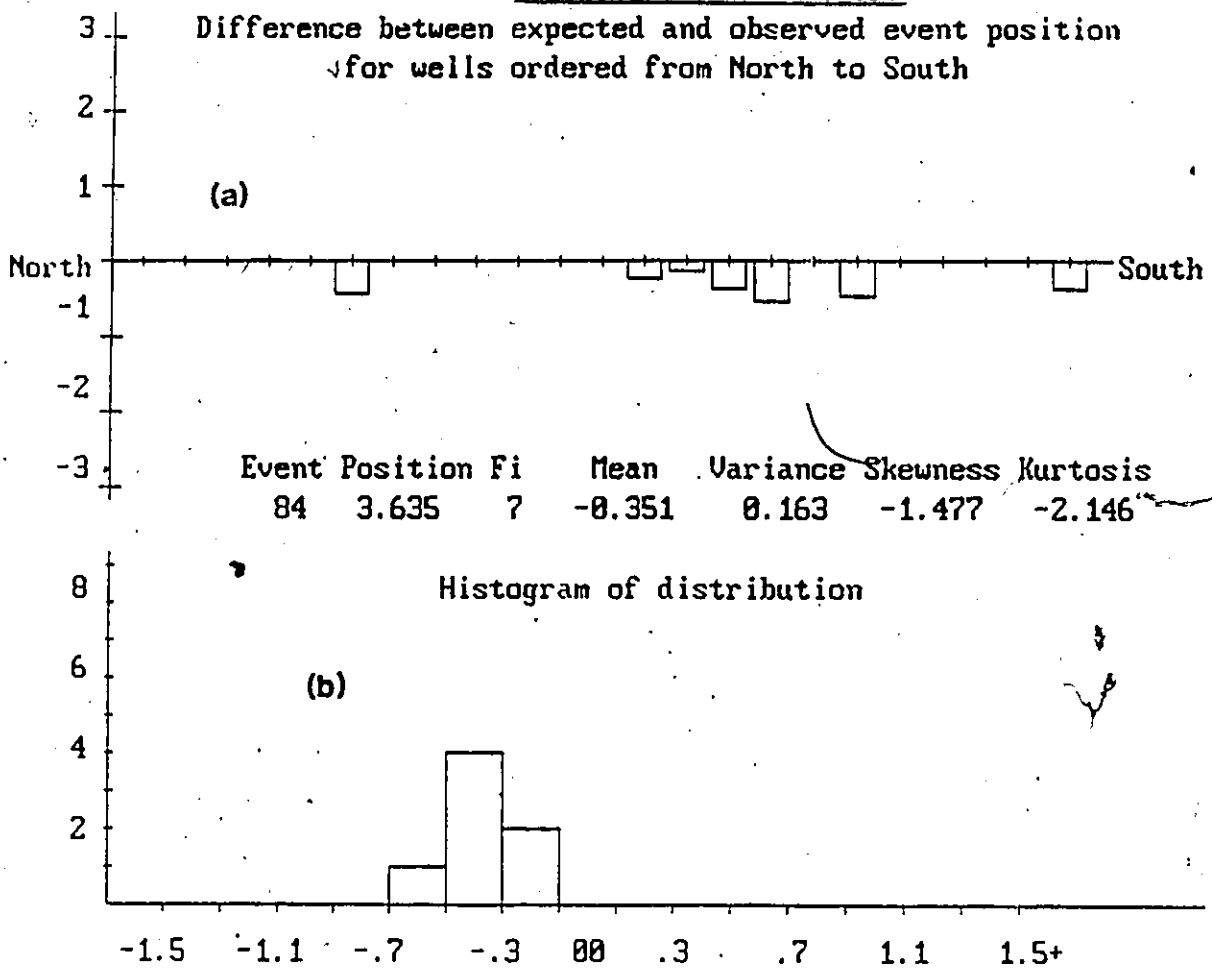

An ideal marker event has a wide horizontal (geographic) and narrow vertical (chronological) distribution. Figure 5.4 illustrates the distribution of event #24 **T. alsatica** which has a broad geographic extent as it was identified in 14 wells; it is also a good marker event because it deviates little from its average position, as indicated by its low variance ($\sigma^2 = 0.103$).

Events dated from 37 to 41 Ma exhibit a scattered frequency distribution. Events 82, 29 and 259 are the notable exceptions to this pattern. The anomalous events are: #390 **D. colligerum**, #487 **C. giuseppei**, #33 **T. pomeroli**, #85 **P. micra**, #591 **W. articulata**, and #298 **A. homomorphum**. Their variances range from $\sigma^2 = 0.428$ to 0.749. It is remarkable that the occurrences of these events in the Herjolf (4th), Bjarni (5th) and Gudrid (6th) wells all show positive deviations, suggesting possible reworking. It also must be noted that the ages of the events approximately correspond to the postulated sea-level drop of the Early Oligocene. Some areas (wells) were probably affected before, and to a greater extent than others, by the environmental changes, causing variations in the relative position of events. Because of these variations, the anomalous events will not be used for chronostratigraphic purposes. All other events listed in Table 3.5 are retained as markers as supported by their respective frequency distributions.

Figure 5.4 (a): Geographical distribution of the deviations between observed and expected positions of event T. alsatica. It has a broad geographic extent as it was identified in 14 wells throughout the study area.

Figure 5.4 (b): Histogram of the frequency distribution of event T. alsatica. The shape of the histogram indicates a normal distribution. The low variance makes this event a good marker.

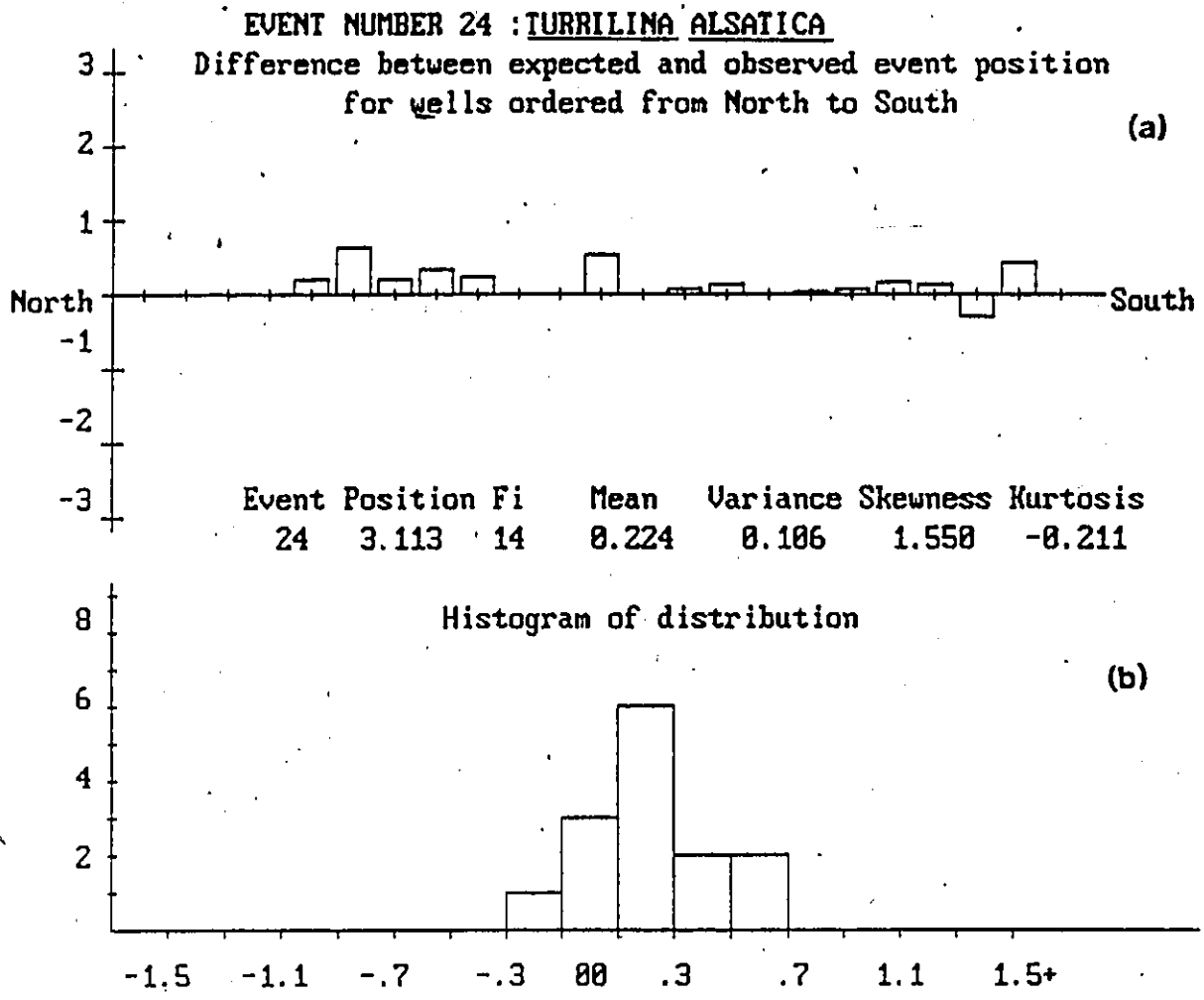
EVENT NUMBER 24 : TURRILINA ALSATICA
Difference between expected and observed event position
for wells ordered from North to South
(a)
3
2
1
North
-1
-2
-3
South
Event Position Fi Mean Variance Skewness Kurtosis
24 3.113 14 0.224 0.106 1.550 -0.211
Histogram of distribution
(b)
8
6
4
2
-1.5 -1.1 -.7 -.3 00 .3 .7 1.1 1.5+

5.5.3 Paleogeographic event migration

This brief section provides an example of new results that can be obtained by frequency distribution analysis. By examining the geographic deviation distribution diagram of each event in Appendix C, latitude-related time-transgressiveness can be detected. Figure 5.5 shows the geographic distribution of deviations of events #264 K. conversa, #41 P. aff. paucicostata and #316 Xenikoon DA. On average, K. conversa disappears sooner in the northern wells and survives longer in southern wells (see Figure 5.5 (a)). This trend is more likely to be related to the greater water depth of southern wells and to the earlier "shallowing" of northern ones (Gradstein, pers. comm., 1988). Conversely, P. aff. paucicostata seemingly survives longer in the north than in the south (see Figure 5.5 (b)). The event Xenikoon DA exhibits a southerly, upward, vertical migration (the species survives longer in the south) especially from wells number 2 (Karlsefni) to 6 (Gudrid) (Figure 5.5 (c)).

Occurrences of the events indicating these types of trends could be reviewed by paleontologists to verify their positions. As they presently occur, these events are probably not reliable and should be avoided in further analysis.

Figure 5.5 (a): Geographic distribution of the deviations between observed and expected position of event #264 K. conversa.

Figure 5.5 (b): Geographic distribution of the deviations between observed and expected position of event #41 P. aff. paucicostata.

Figure 5.5 (c): Geographic distribution of the deviations between observed and expected position of event #316 Xenikoon DA.

(a)

EVENT NUMBER 264 :KARRERIELLA CONVERSA

Difference between expected and observed event position
for wells ordered from North to South

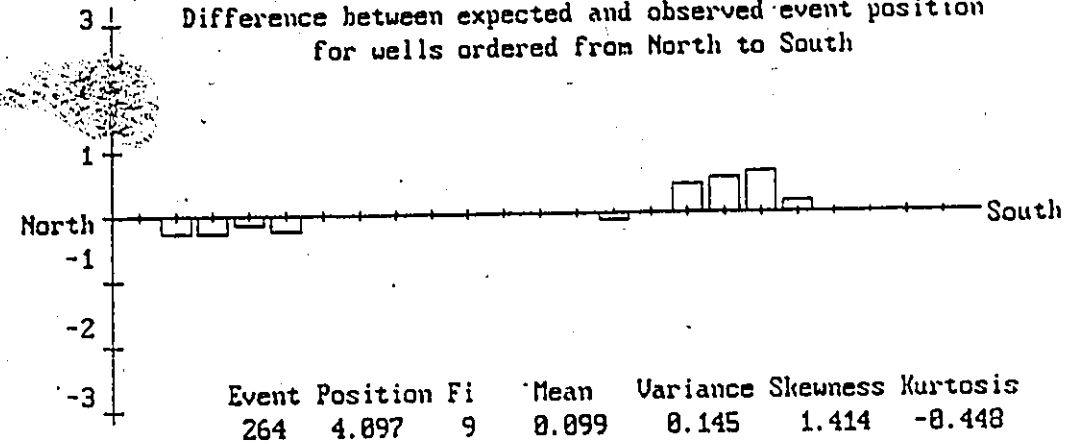

Event	Position	Fi	Mean	Variance	Skewness	Kurtosis
264	4.897	9	0.899	0.145	1.414	-0.448

(b)

EVENT NUMBER 41 :PLECTOFRONDICULARIA AFF. PAUCICOSTATA

Difference between expected and observed event position
for wells ordered from North to South

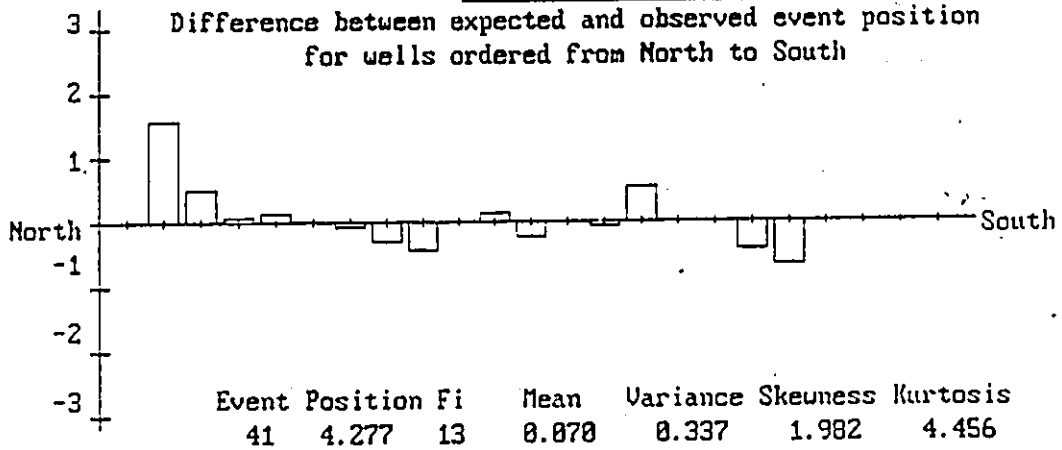

Event	Position	Fi	Mean	Variance	Skewness	Kurtosis
41	4.277	13	0.870	0.337	1.982	4.456

(c)

EVENT NUMBER 316 :XENIKOON DA

Difference between expected and observed event position
for wells ordered from North to South

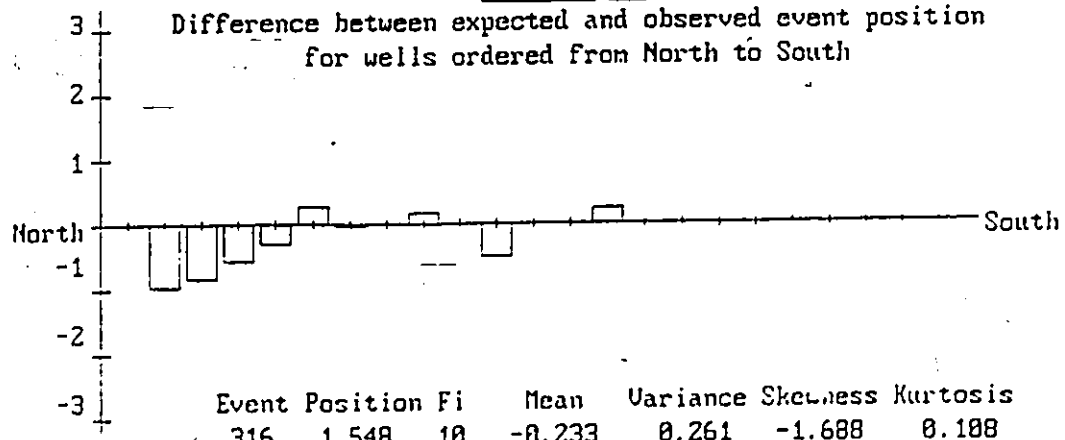

Event	Position	Fi	Mean	Variance	Skewness	Kurtosis
316	1.548	10	-0.233	0.261	-1.688	0.108

5.6 Conclusions

(5a) Because it provides a pooled variance of $\sigma^2 = 0.47$, the frequency distribution estimate method is reliable.

(5b) Based on frequency distribution estimates, events do not have equal variances.

(5c) Using a composite histogram of standardized deviations, the events, as a group, obey a Gaussian distribution according to a chi-squared estimate of 11.63 for 10 degrees of freedom.

(5d) The iterative RASC/frequency distribution estimate procedure converges the values of variances after four cycles.

(5e) Most marker events previously used for chronostratigraphic purposes exhibit a narrow vertical distribution, as confirmed by their frequency distribution histograms.

(5f) Most marker events ranging from 37 to 41 Ma show scattered distributions, possibly due to a major change in environment.

(5g) Frequency distribution results can be used to trace vertical migration of biostratigraphic events.

6. Study of the sensitivity of the RASC model to the critical probit value

6.1 Introduction

The RASC model requires the user to select the value of some parameters. One such parameter is the critical probit value (AAA). The z-value is set equal to this parameter when two events do not crossover. Changing this critical value affects the results of RASC. The nature and magnitude of this effect can be evaluated by a series of RASC runs in which the critical probit value is progressively changed.

6.2 Role of the critical probit value in RASC

The scaling procedure of the RASC model is described in detail in section 3.2.3. To recapitulate, the distance estimates between adjacent events are based on the probability of having consistent relative event positions in the wells. These probabilities are assumed to be equal to the observed frequencies of event position crossovers. The z-values of the probabilities are measured by assuming events have a Gaussian

distribution and by assigning a value to their variance. When an event always occurs above another, the estimated probability becomes $P_{ij} = 1$ and $z_{ij} = \infty$. When this situation occurs, the values of P (and z) are set at a critical value (termed AAA) selected by the user. This situation occurs usually in the indirect distance estimates, when the position of events from different parts of the sequence are compared. The chosen critical value should exceed the largest P_{ij} value that is smaller than 1.

To estimate the effects of the variation of the AAA parameter on the RASC sequence, a series of runs was carried out in which this parameter was gradually increased.

Trial values of the AAA parameter are tested on the data set used to produce Figure 3.5, with all other parameters kept constant. The test values of AAA and their corresponding probabilities are listed in Table 6.1. The lengths of the respective final optimum sequences are also listed in this table.

AAA value	Corresponding probability	Length of the optimum sequence (without final reordering)	Length of the optimum sequence (with final reordering)
1.645	0.95	7.193	7.781
1.75	0.96	7.425	7.336
1.88	0.97	7.730	7.797
1.96	0.975	7.927	9.156
2.06	0.98	8.182	8.718
2.17	0.985	8.473	9.475
2.33	0.99	8.913	9.597
2.575	0.995	9.619	12.351

Table 6.1: List of the AAA value tested in the RASC model on the integrated data set.

6.3 Sensitivity of the scaled optimum sequence

6.3.1 Effects on the length of the scaled sequence

The effects of the probit parameter change with the final reordering option of RASC (see section 3.2). Before the final reordering, the length of the scaled optimum sequence is directly proportional to the probit critical value (see Figure 6.1).

In the final reordering option, a new set of distance estimates are calculated with z-values based on the new sequence of events. The new results of scaling may differ from the previous ones as indirect distance estimates will change according to the reordering of events in the sequence. Because of these procedures, an increased critical probit value does not necessarily result in a longer scaled optimum sequence.

Figure 6.1: Plot of the length of the scaled optimum sequence against the corresponding critical probit value

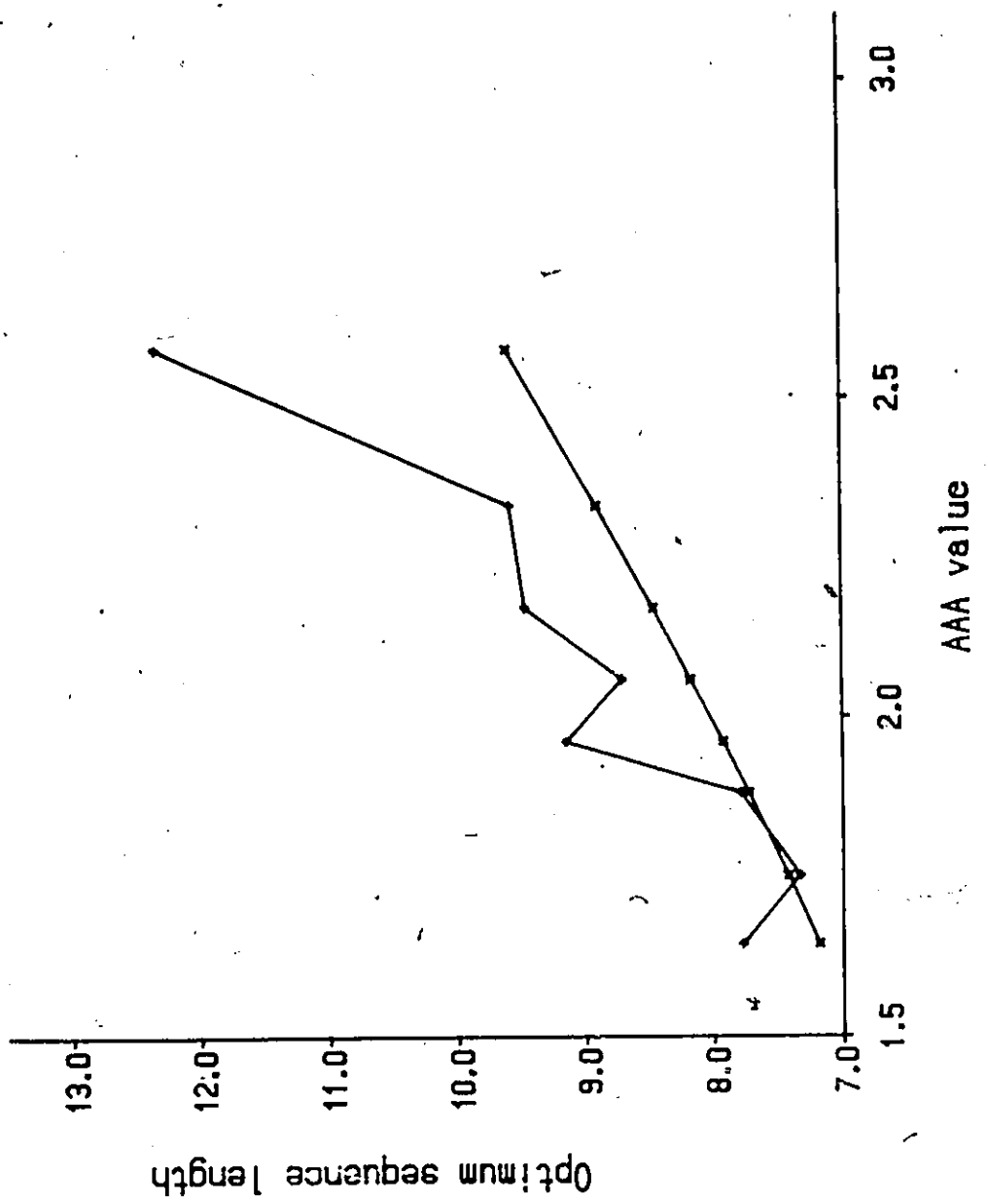
Optimum sequence length
13.0
12.0
11.0
10.0
9.0
8.0
7.0
1.5
2.0
2.5
3.0
AAA value

6.3.2 Effects on the order of events

The relative order of events may change with variations in the probit critical value. The Kendall rank correlation coefficient is calculated between each pair of sequences to assess the fluctuations in the position of events (see Table 6.2). All coefficients indicate an almost perfect correlation between sequences although higher values are observed in the top half of the table, before the application of final reordering.

An obvious trend in the correlation coefficients before final reordering is apparent . The correlation value between two sequences invariably increases as the difference between the respective critical probit values decreases. After the application of final reordering, this trend becomes less apparent though the highest correlation coefficients are observed between sequences that have similar critical probit values.

AAA	1.75	1.88	1.96	2.06	2.17	2.33	2.575
1.645	0.997	0.994	0.991	0.989	0.987	0.985	0.980
1.75		0.997	0.994	0.992	0.990	0.988	0.983
1.88			0.997	0.995	0.993	0.991	0.987
1.96				0.998	0.996	0.994	0.990
2.06					0.998	0.996	0.991
2.17						0.998	0.994
2.33							0.995
1.645	0.967	0.963	0.971	0.967	0.966	0.961	0.956
1.75		0.984	0.983	0.979	0.978	0.970	0.970
1.88			0.984	0.980	0.978	0.968	0.972
1.96				0.993	0.989	0.978	0.980
2.06					0.991	0.980	0.982
2.17						0.980	0.982
2.33							0.976
AAA	1.75	1.88	1.96	2.06	2.17	2.33	2.575

Table 6.2: Kendall rank correlation coefficent measures between runs of RASC with different critical probit values (AAA). The rank of the events in the final scaled optimum sequence is used for these calculations. The final reordering option was not applied in the RASC runs that produced the sequences of the first half of the table (indicated by a single asterisk) while that option was applied for the second half (identified by the double asterisk).

6.3.3 Effects on the relative positions of events

The length of the optimum sequence was normalized to 10 RASC units to better evaluate subtle changes in the scaling of the scaled optimum sequence. The final reordering option was used, as previous results indicated that the effects of the variations in the critical probit values are mostly exhibited after that process.

The positions of the events in the normalized RASC sequences can be compared to the normalized sequence of Figure 3.5. The differences in the events' RASC position in the sequences are plotted against the RASC distance of the event in Figure 3.5, where the critical probit value was 1.645 (see Figure 6.1).

From RASC distance 0 to 5, a trend of diminishing distances with increasing AAA values is observed. The fluctuations seem minimal for critical values from 1.75 to 1.96. A systematic reduction in RASC values seems to occur between values 1.96 and 2.06, regardless of normalization of the lengths of the sequences. This decrease corresponds to the observed reduction in optimum sequence length of Figure 6.1. A marked increase in relative event position is observable from RASC position 5 to 7.5. Values are constant near the bottom of the sequence, from RASC distance 8 to 10.

An inherent problem in interpreting the changes observed in Figure 6.2 is that the normalization process fixes the positions of events at either end of the sequence, and scales the positions of events in the middle. The frequency distribution study of Chapter 5 suggests that the middle part of the sequence provides the most reliable estimates of event positions. Another method for normalization of sequences is applied. In this attempt, the position of the median event is fixed at 5 RASC units, and the remaining event positions are scaled from that point. The normalization process is carried out as follows:

$$NP_{A1} = 5 + (EX_{A1} - EX_{med1}) * 10 / OL_1 \qquad \text{(Eq. 6.1)}$$

where: NP_{A1} is the normalized RASC position of event A in sequence 1;

EX_{A1} is the measured position of event A in sequence 1;

EX_{med1} is the measured position of the median event in sequence 1;

OL_1 is the length of scaled optimum sequence 1.

The plot of the differences in RASC position of events against their RASC position in the sequence in which AAA =

Figure 6.2: Plot of the deviation in normalized RASC position between sequence of varying critical probit values. The AAA value is indicated on top of the apropriate line. All sequences are compared to the scaled optimum sequence of Figure 3.5. The normalization of the RASC distances was accomplished by multiplying the calculated positions by 10 and dividing the product by the length of that sequence.

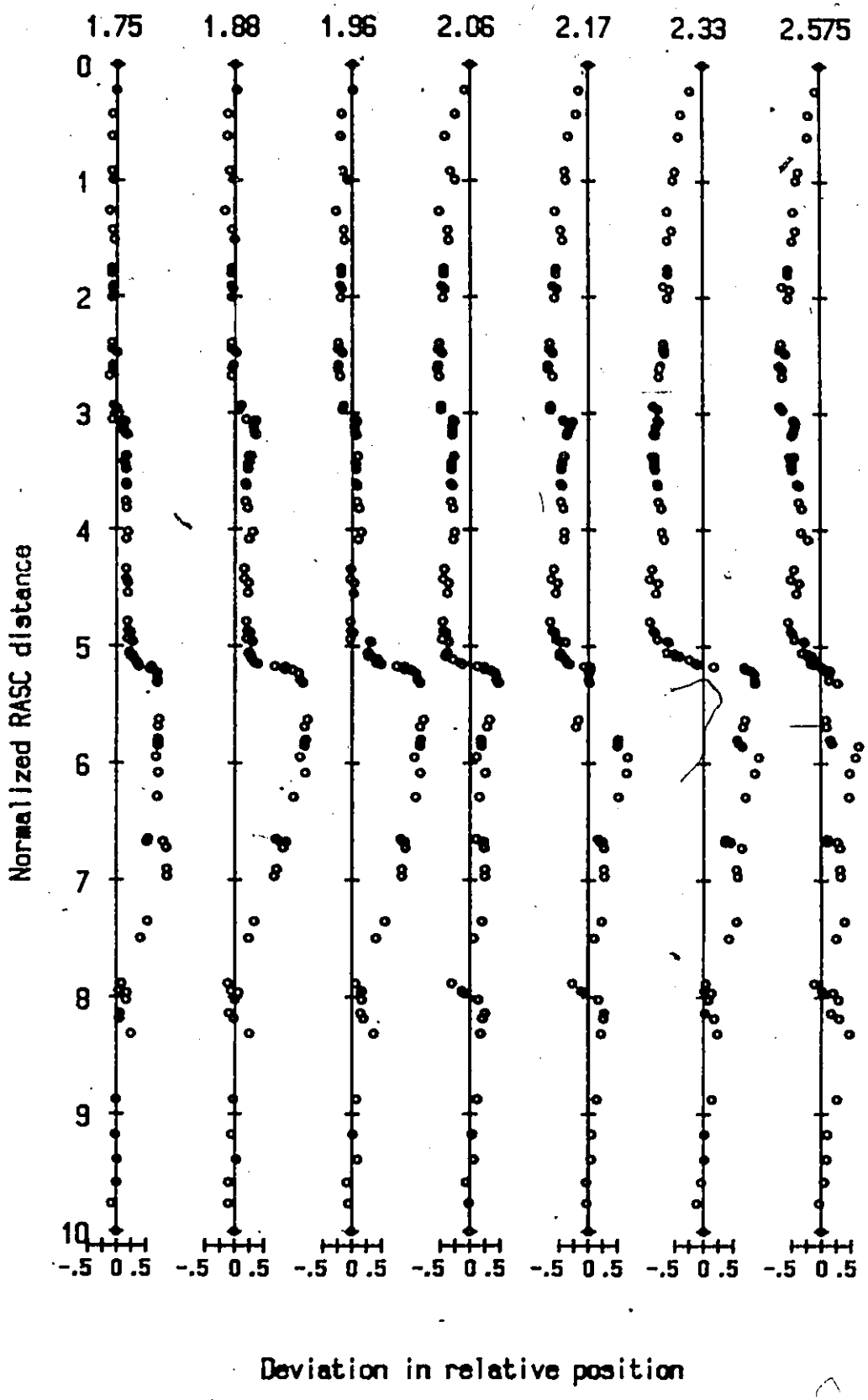
1.75
1.88
1.96
2.06
2.17
2.33
2.575
0
1
2
3
4
5
6
7
8
9
10
-.5 0.5
Normalized RASC distance
Deviation in relative position

1.645 (see Figure 6.3), reveals that systematic deviations occur at both end of the sequence, from RASC distance 0 to 2 and 8 to 10. The deviations from the original sequences increase (positively) with larger values of the probit critical value. The critical value was expected to play a greater role at both extremities of the sequence, because, as previously mentioned, some sampling problems were experienced at the top and bottom of some wells. The scarcity of data and the lower frequency of occurrences of events, led to a greater use of the AAA parameter in individual distance calculations. This is reflected in the continuous increase in deviation from the position of events in the original sequence.

The sequences exhibit small deviations between the RASC positions of events from 2 to 5 normalized RASC units (see Figure 6.3). This implies that the relative position of adjacent events did show crossover between wells and that the effect of the AAA parameter may have canceled out during indirect distance estimation.

The deviations from the original sequence are accentuated with increasing AAA values, from 5 to 7 RASC units, notwithstanding the fact that the RASC distances were normalized starting from the median value. As previously mentioned, the critical probit value will affect the scaling process in the indirect distance estimates, especially when one of the two events being compared will crossover with a

Figure 6.3: Plot of the deviation in modified normalized RASC position between sequence of varying critical probit values. The AAA value is indicated on top of the apropriate line. All sequencesq are compared to the scaled optimum sequence of Figure 3.5. The normalization of the RASC distances was carried out as described in equation 6.1.

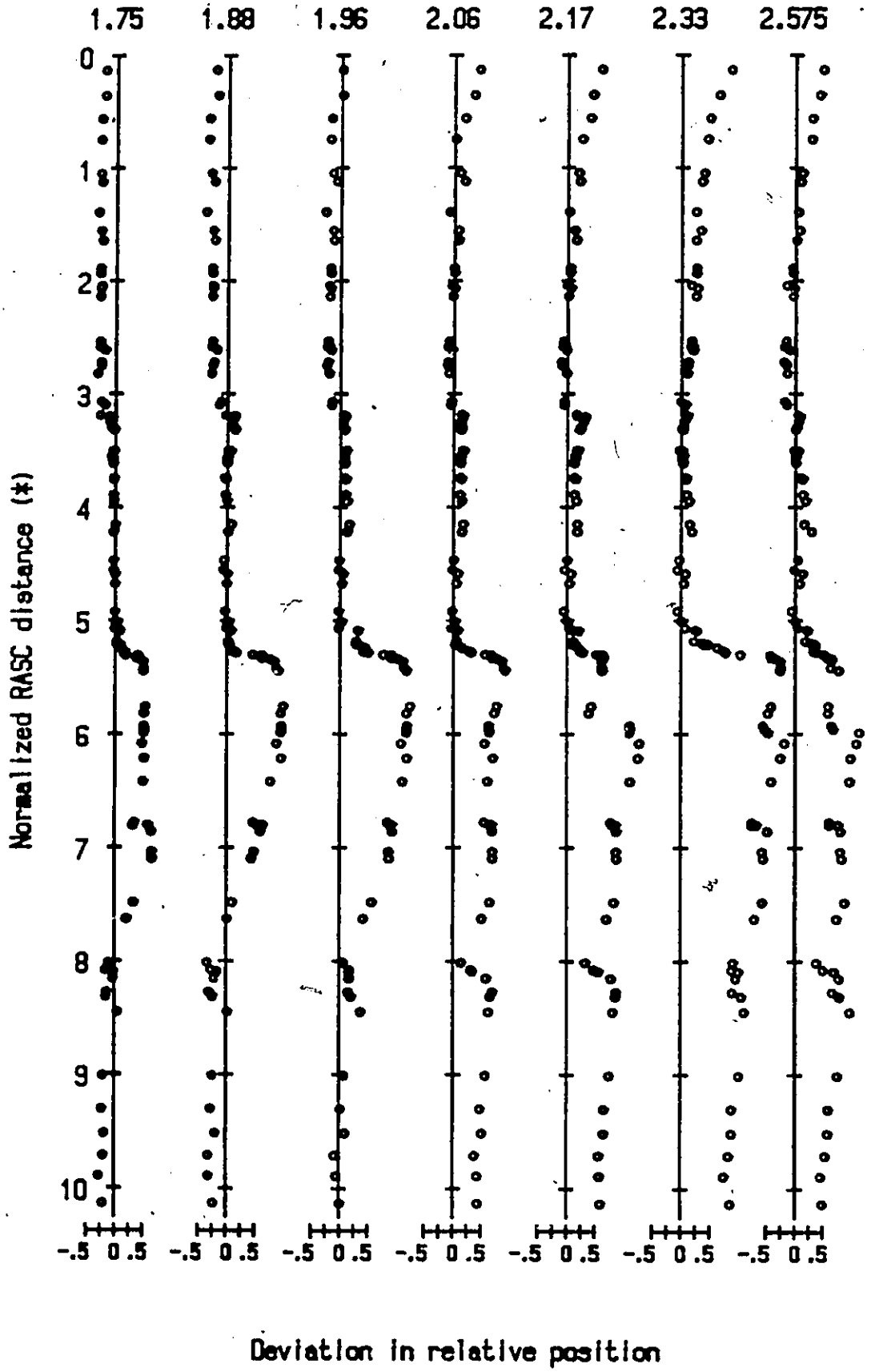
1.75
1.88
1.96
2.06
2.17
2.33
2.575
0
1
2
3
4
5
6
7
8
9
10
-.5 0.5
Normalized RASC distance (*)
Deviation in relative position

third event and the second will not. This situation may occur if certain microfossils are reworked in some wells and not in others. This type of effect is more likely to occur within zones bounded by large intercluster distances. The deviations observed in Figure 6.3 correspond to the Late Eocene (zones V and VI in Figure 3.5). As large intercluster distances occur between zones V, VI and VII, it is likely that microfossils for a few events may have been either reworked or caved-in in some wells, causing the notable and progressively larger deviations of Figure 6.3.

6.4 Conclusions

(6a) Increasing the critical probit value causes a proportional increase in the length of the optimum sequence before the final reordering option of RASC. The latter RASC option obscures this obvious trend, though the general pattern is apparent.

(6b) The ranking of events is not significantly affected by varying the probit critical value, although a general pattern of increasing discrepancies is observed between sequences with increasingly different AAA values.

(6c) The scaling of both ends of the optimum sequence is systematically affected by variations in the critical probit value, presumably because of the lower abundance and frequency of data and of sampling problems at the top and bottom of some wells.

(6d) The scaling of zones V and VI is seemingly more affected by the probit critical value than other parts of the optimum sequence. This is explained by the proximity (in time) of marked unconformities or disconformities and by the postulated presence of a few reworked or caved-in microfossils.

(6e) The effect of the AAA value is related to the quality of the data.

7. Multiple well time and zone correlation

7.1 Introduction

A model for Correlation And SCaling of biostratigraphic events in time (CASC) was devised by Agterberg and Gradstein (cf. Agterberg et al., 1985) as a follow up to the RASC model. This programme was largely developed under the auspices of the IGCP project 148.

The correlation between wells of the study area is carried out using the CASC method. This method draws on the RASC position of the events and on their respective depths and levels in the well to estimate the age-depth and event-depth measures. A regional time scale is obtained by converting distances along the RASC scale into numerical ages.

The preliminary step for chronological correlation is to assign ages to the events of the RASC sequence. Ages are plotted against RASC distances using the approximate literature age of certain events. The plot is spline-fitted to assign ages to all events in the sequence. The advantage of this technique is that it assigns ages that are representative of the regional sequence of events.

CASC is a multiple step processing method that first plots and spline-fits the age of events against their level in the well section. This step allows the regional numerical ages to be calibrated to the local sequence of events. The second processing step is plotting the depth of events against their level. This second step requires a low smoothing factor as depth and level of events are "parallel" measures. By using the two calculated spline curves, an indirect estimate of age versus depth is obtained. This estimate is based on the approximate local age of the events and on their "spline-corrected" depth. With this correlation technique the expected depth and age of an event in a well can be measured even if it was not identified in that well. This estimate facilitates the tracing of biozones from one section to the next.

7.2 The CASC methodology

CASC is an acronym for Correlation And SCaling in time of biostratigraphic events. It is a FORTRAN computer programme that uses either the ranking or scaling results from RASC to draw multiple well comparisons. The following discussion is restricted to the use of CASC with RASC scaling results

(distance CASC) and is partly based on Agterberg et al. (1985).

The CASC routine calibrates the RASC regional zonation with the local sequence of events in each well. The correlation technique depends on the spline-fitting technique described in section 5.2.2. By using spline curves, estimates of event position and age are refined and may be correlated from well to well.

The distance CASC method of correlation is based on three conditions:

(1) that the RASC scaled sequence be calibrated into a numerical time scale by using the approximate age of a subset of its events;

(2) that each well sequence of events be a sample of the optimum sequence; and

(3) that the observed depths of events in the wells are estimates of the true depths.

The first condition was verified in section 3.4.1 by a rank correlation test. The second condition should be fulfilled when one considers that the RASC sequence of events corresponds to a regional average of the well sequences. The third condition depends on the quality of data employed in the study.

7.2.1 CASC input requirements

The data to be used in CASC are made up of three parts. The first is an output of RASC consisting of a list of the events in well sections, as coded for RASC, and their respective position in the RASC sequence. A second file contains the ages of the marker events to be used for chronological correlation and the final input consists of the depths of the events coded in 13F6 format. The application of CASC usually is restricted to events that occur in at least the threshold number of wells in the RASC analysis.

7.2.2 Optimization of smoothing factors by cross-validation

Smoothing factors range between a minimum value that corresponds to the first spline curve that, with respect to the depth axis, has a slope greater than or equal to zero in all points, and a maximum value that represents a best fitting straight line. Wahba (1975) introduced the method of cross-validation to determine the optimum smoothing factor experimentally. The following discussion is based on Craven and Wahba (1979) and on Agterberg and Gradstein (1988).

Given that y_i and s_i represent observed and fitted values, respectively, and that residuals are written as $R_i = y_i - s_i$ $(i = 1,2, \ldots, n)$, then:

$$SF = \left[\frac{1}{n} \sum_{i=1}^{n} R_i^2 \right]^{1/2} \qquad \text{(Eq. 7.1)}$$

The cross-validation method estimates a coefficient based on recalculating and summing up the residuals for spline curves that differ only by a pointwise deletion of values. This coefficient is measured for each smoothing factor to be compared. When separate spline curves are calculated for m different smoothing factors, then s_{ijk} $(i = 1, 2, \ldots, n;\ j = 2; 3, \ldots, m;$ and $k= 1, 2, \ldots, m)$ represents the i^{th} value on a spline curve for the k^{th} smoothing factor fitted to a reduced data set in which the value y_j has been deleted. The cross-validation coefficient, CV_k, is defined as:

$$CV_k = \frac{1}{n-2} \sum_{i=2}^{n-1} (y_i - s_{ijk})^2 \qquad \text{(Eq 7.2)}$$

It may be noted that no estimates are available for the first and last values of the spline such that the sum is based on n-2 comparisons. The optimum smoothing factor minimizes the CV_k value.

7.2.3 Regional age estimates

The first procedure of distance CASC is to convert the RASC distances into numerical ages. This step was also carried in section 3.5.1 to obtain a numerical time scale.

The regional ages of a subgroup of events from the RASC scaled sequence are obtained from literature. A spline curve is fitted to a plot of age versus RASC distance using the best least-square estimate of a curve that always has a positive value (i.e. RASC distance and age always increasing). The spline-curve values provide a regionally calibrated age estimate for all events of the scaled sequence.

7.2.4 Calibration of well data to a regional standard

Once all RASC distances are given a corresponding numerical age, the individual well sequences are interpreted in the context of the modified RASC regional biozonation scheme. This analysis will produce interpolated age-depth and event-depth estimates for each well.

All plots are fitted with smoothing splines as described in section 5.2.2. Three preliminary interpolations are required to obtain the locally calibrated age-depth estimate from which multiple well correlations can be constructed. The local component of age and the calibration of depths are made using the level of events in the well.

The first calibration to be made relates the level of events in the well to the age value as assigned by the first spline-curve. The coordinates of the curve represent the adjusted age/level values.

The second step of the well analysis plots level of events against their depth. Depth is a scaled measure of the level of events. The purpose of this plot is to assign values to all depths for later interpolation and correlation. Because these measures are closely dependent, the smoothing factor is close to zero.

The third plot is a combination of the two previous ones. Age and depth are plotted against each other using the spline-curve estimates. The values estimated from this curve represent the locally calibrated age-depth estimates. Figure 7.1 represents this procedure of age/depth estimation where Figure 7.1 (a) is the age versus level and Figure 7.1 (b) plots the level of an event against its depth.

The fourth plot represents the final results by showing

Figure 7.1 (a): Hypothetical plot of the regional age of events against their level in the well.

Figure 7.1 (b): Hypothetical plot of the observed depth of events against their level in the well. By using the spline curves of plots (a) and (b), the expected depth of time line or of events can be measured.

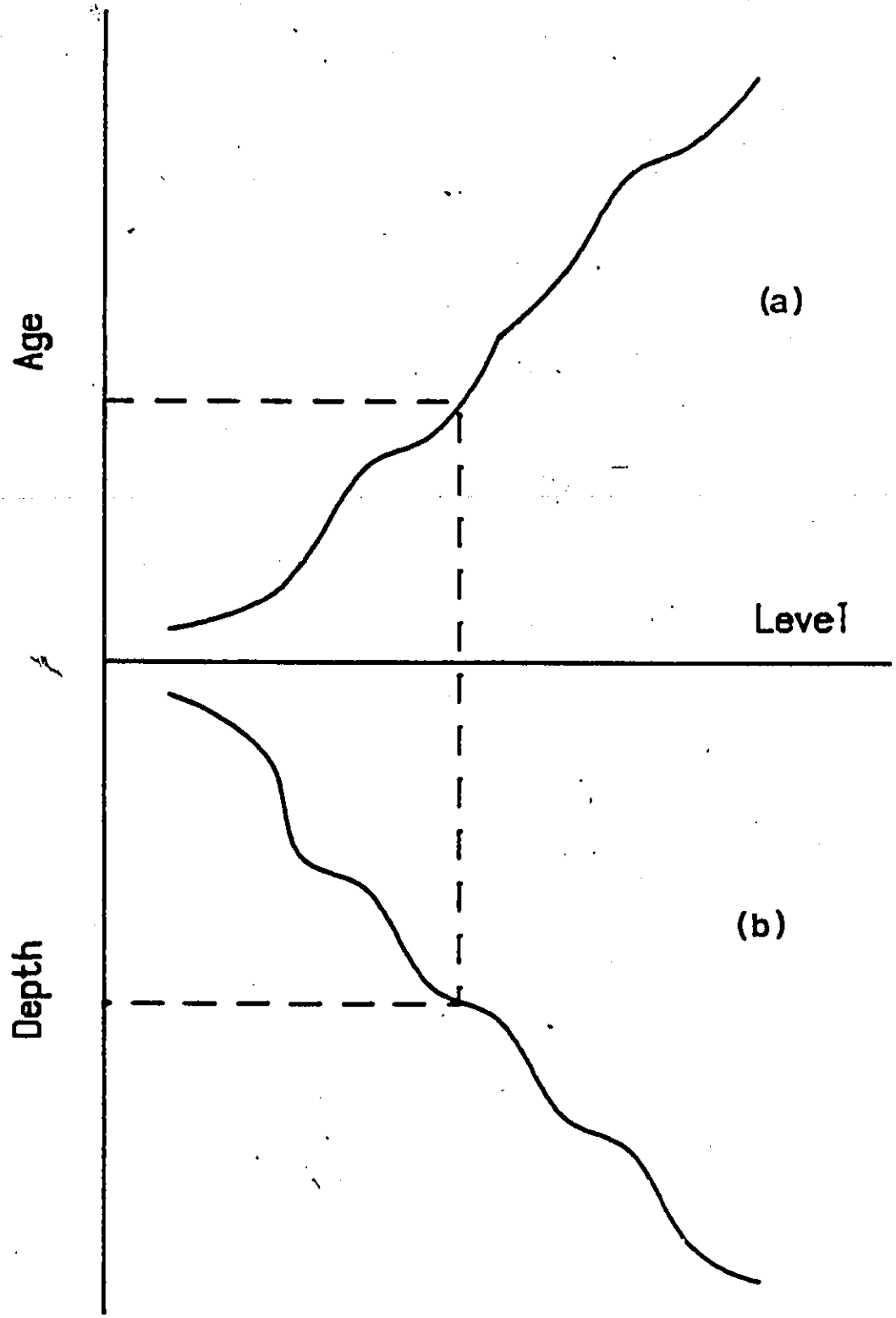
Age
(a)
Level
(b)
Depth

the age/depth spline-curve of the third plot and the observed age depth values. A standard deviation of residuals is calculated for differences between the spline-curve and the observed values.

7.2.5 Well to well correlation

The correlation procedure uses the age-depth values calculated as previously described. CASC offers two types of correlation options, the first being isochron tracing and the second event position correlation. Both options use the spline values determined in the fourth plot described in section 7.2.3.

The isochron correlation requires the input of the time lines to be correlated and extrapolates the corresponding depths from the spline-curve, for each well to be analyzed.

The event position correlation draws on the position of the events in the RASC sequence and on its corresponding numerical age to extrapolate its expected depth in the well from the age-depth spline-curve. This type of correlation is therefore based on the RASC expected depth of events in wells rather than on the recorded depths. This procedure allows the

tracing of events that were not identified in all sections and calibrates the observed depths to the regional standard.

7.2.6 Error bars

The purpose of the error bars is to quantify the inconsistencies of observed and calculated measures of depth.

Error bars to measure the uncertainty of events or isochron positions are constructed by the CASC model in one of three ways.

An error of plus or minus one standard deviation (of residuals in spline-fitting) on the age estimate is determined. This measure can be simply transformed to an error on the depth axis by using the first derivative of the age-depth curve (dz/dy) at that point. The uncertainty in the depth measure is therefore bounded by the ordinates of the error in age reported on a tangent to the age-depth curve at that point. This error estimate is symmetrical and called the local error estimate.

Another method to measure error bars first relies on calculating the sediment accumulation rate (in km per Ma). The modified local error bars are estimated by multiplying the

local error in age (SD) by the sediment accumulation rate. This value corresponds to extrapolating the error measured in age to depth error values through the spline-curve. The resulting error bar will be asymmetrical unless the age-depth curve is locally a straight line.

Finally a global error bar can be constructed by assuming the RASC assigned standard deviation of events of $\sigma = 1/\sqrt{2}$. This value is transformed into a variable error estimate s(age) using the first derivative of the age versus RASC distance curve. This variable error estimate is in turn changed into an error bar by using the first derivative of the age-depth curve (as in the local error estimate).

Assuming the observed depths are normally distributed about their calculated positions, there is approximately a 68% probability of them falling within the local and global error bars as these extend one standard deviation above and below the depth position.

7.3 Application of CASC

The scaled optimum sequence of Figure 3.5 is used as the correlation standard of this study.

The preliminary regional age estimate of events is the same as that obtained from figure 3.8 in section 3.5. The preferred spline-curve is the one that minimized the standard deviation of residuals.

The age versus RASC distance plot was fitted with a smoothing factor of SF = 1.68. The CASC routine is carried out by optimizing smoothing factors with the cross-validation technique. The smoothing factors and standard deviations of residuals used in the CASC analysis of individual wells are listed in Table 7.1.

7.4 RASC zone correlation

For correlation purposes, the study area will be analyzed in two, geographically distinct, groups: the Labrador Shelf and the Grand Banks.

7.4.1 Labrador Shelf wells correlation

Eleven wells are included in the Labrador Shelf group, the southernmost one being Freydis. The Leif E-38 well was

WELL NAME	AvsL	DvsL	AvsD	AvsD'
RUT H-11	5.43 max	0.03 min	0.00 min	4.96
KARLSEFNI H-13	5.81	0.02 min	0.00 min	6.05
SNORRI J-90	5.20 min	0.09 min	0.00 min	5.23
HERJOLF M-92	6.69 min	0.01 min	0.65 min	6.95
BJARNI H-81	6.18	0.01 min	0.00 min	6.21
GUDRID H-55	6.57 min	0.01 min	0.71 min	7.03
CARTIER D-70	6.58	0.01 min	0.00 min	6.42
INDIAN HARBOUR M-52	4.23	0.02 min	0.00 min	4.29
LEIF E-38	9.57 min	0.01 min	0.00 min	10.40
LEIF M-48	5.61	0.01 min	0.00 min	5.70
FREYDIS B-87	7.19 max	0.01 min	0.00 min	7.24
HARE BAY E-21	4.68	0.02 min	0.00 min	4.91
BLUE H-28	5.06	0.01 min	0.00 min	5.39
BONAVISTA C-99	5.10	0.02 min	0.00 min	5.22
CUMBERLAND B-55	5.08 max	0.01 min	0.00 min	5.07
BONANZA M-71	4.23 min	0.01 min	1.01 min	4.89
DOMINION O-23	5.51 max	0.01 min	0.00 min	5.39
SOUTH TEMPEST G-88	4.30 min	0.01 min	0.00 min	3.94
FLYING FOAM I-13	5.98 max	0.01 min	0.00 min	5.89
ADOLPHUS D-50	3.55	0.01 min	0.00 min	3.63
HIBERNIA P-15	4.56 max	0.01 min	0.00 min	4.58
EGRET K-36	6.54	0.01 min	0.00 min	6.29
OSPREY H-84	7.51 max	0.01 min	0.00 min	7.77

Table 7.1: Optimized smoothing factors obtained by cross-validation. AvsL represents the Age versus Level, DvsL is the Depth versus Level, AvsD is the Age vesus Depth and AvsD' is the final Age versus Depth plot used for multiple well correlation purposes. The AvsD' value is the standard deviation of the residuals of the AvsD plot. min indicates that the cross-validation value corresponds to the minimum smoothing factor whereas max corresponds to the maximum smoothing factor.

discarded from further analysis based on its age-depth curve (see Figure 7.2). Most of this well seems much shallower than others and will not be useful for correlation purposes.

RASC biozones are correlated between wells by tracing the depth of zone boundary events. These events are selected from Figure 3.5 and listed in Table 7.2. When an event does not occur in a well, its expected depth can be estimated from its RASC position. The depths of the zone boundaries are listed in Tables 7.3 and 7.4 and plotted in Figure 7.3 for the Labrador Shelf wells.

The zone boundaries in the youngest or oldest part of the wells may not always be observed because of either the scarcity of data points, or the specific shape of the spline-curve.

The Bjarni, Cartier, Leif M-48 and Freydis wells show closer zone boundaries, probably indicating a lower sedimentation rate or greater compaction. In general, the northern wells seem to have been subjected to greater sedimentation rates.

Spacing of zone boundaries indicate greater than average sediment accumulation rates in zone IX of the Karlsefni and Herjolf wells, in zone VIII in the Gudrid well and in zone VI of the Indian Harbour well. Low sedimentation rates or an unconformity would explain the proximity of zone boundaries in

Figure 7.2: Age-depth curve of the Leif E-38 well. The well contains almost exclusively events younger than 20 Ma. This well is not suitable for correlation purposes.

LEIF E-38

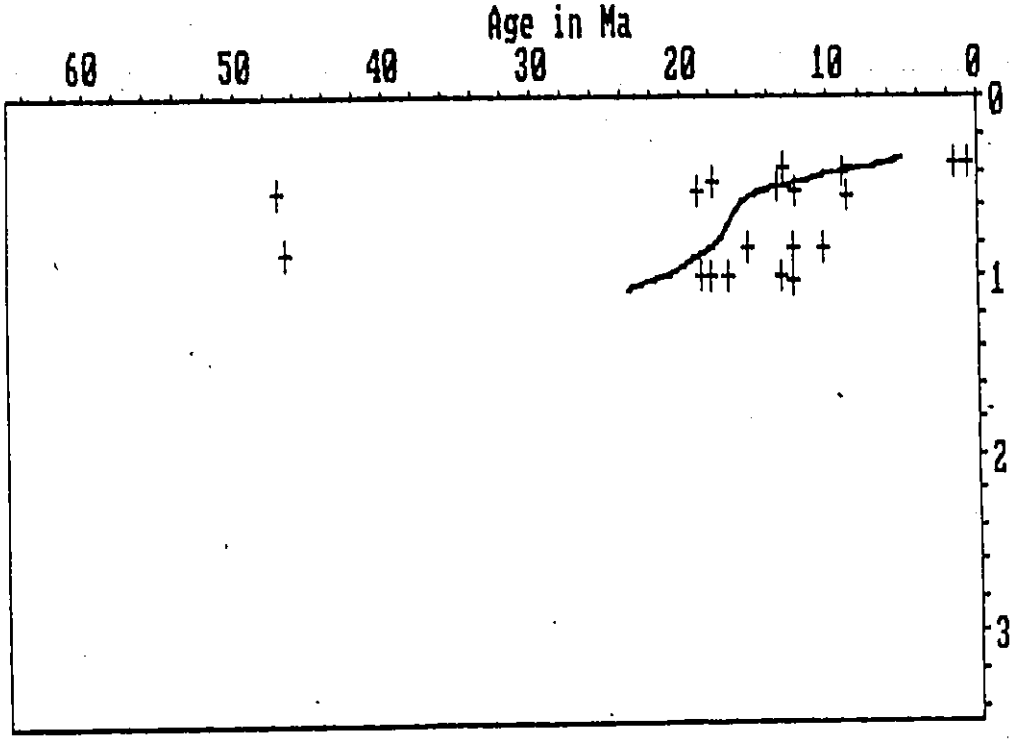

Boundary	Event number	Event name
I - II	52	Acarinina soldadoensis
II - III	37	Acarinina aff. pentacamerata
III - IV	90	Acarinina densa
IV - V	29	Reticulophragmium amplectens
V - VI	263	Ammobaculites aff. polythalamus
VI - VII	259	Ammodiscus latus
VII - VIII	24	Turrilina alsatica
VIII - IX	21	Guttulina problema
IX - X	67	Scaphopod sp. 1
X - XI	17	Asterigerina gurichi

Table 7.2: List of boundary events used to trace RASC biozones in CASC multiple well correlation.

WELL NAME	I - II	II - III	III - IV	IV - V	V - VI
RUT H-11				*3.16 ± 0.63	*3.00 ± 0.63
KARLSEFNI H-13	3.71 ± 0.90	*2.94 ± 0.20	*2.91 ± 0.15	2.76 ± 0.09	*2.74 ± 0.10
SNORRI J-90	*2.95 ± 0.06	*2.53 ± 0.51	*2.48 ± 0.21	2.15 ± 0.05	2.14 ± 0.03
HERJOLF M-92		*1.99 ± 0.19	*1.97 ± 0.18	1.76 ± 0.21	1.72 ± 0.22
BJARNI H-81	*1.99 ± 0.12	*1.83 ± 0.13	*1.82 ± 0.12	1.67 ± 0.08	*1.65 ± 0.08
GUDRID H-55	*2.37 ± 0.39	2.10 ± 0.16	2.08 ± 0.16	1.90 ± 0.11	*1.88 ± 0.09
CARTIER D-70		*1.77 ± 0.08	*1.76 ± 0.08	1.55 ± 0.26	1.50 ± 0.17
INDIAN HARBOUR M-52	2.99 ± 0.07	2.53 ± 0.27	*2.47 ± 0.35	2.28 ± 0.32	2.16 ± 0.47
LEIF M-48		*1.69 ± 0.07	*1.67 ± 0.09	1.59 ± 0.03	1.58 ± 0.04
LEIF E-38					
FREYDIS B-87	*1.54 ± 0.10	*1.39 ± 0.12	*1.38 ± 0.11	1.28 ± 0.05	*1.27 ± 0.07
HARE BAY E-21	*3.06 ± 0.12	*2.88 ± 0.11	*2.86 ± 0.10	2.27 ± 0.67	2.18 ± 0.26
BLUE H-28		4.74 ± 0.05	4.73 ± 0.05	4.43 ± 0.64	*4.29 ± 0.55
BONAVISTA C-99		*3.46 ± 0.13	3.44 ± 0.13	3.21 ± 0.37	3.12 ± 0.25
CUMBERLAND B-55	3.58 ± 0.19	*3.31 ± 0.10	3.29 ± 0.12	2.89 ± 0.28	*2.81 ± 0.28
BONANZA M-71		3.31 ± 0.18	3.28 ± 0.18	2.90 ± 0.40	2.78 ± 0.63
DOMINION O-23		2.50 ± 0.44	2.44 ± 0.29	1.94 ± 0.21	1.89 ± 0.22
SOUTH TEMPEST G-88		2.30 ± 0.11	2.27 ± 0.13	1.71 ± 0.25	1.59 ± 0.44
FLYING FOAM I-13		*1.96 ± 0.15	*1.94 ± 0.18	1.67 ± 0.16	1.62 ± 0.23
ADOLPHUS D-50	*2.63 ± 0.10	2.28 ± 0.45	2.16 ± 0.46	1.78 ± 0.13	1.69 ± 0.34
HIBERNIA P-15				1.25 ± 0.19	1.20 ± 0.10
EGRET K-36					
OSPREY H-84				*0.76 ± 0.06	*0.75 ± 0.06

Table 7.3: CASC depths of zone boundaries I to VI in the wells of the study area. The asterisk denotes that the event used as boundary indicator was not observed in that well.

WELL NAME	VI - VII	VII - VIII	VIII - IX	IX - X	X - XI
RUT H-11	2.24 ± 0.08	*2.16 ± 0.07	*1.74 ± 0.52	*1.26 ± 0.51	0.76 ± 0.52
KARLSEFNI H-13	*2.31 ± 0.37	*2.15 ± 0.08	*2.00 ± 0.19	1.22 ± 1.79	*0.69 ± 0.11
SNORRI J-90	*2.03 ± 0.14	*1.83 ± 0.12	1.73 ± 0.04	1.50 ± 0.68	*1.00 ± 0.97
HERJOLF M-92	1.39 ± 0.15	*1.29 ± 0.12	*1.12 ± 0.28	0.60 ± 0.25	
BJARNI H-81	*1.42 ± 0.19	1.21 ± 0.34	0.87 ± 0.23	0.64 ± 0.58	
GUDRID H-55	1.78 ± 0.06	1.72 ± 0.11	0.70 ± 0.35	*0.58 ± 0.11	0.51 ± 0.10
CARTIER D-70	1.31 ± 0.15	1.20 ± 0.12	0.99 ± 0.55	0.75 ± 0.15	*0.66 ± 0.09
INDIAN HARBOUR M-52	1.46 ± 0.36	1.18 ± 0.15	*0.96 ± 0.42	*0.65 ± 0.22	0.58 ± 0.04
LEIF M-48	*1.20 ± 0.18	1.15 ± 0.08	1.01 ± 0.17	0.77 ± 0.20	*0.56 ± 0.36
LEIF E-38			0.57 ± 0.80	0.45 ± 0.18	0.39 ± 0.06
FREYDIS B-87	*1.14 ± 0.10	*0.87 ± 0.51	0.67 ± 0.41	0.51 ± 0.19	
HARE BAY E-21	1.56 ± 0.22	1.35 ± 0.25	*1.14 ± 0.05	*1.08 ± 0.10	*0.81 ± 0.41
BLUE H-28	*3.70 ± 0.15	*3.52 ± 0.21	*3.22 ± 0.31	*2.96 ± 0.29	*2.69 ± 0.35
BONAVISTA C-99	2.37 ± 0.15	1.95 ± 0.88	1.21 ± 0.49	*0.93 ± 0.13	0.82 ± 0.21
CUMBERLAND B-55	2.22 ± 0.21	1.73 ± 0.90	*1.10 ± 0.37	*0.75 ± 0.16	0.63 ± 0.16
BONANZA M-71	1.62 ± 0.11	*1.52 ± 0.09	1.39 ± 0.08	*1.31 ± 0.08	1.23 ± 0.08
DOMINION O-23	1.30 ± 0.33	1.05 ± 0.29	0.77 ± 0.54	*0.57 ± 0.12	0.44 ± 0.31
SOUTH TEMPEST G-88	1.29 ± 0.17	1.17 ± 0.13	*0.96 ± 0.13	*0.82 ± 0.05	0.76 ± 0.06
FLYING FOAM I-13	1.08 ± 0.32	0.86 ± 0.28	*0.61 ± 0.21	*0.42 ± 0.29	0.31 ± 0.10
ADOLPHUS D-50	1.22 ± 0.17	0.97 ± 0.19	*0.54 ± 0.15	*0.46 ± 0.03	*0.38 ± 0.08
HIBERNIA P-15	0.99 ± 0.05	0.81 ± 0.35	*0.43 ± 0.29	*0.27 ± 0.07	
EGRET K-36	*0.51 ± 0.05	0.48 ± 0.03	0.43 ± 0.08	*0.34 ± 0.15	
OSPREY H-84	*0.62 ± 0.12	*0.54 ± 0.12	*0.43 ± 0.10	*0.37 ± 0.08	0.32 ± 0.09

Table 7.4: CASC depths of zone boundaries VI to XI in the wells of the study area. The asterisk denotes that the event used as boundary indicator was not observed in that well.

Figure 7.3: Biozone correlation chart of the Labrador Shelf wells. The zone boundaries are presented in Table 7.2.

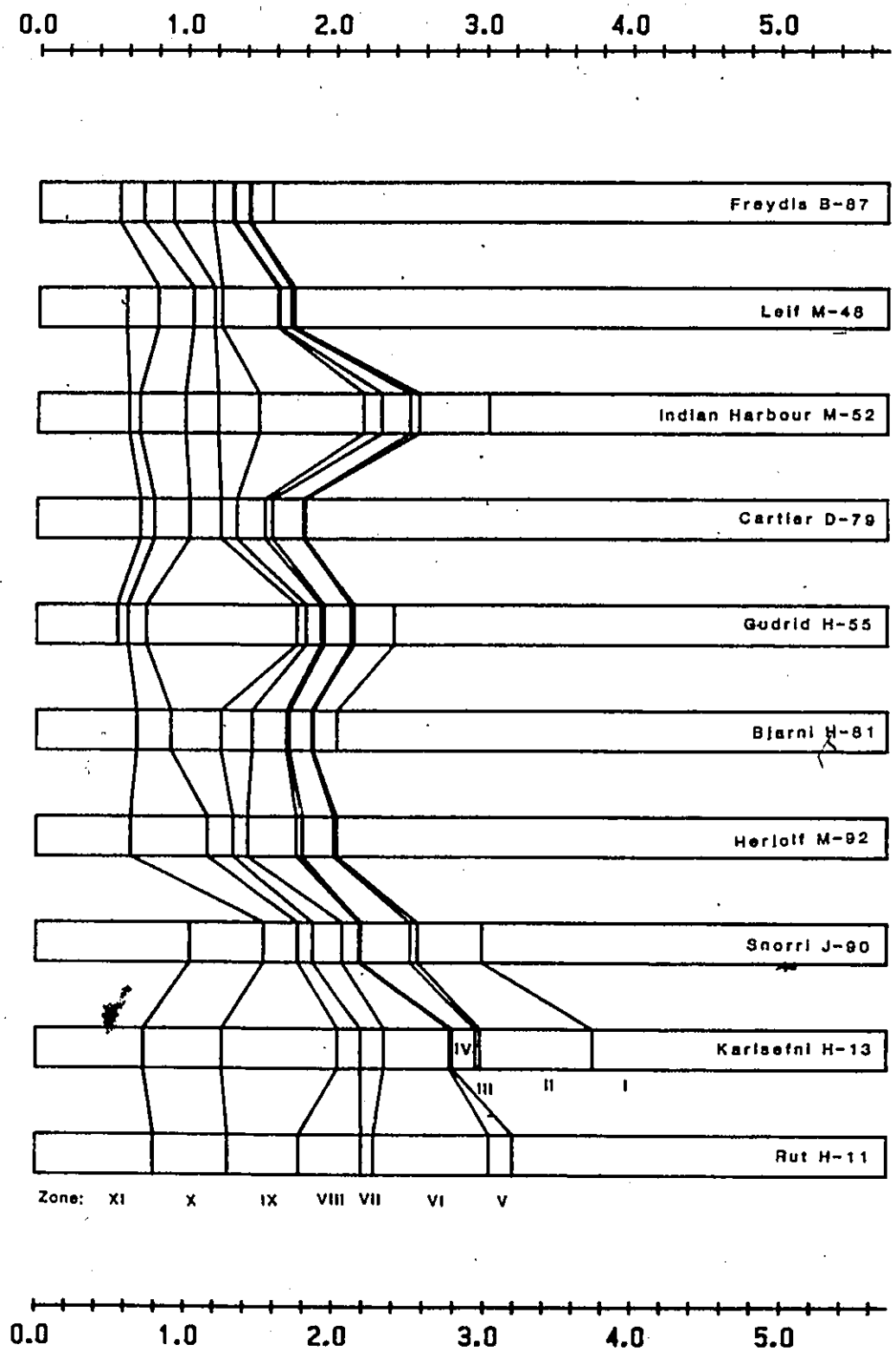
0.0
1.0
2.0
3.0
4.0
5.0
Freydis B-87
Leif M-48
Indian Harbour M-52
Cartier D-79
Gudrid H-55
Bjarni H-81
Herjolf M-92
Snorri J-90
Karlsefni H-13
IV
III
II
I
Rut H-11
Zone: XI X IX VIII VII VI V
0.0
1.0
2.0
3.0
4.0
5.0
Depth (in km)

Snorri from zone VI to VIII, and in Freydis from zone II to VII. The age-depth plots of these two wells (see Figure 7.4 (a) and (b), respectively), reveal a possible hiatus from 20 Ma to 30 Ma B.P. (zone VIII) in the Snorri well, with low sedimentation rates preceding this time. There is no indication of a hiatus in the Freydis section; however, uniformly low sedimentation rates are suggested from zone II to VIII (see Figure 7.4(b), 60 Ma to 30 Ma B.P.).

7.4.2 Grand Banks wells correlation

The Grand Banks group is made up of twelve wells, the northernmost one being Hare Bay. The Egret K-36 well is not included in the correlation figures because it is shallow and has a very condensed section.

The zone boundary events listed in Table 7.2 are traced in the Grand Banks wells and plotted in Figure 7.5. The depth of the boundaries and their respective local error estimates are presented in Tables 7.3 and 7.4.

A noticeable feature of Figure 7.5 is the thickening of zone VI in the Bonanza well suggesting a higher sediment accumulation rate. The Osprey well exhibits relatively closer zone boundaries than other wells; this is presumably because

Figure 7.4 (a): Age-depth plot of the Snorri well. Extremely low or zero sediment accumulation rates are observed from approximately 32 Ma to 42 Ma B.P..

Figure 7.4 (b): Age-depth plot of the Freydis well. No unconformities are observable in this well; the sediment accumulation rate is low but constant in the section of the well older than 30 Ma.

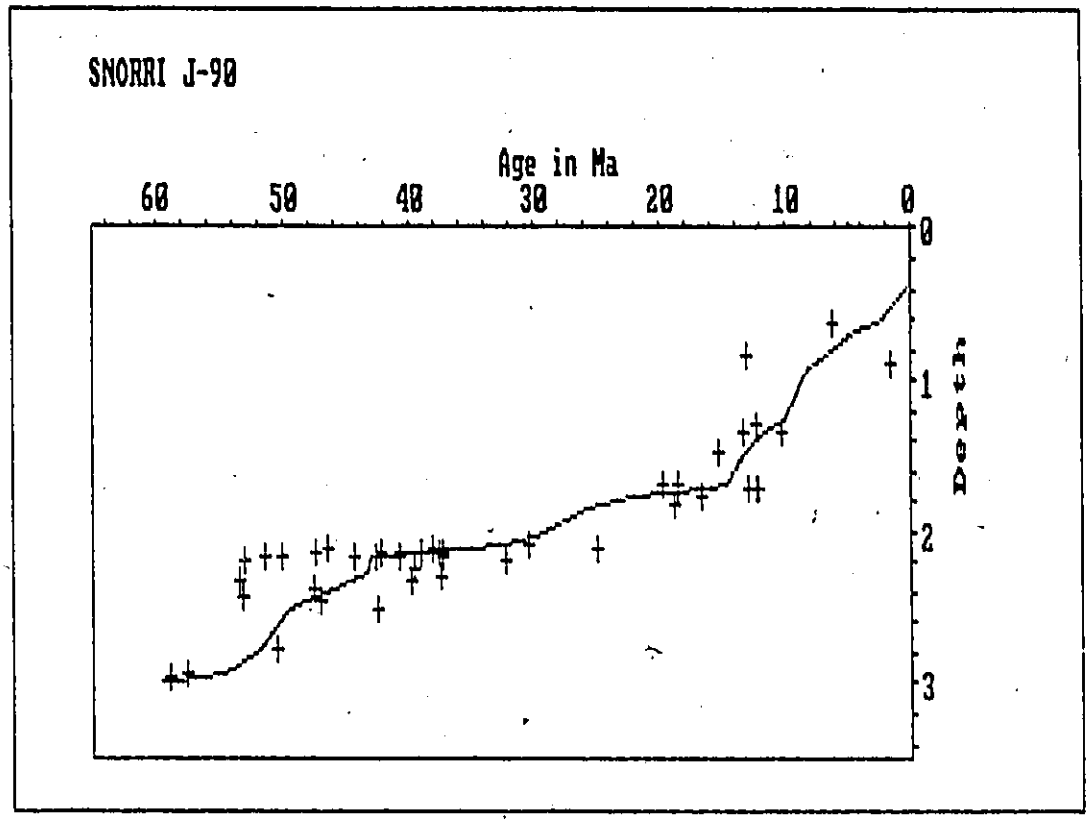
SNORRI J-90
Age in Ma
60
50
40
30
20
10
0
0
1
2
3
Depth

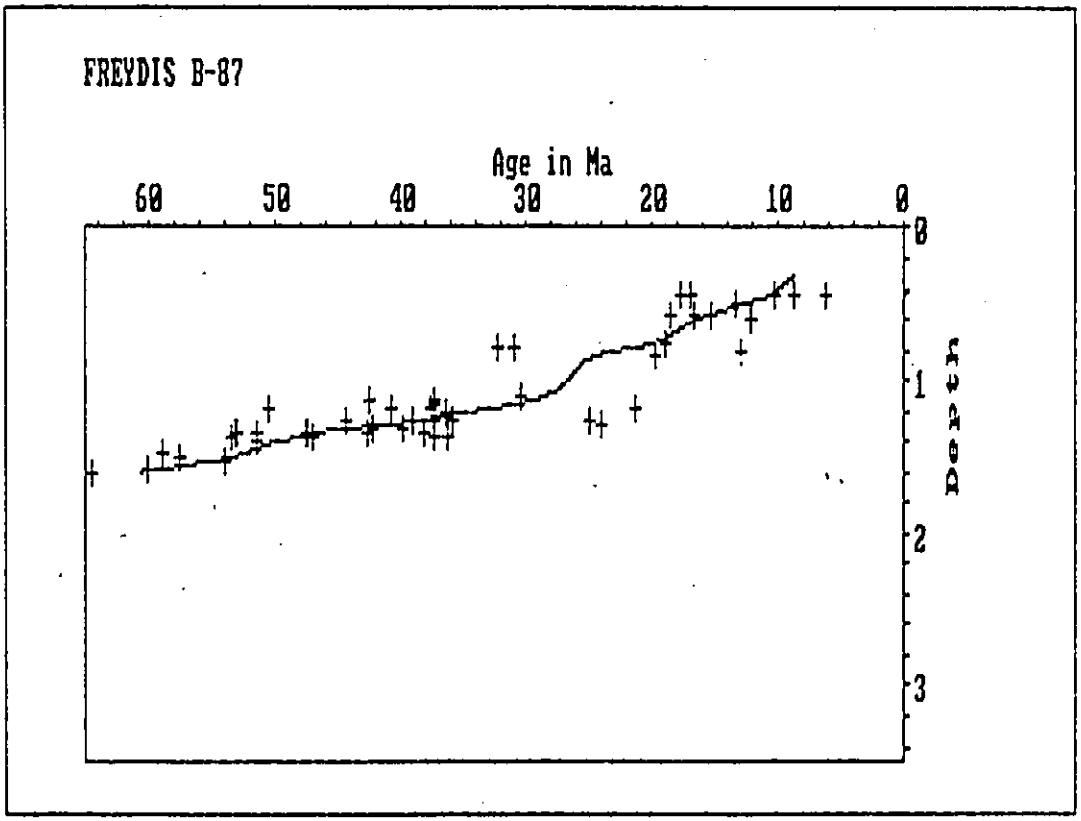
FREYDIS B-87
Age in Ma
60
50
40
30
20
10
0
0
1
2
3
Depth

Figure 7.5: Biozone correlation chart of the Grand Banks wells. The zone boundaries are presented in Table 7.2.

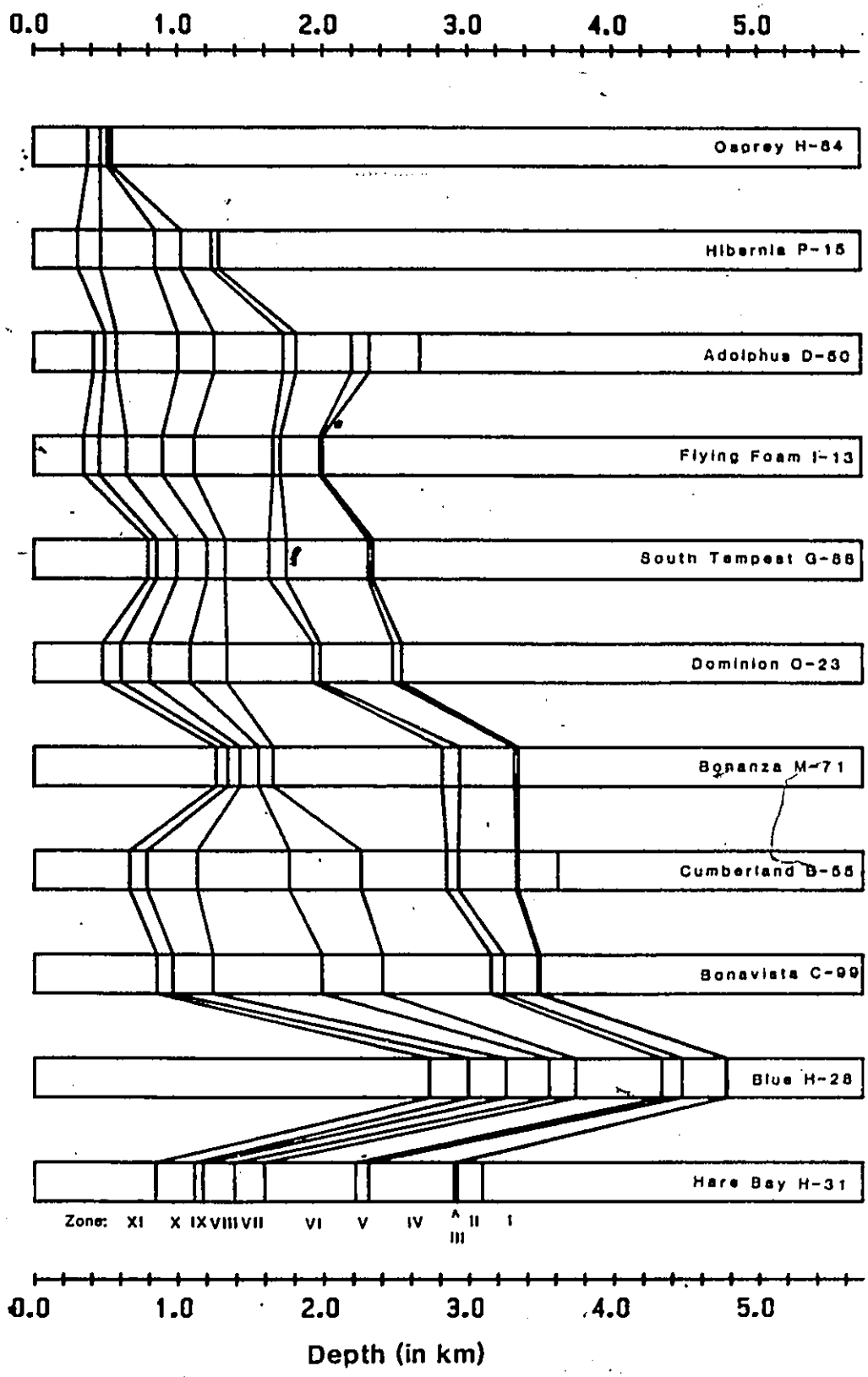
0.0
1.0
2.0
3.0
4.0
5.0
Osprey H-84
Hibernia P-15
Adolphus D-50
Flying Foam I-13
South Tempest G-88
Dominion O-23
Bonanza M-71
Cumberland B-55
Bonavista C-99
Blue H-28
Hare Bay H-31
Zone: XI X IX VIII VII VI V IV III II I
0.0
1.0
2.0
3.0
4.0
5.0
Depth (in km)

of its more distant position from the terrigenous sediment supply (see Figure 2.1).

The Blue well shows all zones in spite of its greater depth to seafloor.

7.5 Isochron correlation

Isochrons were selected at 5 Ma intervals from 60 Ma to 5 Ma. The calculated depth of these isochrons are listed in Tables 7.5 and 7.6. The local error estimate is included in this table. The correlation charts for the isochrons of the Labrador Shelf and Grand Banks wells are presented in Figures 7.6 and 7.7, respectively. The general trends described in sections 7.4.1 and 7.5.1 can be observed in these figures.

Paleontologically estimated depths for epoch boundaries of fifteen wells of the study area were published by Gradstein (1986) in the atlas of the Labrador sea. There are relatively large discrepancies between foraminiferal and palynomorph depth estimates for Cenozoic epoch boundaries. The depths of these epoch boundaries were estimated by CASC and compared to the published values (see Figure 7.8).

WELL NAME	5 Ma	10 Ma	15 Ma	20 Ma	25 Ma	30 Ma
RUT H-11		0.90 ± 0.52	1.43 ± 0.52	1.95 ± 0.52	2.16 ± 0.08	2.24 ± 0.08
KARLSEFNI H-13	0.61 ± 0.20	0.73 ± 0.33	1.69 ± 1.78	2.05 ± 0.15	2.15 ± 0.08	2.29 ± 0.33
SNORRI J-90	0.72 ± 0.38	1.24 ± 0.98	1.68 ± 0.24	1.74 ± 0.05	1.83 ± 0.11	2.03 ± 0.17
HERJOLF M-92		0.50 ± 0.19	0.68 ± 0.41	1.18 ± 0.18	1.28 ± 0.13	1.38 ± 0.15
BJARNI H-81			0.76 ± 0.33	0.99 ± 0.39	1.19 ± 0.39	1.41 ± 0.18
GUDRID H-55		0.53 ± 0.10	0.61 ± 0.14	1.18 ± 1.45	1.72 ± 0.12	1.78 ± 0.07
CARTIER D-70	0.62 ± 0.07	0.68 ± 0.10	0.79 ± 0.18	1.09 ± 0.22	1.20 ± 0.12	1.30 ± 0.16
INDIAN HARBOUR M-52	0.48 ± 0.27	0.59 ± 0.04	0.72 ± 0.22	1.05 ± 0.11	1.17 ± 0.15	1.42 ± 0.35
LEIF M-48	0.43 ± 0.16	0.65 ± 0.35	0.83 ± 0.37	1.05 ± 0.07	1.15 ± 0.11	1.20 ± 0.09
LEIF E-38	0.36 ± 0.11	0.40 ± 0.06	0.48 ± 0.19			
FREYDIS B-87		0.40 ± 0.46	0.56 ± 0.20	0.75 ± 0.20	0.86 ± 0.24	1.14 ± 0.12
HARE BAY E-21	0.50 ± 0.71	0.90 ± 0.26	1.11 ± 0.05	1.17 ± 0.07	1.33 ± 0.26	1.55 ± 0.18
BLUE H-28	2.45 ± 0.35	2.77 ± 0.30	3.05 ± 0.30	3.32 ± 0.21	3.50 ± 0.22	3.69 ± 0.15
BONAVISTA C-99	0.63 ± 0.29	0.86 ± 0.14	1.01 ± 0.33	1.54 ± 0.73	1.87 ± 0.91	2.36 ± 0.16
CUMBERLAND B-55	0.46 ± 0.18	0.67 ± 0.12	0.84 ± 0.39	1.24 ± 0.38	1.65 ± 0.98	2.20 ± 0.23
BONANZA M-71		1.26 ± 0.08	1.34 ± 0.08	1.42 ± 0.08	1.51 ± 0.09	1.61 ± 0.11
DOMINION O-23		0.50 ± 0.17	0.62 ± 0.16	0.91 ± 0.26	1.04 ± 0.19	1.27 ± 0.33
SOUTH TEMPEST G-88		0.78 ± 0.06	0.86 ± 0.12	1.02 ± 0.11	1.16 ± 0.14	1.27 ± 0.16
FLYING FOAM I-13		0.33 ± 0.10	0.49 ± 0.24	0.67 ± 0.18	0.84 ± 0.27	1.06 ± 0.35
ADOLPHUS D-50		0.41 ± 0.09	0.49 ± 0.04	0.61 ± 0.13	0.95 ± 0.19	1.21 ± 0.17
HIBERNIA P-15			0.30 ± 0.08	0.55 ± 0.27	0.78 ± 0.33	0.99 ± 0.06
EGRET K-36			0.38 ± 0.13	0.45 ± 0.07	0.48 ± 0.03	0.51 ± 0.04
OSPREY H-84	0.27 ± 0.12	0.34 ± 0.10	0.39 ± 0.09	0.46 ± 0.12	0.54 ± 0.13	0.62 ± 0.13

Table 7.5: Calculated depth of isochrons in the twenty-three wells of the study area. The estimate of error corresponds to the local error bars as measured in CASC.

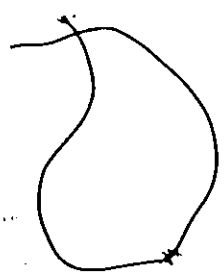

WELL NAME	35 Ma	40 Ma	45 Ma	50 Ma	55 Ma	60 Ma
RUT H-11	2.34 ± 0.19	2.97 ± 0.63	3.61 ± 0.63			
KARLSEFNI H-13	2.63 ± 0.10	2.74 ± 0.11	2.84 ± 0.13	2.95 ± 0.21	3.50 ± 0.95	
SNORRI J-90	2.11 ± 0.04	2.14 ± 0.04	2.33 ± 0.21	2.55 ± 0.65	2.93 ± 0.12	
HERJOLF H-92	1.53 ± 0.27	1.72 ± 0.23	1.87 ± 0.19	2.00 ± 0.20	2.26 ± 0.81	
BJARNI H-81	1.54 ± 0.17	1.65 ± 0.09	1.73 ± 0.13	1.84 ± 0.14	1.96 ± 0.14	
GUDRID H-55	1.83 ± 0.07	1.89 ± 0.09	1.98 ± 0.21	2.11 ± 0.17	2.30 ± 0.39	2.57 ± 0.36
CARTIER D-70	1.42 ± 0.11	1.50 ± 0.17	1.69 ± 0.20	1.78 ± 0.08	1.83 ± 0.07	
INDIAN HARBOUR M-52	1.70 ± 0.09	2.13 ± 0.59	2.37 ± 0.06	2.55 ± 0.28	2.96 ± 0.09	3.11 ± 0.37
LEIF M-48	1.44 ± 0.13	1.58 ± 0.05	1.62 ± 0.05	1.69 ± 0.08		
FREYDIS B-87	1.21 ± 0.10	1.27 ± 0.08	1.32 ± 0.08	1.40 ± 0.14	1.52 ± 0.10	1.59 ± 0.07
HARE BAY E-21	1.91 ± 0.26	2.17 ± 0.28	2.66 ± 0.36	2.89 ± 0.11	3.02 ± 0.13	3.16 ± 0.14
BLUE H-28	3.88 ± 0.31	4.27 ± 0.55	4.68 ± 0.09	4.74 ± 0.05		
BONAVISTA C-99	2.71 ± 0.68	3.12 ± 0.22	3.36 ± 0.11	3.47 ± 0.13		
CUMBERLAND B-55	2.41 ± 0.23	2.80 ± 0.25	3.06 ± 0.69	3.32 ± 0.10	3.51 ± 0.25	
BONANZA M-71	1.75 ± 0.18	2.75 ± 0.72	3.12 ± 0.23	3.33 ± 0.18		
DOMINION O-23	1.66 ± 0.39	1.88 ± 0.24	2.10 ± 0.23	2.52 ± 0.46	2.93 ± 0.53	
SOUTH TEMPEST G-88	1.42 ± 0.05	1.57 ± 0.43	2.00 ± 0.37	2.31 ± 0.11		
FLYING FOAM I-13	1.35 ± 0.38	1.62 ± 0.26	1.75 ± 0.27	1.98 ± 0.16		
ADOLPHUS D-50	1.37 ± 0.08	1.67 ± 0.29	1.88 ± 0.12	2.31 ± 0.32	2.60 ± 0.10	
HIBERNIA P-15	1.10 ± 0.11	1.20 ± 0.08	1.35 ± 0.07			
EGRET K-36	0.58 ± 0.11					
OSPREY H-84	0.70 ± 0.11	0.75 ± 0.06	0.79 ± 0.06			

Table 7.6: Calculated depth of isochrons in the twenty-three wells of the study area. The estimate of error corresponds to the local error bars as measured in CASC.

Figure 7.6: Isochron correlation chart of the Labrador Shelf wells. The time lines are selected at 5 Ma intervals, from 5 Ma to 60 Ma B.P..

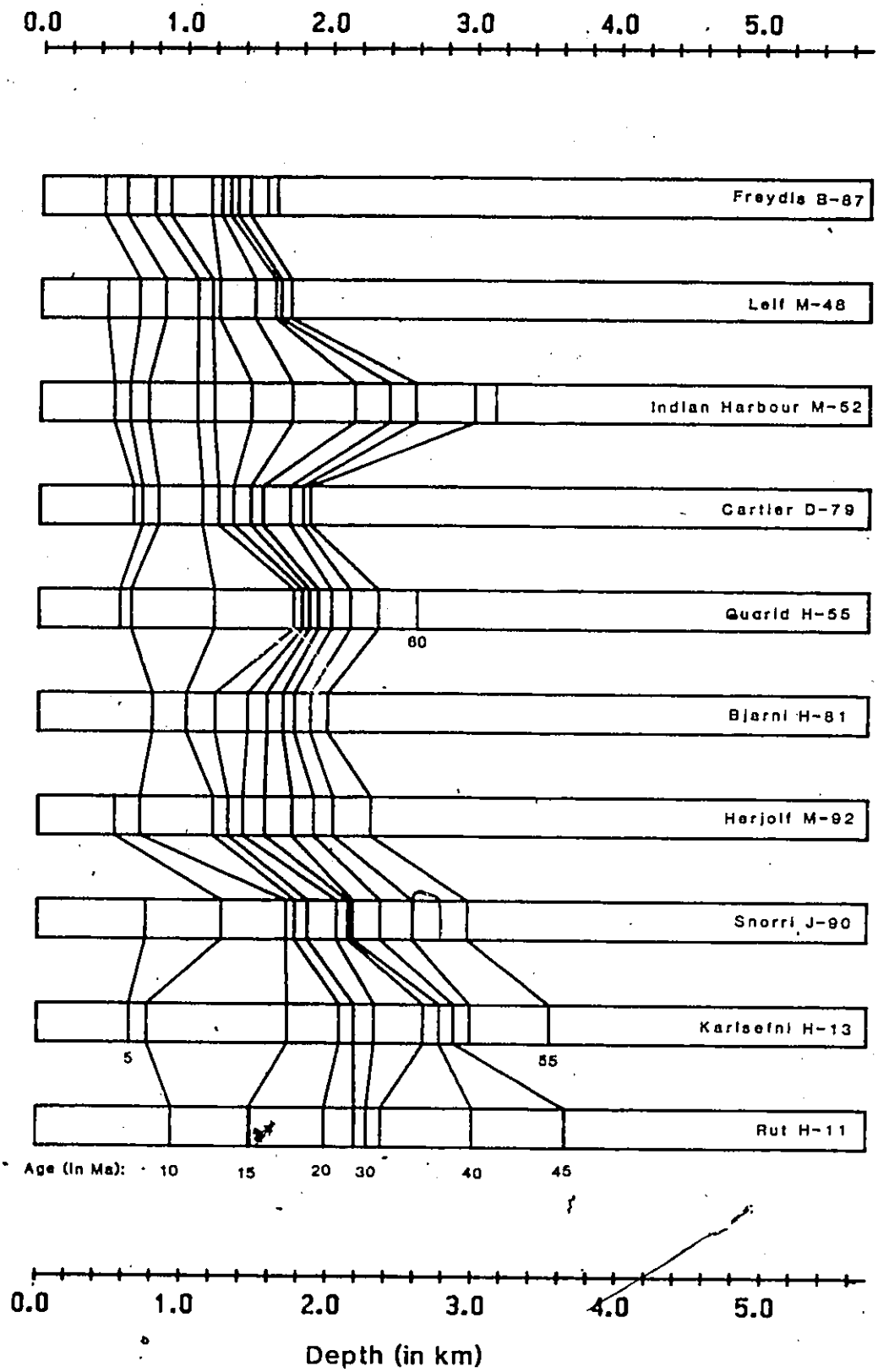
0.0
1.0
2.0
3.0
4.0
5.0
Freydis B-87
Leif M-48
Indian Harbour M-52
Cartier D-79
Quarid H-55
60
Bjarni H-81
Herjolf M-92
Snorri J-90
Karlsefni H-13
5
55
Rut H-11
Age (in Ma):
10
15
20
30
40
45
0.0
1.0
2.0
3.0
4.0
5.0
Depth (in km)

Figure 7.7: Isochron correlation chart of the Grand Banks wells. The time lines are selected at 5 Ma intervals, from 5 Ma to 60 Ma B.P..

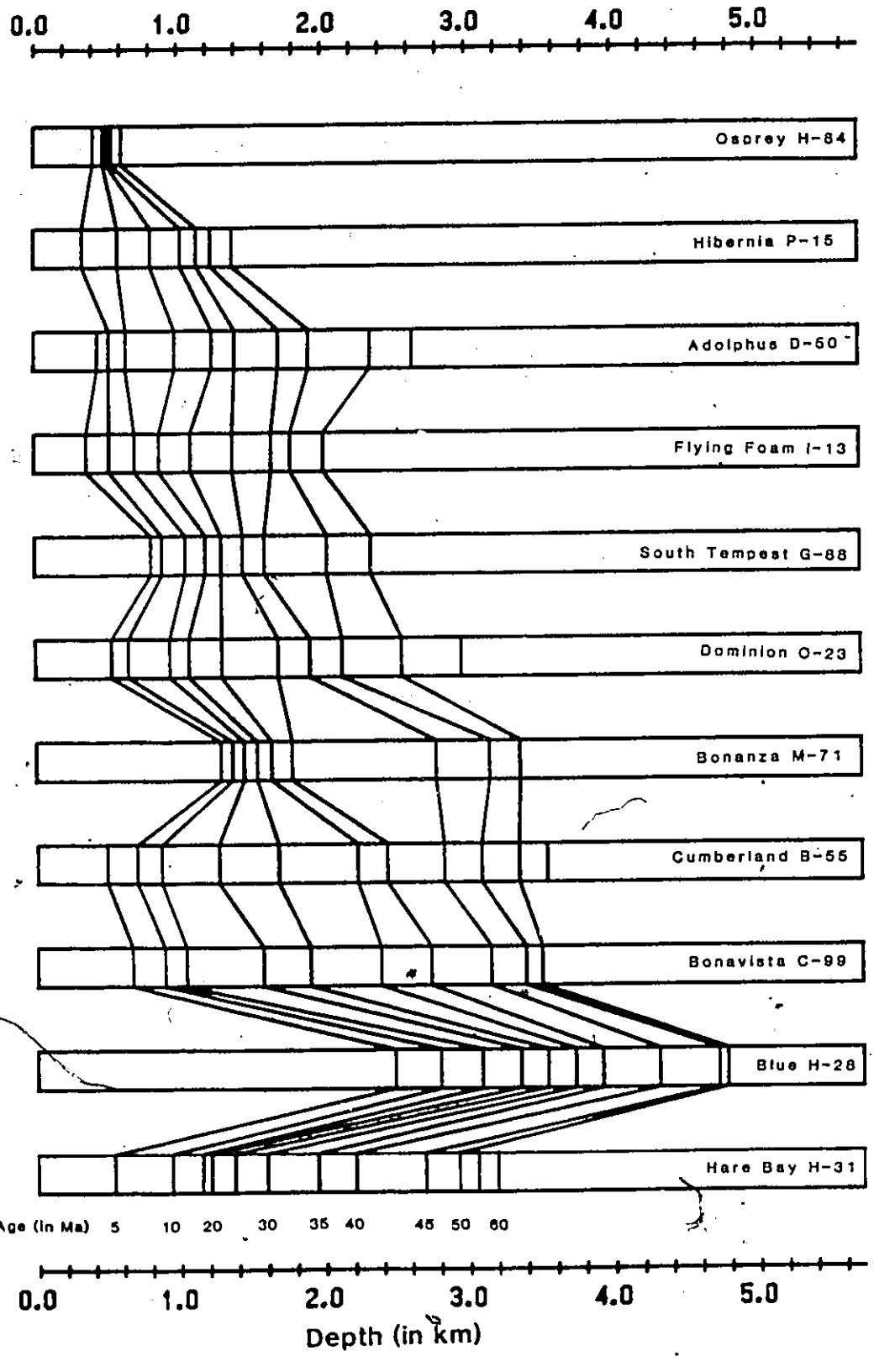
0.0
1.0
2.0
3.0
4.0
5.0
Osprey H-84
Hibernia P-15
Adolphus D-50
Flying Foam I-13
South Tempest G-88
Dominion O-23
Bonanza M-71
Cumberland B-55
Bonavista C-99
Blue H-28
Hare Bay H-31
Age (in Ma) 5 10 20 30 35 40 45 50 60
0.0
1.0
2.0
3.0
4.0
5.0
Depth (in km)

Figure 7.8: Plot the CASC estimated epoch boundary depths versus the biostratigraphically estimated ones. The straight line represent the perfect correlation line with a slope of 1. The squares and circles represent the comparison of CASC depths with foraminifer and palynomorph derived depth estimates, respectively.

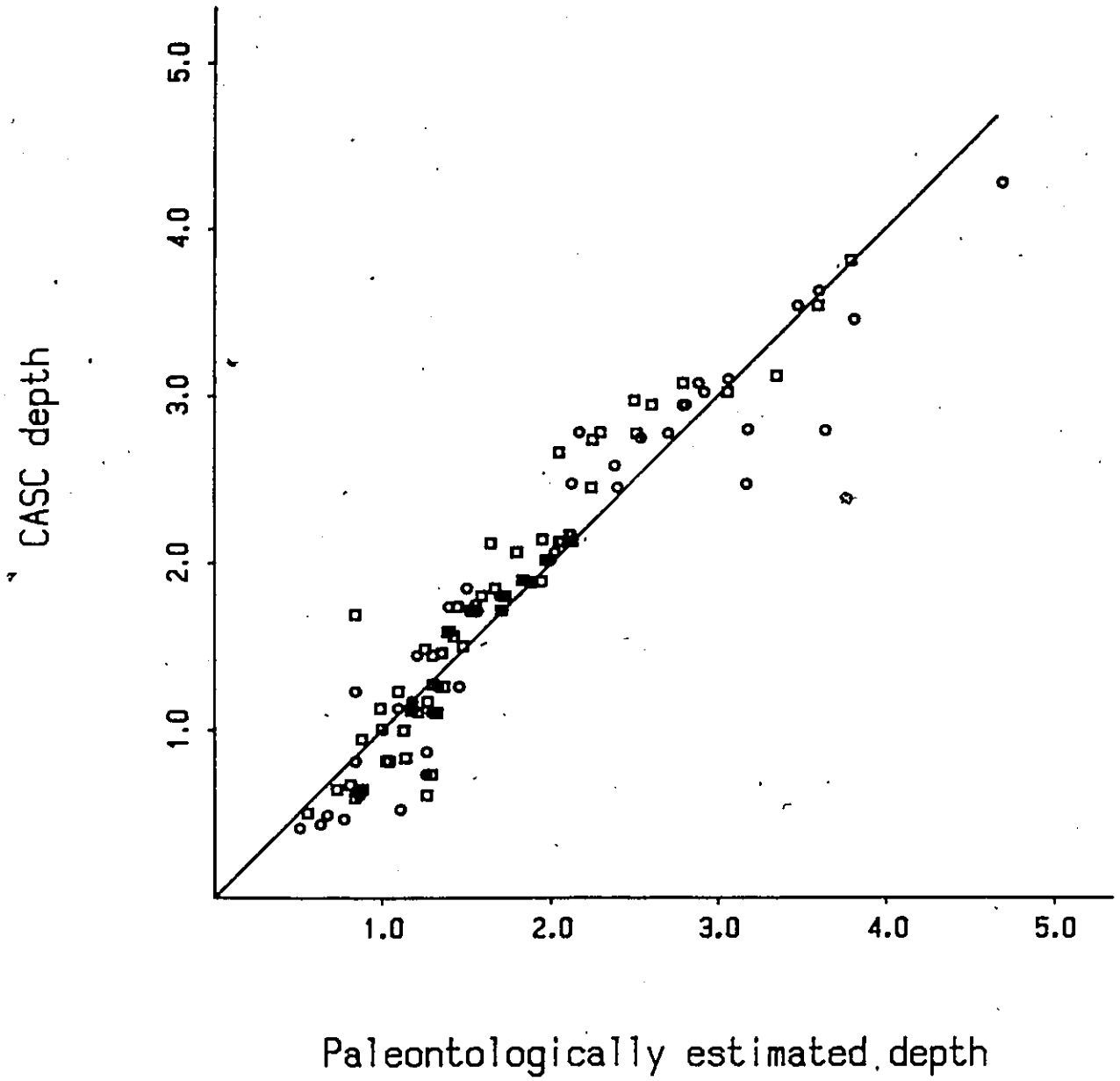
CASC depth
5.0
4.0
3.0
2.0
1.0
1.0
2.0
3.0
4.0
5.0
Paleontologically estimated depth

The comparative plot of Figure 7.8 is based on 58 palynomorph and 49 foraminiferal depth estimates. The mean deviations from the CASC estimate are -0.03 km and 0.07 km for foraminifers and palynomorphs, respectively. Depth estimates based on the three sources (i.e.; CASC, foraminifers and palynomorphs) are available in 30 situations. When both paleontological estimates are available, the mean deviations from CASC values are closer (see Table 7.7). The foraminiferal estimates of depth for the epoch boundaries are, on average, closer than the ones based on palynomorphs. The corresponding unbiased sample standard deviations are, however, similar (see Table 7.7).

Three distinct groups are observable in Figure 7.8. The first consists of CASC depths estimates lesser than approximately 1.3 km and smaller than the paleontological estimates. The third group is made up of CASC depth estimates greater than 2.3 km and more than 150 m smaller than the corresponding paleontological estimates. Finally, the second group is made up of all the estimates that do not belong to groups 1 or 3. In general, the CASC depth estimates the epoch boundaries of group 2 are greater than the paleontological estimates.

By definition, the depth estimates of group 1 represent cases in which the CASC value is smaller than the paleontological estimates. When both foraminiferal and

Table 7.7: Mean deviations of CASC and paleontologically estimated depths of Cenozoic epoch boundaries. The deviations are expressed in km. The three groups are defined in the text. The sub-groups of comparisons represents the epoch boundaries for which foraminiferal, palynomorph, and CASC depth estimates are available. The value n is the number of estimates used in calculating the mean.

			Mean	n
ALL GROUPS	all estimates	foraminifers:	-0.033	49
		palynomorphs:	0.067	58
		Combined:	0.022	107
	sub-group	foraminifers:	0.050	30
		palynomorphs:	0.063	30
		Combined:	0.057	60
GROUP 1	all estimates	foraminifers:	-0.220	15
		palynomorphs:	-0.202	17
		Combined:	-0.211	32
	sub-group	foraminifers:	-0.169	8
		palynomorphs:	-0.270	8
		Combined:	-0.220	16
GROUP 2	all estimates	foraminifers:	0.152	29
		palynomorphs:	0.189	40
		Combined:	0.174	69
	sub-group	foraminifers:	0.148	22
		palynomorphs:	0.167	22
		Combined:	0.157	44
GROUP 3	all estimates	foraminifers:	-0.542	5
		palynomorphs:	-0.234	1
		Combined:	-0.491	6
	sub-group	foraminifers:	N/A	0
		palynomorphs:	N/A	0
		Combined:	N/A	0

palynomorph depth estimates are available, the foraminifers seem to better approximate the CASC estimated depth, as can be observed in Table 7.7. This bias could have been expected because the chronostratigraphic calibration of the RASC scale is based on twice as many foraminiferal ages as palynomorph ages.

A possible cause for the lower CASC epoch boundary estimates is systematic underestimation of depth by the CASC spline-curve. Alternatively, the age of the events could have been systematically overestimated at the top of the optimum sequence causing underestimation of the depth of time lines. This second hypothesis is the preferred explanation for the observed deviations: When overestimated age values are assigned to events, underestimated depth of time line will result (see Figure 7.9 (c)). The overestimation of the age of a chronostratigraphic event in a section can be due to two factors: either the reworking of the fossil species, or an underestimation of its RASC position (see Figure 7.9 (d)). The underestimation of the RASC position of events is consistent with the findings of the frequency distribution study (see section 5.5) where a systematic departure was observed in the youngest section of the optimum sequence.

The second group of epoch boundary depth estimates indicates closer correlations of estimates from the different sources, though the foraminiferal depth estimates are again

Figure 7.9 (a): Theoretical age-depth curve. The number 1 identifies the perfect correlation line.

Figure 7.9 (b): Theoretical age-depth curve using underestimated ages values. The resulting curve 2, exhibits overestimated depths of time lines.

Figure 7.9 (c): Theoretical age-depth curve using overestimated ages values. The resulting curve 3, exhibits underestimated depths of time lines.

Figure 7.9 (d): Theoretical age versus RASC distance curve. For the ages to be overestimated, either the RASC distances are underestimated or the biostratigraphic age assignments are wrong.

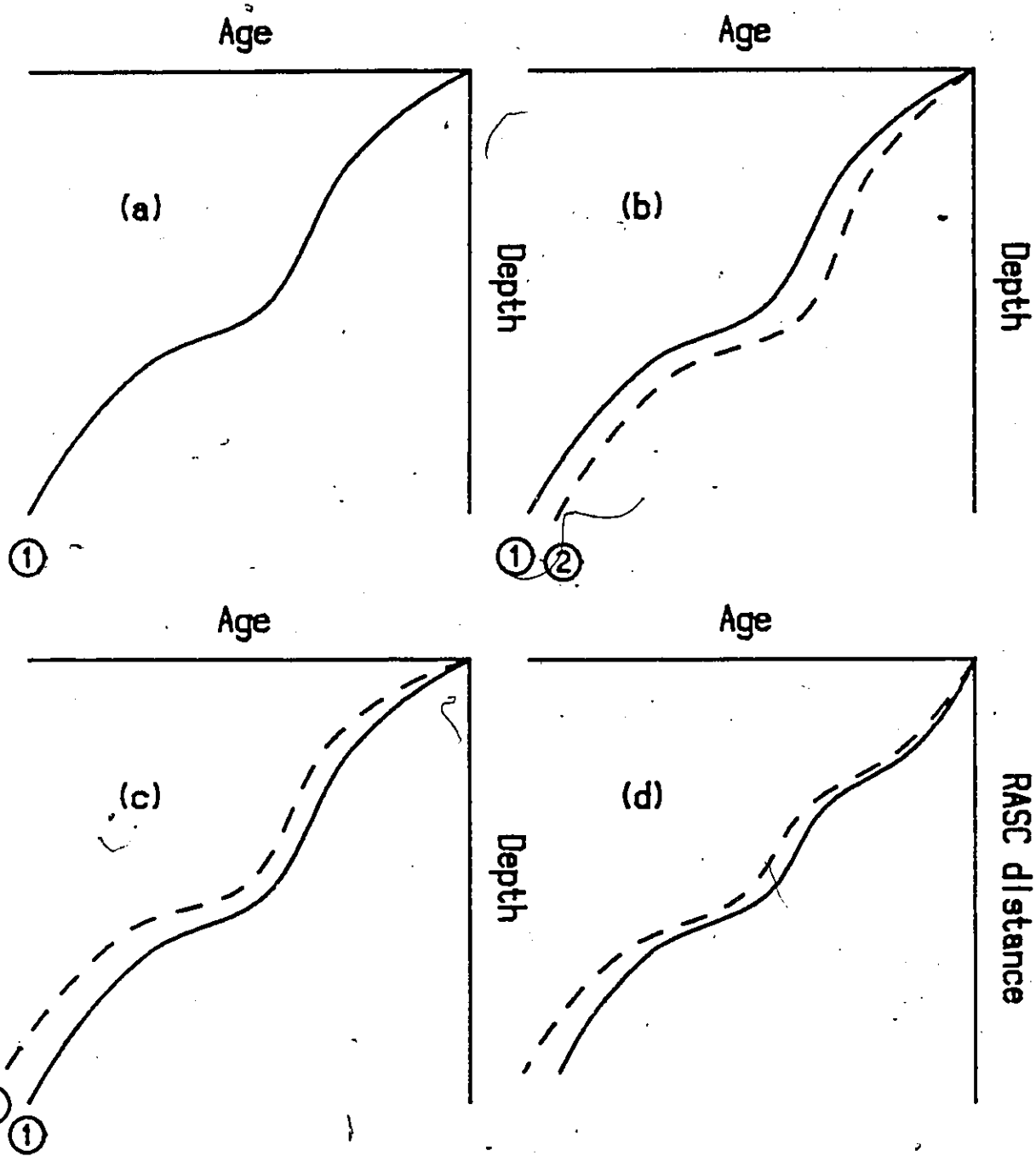
Age
(a)
Depth
1
Age
(b)
Depth
1
2
Age
(c)
Depth
3
1
Age
(d)
RASC distance

closer to the corresponding CASC values. The depths of the boundaries are estimated to be deeper by CASC than by conventional biostratigraphy. Because the CASC age-depth estimates are systematically slightly greater than expected over a considerable range of depth, it is probable that the assigned numerical ages are underestimated for what corresponds to the middle part of the optimum sequence. These results are consistent with a slight overestimation of the RASC position of events (see Figure 7.9 (d)) as was observed in the frequency distribution study (see section 5.5 and Figure 5.2).

The third group of events is small and contains mostly foraminiferally based boundary depth estimates. Further investigation reveal that 5 of the 6 estimates come from the Blue well, which is further offshore than the others used in this compilation. The discrepancies can be explained by either an underestimation of depths by CASC implying again an overestimation of the ages of events. This could be the result of a longer survival of events in the Blue well because of its geographic position. Another possibility is that the biostratigraphic estimates of epoch boundary depths are too large.

7.6 Conclusions

(7a) Tracing RASC biozones between all wells of the study area using the CASC method effectively identifies patterns of rates of sediment accumulations.

(7b) CASC depth estimates of Cenozoic epoch boundaries are consistent with the corresponding boundary depths assigned in the atlas of the Labrador sea (Gradstein, 1986).

(7c) The deviations between CASC estimates of depth and biostratigraphically assigned values exhibit a behaviour similar to that of the calculated frequency distributions of Chapter 5.

8. Epilogue

The integration of palynological and foraminiferal data yields a higher resolution biozonation than was previously available. The increase in resolution is two-fold; the first effect is due to the particular nature of the data sets. As they are partially complementary, the integration produces a geologically more complete data set. The second factor is that the measured RASC interevent distances are based on a greater number of estimates. The integrated biozonation shows a statistically significant rank correlation with a literature sequence of events.

A numerical time scale is built using the positions of the events in the RASC sequence and the published ages of a subset of the events in that sequence. Lithostratigraphic markers show a high correlation between published and RASC inferred ages. Because of resolution of the RASC sequence, the ensuing numerical time scale is useful for chronostratigraphic purposes and objective correlation.

The combined use of RASC and correspondence analysis provides valuable insights into the presence of paleo-environmental gradients, and more specifically into the onset and decline of paleoceanographic currents. There is a strong indication that the Labrador current began at the beginning of

RASC zone X (Middle Miocene). Correspondence analysis results clearly denote that the Eocene climatic warming began early in RASC zone II.

The frequency distribution method provides reliable estimates of frequency distributions, as indicated by a pooled variance measure of $\sigma^2 = 0.48$ compared to an expected value of $\sigma^2 = 0.5$. The event variance estimates indicate unequal variances of events and provide values to be used in a refined RASC model. The new model produces a biozonation that stabilizes after three times estimating the frequency distributions and inputing them into modified RASC. The normality of event distributions is ascertained through a chi-squared test of goodness of fit applied to a composite histogram of standardized event distributions. A systematic deviation indicates underestimation of RASC distances at the top of the scaled optimum sequence and overestimation at the bottom. Because the optimum sequence is constructed starting at a distance of 0, this trend reflects a "stretching" at both ends of the sequence. This is probably caused by an insufficient amount of data in the sections of several wells. To estimate the frequency distributions, the deviations between RASC position and well position of events must be calculated. These estimates provide a valuable insight into the synchroneity of events and, consequently, into their value as markers.

The RASC model seems robust with respect to its critical probit value (AAA). Increasing this parameter yields a proportional increase in scaled optimum sequence length before final reordering and a similar general trend after final reordering. Changes in AAA result in minor reordering of events. The greater the differences in AAA value between two sequences, the more reordering will occur. The amount of deviation of event ranks between sequences is not statistically significant, as reflected by Kendall Tau rank coefficient values in excess of 0.95 between pairs of sequences of different probit critical values. The AAA values produce greater variation at the top and bottom of scaled sequences and in zones bounded by marked unconformities or disconformities where a few events may have been reworked or caved-in. These results are consistent with the deviations observed in the frequency distribution study.

The objective correlation technique of the CASC model provides an effective method of identifying patterns of sediment accumulations by tracing biozones and isochrons through the wells of the study area. The CASC estimated depths of Cenozoic epoch boundaries show good agreement with similar value determined through biostratigraphy. Deviations between the two estimates reflect previously discussed systematic deviations at the top and bottom of the optimum

sequence. These trends are consistent with the frequency distribution results.

LIST OF REFERENCES CITED

REFERENCES

Abramowitz, M., and Stegun, I.A., (eds.), 1965, Handbook of mathematical functions. Applied Mathematics Series, 55, National Bureau of Standards, Washington, 1046 p.

Agterberg, F.P., 1983, Quantitative stratigraphic correlation techniques. Nature and Resources, 19, no.4, p. 20-26.

Agterberg, F.P., 1988 (in press), Quality of time scales- a statistical appraisal. In: Merriam, D.F., (ed.), Computers and Geology 5. Pergamon press, Oxford.

Agterberg, F.P., and D'Iorio, M.A., 1988 (in press), Frequency distribution of highest occurrences of Cenozoic Foraminifera along the northwestern Atlantic Margin. Petrobras.

Agterberg, F.P., and Gradstein, F.M., 1983, Interactive system of computer programs for stratigraphic correlation. Current research, Geological Survey of Canada, paper 83-1A, p. 83-87.

Agterberg, F.P., and Gradstein, F.M., 1988 (in press), Recent developments in quantitative stratigraphy, Earth Science Reviews.

Agterberg, F.P., and Nel, L.D., 1982a, Algorithm for the Ranking of Stratigraphic Events, Computers & Geosciences, 8, no.1, p. 69-90.

Agterberg, F.P., and Nel, L.D., 1982b, Algorithm for the Scaling of Stratigraphic Events, Computers & Geosciences, 8, no.2, p. 163-182.

Agterberg, F.P., Oliver, J., Lew, S.N., Gradstein, F.M., and Williamson, M.A., 1985, CASC FORTRAN IV interactive computer program for correlation and scaling in time of biostratigraphic events. Geological Survey of Canada Open File 1179, 139 p.

Arthur, K.R., Cole, D.R., Henderson, G.G.L., and Kushuir, D.W., 1982, Geology of the Hibernia discovery. Presented at the American Association of Petroleum Geologists general assembly.

Balkwill, H.R., 1987 (in press), Labrador Basin structural and stratigraphic style. Decade of North American Geology, Geological Society of America.

Barss, M.S., Bujak, J.P., and Williams, G.L., 1979, Palynological zonation and correlation of sixty-seven wells, Eastern Canada. Geological Survey of Canada, Paper 78-24, Ottawa, 118 p.

Berggren, W.A., 1977, North Atlantic Cenozoic Foraminifera. In: Swain, F.M., (ed.), Stratigraphic micropaleontology of Atlantic Basin and borderlands. Elsevier Scientific Publishing Company, Amsterdam, p. 389-410.

Berggren, W.A., and Hollister, C.D., 1977, Plate tectonics and paleocirculation - commotion in the ocean. Tectonophysics, 38, p. 11-48.

Berggren W.A., Kent,D.V., Flynn J.J. and van Couvering J.A., 1985, Cenozoic geochronology. Geological Society of America Bulletin, 96, p. 1407-1418.

Boersma, A., 1978, Foraminifera. In: Haq, B.U., and Boersma, A., (eds.), Introduction to marine micropaleontology, Elsevier Biomedical, Amsterdam, p. 19-78.

Bonham-Carter, G.F., Gradstein, F.M., and D'Iorio, M.A., 1986, Distribution of Cenozoic Foraminifera from the northwestern Atlantic margin analysed by correspondence analysis, Computers & Geosciences, 12, no.4b, p. 621-635.

Brauer Hudson, C.B., and Agterberg, F.P., 1982, Paired comparison models in biostratigraphy. Journal of Mathematical Geology, 14, no.2, p. 141-159.

Brazier, M.D., 1980, Microfossils. George Allen & Unwin Ltd., London, 193 p.

Costa, L.I., 1985, A regional zonation for the Tertiary of Northwest Europe and its continental shelf. Norwegian Petroleum Directorate Bulletin, 4, Stavanger, p. 1-14.

Costa, L.I., and Downie, C., 1979, Cenozoic dinocyst stratigraphy of sites 403 to 406 (Rockall Plateau), IPOD, Leg 48, In: Montadert, L., and Roberts, D.G., Deep Sea Drilling Project initial reports, 48, Washington, p. 513-529.

Craven, P., and Wahba, G., 1979, Smoothing noisy data with spline functions. Numerische Mathematik, 31, p. 377-403.

De Boor, C., 1978, A practical guide to splines. Springer-Verlag, New York, 392 p.

D'Iorio, M.A., 1986, Integration of foraminiferal and dinoflagellate data sets in quantitative stratigraphy of the Labrador Shelf and Grand Banks, Bulletin of Canadian Petroleum Geology, 34, no.2, p. 277-283.

D'Iorio, M.A., 1987, Quantitative stratigraphic analysis of 23 Canadian offshore wells. The Compass , 64, no.4, p. 264-277.

Gauch, H.G., 1982, Multivariate analysis in community ecology. Cambridge University Press, 298 p.

Goodman, D.K., and Witmer, R.J., 1985, Archeophyle variation and paratabulation in the dinoflagellate Diphyes colligerum (Deflandre & Cookson 1955) Cookson 1965. Palynology, 9, p. 61-84.

Gradstein, F.M., 1985, Ranking and scaling in exploration micropaleontology. In: Gradstein, F.M., Agterberg, F.P., Brower, J.C., and Schwarzacher, W.W., (eds.), Quantitative stratigraphy, Reidel Publishing Co., and UNESCO, Paris, p. 109-160.

Gradstein, F.M., 1986, Interpretaion of the Biostratigraphy from offshore wells on the Canadian Atlantic Margin. In: Srivastava, S.P. (ed.), 1986, Geophysical maps and geological sections of the Labrador Sea. Geological Survey of Canada, Paper 85-16, Ottawa, 11 p.

Gradstein, F.M., and Agterberg, F.P., 1982, Models of Cenozoic foraminiferal stratigraphy- northwestern Atlantic Margin. In: Cubitt, J.M., and Reyment, R.A., (eds.), Quantitative stratigraphic correlation, John Wiley & Sons, New York, p. 119-170.

Gradstein, F.M., and Agterberg, F.P., 1985, Quantitative correlation in exploration micropaleontology. In: Gradstein, F.M., Agterberg, F.P., Brower, J.C., and Schwarzacher, W.W., (eds.), Quantitative stratigraphy, Reidel Publishing Co., and UNESCO, Paris, p. 309-357

Gradstein, F.M., Agterberg, F.P., Brower, J.C., and Schwarzacher, W.W., (eds.), 1985, Quantitative stratigraphy. Reidel Publishing Co., and UNESCO, Paris, 598 p.

Gradstein, F.M., Agterberg, F.P., and D'Iorio, M.A., 1988a (in press), Quantitative sequence stratigraphy and probabilistic time scale. In: Cross, A.T., Quantitative dynamic stratigraphy.

Gradstein, F.M., Keminsky, M.A., Berggren, W.A., and D'Iorio, M.A., 1988b (in preparation), Cenozoic biostratigraphy and paleoceanography, North Sea and Labrador Sea. Geologie and Mijnbouw (special issue).

Gradstein, F.M., and Srivastava, S.P., 1980, Aspects of Cenozoic stratigraphy and paleoceanography of the Labrador Sea and Baffin Bay, Palaeogeography, Palaeoclimatology, Palaeoecology, 30, p.261-295.

Grant, A.C., 1980, Problems with plate tectonics: The Labrador Sea. Bulletin of Canadian Petroleum of Geology, 28, no.2, p. 252-278.

Hald, A., 1952, Statistical tables and formulas. John Wiley & Sons Publications, New York, 97p.

Harland, R., 1978, Quaternary and Neogene dinoflagellate cysts. In: Thesu B. (ed.), Distribution of biostratigraphically diagnostic dinoflagellate cysts and miospores from the Northwest European continental shelf and adjacent areas. Continental Shelf Institute publication no.100, Trondheim, p. 7-17.

Harper, C.W., 1984, A FORTRAN IV program for comparing ranking algorithms in quantitative biostratigraphy. Computers & Geosciences, 10, no.1, p. 3-29.

Hay, W.W., 1972, Probabilistic stratigraphy. Eclogae Geologicae Helveticae, 65, no.2, p. 255-266.

Heller, M., Gradstein, W.S., Gradstein, F.M. and Agterberg, F.P., 1983, RASC FORTRAN IV computer program for ranking and scaling of biostratigraphic events. Geological Survey of Canada, Open File 924, 54 p.

Heller, M., Gradstein, W.S., Gradstein, F.M., Agterberg, F.P., and Lew, S.N., 1985, RASC FORTRAN 77 computer program for ranking and scaling of biostratigraphic events. Geological Survey of Canada, Open File 1203.

Heuser, L, 1978, Spores and pollen in the marine realm. In: Haq, B.U., and Boersma, A., (ed.), Introduction to marine micropaleontology, Elsevier Biomedical, Amsterdam, p.327-340.

Hill, M.O., 1973, Reciprocal averaging: an eigenvector method of ordination. Journal of Ecology, 61, p. 237-249.

Hill, M.O., 1979, DECORANA a FORTRAN program for detrended correspondence analysis and reciprocal averaging, Cornell University, New York, 30 p.

Hogg, R.V., and Tanis E.A., 1985, Probability and statistical inference, second edition. MacMillan Publishing co., New York, 533 p.

Jan du Chene, R.J., 1977, Etude palynologique du Miocène Supérieur Andalou (Espagne), Revista Española Micropaleontologia, 9, p. 97-114.

Kendall, M.G., 1970, Rank correlation methods, Fourth Edition, Charles Griffin & Company Ltd, London, 202 p.

Manum, S.B., 1976, Dinocysts in Tertiary Norwegian-Greenland Sea sediments (Deep Sea Drilling Project Leg 38), with observations on palynomorphs and palynodebris in relation to environments. In: Talwani, M., and Udintsev, G., et al., Initial reports of the Deep Sea Drilling Project, 38, Washington, p. 897-919.

McWhae, J.R.H., 1981, Structure and spreading history of the Northwest Atlantic from the Scotian Shelf to Baffin Bay. In: Kerr, J.W., and Fergusson, A.J., (eds.), Geology of the North Atlantic Borderlands. Canadian Society of Petroleum Geologists, Memoir 7, p. 299-332.

McWhae, J.R.H., Elie, R., Laughton, D.C., and Gunther, P.R., 1980, Stratigraphy and petroleum prospect of the Labrador Shelf. Bulletin of Canadian Petroleum Geololgy, 28, p. 460-488.

Reinsch, C.H., 1967, Smoothing by spline functions. Numerische Mathematik, 10, p. 177-183.

Reinsch, C.H., 1971, Smoothing by spline functions II. Numerische Mathematik, 16, p. 451-454.

Sarjeant, W.A.S., 1984, Re-study of some dinoflagellate cysts from the Oligocene and Miocene of Germany. Journal of Micropaleontology, 3, no.2, p. 73-94.

Sclater J.G., Hellinger, S., and Tapscott C.R., 1977, The paleobathymetry of the Atlantic Ocean from the Jurassic to the present. Journal of Geology, 85, no.5, p. 509-551.

Srivastava, S.P., 1978, Evolution of the Labrador Sea and its bearing on the early evolution of the North Atlantic. Geophysical Journal of the Royal Astronomical Society, 52, p. 313-357.

Srivastava, S.P. (ed.), 1986, Geophysical maps and geological sections of the Labrador Sea. Geological Survey of Canada, Paper 85-16, 11 p.

Srivastava, S.P., and Tapscott, C.R., 1986, Plate kinematics of the North Atlantic. In: Vogt, P.R., and Tucholke, B.E., (eds.), The Geology of North America, M, The Western North Atlantic Region, Geological Society of America, p. 379-404.

Stover, L.E., 1977, Oligocene and early Miocene dinoflagellates from Atlantic core hole 5/5B, Blake Plateau. In: Elsik, W.C., (ed.), Contributions of stratigraphic palynology volume 1, Cenozoic palynology, American Association of Stratigraphic Palynologists, Contribution Series no.5a, p. 66-89.

Tjalsma, R.C., and Lohmann, G.P., 1983, Paleocene-Eocene bathyal and abyssal benthic Foraminifera from the Atlantic Ocean. Micropaleontology Special Publication, 4, 76 p.

Umpleby, D.C., 1979, Geology of the Labrador Shelf. Geological Survey of Canada, Paper 79-13, Ottawa, 34 p.

Van der Linden, W.J., Fillon, R.H., and Monahan, D., 1976, Hamilton Bank, Labrador Margin: Origin and Evolution of a glaciated Shelf. Geological Survey of Canada, Paper 75-40.

Vogt, P.R., Avery, O.E., Anderson, C.N., Bracey, D.R., and Schneider, E.D., 1969, Discontinuity in sea-floor spreading. Tectonophysics, 8, p. 285-317.

Wahba, G., 1975, Smoothing noisy data with spline functions. Numerische Mathematik, 24, p. 383-393.

Williams, G.L., 1978, Dinoflagellates, acritarchs and tasmanitids. In: Haq, B.U., and Boersma, A., (eds.), Introduction to marine micropaleontology, Elsevier Biomedical, Amsterdam, p.293-326.

Williams, G.L., and Bujak, J.P., 1985, Mesozoic and Cenozoic Dinoflagellates. In: Bolli, Saunders, and Perch-Nielsen, (eds.), Plankton stratigraphy, Cambridge University Press, U.K., p. 847-964.

Williamson, M.A., 1987, A quantitative foraminiferal biozonation of the Late Jurassic and Early Cretaceous of the East Newfoundland Basin. Micropaleontology, 33, no.1, p.37-65.

Williamson, M.A., and Agterberg, F.P., 1988 (in press), A quantitative correlation of the Jurassic-Cretaceous of the Hibernia area. Canadian Journal of Earth Sciences.

Wold, S., 1974, Spline functions in data analysis. Technometrics, 16, no.1, p. 1-11.

APPENDIX A

LIST OF DATA AND DICTIONARY

APPENDIX

LIST OF FORAMINIFERA, DINOFLAGELLATE AND SPORES AND POLLEN DATA SET

RUT H-11 (M)

Rotary table height: 12.0M
Water depth: 124.0M

Depth	Number	Fossil Name
675.	17	ASTERIGERINA GURICHI
	77	ELPHIDIUM SPP.
2150.	25	COARSE ARENACEOUS SPP.
	80	CYCLAMMINA CANCELLATA
2270.	259	AMMODISCUS LATUS
2910.	129	CYCLAMMINA PLACENTA
2950.	53	UVIGERINA PATJESI
3030.	205	NUTTALINELLA FLOREALIS
	39	ALABAMINA WILCOXENSIS
3110.	96	ACARININA INTERMEDIA WILCOXENSIS
3150.	63	NODOSARIA CF. POZOENSIS
3470.	230	BULIMINA OVATA
4070.	68	SPIROPLECTAMMINA SPECTABILIS LO

KARLSEFNI H-13 (F)

Rotary table height: 40.0F
Water depth: 573.0F

Depth	Number	Fossil Name
1760.	228	CASSIDULINA TERETIS
	283	PINUS
1960.	287	PODOCARPIDITES DA
	293	TSUGAEPOLLENITES INGNICULUS
2260.	501	OPERCULOPINIUM CENTROCARPUM
	276	ABIES
	282	OSMUNDACIDITES DA
2350.	552	SPINIFERITES PSEUDOFURCATUS
	569	SYSTEMATOPHORA ANCYREA
3150.	279	BOMBACACIDITES DA
3570.	585	TRITHYRODINIUM
4150.	289	SEQUOIAPOLLENITES
4350.	342	CHLAMYDOPHORELLA NYEI
4450.	345	ALTERBIA
	515	PARALECANIELLA INDENTATA
5894.	576	THALASSIPHORA DELICATA

KARLSEFNI H-13 (F)

Depth	Number	Fossil Name
6260.	67	SCAPHOPOD SP. 1
6374.	369	CYCLOPSIELLA VIETA
	294	NYSSAPOLLENITES DA
6460.	478	LINGULODINIUM MACHAEROPHORUM
6720.	358	CYCLONEPHELIUM DISTINCTUM
	405	EPICEPHALOPYXIS
	288	POLYPODIACIDITES DA
6760.	25	COARSE ARENACEOUS SPP.
6860.	434	HYSTRICHOSPHAERIDIUM
	470	LENTINIA
7020.	479	LINGULODINIUM DC
	316	XENIKOON DA
	295	NYASSAPOLLENITES DB
7060.	118	EPISTOMINA SP. 5
	321	CARPODINIUM
	338	CHIROPTERIDIUM MESPILANUM
	433	HYSTRICHOKOLPOMA RIGAUDIAE
	41	PLECTOFRONDICULARIA AFF. PAUCICOSTATA
7200.	558	SPINIFERITES DA
7250.	69	NODOSARIA CF. ELEGANTISSIMA
	419	GLADHROCYSTA PASTIELSII
	577	THALASSIPHORA PATULA
7380.	480	LITHODINIA
7514.	372	DAPSILIDINIUM SIMPLEX
	296	OSMUNDACIDITES
7972.	284	PISTILLIPOLLENITES MCGREGORII
8600.	377	DEFLANDREA PHOSPHORITICA
	397	EATONICYSTA URSULAE
	570	SYSTEMATOPHORA AREOLATA
8660.	260	HAPLOPHRAGMOIDES KIRKI
	261	HAPLOPHRAGMOIDES WALTERI
	301	APECTODINIUM QUINQUELATUM
8760.	68	SPIROPLECTAMMINA SPECTABILIS LO
	39	ALABAMINA WILCOXENSIS
8800.	317	ACHILLEODINIUM BIFORMOIDES
8960.	53	UVIGERINA BATJESI
	206	EPONIDES POLYGONUS
	173	ANOMALINA SP. 1
	591	WETZELIELLA ARTICULATA
9060.	29	CYCLAMMINA AMPLECTENS
9080.	378	DEFLANDREA CF PHOSPHORITICA
9160.	86	TURRILINA ROBERTSI
	30	CIBICIDOIDES BLANPIEDI
	63	NODOSARIA CF. POZOENSIS
	34	MARGINULINA DECORATA
	300	APECTODINIUM PARVUM
9260.	297	MEGASPORE SP. 1

KARLSEFNI H-13 (F)

Depth	Number	Fossil Name
	264	KARRERIELLA CONVERSA
9260.	376	DEFLANDREA OEBISFELDENSIS
9360.	500	OPERCULOPINIUM CF HIRSUTUM
	599	WILSONIDIUM ECHINOSUTURATUM
9460.	230	BULIMINA OVATA
	44	CIBICIDOIDES AFF. WESTI
	42	CIBICIDOIDES ALLENI
9464.	348	CORDOSPHAERIDIUM GRACILE
	388	DINOPETEIGIUM CLADOIDES SENSU MORG.
9660.	96	ACARININA INTERMEDIA WILCOXENSIS
	36	PSEUDOHASTIGERINA WILCOXENSIS
	314	AZOLLA
	403	EOCLADOPYXIS PENICULATA (REWORKED)
	427	HOMOTRYBLIUM TENUISPINOSUM
	438	HYSTRICHOSPHAERIDIUM SALPINGOPHORUM
9752.	326	CERATIOPSIS SPECIOSA
9760.	313	AREOSPHAERIDIUM DA
	373	DEFLANDREA DENTICULATA
9968.	375	DEFLANDREA HYALINA
10044.	582	TRIGONOPYXIDIA
10192.	270	CIBICIDOIDES GROSSA
	424	HETERAULACACYSTA LEPTALEA
10260.	164	NUTTALIDES TRUMPYI
	50	SUBBOTINA PATAGONICA
10843.	286	PLATYCARYAPOLLENITES DA
10952.	52	ACARININA SOLDADOENSIS
11043.	533	PTERODINIUM CINGULATUM
11440.	467	LEJEUNECYSTA HYALINA
11663.	45	BULIMINA TRIGONALIS
	54	SPIROPLECTAMMINA NAVARROANA
11851.	363	CYCLONEPHELIUM VANNOPHORUM
12450.	322	CERATIOPSIS DARTMOORIA
12460.	56	GLOMOSPIRA CORONA
12560.	55	GAVELINELLA BECCARIIFORMIS
	62	GAVELINELLA DANICA
12650.	512	PALAEOPERIDINIUM PYROPHORUM
12760.	61	SUBBOTINA PSEUDOBULLOIDES
	253	SUBBOTINA TRILOCULINOIDES
12950.	559	SPINIFERITES DB
12960.	258	TAPPANINA SELMENSIS
13150.	334	ALISOCYSTA CIRCUMTABULATA
13350.	308	XENASCUS
13450.	483	MELITASPHAERIDIUM

SNORRI J-90 (F)

Rotary table height: 37.0F
Water depth: 462.0F

Depth	Number	Fossil Name
1026.	296	OSMUNDACIDITES
1260.	77	ELPHIDIUM SPP.
	330	CHATANGIELLA
	358	CYCLONEPHELIUM DISTINCTUM
	283	PINUS
2060.	276	ABIES
2160.	293	TSUGAEPOLLENITES INGNICULUS
2660.	417	GLAPHROCYSTA INTRICATA
2760.	279	BOMBACACIDITES DA
2940.	228	CASSIDULINA TERETIS
3120.	339	CHIROPTERIDIUM LOBOSPINOSUM
4140.	560	SPONGODINIUM DELITIENSE
4250.	16	CERATOBULIMINA CONTRARIA
4410.	342	CHLAMYDOPHORELLA NYEI
	461	LACINIADINIUM
	282	OSMUNDACIDITES DA
	287	PODOCARPIDITES DA
4860.	67	SCAPHOPOD SP. 1
5040.	290	SEQUOIAPOLLENITES DA
5310.	415	GLAPHROCYSTA DIVARICATA
	288	POLYPODIACIDITES DA
5400.	502	OPERCULOPINIUM ISRAELIANUM
5490.	15	GLOBIGERINA PRAEBULLOIDES
	21	GUTTULINA PROBLEMA
5580.	347	CORDOSPHAERIDIUM FIBROSPINOSUM
	365	CYCLONEPHELIUM SP. C
	433	HYSTRICHOKOLPOMA RIGAUDIAE
	478	LINGULODINIUM MACHAEROPHORUM
	316	XENIKOON DA
5670.	431	HYSTRICHOKOLPOMA CINCTUM (REWORKED)
	600	WILSONIDIUM INTERMEDIUM
5760.	18	SPIROPLECTAMMINA CARINATA
5830.	328	CERATIOPSIS WARDENENSIS
	534	PYXIDIELLA
	547	SPINIFERITES MEMBRANACEUS
5940.	470	LENTINIA
	522	PHTHANOPERIDINIUM
6030.	435	HYSTRICHOSPHAERIDIUM DIFFICILE
6120.	447	IMPLETOSPHAERIDIUM SCALENFURCATUM
	294	NYSSAPOLLENITES DA
6480.	284	PISTILLIPOLLENITES MCGREGORII
6800.	25	COARSE ARENACEOUS SPP.
6930.	304	AREOLIGERA CORONATA
	372	DAPSILIDINIUM SIMPLEX

SNORRI J-90 (F)

Depth	Number	Fossil Name
6930.	377	DEFLANDREA PHOSPHORITICA
7020.	57	SPIROPLECTAMMINA SPECTABILIS LCO
	263	AMMOBACULITES AFF. POLYTHALAMUS
	32	AMMOSPHAEROIDINA SP. 1
	34	MARGINULINA DECORATA
	298	APECTODINIUM HOMOMORPHUM
7090.	29	CYCLAMMINA AMPLECTENS
	260	HAPLOPHRAGMOIDES KIRKI
	53	UVIGERINA BATJESI
	41	PLECTOFRONDICULARIA AFF. PAUCICOSTATA
	30	CIBICIDOIDES BLANPIEDI
	36	PSEUDOHASTIGERINA WILCOXENSIS
	173	ANOMALINA SP. 1
	440	HYSTRICHOSPHAERIDIUM TUBIFERUM
7110.	317	ACHILLEODINIUM BIFORMOIDES
	325	ACHOMOSPHAERA RAMULIFERA
	387	DINOPTERIGIUM CLADOIDES
	427	HOMOTRYBLIUM TENUISPINOSUM
	487	CRIBROPERIDINIUM GIUSEPPEI
7200.	27	EPONIDES UMBONATUS
	297	MEGASPORE SP. 1
7290.	397	EATONICYSTA URSULAE
7310.	118	EPISTOMINA SP. 5
7350.	264	KARRERIELLA CONVERSA
7380.	577	THALASSIPHORA PATULA
7525.	311	AREOSPHAERIDIUM DIKTYOPLOCUS
	314	AZOLLA
	426	HOMOTRYBLIUM ACULEATUM
	456	KISSELOVIA CLATHRATA
	591	WETZELIELLA ARTICULATA
	599	WILSONIDIUM ECHINOSUTURATUM
7650.	309	AREOSPHAERIDIUM
	326	CERATIOPSIS SPECIOSA
	390	DIPHYES COLLIGERUM
	536	RHOMBOIDINIUM GLABRUM
7680.	230	BULIMINA OVATA
7740.	376	DEFLANDREA OEBISFELDENSIS
	446	IMPAGIDINIUM VICTORIANUM
7830.	86	TURRILINA ROBERTSI
	63	NODOSARIA CF. POZOENSIS
	507	PALEOCYSTODINIUM BENJAMINII
	531	POLYSTEPHANOPHORUS
7940.	373	DEFLANDREA DENTICULATA
	393	DRACODINIUM CONDYLOS
8100.	348	CORDOSPHAERIDIUM GRACILE
8200.	42	CIBICIDOIDES ALLENI
	432	HYSTRICHOKOLPOMA CINCTUM TURGIDUM
	576	THALASSIPHORA DELICATA

SNORRI J-90 (F)

Depth	Number	Fossil Name
8270.	322	CERATIOPSIS DARTMOORIA
8370.	349	CORDOSPHAERIDIUM INODES
8940.	299	APECTODINIUM HYPERACANTHUM
9020.	505	PALEOCYSTODINIUM
9120.	45	BULIMINA TRIGONALIS
9620.	56	GLOMOSPIRA CORONA
9720.	343	ALISOCYSTA ORNATA
	512	PALAEOPERIDINIUM PYROPHORUM
9820.	59	RZEHAKINA EPIGONA
	54	SPIROPLECTAMMINA NAVARROANA

HERJOLF M-92 (F)

Rotary table height: 88.0F
Water depth: 456.0F

Depth	Number	Fossil Name
1600.	434	HYSTRICHOSPHAERIDIUM
	478	LINGULODINIUM MACHAEROPHORUM
	513	PALEOSTOMOCYSTIS DA
	552	SPINIFERITES PSEUDOFURCATUS
	565	SUMATRADINIUM
	569	SYSTEMATOPHORA ANCYREA
	276	ABIES
	283	PINUS
	293	TSUGAEPOLLENITES INGNICULUS
1700.	433	HYSTRICHOKOLPOMA RIGAUDIAE
1800.	340	CHIROPTERIDIUM PARTISPINATUM
	431	HYSTRICHOKOLPOMA CINCTUM (REWORKED)
	282	OSMUNDACIDITES DA
1900.	280	CHENOPODIUMSPORITES DA
2000.	338	CHIROPTERIDIUM MESPILANUM
	339	CHIROPTERIDIUM LOBOSPINOSUM
2200.	568	SVALBARDELLA
2400.	295	NYASSAPOLLENITES DB
2600.	330	CHATANGIELLA
	525	HANOPERIDINIUM COMATUM (REWORKED)
	546	SPINIDINIUM [illegible] VESTITUM
2800.	312	SPHAERIDIUM PECTINIFORME (REWORKED)
	287	PODOCARPIDITES DA
2900.	503	OVOIDINIUM
3000.	288	POLYPODIACIDITES DA
3300.	504	OVOIDINIUM VERRUCOSUM
3400.	347	CORDOSPHAERIDIUM FIBROSPINOSUM
	482	METOUROGONYAULAX
3500.	377	DEFLANDREA PHOSPHORITICA

HERJOLF M-92 (F)

Depth	Number	Fossil Name
3700.	501	OPERCULOPINIUM CENTROCARPUM
	316	XENIKOON DA
	294	NYSSAPOLLENITES DA
3750.	67	SCAPHOPOD SP. 1
3840.	18	SPIROPLECTAMMINA CARINATA
	15	GLOBIGERINA PRAEBULLOIDES
	20	GYROIDINA GIRARDANA
	16	CERATOBULIMINA CONTRARIA
4000.	526	PHTHANOPERIDINIUM ECHINATUM
	567	SURCULOSPHAERIDIUM LONGIFURCATUM A
4020.	78	UVIGERINA PEREGRINA
4110.	70	ALABAMINA SCITULA
4200.	448	IMPLETOSPHAERIDIUM TRANSFODUM
4300.	25	COARSE ARENACEOUS SPP.
	259	AMMODISCUS LATUS
4600.	390	DIPHYES COLLIGERUM
	417	GLAPHROCYSTA INTRICATA
	447	IMPLETOSPHAERIDIUM SCALENFURCATUM
	470	LENTINIA
	471	LENTINIA SERRATA
	533	PTERODINIUM CINGULATUM
4650.	85	PSEUDOHASTIGERINA MICRA
	145	ANOMALINOIDES ALLENI
	71	EPISTOMINA ELEGANS
	40	BULIMINA ALAZANENSIS
4900.	337	CHATANGIELLA VNIGRI
	459	KISSELOVIA TENUIVIRGULA
5100.	307	AREOLIGERA SENONENSIS
5200.	371	DAPSILIDINIUM PASTIELSII
	593	WETZELIELLA OVALIS
5400.	380	DEFLANDREA SP. B
	290	SEQUOIAPOLLENITES DA
5500.	326	CERATIOPSIS SPECIOSA
	286	PLATYCARYAPOLLENITES DA
5600.	357	CTENIDODINIUM DB
	547	SPINIFERITES MEMBRANACEUS
5640.	45	BULIMINA TRIGONALIS
	35	SPIROPLECTAMMINA DENTATA
	263	AMMOBACULITES AFF. POLYTHALAMUS
	261	HAPLOPHRAGMOIDES WALTERI
	34	MARGINULINA DECORATA
5700.	403	EOCLADOPYXIS PENICULATA (REWORKED)
5740.	29	CYCLAMMINA AMPLECTENS
5800.	314	AZOLLA
5900.	298	APECTODINIUM HOMOMORPHUM
	300	APECTODINIUM PARVUM
6000.	41	PLECTOFRONDICULARIA AFF. PAUCICOSTATA
	58	UVIGERINA BATJESI

HERJOLF M-92 (F)

Depth	Number	Fossil Name
6000.	30	CIBICIDOIDES BLANPIEDI
	32	AMMOSPHAEROIDINA SP.. 1
	264	KARRERIELLA CONVERSA
6100.	389	DIPHYES AIREANA
	594	WETZELIELLA SYMMETRICA
6180.	86	TURRILINA ROBERTSI
6200.	299	APECTODINIUM HYPERACANTHUM
	427	HOMOTRYBLIUM TENUISPINOSUM
	440	HYSTRICHOSPHAERIDIUM TUBIFERUM
6300.	372	DAPSILIDINIUM SIMPLEX
	425	HOMOTRYBLIUM
	539	SAMLANDIA
	578	THALASSIPHORA PELAGICA
6450.	57	SPIROPLECTAMMINA SPECTABILIS LCO
6540.	54	SPIROPLECTAMMINA NAVARROANA
6600.	304	AREOLIGERA CORONATA
6630.	297	MEGASPORE SP. 1
6700.	319	ACHOMOSPHAERA CRASSIPELUS
	329	ADNATOSPHAERIDIUM RETICULENSE
	328	CERATIOPSIS WARDENENSIS
	394	DRACODINIUM CF CONDYLOS
6720.	190	ANOMALINOIDES ACUTA
7060.	47	PLANOROTALITES PLANOCONICUS
	154	ANOMALINOIDES MIDWAYENSIS
	56	GLOMOSPIRA CORONA
7250.	55	GAVELINELLA BECCARIIFORMIS
7300.	323	CERATIOPSIS DIEBELII
7400.	373	DEFLANDREA DENTICULATA
	512	PALAEOPERIDINIUM PYROPHORUM
7500.	349	CORDOSPHAERIDIUM INODES
	506	PALEOCYSTODINIUM AUSTRALINIUM
7600.	415	GLAPHROCYSTA DIVARICATA
	416	GLAPHROCYSTA EXUBERANS
	560	SPONGODINIUM DELITIENSE
7610.	60	PLANOROTALITES COMPRESSUS
7790.	59	RZEHAKINA EPIGONA

BJARNI H-81 (F)

Rotary table height: 40.0F
Water depth: 456.0F

Depth	Number	Fossil Name
1480.	433	HYSTRICHOKOLPOMA RIGAUDIAE
	501	OPERCULOPINIUM CENTROCARPUM
	552	SPINIFERITES PSEUDOFURCATUS

BJARNI H-81 (F)

Depth	Number	Fossil Name
1480.	569	SYSTEMATOPHORA ANCYREA
	293	TSUGAEPOLLENITES INGNICULUS
1510.	518	PERISSEIASPHAERIDIUM
1900.	338	CHIROPTERIDIUM MESPILANUM
	346	CORDOSPHAERIDIUM CANTHARELLUM
	369	CYCLOPSIELLA VIETA
	379	DEFLANDREA SPINULOSA (REWORKED)
2110.	553	SPINIFERITES RAMOSUS MULTIBREVIS
2460.	522	PHTHANOPERIDINIUM
2560.	319	ACHOMOSPHAERA CRASSIPELUS
2650.	367	CYCLONEPHELIUM DY
	371	DAPSILIDINIUM PASTIELSII
	391	DISTATODINIUM PARADOXUM
	448	IMPLETOSPHAERIDIUM TRANSFODUM
	502	OPERCULOPINIUM ISRAELIANUM
	593	WETZELIELLA OVALIS
2760.	316	XENIKOON DA
	282	OSMUNDACIDITES DA
2860.	16	CERATOBULIMINA CONTRARIA
	347	CORDOSPHAERIDIUM FIBROSPINOSUM
	287	PODOCARPIDITES DA
3360.	67	SCAPHOPOD SP. 1
	478	LINGULODINIUM MACHAEROPHORUM
3460.	20	GYROIDINA GIRARDANA
	21	GUTTULINA PROBLEMA
	487	CRIBROPERIDINIUM GIUSEPPEI
	566	SURCULOSPHAERIDIUM LONGIFURCATUM
3560.	18	SPIROPLECTAMMINA CARINATA
	69	NODOSARIA CF. ELEGANTISSIMA
	70	ALABAMINA SCITULA
	71	EPISTOMINA ELEGANS
	511	PALAEOPERIDINIUM CRETACEUM
	543	SPINIDINIUM ECHINOIDEUM
	292	TILIAEPOLLENITES DA
3760.	335	CHATANGIELLA TRIPARTITA
3860.	358	CYCLONEPHELIUM DISTINCTUM
4060.	15	GLOBIGERINA PRAEBULLOIDES
4260.	24	TURRILINA ALSATICA
4360.	314	AZOLLA
	361	CYCLONEPHELIUM MEMBRANIPHORUM
	471	LENTINIA SERRATA
	535	RHOMBOIDINIUM
4560.	390	DIPHYES COLLIGERUM
4760.	591	WETZELIELLA ARTICULATA
4860.	25	COARSE ARENACEOUS SPP.
5060.	34	MARGINULINA DECORATA
5260.	29	CYCLAMMINA AMPLECTENS
	261	HAPLOPHRAGMOIDES WALTERI

BJARNI H-81 (F)

Depth	Number	Fossil Name
5260.	444	HYSTRICHOSPHAERANA ORBIFERA
	529	POLYSPHAERIDIUM
	571	SYSTEMATOPHORA PLACACANTHA
	587	TUBIDERMODINIUM SULCATUM
5360.	354	CORRUDINIUM INCOMPOSITUM
	377	DEFLANDREA PHOSPHORITICA
	396	DRACODINIUM VARIELONGITUDUM
	472	LENTINIA WETZELII
5460.	42	CIBICIDOIDES ALLENI
	74	EPONIDES SP. 5
	41	PLECTOFRONDICULARIA AFF. PAUCICOSTATA
	32	AMMOSPHAEROIDINA SP. 1
5560.	30	CIBICIDOIDES BLANPIEDI
	264	KARRERIELLA CONVERSA
	75	LENTICULINA ULATISENSIS
5660.	57	SPIROPLECTAMMINA SPECTABILIS LCO
5960.	298	APECTODINIUM HOMOMORPHUM
6010.	297	MEGASPORE SP. 1
	306	AREOLIGERA SENONENSIS
	393	DRACODINIUM CONDYLOS
6060.	459	KISSELOVIA TENUIVIRGULA
6260.	326	CERATIOPSIS SPECIOSA
	418	GLAPHROCYSTA ORDINATA
6360.	441	HYSTRICHOSPHAERIDIUM DB
	512	PALAEOPERIDINIUM PYROPHORUM
6560.	514	PALEOTETRADINIUM
	520	PHELODINIUM MAGNIFICUM
6590.	56	GLOMOSPIRA CORONA
6660.	54	SPIROPLECTAMMINA NAVARROANA
	55	GAVELINELLA BECCARIIFORMIS
	419	GLADHROCYSTA PASTIELSII
6740.	323	CERATIOPSIS DIEBELII
	411	FORMA P EVITT
	430	HYSTRICHODINIUM DA
	454	ISABELIDINIUM MAGNUM
	498	OLIGOSPHAERIDIUM PULCHERRIMUM
	505	PALEOCYSTODINIUM

GUDRID H-55 (F)

Rotary table height: 40.0F
Water depth: 982.0F

Depth	Number	Fossil Name
1660.	10	UVIGERINA CANARIENSIS
	17	ASTERIGERINA GURICHI

GUDRID H-55 (F)

Depth	Number	Fossil Name
1660.	569	SYSTEMATOPHORA ANCYREA
	316	XENIKOON DA
	282	OSMUNDACIDITES DA
	283	PINUS
	293	TSUGAEPOLLENITES INGNICULUS
1750.	501	OPERCULOPINIUM CENTROCARPUM
1840.	554	SPINIFERITES SCABRATUS
1960.	265	ASTERIGERINA GURICHI (PEAK)
2010.	20	GYROIDINA GIRARDANA
	21	GUTTULINA PROBLEMA
	18	SPIROPLECTAMMINA CARINATA
	16	CERATOBULIMINA CONTRARIA
2130.	377	DEFLANDREA PHOSPHORITICA
2220.	492	NEMATOSPHAEROPSIS BALCOMBIANA
2310.	522	PHTHANOPERIDINIUM
2400.	371	DAPSILIDINIUM PASTIELSII
	469	LEJEUNECYSTA TENELLA
	485	MEMBRANOPHORIDIUM ASPINATUM
	279	BOMBACACIDITES DA
2490.	468	LEJEUNECYSTA PSILODORA
2670.	287	PODOCARPIDITES DA
2760.	305	AREOLIGERA SEMICIRCULATA
	388	DINOPETEIGIUM CLADOIDES SENSU MORG.
	497	OLIGOSPHAERIDIUM COMPLEX
	528	PHTHANOPERIDINIUM MICROSPINATUM
3500.	24	TURRILINA ALSATICA
4160.	276	ABIES
4400.	383	DIACROCANTHIPIUM
	280	CHENOPODIUMSPORITES DA
	288	POLYPODIACIDITES DA
4460.	15	GLOBIGERINA PRAEBULLOIDES
	25	COARSE ARENACEOUS SPP.
4520.	292	TILIAEPOLLENITES DA
4760.	526	PHTHANOPERIDINIUM ECHINATUM
4880.	451	ISABELIDINIUM BELFASTENSE
4940.	33	TURBOROTALIA POMEROLI
5380.	315	XENIKOON
5600.	428	HOROLOGINELLA
	478	LINGULODINIUM MACHAEROPHORUM
5720.	433	HYSTRICHOKOLPOMA RIGAUDIAE
	500	OPERCULOPINIUM CF HIRSUTUM
	291	TILIAEPOLLENITES
5810.	259	AMMODISCUS LATUS
5900.	338	CHIROPTERIDIUM MESPILANUM
5990.	284	PISTILLIPOLLENITES MCGREGORII
6020.	40	BULIMINA ALAZANENSIS
	34	MARGINULINA DECORATA

GUDRID H-55 (F)

Depth	Number	Fossil Name
6080.	537	[illegible]TTNESTIA BORUSSICA
	285	PLATYCARYAPOLLENITES
6110.	84	GLOBIGERINA YEGUAENSIS
	90	ACARININA DENSA
	36	PSEUDOHASTIGERINA WILCOXENSIS
6200.	37	ACARININA AFF. PENTACAMERATA
	260	HAPLOPHRAGMOIDES KIRKI
	261	HAPLOPHRAGMOIDES WALTERI
6410.	29	CYCLAMMINA AMPLECTENS
6440.	35	SPIROPLECTAMMINA DENTATA
6530.	45	BULIMINA TRIGONALIS
	74	EPONIDES SP. 5
6590.	42	CIBICIDOIDES ALLENI
6680.	57	SPIROPLECTAMMINA SPECTABILIS LCO
	88	SIPHOGENEROIDES ELEGANTA
	30	CIBICIDOIDES BLANPIEDI
6830.	298	APECTODINIUM HOMOMORPHUM
	307	AREOLIGERA SENONENSIS
	328	CERATIOPSIS WARDENENSIS
6860.	32	AMMOSPHAEROIDINA SP. 1
6950.	297	MEGASPORE SP. 1
	50	SUBBOTINA PATAGONICA
7860.	56	GLOMOSPIRA CORONA
	59	RZEHAKINA EPIGONA
	54	SPIROPLECTAMMINA NAVARROANA
8550.	55	GAVELINELLA BECCARIIFORMIS

CARTIER D-70 (F)

Rotary table height: 41.0F
Water depth: 1017.0F

Depth	Number	Fossil Name
1940.	350	CORDOSPHAERIDIUM MULTISPINOSUM
	283	PINUS
	293	TSUGAEPOLLENITES INGNICULUS
	296	OSMUNDACIDITES
2050.	276	ABIES
2140.	279	BOMBACACIDITES DA
	291	TILIAEPOLLENITES
2270.	16	CERATOBULIMINA CONTRARIA
2420.	515	PARALECANIELLA INDENTATA
	347	CORDOSPHAERIDIUM FIBROSPINOSUM
	489	MUDERONGIA
	524	PHTHANOPERIDINIUM AMOENUM
	525	PHTHANOPERIDINIUM COMATUM (REWORKED)

CARTIER D-70 (F)

Depth	Number	Fossil Name
2520.	18	SPIROPLECTAMMINA CARINATA
2620.	433	HYSTRICHOKOLPOMA RIGAUDIAE
	569	SYSTEMATOPHORA ANCYREA
2700.	316	XENIKOON DA
2780.	416	GLAPHROCYSTA EXUBERANS
	501	OPERCULOPINIUM CENTROCARPUM
2960.	15	GLOBIGERINA PRAEBULLOIDES
	428	HOROLOGINELLA
3050.	338	CHIROPTERIDIUM MESPILANUM
	493	ODONTOCHITINA COSTATA
3160.	282	OSMUNDACIDITES DA
3360.	21	GUTTULINA PROBLEMA
	70	ALABAMINA SCITULA
3460.	67	SCAPHOPOD SP. 1
	335	CHATANGIELLA TRIPARTITA
3660.	69	NODOSARIA CF. ELEGANTISSIMA
	363	CYCLONEPHELIUM VANNOPHORUM
	371	DAPSILIDINIUM PASTIELSII
3750.	346	CORDOSPHAERIDIUM CANTHARELLUM
	478	LINGULODINIUM MACHAEROPHORUM
3870.	24	TURRILINA ALSATICA
	172	PSEUDOHASTIGERINA SP.
	345	ALTERBIA
	522	PHTHANOPERIDINIUM
	526	PHTHANOPERIDINIUM ECHINATUM
3960.	314	AZOLLA
	474	LEPTODINIUM
4060.	25	COARSE ARENACEOUS SPP.
	537	ROTTNESTIA BORUSSICA
4170.	259	AMMODISCUS LATUS
	471	LENTINIA SERRATA
4270.	328	CERATIOPSIS WARDENENSIS
	447	IMPLETOSPHAERIDIUM SCALENFURCATUM
	448	IMPLETOSPHAERIDIUM TRANSFODUM
	470	LENTINIA
	294	NYSSAPOLLENITES DA
4670.	487	CRIBROPERIDINIUM GIUSEPPEI
	591	WETZELIELLA ARTICULATA
	281	CUPANIEIDITES DA
4750.	298	APECTODINIUM HOMOMORPHUM
	596	WETZELIELLA DA
	292	TILIAEPOLLENITES DA
4760.	34	MARGINULINA DECORATA
4860.	260	HAPLOPHRAGMOIDES KIRKI
	261	HAPLOPHRAGMOIDES WALTERI
4860.	284	PISTILLIPOLLENITES MCGREGORII
4960.	118	EPISTOMINA SP. 5
	173	ANOMALINA SP. 1

CARTIER D-70 (F)

Depth	Number	Fossil Name
4960.	85	PSEUDOHASTIGERINA MICRA
	29	CYCLAMMINA AMPLECTENS
	263	AMMOBACULITES AFF. POLYTHALAMUS
5160.	32	AMMOSPHAEROIDINA SP. 1
	42	CIBICIDOIDES ALLENI
	297	MEGASPORE SP. 1
	531	POLYSTEPHANOPHORUS
5260.	35	SPIROPLECTAMMINA DENTATA
5360.	457	KISSELOVIA COLEOTHRYPTA (REWORKED)
5470.	41	PLECTOFRONDICULARIA AFF. PAUCICOSTATA
	57	SPIROPLECTAMMINA SPECTABILIS LCO
	372	DAPSILIDINIUM SIMPLEX
5560.	299	APECTODINIUM HYPERACANTHUM
	304	AREOLIGERA CORONATA
	472	LENTINIA WETZELII
5670.	54	SPIROPLECTAMMINA NAVARROANA
	309	AREOSPHAERIDIUM
	390	DIPHYES COLLIGERUM
	393	DRACODINIUM CONDYLOS.
	397	EATONICYSTA URSULAE
	415	GLAPHROCYSTA DIVARICATA
	427	HOMOTRYBLIUM TENUISPINOSUM
	481	LUXADINIUM
5750.	312	AREOSPHAERIDIUM PECTINIFORME (REWORKED)
	423	HETERAULACACYSTA CAMPANULA
5870.	56	GLOMOSPIRA CORONA
5970.	326	CERATIOPSIS SPECIOSA
	378	DEFLANDREA CF PHOSPHORITICA
	418	GLAPHROCYSTA ORDINATA
	512	PALAEOPERIDINIUM PYROPHORUM
6070.	59	RZEHAKINA EPIGONA
	175	ALLOGROMIA SP.
	300	APECTODINIUM PARVUM
	440	HYSTRICHOSPHAERIDIUM TUBIFERUM
	500	OPERCULOPINIUM CF HIRSUTUM
6170.	351	AMPHIDIADEMA NUCULA
	323	CERATIOPSIS DIEBELII

INDIAN HARBOUR M-52 (F)

Rotary table height: 98.0F
Water depth: 649.0F

Depth	Number	Fossil Name
1000.	276	ABIES
	283	PINUS

INDIAN HARBOUR M-52 (F)

Depth	Number	Fossil Name
1000.	293	TSUGAEPOLLENITES INGNICULUS
1360.	291	TILIAEPOLLENITES
1450.	330	CHATANGIELLA
1740.	1	NEOGLOBOQUADRINA PACHYDERMA
	3	GLOBIGERINA PSEUDOBESA
	4	GLOBOROTALIA INFLATA
	5	GLOBOROTALIA CRASSAFORMIS
	8	ORBULINA UNIVERSA
1780.	569	SYSTEMATOPHORA ANCYREA
	296	OSMUNDACIDITES
1870.	302	APTEA
	425	HOMOTRYBLIUM
	433	HYSTRICHOKOLPOMA RIGAUDIAE
1890.	9	FURSENKOINA GRACILIS
	10	UVIGERINA CANARIENSIS
1930.	282	OSMUNDACIDITES DA
	288	POLYPODIACIDITES DA
1950.	269	NEOGLOBOQUADRINA ATLANTICA
2040.	2	GLOBIGERINA APERTURA
	7	GLOBIGERINOIDES RUBER
2110.	415	GLAPHROCYSTA DIVARICATA
	502	OPERCULOPINIUM ISRAELIANUM
	277	ARTEMISIA
2130.	6	NEOGLOBOQUADRINA ACOSTAENSIS
	18	SPIROPLECTAMMINA CARINATA
2200.	428	HOROLOGINELLA
	478	LINGULODINIUM MACHAEROPHORUM
	279	BOMBACACIDITES DA
2260.	548	SPINIFERITES MIRABILIS
2350.	346	CORDOSPHAERIDIUM CANTHARELLUM
2460.	15	GLOBIGERINA PRAEBULLOIDES
	20	GYROIDINA GIRARDANA
	16	CERATOBULIMINA CONTRARIA
2530.	491	NEMATOSPHAEROPSIS
2550.	17	ASTERIGERINA GURICHI
2620.	338	CHIROPTERIDIUM MESPILANUM
	501	OPERCULOPINIUM CENTROCARPUM
	570	SYSTEMATOPHORA AREOLATA
2710.	312	AREOSPHAERIDIUM PECTINIFORME (REWORKED)
	322	CERATIOPSIS DARTMOORIA
	376	DEFLANDREA OEBISFELDENSIS
	448	IMPLETOSPHAERIDIUM TRANSFODUM
	485	MEMBRANOPHORIDIUM ASPINATUM
	505	PALEOCYSTODINIUM
	596	WETZELIELLA DA
2800.	294	NYSSAPOLLENITES DA
3070.	461	LACINIADINIUM
	281	CUPANIEIDITES DA

INDIAN HARBOUR M-52 (F)

Depth	Number	Fossil Name
3070.	295	NYASSAPOLLENITES DB
3160.	337	CHATANGIELLA VNIGRI
	342	CHLAMYDOPHORELLA NYEI
	522	PHTHANOPERIDINIUM
3250.	350	CORDOSPHAERIDIUM MULTISPINOSUM
	379	DEFLANDREA SPINULOSA (REWORKED)
	350	CORDOSPHAERIDIUM MULTISPINOSUM
	471	LENTINIA SERRATA
3430.	287	PODOCARPIDITES DA
3490.	519	PHELODINIUM
3580.	354	CORRUDINIUM INCOMPOSITUM
	371	DAPSILIDINIUM PASTIELSII
	479	LINGULODINIUM DC
3600.	446	IMPAGIDINIUM VICTORIANUM
	467	LEJEUNECYSTA HYALINA
	575	TANYOSPHAERIDIUM DA
3650.	24	TURRILINA.ALSATICA
	25	COARSE ARENACEOUS SPP.
	289	SEQUOIAPOLLENITES
	345	ALTERBIA
	323	CERATIOPSIS DIEBELII
	494	ODONTOCHITINA OPERCULATA
	525	PHTHANOPERIDINIUM COMATUM (REWORKED)
3940.	369	CYCLOPSIELLA VIETA
	493	ODONTOCHITINA COSTATA
	587	TUBIDERMODINIUM SULCATUM
4030.	374	DEFLANDREA EOCENICA
	431	HYSTRICHOKOLPOMA CINCTUM (REWORKED)
4120.	305	AREOLIGERA SEMICIRCULATA
	529	POLYSPHAERIDIUM
4140.	26	UVIGERINA EX.GR.MIOZEA-NUTTALI
	27	EPONIDES UMBONATUS
	28	CIBICIDOIDES SP. 5
4300.	368	CYCLOPSIELLA ELLIPTICA
	540	SCHIZOCYSTIA RUGOSA
4750.	344	COMASPHAERIDIUM COMETES
	463	LACINIADINIUM BICONICULUM
	504	OVOIDINIUM VERRUCOSUM
	526	PHTHANOPERIDINIUM ECHINATUM
	527	PHTHANOPERIDINIUM LEVIMURUM
4840.	447	IMPLETOSPHAERIDIUM SCALENFURCATUM
	484	MEMBRANILARNACIA
	578	THALASSIPHORA PELAGICA
5200.	523	PHTHANOPERIDINIUM ALECTROLOPHUM
	551	SPINIFERITES POROSUS
5380.	259	AMMODISCUS LATUS
5480.	261	HAPLOPHRAGMOIDES WALTERI
	470	LENTINIA

INDIAN HARBOUR M-52 (F)

Depth	Number	Fossil Name
5590.	382	DEFLANDREA SP. C
5690.	30	CIBICIDOIDES BLANPIEDI
5780.	487	CRIBROPERIDINIUM GIUSEPPEI
5880.	335	CHATANGIELLA TRIPARTITA
	497	OLIGOSPHAERIDIUM COMPLEX
	509	PALEOHYSTRICHOPHORA INFUSORIOIDES
	554	SPINIFERITES SCABRATUS
6080.	260	HAPLOPHRAGMOIDES KIRKI
	32	AMMOSPHAEROIDINA SP. 1
	531	POLYSTEPHANOPHORUS
6370.	363	CYCLONEPHELIUM VANNOPHORUM
6770.	33	TURBOROTALIA POMEROLI
6970.	314	AZOLLA
6980.	591	WETZELIELLA ARTICULATA
7260.	375	DEFLANDREA HYALINA
	440	HYSTRICHOSPHAERIDIUM TUBIFERUM
	540	SCHIZOCYSTIA RUGOSA
	593	WETZELIELLA OVALIS
	594	WETZELIELLA SYMMETRICA
7460.	599	WILSONIDIUM ECHINOSUTURATUM
7560.	34	MARGINULINA DECORATA
	35	SPIROPLECTAMMINA DENTATA
7660.	263	AMMOBACULITES AFF. POLYTHALAMUS
	36	PSEUDOHASTIGERINA WILCOXENSIS
	39	ALABAMINA WILCOXENSIS
7760.	29	CYCLAMMINA AMPLECTENS
	40	BULIMINA ALAZANENSIS
	41	PLECTOFRONDICULARIA AFF. PANICOSTATA
	42	CIBICIDOIDES ALLENI
7860.	380	DEFLANDREA SP. B
	458	KISSELOVIA CRASSIRAMOSA
7870.	86	TURRILINA ROBERTSI
	544	SPINIDINIUM STYLONIFERUM
7960.	473	LENTINIA DA
8050.	37	ACARININA AFF. PENTACAMERATA
	38	LENTICULINA SUBPAPILLOSA
8140.	44	CIBICIDOIDES AFF. WESTI
8230.	309	AREOSPHAERIDIUM
8350.	45	BULIMINA TRIGONALIS
	297	MEGASPORE SP. 1
	47	PLANOROTALITES PLANOCONICUS
8860.	49	OSANGULARIA EXPANSA
	392	DOROCYSTA
	479	LINGULODINIUM DC
	508	PALEOCYSTODINIUM GOLZOWENSE
9130.	381	DEFLANDREA SP. B 2
9490.	57	SPIROPLECTAMMINA SPECTABILIS LCO
	54	SPIROPLECTAMMINA NAVARROANA

INDIAN HARBOUR M-52 (F)

Depth	Number	Fossil Name
9490.	50	SUBBOTINA PATAGONICA
	52	ACARININA SOLDADOENSIS
9560.	299	APECTODINIUM HYPERACANTHUM
9580.	300	APECTODINIUM PARVUM
	393	DRACODINIUM CONDYLOS
9670.	333	ADNATOSPHAERIDIUM VITTATUM
9760.	328	CERATIOPSIS WARDENENSIS
	490	MURATODINIUM FIMBRIATUM
9850.	55	GAVELINELLA BECCARIIFORMIS
	56	GLOMOSPIRA CORONA
9940.	326	CERATIOPSIS SPECIOSA
	507	PALEOCYSTODINIUM BENJAMINII
10030.	59	RZEHAKINA EPIGONA
10090.	60	PLANOROTALITES COMPRESSUS
	61	SUBBOTINA PSEUDOBULLOIDES
	62	GAVELINELLA DANICA
10230.	334	ALISOCYSTA CIRCUMTABULATA
10930.	512	PALAEOPERIDINIUM PYROPHORUM.

LEIF E-38 (F)

Rotary table height: 40.0F
Water depth: 550.0F

Depth	Number	Fossil Name
1100.	276	ABIES
	283	PINUS
	293	TSUGAEPOLLENITES INGNICULUS
1210.	228	CASSIDULINA TERETIS
	77	ELPHIDIUM SPP.
	270	CIBICIDOIDES GROSSA
	278	ARTEMISIA DA
	292	TILIAEPOLLENITES DA
1300.	478,	LINGULODINIUM MACHAEROPHORUM
	508	PALEOCYSTODINIUM GOLZOWENSE
	529	POLYSPHAERIDIUM
1310.	17	ASTERIGERINA GURICHI
1410.	350	CORDOSPHAERIDIUM MULTISPINOSUM
	367	CYCLONEPHELIUM DY
1500.	525	PHTHANOPERIDINIUM COMATUM (REWORKED)
1590.	287	PODOCARPIDITES DA
1690.	348	CORDOSPHAERIDIUM GRACILE
	446	IMPAGIDINIUM VICTORIANUM
	503	OVOIDINIUM
	522	PHTHANOPERIDINIUM
	316	XENIKOON DA

LEIF E-38 (F)

Depth	Number	Fossil Name
1790.	569	SYSTEMATOPHORA ANCYREA
2090.	373	DEFLANDREA DENTICULATA
2190.	474	LEPTODINIUM
2710.	16	CERATOBULIMINA CONTRARIA
	67	SCAPHOPOD SP. 1
	282	OSMUNDACIDITES DA
2840.	304	AREOLIGERA CORONATA
	576	THALASSIPHORA DELICATA
2920.	335	CHATANGIELLA TRIPARTITA
	497	OLIGOSPHAERIDIUM COMPLEX
3030.	488	MILLIOUDODINIUM TENUITABULATUM
3120.	399	ELLIPSOIDICTYUM
3230.	18	SPIROPLECTAMMINA CARINATA
	21	GUTTULINA PROBLEMA
	371	DAPSILIDINIUM PASTIELSII
	449	ISABELIDINIUM ACUMINATUM
	279	BOMBACACIDITES DA
3330.	370	DANEA CALIFORNICA
	433	HYSTRICHOKOLPOMA RIGAUDIAE
	457	KISSELOVIA COLEOTHRYPTA (REWORKED)
	469	LEJEUNECYSTA TENELLA
	550	SPINIFERITES NODOSUS
3430.	307	AREOLIGERA SENONENSIS
	517	PENTADINIUM LATICINCTUM
3520.	20	GYROIDINA GIRARDANA

LEIF M-48 (F)

Rotary table height: 40.0F
Water depth: 542.0F

Depth	Number	Fossil Name
1290.	280	CHENOPODIUMSPORITES DA
	283	PINUS
	292	TILIAEPOLLENITES DA
1300.	339	CHIROPTERIDIUM LOBOSPINOSUM
	228	CASSIDULINA TERETIS
	77	ELPHIDIUM SPP.
	10	UVIGERINA CANARIENSIS
	303	APTEODINIUM SPIRIDOIDES
	320	CANNOSPHAEROPSIS DA
	437	HYSTRICHOSPHAERIDIUM PALMATUM
	293	TSUGAEPOLLENITES INGNICULUS
1326.	335	CHATANGIELLA TRIPARTITA
1500.	282	OSMUNDACIDITES DA
1600.	323	CERATIOPSIS DIEBELII

LEIF M-48 (F)

Depth	Number	Fossil Name
1600.	503	OVOIDINIUM
	529	POLYSPHAERIDIUM
1690.	415	GLAPHROCYSTA DIVARICATA
	496	OLIGOSPHAERIDIUM ASTERIGERUM
	316	XENIKOON DA
1700.	543	SPINIDINIUM ECHINOIDEUM
2100.	385	DINOGYMNIUM EUCLAENSE
	584	TRINOVANTEDINIUM
2380.	287	PODOCARPIDITES DA
	181	CYCLOGYRA INVOLVENS
2470.	16	CERATOBULIMINA CONTRARIA
	67	SCAPHOPOD SP. 1
2500.	493	ODONTOCHITINA COSTATA
2600.	569	SYSTEMATOPHORA ANCYREA
2900.	599	WILSONIDIUM ECHINOSUTURATUM
3100.	494	ODONTOCHITINA OPERCULATA
3290.	15	GLOBIGERINA PRAEBULLOIDES
	522	PHTHANOPERIDINIUM
3380.	20	GYROIDINA GIRARDANA
	21	GUTTULINA PROBLEMA
	18	SPIROPLECTAMMINA CARINATA
3480.	70	ALABAMINA SCITULA
3580.	371	DAPSILIDINIUM PASTIELSII
3790.	69	NODOSARIA CF. ELEGANTISSIMA
3850.	347	CORDOSPHAERIDIUM FIBROSPINOSUM
	474	LEPTODINIUM
	478	LINGULODINIUM MACHAEROPHORUM
	588	VOZZHENNIKOVIA EXTENSA
3880.	85	PSEUDOHASTIGERINA MICRA
	24	TURRILINA ALSATICA
3940.	346	CORDOSPHAERIDIUM CANTHARELLUM
	416	GLAPHROCYSTA EXUBERANS
	593	WETZELIELLA OVALIS
4030.	328	CERATIOPSIS WARDENENSIS
	367	CYCLONEPHELIUM DY
	571	SYSTEMATOPHORA PLACACANTHA
	578	THALASSIPHORA PELAGICA
4120.	315	XENIKOON
4210.	318	ACHOMOSPHAERA ALCICORNU
	592	WETZELIELLA LUNARIS
4248.	459	KISSELOVIA TENUIVIRGULA
	591	WETZELIELLA ARTICULATA
4480.	333	ADNATOSPHAERIDIUM VITTATUM
4630.	25	COARSE ARENACEOUS SPP.
	238	CIBICIDOIDES SP. 7
4660.	577	THALASSIPHORA PATULA
4720.	42	CIBICIDOIDES ALLENI
4750.	390	DIPHYES COLLIGERUM

LEIF M-48 (F)

Depth	Number	Fossil Name
4850.	29	CYCLAMMINA AMPLECTENS
5010.	307	AREOLIGERA SENONENSIS
	403	EOCLADOPYXIS PENICULATA (REWORKED)
	448	IMPLETOSPHAERIDIUM TRANSFODUM
	533	PTERODINIUM CINGULATUM
5150.	260	HAPLOPHRAGMOIDES KIRKI
	34	MARGINULINA DECORATA
5190.	443	HYSTRICHOSPHAERIDIUM SP. A
	487	CRIBROPERIDINIUM GIUSEPPEI
5250.	57	SPIROPLECTAMMINA SPECTABILIS LCO
	74	EPONIDES SP. 5
	118	EPISTOMINA SP. 5
	263	AMMOBACULITES AFF. POLYTHALAMUS
5280.	393	DRACODINIUM CONDYLOS
5340.	30	CIBICIDOIDES BLANPIEDI
	41	PLECTOFRONDICULARIA AFF. PAUCICOSTATA
5370.	329	ADNATOSPHAERIDIUM RETICULENSE
	465	LANTERNOSPHAERIDIUM
	467	LEJEUNECYSTA HYALINA
5410.	286	PLATYCARYAPOLLENITES DA
5550.	298	APECTODINIUM HOMOMORPHUM
5620.	297	MEGASPORE SP. 1
	56	GLOMOSPIRA CORONA
	54	SPIROPLECTAMMINA NAVARROANA
5712.	322	CERATIOPSIS DARTMOORIA
	326	CERATIOPSIS SPECIOSA
	398	EISENACKIA CRASSITABULATA

FREYDIS B-87 (F)

Rotary table height: 41.0F
Water depth: 586.0F

Depth	Number	Fossil Name
1000.	16	CERATOBULIMINA CONTRARIA
1480.	330	CHATANGIELLA
	376	DEFLANDREA OEBISFELDENSIS
	379	DEFLANDREA SPINULOSA (REWORKED)
	525	PHTHANOPERIDINIUM COMATUM (REWORKED)
	569	SYSTEMATOPHORA ANCYREA
	276	ABIES
	282	OSMUNDACIDITES DA
	283	PINUS
	292	TILIAEPOLLENITES DA
	293	TSUGAEPOLLENITES INGNICULUS
1570.	287	PODOCARPIDITES DA

FREYDIS B-87 (F)

Depth	Number	Fossil Name
1840.	181	CYCLOGYRA INVOLVENS
	67	SCAPHOPOD SP. 1
	21	GUTTULINA PROBLEMA
	18	SPIROPLECTAMMINA CARINATA
	400	ELONGOSPHAERA DA SPINOSUS
1930.	316	XENIKOON DA
2190.	290	SEQUOIAPOLLENITES DA
2460.	533	PTERODINIUM CINGULATUM
	281	CUPANIEIDITES DA
2470.	20	GYROIDINA GIRARDANA
2560.	69	NODOSARIA CF. ELEGANTISSIMA
	27	EPONIDES UMBONATUS
	524	PHTHANOPERIDINIUM AMOENUM
	295	NYASSAPOLLENITES DB
2670.	474	LEPTODINIUM
	478	LINGULODINIUM MACHAEROPHORUM
	280	CHENOPODIUMSPORITES DA
	291	TILIAEPOLLENITES
2760.	364	CYCLONEPHELIUM SP. B
	526	PHTHANOPERIDINIUM ECHINATUM
2770.	15	GLOBIGERINA PRAEBULLOIDES
	70	ALABAMINA SCITULA
2860.	419	GLADHROCYSTA PASTIELSII
	284	PISTILLIPOLLENITES MCGREGORII
2960.	545	SPINIDINIUM SVERDRUPIANUM
	294	NYSSAPOLLENITES DA
3360.	515	PARALECANIELLA INDENTATA
	531	POLYSTEPHANOPHORUS
3430.	354	CORRUDINIUM INCOMPOSITUM
3500.	395	DRACODINIUM SIMILE
3600.	25	COARSE ARENACEOUS SPP.
	391	DISTATODINIUM PARADOXUM
3700.	190	ANOMALINOIDES ACUTA
	34	MARGINULINA DECORATA
	206	EPONIDES POLYGONUS
	42	CIBICIDOIDES ALLENI
	74	EPONIDES SP. 5
	173	ANOMALINA SP. 1
	493	ODONTOCHITINA COSTATA
	577	THALASSIPHORA PATULA
3810.	260	HAPLOPHRAGMOIDES KIRKI
3910.	29	CYCLAMMINA AMPLECTENS
	261	HAPLOPHRAGMOIDES WALTERI
	45	BULIMINA TRIGONALIS
	422	HEMIPLACOPHORA SEMILUNIFERA
	448	IMPLETOSPHAERIDIUM TRANSFODUM
	566	SURCULOSPHAERIDIUM LONGIFURCATUM
4000.	593	WETZELIELLA OVALIS

FREYDIS B-87 (F)

Depth	Number	Fossil Name
4100.	307	AREOLIGERA SENONENSIS
	377	DEFLANDREA PHOSPHORITICA
4180.	33	TURBOROTALIA POMEROLI
	81	GLOBIGERINA VENEZUELANA
	41	PLECTOFRONDICULARIA AFF. PAUCICOSTATA
	75	LENTICULINA ULATISENSIS
	210	LOXOSTOMOIDES APPLINAE
	32	AMMOSPHAEROIDINA SP. 1
4250.	312	AREOSPHAERIDIUM PECTINIFORME (REWORKED)
	363	CYCLONEPHELIUM VANNOPHORUM
	529	POLYSPHAERIDIUM
4270.	211	HANTKENINA SP.
	85	PSEUDOHASTIGERINA MICRA
	94	GLOBIGERINATHEKA KUGLERI
	298	APECTODINIUM HOMOMORPHUM
	309	AREOSPHAERIDIUM
	423	HETERAULACACYSTA CAMPANULA
	599	WILSONIDIUM ECHINOSUTURATUM
4360.	57	SPIROPLECTAMMINA SPECTABILIS LCO
	88	SIPHOGENEROIDES ELEGANTA
	86	TURRILINA ROBERTSI
	30	CIBICIDOIDES BLANPIEDI
	297	MEGASPORE SP. 1
	35	SPIROPLECTAMMINA DENTATA
	300	APECTODINIUM PARVUM
	372	DAPSILIDINIUM SIMPLEX
	374	DEFLANDREA EOCENICA
	393	DRACODINIUM CONDYLOS
	418	GLAPHROCYSTA ORDINATA
	530	POLYSPHAERIDIUM ZOHARYI
	587	TUBIDERMODINIUM SULCATUM
4450.	373	DEFLANDREA DENTICULATA
4500.	299	APECTODINIUM HYPERACANTHUM
	326	CERATIOPSIS SPECIOSA
	344	COMASPHAERIDIUM COMETES
	348	CORDOSPHAERIDIUM GRACILE
	397	EATONICYSTA URSULAE
	416	GLAPHROCYSTA EXUBERANS
	446	IMPAGIDINIUM VICTORIANUM
	487	CRIBROPERIDINIUM GIUSEPPEI
4520.	306	AREOLIGERA SENONENSIS
	398	EISENACKIA CRASSITABULATA
4550.	440	HYSTRICHOSPHAERIDIUM TUBIFERUM
4600.	415	GLAPHROCYSTA DIVARICATA
4690.	322	CERATIOPSIS DARTMOORIA
	324	CERATIOPSIS OBLIQUIPES
4870.	512	PALAEOPERIDINIUM PYROPHORUM
	460	KLEITHRIASPHAERIDIUM LOFFRENSE

FREYDIS B-87 (F)

Depth	Number	Fossil Name
4960.	56	GLOMOSPIRA CORONA
5050.	54	SPIROPLECTAMMINA NAVARROANA
5170.	213	ARENOBULIMINA SP. 2
	55	GAVELINELLA BECCARIIFORMIS
5230.	59	RZEHAKINA EPIGONA

HARE BAY E-21 (M)

Rotary table height: 24.2M
Water depth: 239.1M

Depth	Number	Fossil Name
393.	228	CASSIDULINA TERETIS
	270	CIBICIDOIDES GROSSA
420.	77	ELPHIDIUM SPP.
450.	1	NEOGLOBOQUADRINA PACHYDERMA
870.	10	UVIGERINA CANARIENSIS
990.	136	MELONIS BARLEEANUM
1110.	16	CERATOBULIMINA CONTRARIA
1140.	70	ALABAMINA SCITULA
	15	GLOBIGERINA PRAEBULLOIDES
1170.	24	TURRILINA ALSATICA
1430.	18	SPIROPLECTAMMINA CARINATA
	20	GYROIDINA GIRARDANA
	25	COARSE ARENACEOUS SPP.
1550.	260	HAPLOPHRAGMOIDES KIRKI
	263	AMMOBACULITES AFF. POLYTHALAMUS
1910.	259	AMMODISCUS LATUS
2060.	29	CYCLAMMINA AMPLECTENS
	233	CATAPSYDRAX UNICAVUS
	69	NODOSARIA CF. ELEGANTISSIMA
	118	EPISTOMINA SP. 5
	32	AMMOSPHAEROIDINA SP. 1
	81	GLOBIGERINA VENEZUELANA
2210.	68	SPIROPLECTAMMINA SPECTABILIS LO
2400.	49	OSANGULARIA EXPANSA
2630.	41	PLECTOFRONDICULARIA AFF. PAUCICOSTATA
2660.	227	CIBICIDOIDES AFF. TUXPAMENSIS
2840.	93	ACARININA AFF. BROEDERMANNI
	42	CIBICIDOIDES ALLENI
	96	ACARININA INTERMEDIA WILCOXENSIS
2870.	50	SUBBOTINA PATAGONICA
2960.	57	SPIROPLECTAMMINA SPECTABILIS LCO
3020.	66	COLEITES RETICULOSUS
	54	SPIROPLECTAMMINA NAVARROANA

HARE BAY E-21 (M)

Depth	Number	Fossil Name
3080.	55	GAVELINELLA BECCARIIFORMIS
	161	PLANOROTALITES AUSTRALIFORMIS
	56	GLOMOSPIRA CORONA
3140.	59	RZEHAKINA EPIGONA
3200.	253	SUBBOTINA TRILOCULINOIDES
	255	MOROZOVELLA CONICOTRUNCATA
	297	MEGASPORE SP. 1

BLUE H-28 (M)

Rotary table height: 15.0M
Water depth: 1486.0M

Depth	Number	Fossil Name
2090.	77	ELPHIDIUM SPP.
2150.	1	NEOGLOBOQUADRINA PACHYDERMA
2240.	4	GLOBOROTALIA INFLATA
2540.	267	GLOBOROTALIA HIRSUTA
2600.	269	NEOGLOBOQUADRINA ATLANTICA
2720.	110	GLOBIGERINA BULLOIDES
	10	UVIGERINA CANARIENSIS
	64	CASSIDULINA ISLANDICA
2870.	266	GLOBOROTALIA PUNCTICULATA (D'ORBIGNY)
3170.	124	GLOBOQUADRINA DEHISCENS
	125	GLOBOROTALIA CONTINUOSA
	6	NEOGLOBOQUADRINA ACOSTAENSIS
	113	GLOBOROTALIA MENARDII GROUP
3220.	122	SPHAEROIDINELLOPSIS SEMINULINA
3310.	26	UVIGERINA EX.GR.MIOZEA-NUTTALI
	71	EPISTOMINA ELEGANS
3550.	268	GLOBOROTALIA AFF. KUGLERI
	2	GLOBIGERINA APERTURA
3640.	147	CATAPSYDRAX AFF. DISSIMILIS
	27	EPONIDES UMBONATUS
3830.	29	CYCLAMMINA AMPLECTENS
3830.	261	HAPLOPHRAGMOIDES WALTERI
	81	GLOBIGERINA VENEZUELANA
	150	GLOBIGERINA GORTANII
3920.	82	GLOBIGERINA LINAPERTA
	15	GLOBIGERINA PRAEBULLOIDES
	118	EPISTOMINA SP. 5
	138	GLOBIGERINA ANGUSTIUMBILICATA
4070.	146	SUBBOTINA EOCAENA
	84	GLOBIGERINA YEGUAENSIS
4340.	32	AMMOSPHAEROIDINA SP. 1
	79	GLOBIGERINA TRIPARTITA

BLUE H-28 (M)

Depth	Number	Fossil Name
4340.	172	PSEUDOHASTIGERINA SP.
	53	UVIGERINA BATJESI
	68	SPIROPLECTAMMINA SPECTABILIS LO
4490.	164	NUTTALIDES TRUMPYI
	190	ANOMALINOIDES ACUTA
4635.	42	CIBICIDOIDES ALLENI
4670.	86	TURRILINA ROBERTSI
	151	BULIMINA BRADBURYI
4700.	33	TURBOROTALIA POMEROLI
	94	GLOBIGERINATHEKA KUGLERI
	57	SPIROPLECTAMMINA SPECTABILIS LCO
4730.	37	ACARININA AFF. PENTACAMERATA
4760.	90	ACARININA DENSA
	52	ACARININA SOLDADOENSIS

BONAVISTA C-99 (F)

Rotary table height: 42.6F
Water depth: 1080.0F

Depth	Number	Fossil Name
1500.	283	PINUS
	293	TSUGAEPOLLENITES INGNICULUS
1590.	76	CASSIDULINA SP.
	77	ELPHIDIUM SPP.
2220.	569	SYSTEMATOPHORA ANCYREA
2370.	545	SPINIDINIUM SVERDRUPIANUM
2460.	501	OPERCULOPINIUM CENTROCARPUM
2820.	10	UVIGERINA CANARIENSIS
	316	XENIKOON DA
2910.	17	ASTERIGERINA GURICHI
	16	CERATOBULIMINA CONTRARIA
	371	DAPSILIDINIUM PASTIELSII
	399	ELLIPSOIDICTYUM
	508	PALEOCYSTODINIUM GOLZOWENSE
	571	SYSTEMATOPHORA PLACACANTHA
	575	TANYOSPHAERIDIUM DA
	282	OSMUNDACIDITES DA
3000.	320	CANNOSPHAEROPSIS DA
	433	HYSTRICHOKOLPOMA RIGAUDIAE
	280	CHENOPODIUMSPORITES DA
3090.	319	ACHOMOSPHAERA CRASSIPELUS
	478	LINGULODINIUM MACHAEROPHORUM
	296	OSMUNDACIDITES
3390.	552	SPINIFERITES PSEUDOFURCATUS
	587	TUBIDERMODINIUM SULCATUM

BONAVISTA C-99 (F)

Depth	Number	Fossil Name
3720.	312	AREOSPHAERIDIUM PECTINIFORME (REWORKED)
	388	DINOPETEIGIUM CLADOIDES SENSU MORG.
3810.	448	IMPLETOSPHAERIDIUM TRANSFODUM
3990.	303	APTEODINIUM SPIRIDOIDES
	338	CHIROPTERIDIUM MESPILANUM
4150.	457	KISSELOVIA COLEOTHRYPTA (REWORKED)
4380.	287	PODOCARPIDITES DA
5010.	379	DEFLANDREA SPINULOSA (REWORKED)
	485	MEMBRANOPHORIDIUM ASPINATUM
5370.	518	PERISSEIASPHAERIDIUM
	522	PHTHANOPERIDINIUM
	526	PHTHANOPERIDINIUM ECHINATUM
5430.	367	CYCLONEPHELIUM DY
5490.	346	CORDOSPHAERIDIUM CANTHARELLUM
	377	DEFLANDREA PHOSPHORITICA
	416	GLAPHROCYSTA EXUBERANS
	525	PHTHANOPERIDINIUM COMATUM (REWORKED)
5760.	524	PHTHANOPERIDINIUM AMOENUM
5820.	21	GUTTULINA PROBLEMA
	419	GLADHROCYSTA PASTIELSII
5827.	25	COARSE ARENACEOUS SPP.
	20	GYROIDINA GIRARDANA
5830.	363	CYCLONEPHELIUM VANNOPHORUM
5832.	279	BOMBACACIDITES DA
5833.	451	ISABELIDINIUM BELFASTENSE
	452	ISABELIDINIUM COOKSONIAE
5837.	528	PHTHANOPERIDINIUM MICROSPINATUM
	291	TILIAEPOLLENITES
5839.	330	CHATANGIELLA
5843.	591	WETZELIELLA ARTICULATA
5940.	318	ACHOMOSPHAERA ALCICORNU
6030.	369	CYCLOPSIELLA VIETA
6210.	310	AREOSPHAERIDIUM ARCUATUM
6660.	18	SPIROPLECTAMMINA CARINATA
	578	THALASSIPHORA PELAGICA
7290.	365	CYCLONEPHELIUM SP. C
7380.	79	GLOBIGERINA TRIPARTITA
	15	GLOBIGERINA PRAEBULLOIDES
7600.	259	AMMODISCUS LATUS
	469	LEJEUNECYSTA TENELLA
7800.	24	TURRILINA ALSATICA
	26	UVIGERINA EX.GR.MIOZEA-NUTTALI
7900.	390	DIPHYES COLLIGERUM
8200.	496	OLIGOSPHAERIDIUM ASTERIGERUM
8200.	545	SPINIDINIUM SVERDRUPIANUM
8400.	81	GLOBIGERINA VENEZUELANA
	33	TURBOROTALIA POMEROLI
8730.	82	GLOBIGERINA LINAPERTA

BONAVISTA C-99 (F)

Depth	Number	Fossil Name
9400.	83	PLANOROTALITES PSEUDOSCITULUS
9800.	40	BULIMINA ALAZANENSIS
10000.	84	GLOBIGERINA YEGUAENSIS
	27	EPONIDES UMBONATUS
10100.	29	CYCLAMMINA AMPLECTENS
	261	HAPLOPHRAGMOIDES WALTERI
10200.	32	AMMOSPHAEROIDINA SP. 1
	263	AMMOBACULITES AFF. POLYTHALAMUS
10656.	85	PSEUDOHASTIGERINA MICRA
	86	TURRILINA ROBERTSI
	87	BULIMINA AFF. JACKSONENSIS
	264	KARRERIELLA CONVERSA
10910.	41	PLECTOFRONDICULARIA AFF. PAUCICOSTATA
	34	MARGINULINA DECORATA
11010.	57	SPIROPLECTAMMINA SPECTABILIS LCO
11110.	88	SIPHOGENEROIDES ELEGANTA
	42	CIBICIDOIDES ALLENI
	90	ACARININA DENSA
11110.	89	MOROZOVELLA SPINULOSA
11310.	159	MOROZOVELLA ARAGONENSIS
	92	MOROZOVELLA CAUCASICA
	93	ACARININA AFF. BROEDERMANNI
	94	GLOBIGERINATHEKA KUGLERI
11410.	56	GLOMOSPIRA CORONA
	50	SUBBOTINA PATAGONICA
	30	CIBICIDOIDES BLANPIEDI
11510.	47	PLANOROTALITES PLANOCONICUS
	96	ACARININA INTERMEDIA WILCOXENSIS
	36	PSEUDOHASTIGERINA WILCOXENSIS
11910.	297	MEGASPORE SP. 1

CUMBERLAND B-55 (F)

Rotary table height: 98.0F
Water depth: 639.0F

Depth	Number	Fossil Name
920.	76	CASSILULINA SP.
1380.	293	TSUGAEPOLLENITES INGNICULUS
1470.	283	PINUS
1830.	478	LINGULODINIUM MACHAEROPHORUM
1920.	335	CHATANGIELLA TRIPARTITA
	554	SPINIFERITES SCABRATUS
	296	OSMUNDACIDITES
2010.	501	OPERCULOPINIUM CENTROCARPUM
	280	CHENOPODIUMSPORITES DA

CUMBERLAND B-55 (F)

Depth	Number	Fossil Name
2190.	228	CASSIDULINA TERETIS
	1	NEOGLOBOQUADRINA PACHYDERMA
	431	HYSTRICHOKOLPOMA CINCTUM (REWORKED)
2280.	17	ASTERIGERINA GURICHI
	384	DICONODINIUM
	433	HYSTRICHOKOLPOMA RIGAUDIAE
	505	PALEOCYSTODINIUM
	565	SUMATRADINIUM
2360.	451	ISABELIDINIUM BELFASTENSE
	474	LEPTODINIUM
	479	LINGULODINIUM DC
	494	ODONTOCHITINA OPERCULATA
	508	PALEOCYSTODINIUM GOLZOWENSE
	531	POLYSTEPHANOPHORUS
	571	SYSTEMATOPHORA PLACACANTHA
2370.	10	UVIGERINA CANARIENSIS
	11	NONIONELLA PIZARRENSE
	9	FURSENKOINA GRACILIS
	109	CASSIDULINA CURVATA
	71	EPISTOMINA ELEGANS
2550.	265	ASTERIGERINA GURICHI (PEAK)
	16	CERATOBULIMINA CONTRARIA
	20	GYROIDINA GIRARDANA
	320	CANNOSPHAEROPSIS DA
	331	CHATANGIELLA DECOROSA
	371	DAPSILIDINIUM PASTIELSII
	428	HOROLOGINELLA
	448	IMPLETOSPHAERIDIUM TRANSFODUM
	497	OLIGOSPHAERIDIUM COMPLEX
	538	SAEPTODINIUM EURYPYLUM
	552	SPINIFERITES PSEUDOFURCATUS
	569	SYSTEMATOPHORA ANCYREA
	282	OSMUNDACIDITES DA
2730.	319	ACHOMOSPHAERA CRASSIPELUS
	303	APTEODINIUM SPIRIDOIDES
	332	CHATANGIELLA DITISSIMA
	423	HETERAULACACYSTA CAMPANULA
	435	HYSTRICHOSPHAERIDIUM DIFFICILE
	445	HYSTRICHOSPHAEROPSIS OVUM
	515	PARALECANIELLA INDENTATA
2820.	280	CHENOPODIUMSPORITES DA
2910.	18	SPIROPLECTAMMINA CARINATA
	346	CORDOSPHAERIDIUM CANTHARELLUM
	347	CORDOSPHAERIDIUM FIBROSPINOSUM
	504	OVOIDINIUM VERRUCOSUM
	549	SPINIFERITES MONILIS
3000.	502	OPERCULOPINIUM ISRAELIANUM
3260.	575	TANYOSPHAERIDIUM DA

CUMBERLAND/B-55 (F)

Depth	Number	Fossil Name
3360.	383	DIACROCANTHIPIUM
3450.	15	GLOBIGERINA PRAEBULLOIDES
	119	SPHAEROIDINELLA SUBDEHISCENS
	345	ALTERBIA
	361	CYCLONEPHELIUM MEMBRANIPHORUM
3540.	117	SPHAEROIDINA BULLOIDES
	581	TRICHODINIUM CASTANEUM
3630.	517	PENTADINIUM LATICINCTUM
3810.	219	MARTINOTIELLA COMMUNIS
	338	CHIROPTERIDIUM MESPILANUM
4080.	379	DEFLANDREA SPINULOSA (REWORKED)
4170.	388	DINOPETEIGIUM CLADOIDES SENSU MORG.
	485	MEMBRANOPHORIDIUM ASPINATUM
4620.	568	SVALBARDELLA
4710.	312	AREOSPHAERIDIUM PECTINIFORME (REWORKED)
4890.	26	UVIGERINA EX.GR.MIOZEA-NUTTALI
5250.	375	DEFLANDREA HYALINA
	522	PHTHANOPERIDINIUM
5610.	523	PHTHANOPERIDINIUM ALECTROLOPHUM
5880.	426	HOMOTRYBLIUM ACULEATUM
6330.	24	TURRILINA ALSATICA
6420.	403	EOCLADOPYXIS PENICULATA (REWORKED)
6600.	25	COARSE ARENACEOUS SPP.
	259	AMMODISCUS LATUS
	457	KISSELOVIA COLEOTHRYPTA (REWORKED)
	535	RHOMBOIDINIUM[a]
6690.	374	DEFLANDREA EOCENICA
6870.	471	LENTINIA SERRATA
7140.	594	WETZELIELLA SYMMETRICA
7230.	525	PHTHANOPERIDINIUM COMATUM (REWORKED)
7320.	416	GLAPHROCYSTA EXUBERANS
7500.	364	CYCLONEPHELIUM SP. B
7590.	358	CYCLONEPHELIUM DISTINCTUM
	372	DAPSILIDINIUM SIMPLEX
	593	WETZELIELLA OVALIS
7700.	132	GLOBOROTALIA OPIMA NANA
7800.	42	CIBICIDOIDES ALLENI
7900.	261	HAPLOPHRAGMOIDES WALTERI
	367	CYCLONEPHELIUM DY
8100.	310	AREOSPHAERIDIUM ARCUATUM
8600.	458	KISSELOVIA CRASSIRAMOSA
8710.	41	PLECTOFRONDICULARIA AFF. PAUCICOSTATA
	341	CHLAMYDOPHORELLA GROSSA
9000.	377	DEFLANDREA PHOSPHORITICA
9100.	84	GLOBIGERINA YEGUAENSIS
	459	KISSELOVIA TENUIVIRGULA
9200.	460	KLEITHRIASPHAERIDIUM LOFFRENSE
	467	LEJEUNECYSTA HYALINA

CUMBERLAND B-55 (F)

Depth	Number	Fossil Name
9200.	545	SPINIDINIUM SVERDRUPIANUM
9300.	570	SYSTEMATOPHORA AREOLATA
	580	TRICHODINIUM
9400.	318	ACHOMOSPHAERA ALCICORNU
9600.	390	DIPHYES COLLIGERUM
	577	THALASSIPHORA PATULA
9700.	29	CYCLAMMINA AMPLECTENS
9800.	32	AMMOSPHAEROIDINA SP. 1
	365	CYCLONEPHELIUM SP. C
9900.	226	GLOBIGERINA SENNI
10140.	144	GLOBOROTALIA CERROAZULENSIS
	419	GLADHROCYSTA PASTIELSII
10440.	49	OSANGULARIA EXPANSA
	333	ADNATOSPHAERIDIUM VITTATUM
	432	HYSTRICHOKOLPOMA CINCTUM TURGIDUM
	446	IMPAGIDINIUM VICTORIANUM
	587	TUBIDERMODINIUM SULCATUM
10560.	57	SPIROPLECTAMMINA SPECTABILIS LCO
	36	PSEUDOHASTIGERINA WILCOXENSIS
	373	DEELANDREA DENTICULATA
	600	WILSONIDIUM INTERMEDIUM
10680.	90	ACARININA DENSA
	396	DRACODINIUM VARIELONGITUDUM
	418	GLAPHROCYSTA ORDINATA
10830.	52	ACARININA SOLDADOENSIS
	54	SPIROPLECTAMMINA NAVARROANA
	329	ADNATOSPHAERIDIUM RETICULENSE
	309	AREOSPHAERIDIUM
	348	CORDOSPHAERIDIUM GRACILE
	447	IMPLETOSPHAERIDIUM SCALENFURCATUM
10930.	161	PLANOROTALITES AUSTRALIFORMIS
	93	ACARININA AFF. BROEDERMANNI
	96	ACARININA INTERMEDIA WILCOXENSIS
	151	BULIMINA BRADBURYI
	164	NUTTALIDES TRUMPYI
	157	TRITAXIA SP. 3
11030.	297	MEGASPORE SP. 1
	50	SUBBOTINA PATAGONICA
	159	MOROZOVELLA ARAGONENSIS
	427	HOMOTRYBLIUM TENUISPINOSUM
11130.	317	ACHILLEODINIUM BIFORMOIDES
	397	EATONICYSTA URSULAE
	597	WETZELIELLA LV
11330.	298	APECTODINIUM HOMOMORPHUM
	539	SAMLANDIA
11530.	311	AREOSPHAERIDIUM DIKTYOPLOCUS
	376	DEFLANDREA OEBISFELDENSIS
	393	DRACODINIUM CONDYLOS

CUMBERLAND B-55 (F)

Depth	Number	Fossil Name
11530.	440	HYSTRICHOSPHAERIDIUM TUBIFERUM
	599	WILSONIDIUM ECHINOSUTURATUM
11830.	55	GAVELINELLA BECCARIIFORMIS
	56	GLOMOSPIRA CORONA
	254	PLANOROTALITES PSEUDOMENARDII
	194	PLANOROTALITES CHAPMANI
11930.	326	CERATIOPSIS SPECIOSA
	512	PALAEOPERIDINIUM PYROPHORUM
	576	THALASSIPHORA DELICATA
12030.	334	ALISOCYSTA CIRCUMTABULATA

DOMINION O-23 (F)

Rotary table height: 98.0F
Water depth: 530.0F

Depth	Number	Fossil Name
1200.	283	PINUS
1380.	177	BOLIVINA DILATATA
	109	CASSIDULINA CURVATA
	169	EPISTOMINELLA TAKAYANAGII
1470.	451	ISABELIDINIUM BELFASTENSE
	501	OPERCULOPINIUM CENTROCARPUM
	502	OPERCULOPINIUM ISRAELIANUM
1560.	11	NONIONELLA PIZARRENSE
	9	FURSENKOINA GRACILIS
	546	SPINIDINIUM CF VESTITUM
1650.	17	ASTERIGERINA GURICHI
1740.	10	UVIGERINA CANARIENSIS
	117	SPHAEROIDINA BULLOIDES
	78	UVIGERINA PEREGRINA
	433	HYSTRICHOKOLPOMA RIGAUDIAE
	474	LEPTODINIUM
	478	LINGULODINIUM MACHAEROPHORUM
1830.	112	MARGINULINA BACHEI
	329	ADNATOSPHAERIDIUM RETICULENSE
	492	NEMATOSPHAEROPSIS BALCOMBIANA
	517	PENTADINIUM LATICINCTUM
	552	SPINIFERITES PSEUDOFURCATUS
1920.	18	SPIROPLECTAMMINA CARINATA
	569	SYSTEMATOPHORA ANCYREA
2010.	179	GLOBOROTALIA SCITULA PRAESCITULA
	16	CERATOBULIMINA CONTRARIA
	15	GLOBIGERINA PRAEBULLOIDES
	71	EPISTOMINA ELEGANS
	511	PALAEOPERIDINIUM CRETACEUM

DOMINION O-23 (F)

Depth	Number	Fossil Name
2100.	122	SPHAEROIDINELLOPSIS SEMINULINA
	494	ODONTOCHITINA OPERCULATA
2190.	549	SPINIFERITES MONILIS
	279	BOMBACACIDITES DA
2280.	371	DAPSILIDINIUM PASTIELSII
2370.	391	DISTATODINIUM PARADOXUM
	452	ISABELIDINIUM COOKSONIAE
2460.	319	ACHOMOSPHAERA CRASSIPELUS
	508	PALEOCYSTODINIUM GOLZOWENSE
	547	SPINIFERITES MEMBRANACEUS
2550.	576	THALASSIPHORA DELICATA
2670.	180	GYROIDINA SP. 4
2760.	346	CORDOSPHAERIDIUM CANTHARELLUM
2850.	515	PARALECANIELLA INDENTATA
2940.	26	UVIGERINA EX.GR.MIOZEA-NUTTALI
	123	GLOBIGERINOIDES TRILOBUS
	137	GLOBIGERINOIDES PRIMORDIUS
	343	ALISOCYSTA ORNATA
	431	HYSTRICHOKOLPOMA CINCTUM (REWORKED)
3030.	14	TEXTULARIA AGGLUTINANS
	136	MELONIS BARLEEANUM
	571	SYSTEMATOPHORA PLACACANTHA
3120.	27	EPONIDES UMBONATUS
	338	CHIROPTERIDIUM MESPILANUM
3210.	20	GYROIDINA GIRARDANA
	372	DAPSILIDINIUM SIMPLEX
3300.	312	AREOSPHAERIDIUM PECTINIFORME (REWORKED)
3330.	21	GUTTULINA PROBLEMA
	181	CYCLOGYRA INVOLVENS
3390.	310	AREOSPHAERIDIUM ARCUATUM
3480.	327	CERATIOPSIS STRIATA
	339	CHIROPTERIDIUM LOBOSPINOSUM
3570.	377	DEFLANDREA PHOSPHORITICA
3660.	593	WETZELIELLA OVALIS
3840.	379	DEFLANDREA SPINULOSA (REWORKED)
	417	GLAPHROCYSTA INTRICATA
	485	MEMBRANOPHORIDIUM ASPINATUM
	578	THALASSIPHORA PELAGICA
3930.	545	SPINIDINIUM SVERDRUPIANUM
4110.	591	WETZELIELLA ARTICULATA
4250.	201	SEISMIC EVENT #1
4290.	358	CYCLONEPHELIUM DISTINCTUM
4380.	24	TURRILINA ALSATICA
4470.	349	CORDOSPHAERIDIUM INODES
	471	LENTINIA SERRATA
	520	PHELODINIUM MAGNIFICUM
4560.	25	COARSE ARENACEOUS SPP.

DOMINION O-23 (F)

Depth	Number	Fossil Name
5190.	318	ACHOMOSPHAERA ALCICORNU
	348	CORDOSPHAERIDIUM GRACILE
	388	DINOPETEIGIUM CLADOIDES SENSU MORG.
	530	POLYSPHAERIDIUM ZOHARYI
5280.	34	MARGINULINA DECORATA
5370.	457	KISSELOVIA COLEOTHRYPTA (REWORKED)
5460.	355	CRIBROPERIDINIUM EDWARDSII
	527	PHTHANOPERIDINIUM LEVIMURUM
5640.	264	KARRERIELLA CONVERSA
	260	HAPLOPHRAGMOIDES KIRKI
	38	LENTICULINA SUBPAPILLOSA
5820.	259	AMMODISCUS LATUS
5910.	142	GYROIDINA SOLDANII MAMILLIGERA
	81	GLOBIGERINA VENEZUELANA
	416	GLAPHROCYSTA EXUBERANS
6090.	184	GYROIDINA OCTOCAMERATA
	82	GLOBIGERINA LINAPERTA
	30	CIBICIDOIDES BLANPIEDI
	146	SUBBOTINA EOCAENA
6270.	69	NODOSARIA CF. ELEGANTISSIMA
	263	AMMOBACULITES AFF. POLYTHALAMUS
6360.	418	GLAPHROCYSTA ORDINATA
	424	HETERAULACACYSTA LEPTALEA
6720.	304	AREOLIGERA CORONATA
6800.	202	SEISMIC EVENT #2
6810.	32	AMMOSPHAEROIDINA SP. 1
6900.	68	SPIROPLECTAMMINA SPECTABILIS LO
7080.	187	CIBICIDOIDES TRUNCANUS
	523	PHTHANOPERIDINIUM ALECTROLOPHUM
7270.	49	OSANGULARIA EXPANSA
	188	PLEUROSTOMELLA SP. 1
	147	CATAPSYDRAX AFF. DISSIMILIS
	190	ANOMALINOIDES ACUTA
	140	ROTALIATINA BULIMINOIDES
7320.	411	FORMA P EVITT
7370.	472	LENTINIA WETZELII
7470.	29	CYCLAMMINA AMPLECTENS
	40	BULIMINA ALAZANENSIS
7570.	191	GLOBIGERINA AFF. HIGGINSI
	156	SUBBOTINA FRONTOSA
7670.	151	BULIMINA BRADBURYI
7820.	250	VULVULINA JARVISI
	226	GLOBIGERINA SENNI
7920.	512	PALAEOPERIDINIUM PYROPHORUM
8070.	36	PSEUDOHASTIGERINA WILCOXENSIS
	44	CIBICIDOIDES AFF. WESTI
8320.	340	CHIROPTERIDIUM PARTISPINATUM

DOMINION O-23 (F)

Depth	Number	Fossil Name
8370.	194	PLANOROTALITES CHAPMANI
	90	ACARININA DENSA
	57	SPIROPLECTAMMINA SPECTABILIS LCO
8800.	203	SEISMIC EVENT #3
9070.	50	SUBBOTINA PATAGONICA
	47	PLANOROTALITES PLANOCONICUS
9070.	158	SUBBOTINA INAEQUISPIRA
9170.	161	PLANOROTALITES AUSTRALIFORMIS
	52	ACARININA SOLDADOENSIS
	297	MEGASPORE SP. 1
9320.	37	ACARININA AFF. PENTACAMERATA
	159	MOROZOVELLA ARAGONENSIS
	162	MOROZOVELLA AEQUA
9570.	196	OSANGULARIA SP. 4
9770.	45	BULIMINA TRIGONALIS
	230	BULIMINA OVATA
10230.	164	NUTTALIDES TRUMPYI

FLYING FOAM I-13 (F)

Rotary table height: 98.0F
Water depth: 300.0F

Depth	Number	Fossil Name
990.	9	FURSENKOINA GRACILIS
	10	UVIGERINA CANARIENSIS
	508	PALEOCYSTODINIUM GOLZOWENSE
	283	PINUS
1080.	379	DEFLANDREA SPINULOSA (REWORKED)
	279	BOMBACACIDITES DA
1170.	16	CERATOBULIMINA CONTRARIA
	325	ACHOMOSPHAERA RAMULIFERA
	384	DICONODINIUM
1260.	71	EPISTOMINA ELEGANS
	449	ISABELIDINIUM ACUMINATUM
	478	LINGULODINIUM MACHAEROPHORUM
	502	OPERCULOPINIUM ISRAELIANUM
	552	SPINIFERITES PSEUDOFURCATUS
1530.	17	ASTERIGERINA GURICHI
	371	DAPSILIDINIUM PASTIELSII
	433	HYSTRICHOKOLPOMA RIGAUDIAE
	501	OPERCULOPINIUM CENTROCARPUM
	569	SYSTEMATOPHORA ANCYREA
1620.	275	PARAROTALIA SP. 2
	265	ASTERIGERINA GURICHI (PEAK)
1710.	346	CORDOSPHAERIDIUM CANTHARELLUM

FLYING FOAM I-13 (F)

Depth	Number	Fossil Name
1800.	515	PARALECANIELLA INDENTATA
1890.	18	SPIROPLECTAMMINA CARINATA
	110	GLOBIGERINA BULLOIDES
	338	CHIROPTERIDIUM MESPILANUM
2070.	312	AREOSPHAERIDIUM PECTINIFORME (REWORKED)
	339	CHIROPTERIDIUM LOBOSPINOSUM
	592	WETZELIELLA LUNARIS
2160.	310	AREOSPHAERIDIUM ARCUATUM
2250.	377	DEFLANDREA PHOSPHORITICA
	539	SAMLANDIA
2340.	70	ALABAMINA SCITULA
2520.	26	UVIGERINA EX.GR.MIOZEA-NUTTALI
	15	GLOBIGERINA PRAEBULLOIDES
	81	GLOBIGERINA VENEZUELANA
2700.	201	SEISMIC EVENT #1
	525	PHTHANOPERIDINIUM COMATUM (REWORKED)
2970.	487	CRIBROPERIDINIUM GIUSEPPEI
3060.	452	ISABELIDINIUM COOKSONIAE
	517	PENTADINIUM LATICINCTUM
3150.	24	TURRILINA ALSATICA
	20	GYROIDINA GIRARDANA
	27	EPONIDES UMBONATUS
	319	ACHOMOSPHAERA CRASSIPELUS
	391	DISTATODINIUM PARADOXUM
	403	EOCLADOPYXIS PENICULATA (REWORKED)
	527	PHTHANOPERIDINIUM LEVIMURUM
3240.	431	HYSTRICHOKOLPOMA CINCTUM (REWORKED)
3420.	523	PHTHANOPERIDINIUM ALECTROLOPHUM
3690.	416	GLAPHROCYSTA EXUBERANS
	522	PHTHANOPERIDINIUM
	571	SYSTEMATOPHORA PLACACANTHA
3700.	25	COARSE ARENACEOUS SPP.
4230.	259	AMMODISCUS LATUS
4400.	202	SEISMIC EVENT #2
4500.	263	AMMOBACULITES AFF. POLYTHALAMUS
	32	AMMOSPHAEROIDINA SP. 1
	34	MARGINULINA DECORATA
4770.	260	HAPLOPHRAGMOIDES KIRKI
	261	HAPLOPHRAGMOIDES WALTERI
4950.	264	KARRERIELLA CONVERSA
5130.	570	SYSTEMATOPHORA AREOLATA
5300.	29	CYCLAMMINA AMPLECTENS
	57	SPIROPLECTAMMINA SPECTABILIS LCO
	203	SEISMIC EVENT #3
5490.	54	SPIROPLECTAMMINA NAVARROANA
5580.	591	WETZELIELLA ARTICULATA
5650.	297	MEGASPORE SP. 1
5760.	530	POLYSPHAERIDIUM ZOHARYI

FLYING FOAM I-13 (F)

Depth	Number	Fossil Name
5850.	418	GLAPHROCYSTA ORDINATA
	440	HYSTRICHOSPHAERIDIUM TUBIFERUM
5940.	417	GLAPHROCYSTA INTRICATA
6200.	36	PSEUDOHASTIGERINA WILCOXENSIS
	307	AREOLIGERA SENONENSIS
	447	IMPLETOSPHAERIDIUM SCALENFURCATUM
	485	MEMBRANOPHORIDIUM ASPINATUM
	578	THALASSIPHORA PELAGICA
6300.	376	DEFLANDREA OEBISFELDENSIS
6390.	41	PLECTOFRONDICULARIA AFF. PAUCICOSTATA
	348	CORDOSPHAERIDIUM GRACILE
	349	CORDOSPHAERIDIUM INODES
	388	DINOPETEIGIUM CLADOIDES SENSU MORG.
	424	HETERAULACACYSTA LEPTALEA
	457	KISSELOVIA COLEOTHRYPTA (REWORKED)
	593	WETZELIELLA OVALIS
6480.	390	DIPHYES COLLIGERUM
6570.	230	BULIMINA OVATA
6660.	304	AREOLIGERA CORONATA
6750.	427	HOMOTRYBLIUM TENUISPINOSUM
6840.	458	KISSELOVIA CRASSIRAMOSA

ADOLPHUS D-50 (F)

Rotary table height: 98.0F
Water depth: 377.0F

Depth	Number	Fossil Name
1140.	10	UVIGERINA CANARIENSIS
1410.	71	EPISTOMINA ELEGANS
1500.	218	MARGINULINA AMERICANA
1590.	16	CERATOBULIMINA CONTRARIA
	136	MELONIS BARLEEANUM
1680.	18	SPIROPLECTAMMINA CARINATA
1980.	20	GYROIDINA GIRARDANA
2700.	179	GLOBOROTALIA SCITULA PRAESCITULA
2900.	201	SEISMIC EVENT #1
3060.	26	UVIGERINA EX.GR.MIOZEA-NUTTALI
3660.	15	GLOBIGERINA PRAEBULLOIDES
	81	GLOBIGERINA VENEZUELANA
	69	NODOSARIA CF. ELEGANTISSIMA
4200.	24	TURRILINA ALSATICA
	33	TURBOROTALIA POMEROLI
	202	SEISMIC EVENT #2
4440.	259	AMMODISCUS LATUS
	25	COARSE ARENACEOUS SPP.

ADOLPHUS D-50 (F)

Depth	Number	Fossil Name
4562.	263	AMMOBACULITES AFF. POLYTHALAMUS
4920.	82	GLOBIGERINA LINAPERTA
4950.	85	PSEUDOHASTIGERINA MICRA
	261	HAPLOPHRAGMOIDES WALTERI
5400.	203	SEISMIC EVENT #3
5420.	147	CATAPSYDRAX AFF. DISSIMILIS
	260	HAPLOPHRAGMOIDES KIRKI
5550.	68	SPIROPLECTAMMINA SPECTABILIS LO
5778.	32	AMMOSPHAEROIDINA SP. 1
5896.	40	BULIMINA ALAZANENSIS
6018.	30	CIBICIDOIDES BLANPIEDI
6200.	49	OSANGULARIA EXPANSA
	29	CYCLAMMINA AMPLECTENS
6646.	144	GLOBOROTALIA CERROAZULENSIS
	90	ACARININA DENSA
	156	SUBBOTINA FRONTOSA
	37	ACARININA AFF. PENTACAMERATA
	89	MOROZOVELLA SPINULOSA
6975.	234	TRUNCAROTALITES AFF. ROHRI
7596.	160	ACARININA PSEUDOTOPILENSIS
	93	ACARININA AFF. BROEDERMANNI
7917.	36	PSEUDOHASTIGERINA WILCOXENSIS
8020.	161	PLANOROTALITES AUSTRALIFORMIS
	164	NUTTALIDES TRUMPYI
8258.	50	SUBBOTINA PATAGONICA
	230	BULIMINA OVATA
8384.	54	SPIROPLECTAMMINA NAVARROANA
8520.	57	SPIROPLECTAMMINA SPECTABILIS LCO
	56	GLOMOSPIRA CORONA
8700.	55	GAVELINELLA BECCARIIFORMIS
8726.	194	PLANOROTALITES CHAPMANI
	95	ARAGONIA VELASCOENSIS

HIBERNIA P-15 (M)

Rotary table height: 11.3M
Water depth: 80.2M

Depth	Number	Fossil Name
255.	17	ASTERIGERINA GURICHI
275.	18	SPIROPLECTAMMINA CARINATA
	265	ASTERIGERINA GURICHI (PEAK)
310.	16	CERATOBULIMINA CONTRARIA
410.	20	GYROIDINA GIRARDANA
	100	GLOBIGERINA RIVEROA
550.	26	UVIGERINA EX.GR.MIOZEA-NUTTALI

HIBERNIA P-15 (M)

Depth	Number	Fossil Name
620.	201	SEISMIC EVENT #1
695.	15	GLOBIGERINA PRAEBULLOIDES
720.	71	EPISTOMINA ELEGANS
915.	72	CYCLOGYRA DECORATA
945.	69	NODOSARIA CF. ELEGANTISSIMA
960.	202	SEISMIC EVENT #2
975.	81	GLOBIGERINA VENEZUELANA
1005.	27	EPONIDES UMBONATUS
1035.	147	CATAPSYDRAX AFF. DISSIMILIS
1075.	24	TURRILINA ALSATICA
1125.	25	COARSE ARENACEOUS SPP.
	32	AMMOSPHAEROIDINA SP. 1
	57	SPIROPLECTAMMINA SPECTABILIS LCO
	259	AMMODISCUS LATUS
	260	HAPLOPHRAGMOIDES KIRKI
1185.	261	HAPLOPHRAGMOIDES WALTERI
1195.	29	CYCLAMMINA AMPLECTENS
1200.	203	SEISMIC EVENT #3
1315.	53	UVIGERINA BATJESI
	263	AMMOBACULITES AFF. POLYTHALAMUS
1345.	40	BULIMINA ALAZANENSIS
1375.	45	BULIMINA TRIGONALIS
1400.	204	SEISMIC EVENT #4

EGRET K-36 (F)

Rotary table height: 98.0F
Water depth: 222.0F

Depth	Number	Fossil Name
860.	17	ASTERIGERINA GURICHI
	369	CYCLOPSIELLA VIETA
	377	DEFLANDREA PHOSPHORITICA
	279	BOMBACACIDITES DA
	283	PINUS
	287	PODOCARPIDITES DA
	293	TSUGAEPOLLENITES INGNICULUS
1040.	26	UVIGERINA EX.GR.MIOZEA-NUTTALI
1130.	478	LINGULODINIUM MACHAEROPHORUM
1340.	16	CERATOBULIMINA CONTRARIA
1520.	20	GYROIDINA GIRARDANA
	21	GUTTULINA PROBLEMA
	18	SPIROPLECTAMMINA CARINATA
	71	EPISTOMINA ELEGANS
	15	GLOBIGERINA PRAEBULLOIDES
1580.	24	TURRILINA ALSATICA

EGRET K-36 (F)

Depth	Number	Fossil Name
1610.	27	EPONIDES UMBONATUS
	42	CIBICIDOIDES ALLENI
1640.	202	SEISMIC EVENT #2
1940.	69	NODOSARIA CF. ELEGANTISSIMA
2240.	82	GLOBIGERINA LINAPERTA

OSPREY H-84 (F)

Rotary table height: 85.0F
Water depth: 201.0F

Depth	Number	Fossil Name
830.	478	LINGULODINIUM MACHAEROPHORUM
	554	SPINIFERITES SCABRATUS
	565	SUMATRADINIUM
	282	OSMUNDACIDITES DA
	283	PINUS
	293	TSUGAEPOLLENITES INGNICULUS
1100.	501	OPERCULOPINIUM CENTROCARPUM
	569	SYSTEMATOPHORA ANCYREA
1190.	17	ASTERIGERINA GURICHI
1280.	338	CHIROPTERIDIUM MESPILANUM
	279	BOMBACACIDITES DA
1370.	18	SPIROPLECTAMMINA CARINATA
	20	GYROIDINA GIRARDANA
1460.	310	AREOSPHAERIDIUM ARCUATUM
1640.	15	GLOBIGERINA PRAEBULLOIDES
	16	CERATOBULIMINA CONTRARIA
1820.	26	UVIGERINA EX.GR.MIOZEA-NUTTALI
	181	CYCLOGYRA INVOLVENS
1910.	81	GLOBIGERINA VENEZUELANA
2180.	82	GLOBIGERINA LINAPERTA
2360.	84	GLOBIGERINA YEGUAENSIS
	147	CATAPSYDRAX AFF. DISSIMILIS
	69	NODOSARIA CF. ELEGANTISSIMA
	148	LOBIGERINATHEKA INDEX
2450.	90	ACARININA DENSA
	89	MOROZOVELLA SPINULOSA
	33	TURBOROTALIA POMEROLI
	187	CIBICIDOIDES TRUNCANUS
	234	TRUNCAROTALITES AFF. ROHRI
	34	MARGINULINA DECORATA
	244	GAUDRYINA SP. 10
2540.	52	ACARININA SOLDADOENSIS
	51	ACARININA PRIMITIVA

OSPREY H-84 (F)

Depth	Number	Fossil Name
2540.	162	MOROZOVELLA AEQUA
	159	MOROZOVELLA ARAGONENSIS
	166	MOROZOVELLA SUBBOTINAE
	50	SUBBOTINA PATAGONICA
	93	ACARININA AFF. BROEDERMANNI
	472	LENTINIA WETZELII
	509	PALEOHYSTRICHOPHORA INFUSORIOIDES
	593	WETZELIELLA OVALIS
2630.	329	ADNATOSPHAERIDIUM RETICULENSE
	298	APECTODINIUM HOMOMORPHUM
	304	AREOLIGERA CORONATA
	348	CORDOSPHAERIDIUM GRACILE
	403	EOCLADOPYXIS PENICULATA (REWORKED)
	418	GLAPHROCYSTA ORDINATA
	431	HYSTRICHOKOLPOMA CINCTUM (REWORKED)

BONANZA M-71 (M)

Rotary table height: 26.8M
Water depth: 194.0M

Depth	Number	Fossil Name
1210.	10	UVIGERINA CANARIENSIS
	77	ELPHIDIUM SPP.
1240.	17	ASTERIGERINA GURICHI
1320.	26	UVIGERINA EX.GR.MIOZEA-NUTTALI
1370.	18	SPIROPLECTAMMINA CARINATA
1410.	21	GUTTULINA PROBLEMA
1440.	70	ALABAMINA SCITULA
1480.	16	CERATOBULIMINA CONTRARIA
	20	GYROIDINA GIRARDANA
	71	EPISTOMINA ELEGANS
1510.	25	COARSE ARENACEOUS SPP.
	97	MAIN SAND MEMBER TOP
	98	MAIN SAND MEMBER BOTTOM
1560.	34	MARGINULINA DECORATA
	15	GLOBIGERINA PRAEBULLOIDES
1600.	259	AMMODISCUS LATUS
1680.	260	HAPLOPHRAGMOIDES KIRKI
1710.	27	EPONIDES UMBONATUS
1760.	264	KARRERIELLA CONVERSA
1800.	263	AMMOBACULITES AFF. POLYTHALAMUS
1840.	29	CYCLAMMINA AMPLECTENS
1960.	72	CYCLOGYRA DECORATA
2130.	81	GLOBIGERINA VENEZUELANA
2370.	261	HAPLOPHRAGMOIDES WALTERI

BONANZA M-71 (M)

Depth	Number	Fossil Name
2885.	84	GLOBIGERINA YEGUAENSIS
3125.	94	GLOBIGERINATHEKA KUGLERI
	90	ACARININA DENSA
	32	AMMOSPHAEROIDINA SP. 1
3125.	85	PSEUDOHASTIGERINA MICRA
3285.	36	PSEUDOHASTIGERINA WILCOXENSIS
	50	SUBBOTINA PATAGONICA
3405.	159	MOROZOVELLA ARAGONENSIS
	93	ACARININA AFF. BROEDERMANNI
	37	ACARININA AFF. PENTACAMERATA
	56	GLOMOSPIRA CORONA

SOUTH TEMPEST G-88 (M)

Rotary table height: 26.8M
Water depth: 158:2M

Depth	Number	Fossil Name
740.	228	CASSIDULINA TERETIS
	240	ELPHIDIUM CLAVATUM
	71	EPISTOMINA ELEGANS
800.	16	CERATOBULIMINA CONTRARIA
830.	17	ASTERIGERINA GURICHI
980.	18	SPIROPLECTAMMINA CARINATA
	20	GYROIDINA GIRARDANA
	110	GLOBIGERINA BULLOIDES
	6	NEOGLOBOQUADRINA ACOSTAENSIS
1065.	26	UVIGERINA EX.GR.MIOZEA-NUTTALI
1215.	25	COARSE ARENACEOUS SPP.
1245.	24	TURRILINA ALSATICA
1245.	15	GLOBIGERINA PRAEBULLOIDES
1395.	263	AMMOBACULITES AFF. POLYTHALAMUS
	260	HAPLOPHRAGMOIDES KIRKI
1425.	264	KARRERIELLA CONVERSA
	259	AMMODISCUS LATUS
1455.	29	CYCLAMMINA AMPLECTENS
1515.	261	HAPLOPHRAGMOIDES WALTERI
1695.	86	TURRILINA ROBERTSI
1725.	32	AMMOSPHAEROIDINA SP. 1
1845.	82	GLOBIGERINA LINAPERTA
	84	GLOBIGERINA YEGUAENSIS
1905.	187	CIBICIDOIDES TRUNCANUS
	68	SPIROPLECTAMMINA SPECTABILIS LO
	30	CIBICIDOIDES BLANPIEDI
2005.	57	SPIROPLECTAMMINA SPECTABILIS LCO

SOUTH TEMPEST G-88 (M)

Depth	Number	Fossil Name
2145.	54	SPIROPLECTAMMINA NAVARROANA
	151	BULIMINA BRADBURYI
2205.	90	ACARININA DENSA
2265.	41	PLECTOFRONDICULARIA AFF. PAUCICOSTATA
	85	PSEUDOHASTIGERINA MICRA
2335.	36	PSEUDOHASTIGERINA WILCOXENSIS
	96	ACARININA INTERMEDIA WILCOXENSIS
2355.	194	PLANOROTALITES CHAPMANI
	50	SUBBOTINA PATAGONICA
	93	ACARININA AFF. BROEDERMANNI
	37	ACARININA AFF. PENTACAMERATA
2535.	164	NUTTALIDES TRUMPYI
2655.	52	ACARININA SOLDADOENSIS
	56	GLOMOSPIRA CORONA

DICTIONARY USED IN RASC TO CODE STRATIGRAPHIC EVENTS

NEOGLOBOQUADRINA PACHYDERMA	1	SUBBOTINA PATAGONICA	50
GLOBIGERINA APERTURA	2	ACARININA PRIMITIVA	51
GLOBIGERINA PSEUDOBESA	3	ACARININA SOLDADOENSIS	52
GLOBOROTALIA INFLATA	4	UVIGERINA BATJSSI	53
GLOBOROTALIA CRASSAFORMIS	5	SPIROPLECTAMMINA NAVARROANA	54
NEOGLOBOQUADRINA ACOSTAENSIS	6	GAVELINELLA BECCARIIFORMIS	55
GLOBIGERINOIDES RUBER	7	GLOMOSPIRA CORONA	56
ORBULINA UNIVERSA	8	SPIROPLECTAMMINA SPECTABILIS LCO	57
TURSENKOINA GRACILIS	9	EPONIDES SP. 8	58
UVIGERINA CANARIENSIS	10	RZEHAKINA EPIGONA	59
NONIONELLA PIZARRENSE	11	PLANOROTALITES COMPRESSUS	60
EHRENBERGINA SERRATA	12	SUBBOTINA PSEUDOBULLOIDES	61
HANZAWAIA CONCENTRICA	13	GAVELINELLA DANICA	62
TEXTULARIA AGGLUTINANS	14	NODOSARIA CF. POZOENSIS	63
GLOBIGERINA PRAEBULLOIDES	15	CASSIDULINA ISLANDICA	64
CERATOBULIMINA CONTRARIA	16	COSCINODISCUS SP. 1	65
ASTERIGERINA GURICHI	17	COLEITES RETICULOSUS	66
SPIROPLECTAMMINA CARINATA	18	SCAPHOPOD SP. 1	67
GLOBIGERINOIDES SP.	19	SPIROPLECTAMMINA SPECTABILIS LO	68
GYROIDINA GIRARDANA	20	NODOSARIA CF. ELEGANTISSIMA	69
GUTTULINA PROBLEMA	21	ALABAMINA SCITULA	70
DUMMY	22	EPISTOMINA ELEGANS	71
DUMMY	23	CYCLOGYRA DECORATA	72
TURRILINA ALSATICA	24	EPONIDES SP. 3	73
COARSE ARENACEOUS SPP.	25	EPONIDES SP. 5	74
UVIGERINA EX.GR.MIOZEA-NUTTALI	26	LENTICULINA ULATISENSIS	75
EPONIDES UMBONATUS	27	CASSIDULINA SP.	76
CIBICIDOIDES SP. 5	28	ELPHIDIUM SPP.	77
CYCLAMMINA AMPLECTENS	29	UVIGERINA PEREGRINA	78
CIBICIDOIDES BLAMPIEDI	30	GLOBIGERINA TRIPARTITA	79
PTEROPOD SP. 1	31	CYCLAMMINA CANCELLATA	80
AMMOSPHAEROIDINA SP. 1	32	GLOBIGERINA VENEZUELANA	81
TURBOROTALIA POMEROLI	33	GLOBIGERINA LINAPERTA	82
MARGINULINA DECORATA	34	PLANOROTALITES PSEUDOSCITULUS	83
SPIROPLECTAMMINA DENTATA	35	GLOBIGERINA YEGUAENSIS	84
PSEUDOHASTIGERINA WILCOXENSIS	36	PSEUDOHASTIGERINA MICRA	85
ACARININA AFF. PENTACAMERATA	37	TURRILINA ROBERTSI	86
LENTICULINA SUBPAPILLOSA	38	BULIMINA AFF. JACKSONENSIS	87
ALABAMINA WILCOXENSIS	39	SIPHOGENEROIDES ELEGANTA	88
BULIMINA ALAZANENSIS	40	MOROZOVELLA SPINULOSA	89
PLECTOFRONDICULARIA AFF. PAUCICOSTATA	41	ACARININA DENSA	90
CIBICIDOIDES ALLENI	42	RADIOLARIANS	91
BULIMINA MIDWAYENSIS	43	MOROZOVELLA CAUCASICA	92
CIBICIDOIDES AFF. WESTI	44	ACARININA AFF. BROEDERMANNI	93
BULIMINA TRIGONALIS	45	GLOBIGERINATHEKA KUGLERI	94
**********	46	ARAGONIA VELASCOENSIS	95
PLANOROTALITES PLANOCONICUS	47	ACARININA INTERMEDIA WILCOXENSIS	96
ANOMALINA SP. 5	48	MAIN SAND MEMBER TOP	97
OSANGULARIA EXPANSA	49	MAIN SAND MEMBER BOTTOM	98

BOLIVINA PASTIGIA	99	GLOBIGERINA GORTANII	150
GLOBIGERINA RIVEROA	100	BULIMINA BRADBURYI	151
BROWN MUDSTONE MEMBER TOP	101	CASSIDULINA SUBGLOBOSA	152
BROWN MUDSTONE MEMBER BOTTOM	102	BULIMINA COOPERENSIS	153
GUDRID SAND MEMBER TOP	103	ANOMALINOIDES MIDWAYENSIS	154
GUDRID SAND MEMBER BOTTOM	104	ANOMALINOIDES GROSSERUGOSA	155
LEIF SAND MEMBER TOP	105	SUBBOTINA FRONTOSA	156
LEIF SAND MEMBER BOTTOM	106	TRITAXIA SP. 3	157
CARTWRIGHT FORMATION TOP	107	SUBBOTINA INAEQUISPIRA	158
CARTWRIGHT FORMATION BOTTOM	108	MOROZOVELLA ARAGONENSIS	159
CASSIDULINA CURVATA	109	ACARININA PSEUDOTOPILENSIS	160
GLOBIGERINA BULLOIDES	110	PLANOROTALITES AUSTRALIFORMIS	161
PARAROTALIA SP. 1	111	MOROZOVELLA AEQUA	162
MARGINULINA BACHEI	112	**********	163
GLOBOROTALIA MENARDII GROUP	113	NUTTALIDES TRUMPYI	164
GLOBIGERINOIDES SACCULIFER	114	HETEROLEPA AFF. MEXICANA	165
GLOBOROTALIA OBESA	115	MOROZOVELLA SUBBOTINAE	166
ORBULINA SUTURALIS	116	MOROZOVELLA FORMOSA GRACILIS	167
SPHAEROIDINA BULLOIDES	117	MOROZOVELLA VELACOENSIS	168
EPISTOMINA SP. 5	118	EPISTOMINELLA TAKAYANAGII	169
SPHAEROIDINELLA SUBDEHISCENS	119	GLOBIGERINA AFF. FALCONENSIS	170
GLOBOROTALIA SIAKENSIS	120	BUCELLA FRIGIDA	171
GLOBIGERINA NEPENTHES	121	PSEUDOHASTIGERINA SP.	172
SPHAEROIDINELLOPSIS SEMINULINA	122	ANOMALINA SP. 1	173
GLOBIGERINOIDES TRILOBUS	123	**********	174
GLOBOQUADRINA DEHISCENS	124	ALLOGROMIA SP.	175
GLOBOROTALIA CONTINUOSA	125	QUADRIMORPHINA AFF.ALLOMORPHINOIDES	176
GLOBIGERINOIDES OBLIQUUS	126	BOLIVINA DILATATA	177
GLOBIGERINITA NAPARIMAENSIS	127	GLOBOROTALIA ARCHEOMENARDII	178
GLOBOROTALIA PRAEMENARDII	128	GLOBOROTALIA SCITULA PRAESCITULA	179
CYCLAMMINA PLACENTA	129	GYROIDINA SP. 4	180
SIPHONINA ADVENA	130	CYCLOGYRA INVOLVENS	181
CIBICIDOIDES TENELLUS	131	PLECTOFRONDICULARIA SP. 3	182
GLOBOROTALIA OPIMA NANA	132	CYCLAMMINA ROTUNDIDORSATA	183
LENTICULINA SP. 3	133	GYROIDINA OCTOCAMERATA	184
LENTICULINA SP. 4	134	TRITAXIA SP. 4	185
GLOBIGERINA SP. 40	135	ACARININA AFF. QUETRA	186
MELONIS BARLEEANUM	136	CIBICIDOIDES TRUNCANUS	187
GLOBIGERINOIDES PRIMORDIUS	137	PLEUROSTOMELLA SP. 1	188
GLOBIGERINA ANGUSTIUMBILICATA	138	KARRERIELLA SP. 2	189
GLOBOROTALIA OPIMA OPIMA	139	ANOMALINOIDES ACUTA	190
ROTALIATINA BULIMINOIDES	140	GLOBIGERINA AFF. HIGGINSI	191
PLANULINA RENZI	141	KARRERIELA CONIFORMIS	192
GYROIDINA SOLDANII MANILLIGERA	142	**********	193
UVIGERINA GALLOWAY	143	PLANOROTALITES CHAPMANI	194
GLOBOROTALIA CERROAZULENSIS	144	GLOBIGERINOIDES SUBCONGLOBATUS	195
ANOMALINOIDES ALLENI	145	OSANGULARIA SP. 4	196
SUBBOTINA EOCAENA	146	BULIMINA CACUMINATA	197
CATAPSYDRAX AFF. DISSIMILIS	147	GLOBIGERINATHEKA MEXICANA	198
LOBIGERINATHEKA INDEX	148	BOLIVINA FLORIDANA	199
GLOBIGERINATHEKA TROPICALIS	149	**********	200

SEISMIC EVENT #1	201	MOROZOVELLA AFF. QUETRA	252
SEISMIC EVENT #2	202	SUBBOTINA TRILOCULINOIDES	253
SEISMIC EVENT #3	203	PLANOROTALITES PSEUDOMENARDII	254
SEISMIC EVENT #4	204	MOROZOVELLA CONICOTRUNCATA	255
NUTTALINELLA FLOREALIS	205	MOROZOVELLA AFF. PUSILLA	256
EPONIDES POLYGONUS	206	CHILOGUEMBELINA SP.	257
GLOBIGERINA MUNDA	207	TAPPANINA SELMENSIS	258
GLOBIGERINA AFF. ANGIPOROIDES	208	AMMODISCUS LATUS	259
BULIMINA TRINITATENSIS	209	HAPLOPHRAGMOIDES KIRKI	260
LOXOSTOMOIDES APPLINAE	210	HAPLOPHRAGMOIDES WALTERI	261
HANTKENINA SP.	211	KARRERIELLA APICULARIS	262
**********	212	AMMOBACULITES AFF. POLYTHALAMUS	263
ARENOBULIMINA SP. 2	213	KARRERIELLA CONVERSA	264
**********	214	ASTERIGERINA GURICHI (PEAK)	265
**********	215	GLOBOROTALIA PUNCTICULATA (D'ORBIGNY)	266
GLOBIGERINOIDES SICANUS	216	GLOBOROTALIA HIRSUTA	267
GLOBOROTALIA SCITULA	217	GLOBOROTALIA AFF. KUGLERI	268
MARGINULINA AMERICANA	218	NEOGLOBOQUADRINA ATLANTICA	269
MARTINOTIELLA COMMUNIS	219	CIBICIDOIDES GROSSA	270
CIBICIDOIDES WUELLERSTORFFI	220	GLOBOROTALIA INCREBESCENS	271
GLOBIGERINOIDES SUBQUADRATUS	221	GLOBOQUADRINA BAROEMENSIS	272
GLOBOQUADRINA ALTISPIRA	222	BULIMINA GRATA	273
GLOBIGERINA CIPEROENSIS	223	GAUDRYINA AFF. HILTERMANNI	274
UVIGERINA MEXICANA	224	PARAROTALIA SP. 2	275
GLOBIGERINA AFF. AMPLIAPERTURA	225	ABIES	276
GLOBIGERINA SENNI	226	ARTEMISIA	277
CIBICIDOIDES AFF. TUXPAMENSIS	227	ARTEMISIA DA	278
CASSIDULINA TERETIS	228	BOMBACACIDITES DA	279
**********	229	CHENOPODIUMSPORITES DA	280
BULIMINA OVATA	230	CUPANIEIDITES DA	281
UVIGERINA RUSTICA	231	OSMUNDACIDITES DA	282
GLOBIGERINOIDES IMMATURUS	232	PINUS	283
CATAPSYDRAX UNICAVUS	233	PISTILLIPOLLENITES MCGREGORII	284
TRUNCAROTALITES AFF. ROHRI	234	PLATYCARYAPOLLENITES	285
SUBBOTINA BOLIVARIANA	235	PLATYCARYAPOLLENITES DA	286
EPONIDES SP. 4	236	PODOCARPIDITES DA	287
LENTICULINA AFF. ALATOLIMBATA	237	POLYPODIACIDITES DA	288
CIBICIDOIDES SP. 7	238	SEQUOIAPOLLENITES	289
NONIONELLA LABRADORICA	239	SEQUOIAPOLLENITES DA	290
ELPHIDIUM CLAVATUM	240	TILIAEPOLLENITES	291
GLOBOROTALIA TRUNCATULINOIDES	241	TILIAEPOLLENITES DA	292
GLOBOROTALIA FOHSI GROUP	242	TSUGAEPOLLENITES INGNICULUS	293
GLOBIGERINA DECAPERTA	243	NYSSAPOLLENITES DA	294
GAUDRYINA SP. 10	244	NYASSAPOLLENITES DB	295
PRAEORBULINA GLOMEROSA	245	OSMUNDACIDITES	296
GLOBIGERINATELLA INSUETA	246	MEGASPORE SP. 1	297
GLOBIGERINOIDES ALTIAPERTURA	247	APECTODINIUM HOMOMORPHUM	298
GLOBOROTALIA AFF. INCREBESCENS	248	APECTODINIUM HYPERACANTHUM	299
GLOBIGERINATHEKA SEMIINVOLUTA	249	APECTODINIUM PARVUM	300
VULVULINA JARVISI	250	APECTODINIUM QUINQUELATUM	301
ANOMALINA SP. 4	251	APTEA	302

PALEOCYSTODINIUM BENJAMINII 507
PALEOCYSTODINIUM GOLZOWENSE 508
PALEOHYSTRICHOPHORA INFUSORIOIDES 509
PALEOHYSTRICHOPHORA 510
PALAEOPERIDINIUM CRETACEUM 511
PALAEOPERIDINIUM PYROPHORUM 512
PALEOSTOMOCYSTIS DA 513
PALEOTETRADINIUM 514
PARALECANIELLA INDENTATA 515
PALYNODINIUM GRALLATOR 516
PENTADINIUM LATICINCTUM 517
PERISSEIASPHAERIDIUM 518
PHELODINIUM 519
PHELODINIUM MAGNIFICUM 520
PHELODINIUM TRICUSPE 521
PHTHANOPERIDINIUM 522
PHTHANOPERIDINIUM ALECTROLOPHUM 523
PHTHANOPERIDINIUM AMOSNUM 524
PHTHANOPERIDINIUM COMATUM (REWORKED) 525
PHTHANOPERIDINIUM ECHINATUM 526
PHTHANOPERIDINIUM LEVIMURUM 527
PHTHANOPERIDINIUM MICROSPINATUM 528
POLYSPHAERIDIUM 529
POLYSPHAERIDIUM ZOHARYI 530
POLYSTEPHANOPHORUS 531
PSEUDOCERATIUM 532
PTERODINIUM CINGULATUM 533
PYXIDIELLA 534
RHOMBOIDINIUM 535
RHOMBOIDINIUM GLABRUM 536
ROTTNESTIA BORUSSICA 537
SAEPTODINIUM EURYPYLUM 538
SAHLANDIA 539
SCHIZOCYSTIA RUGOSA 540
SENEGALINIUM MACROCYSTUM 541
SENDNIASPHAERA ROTUNDATA 542
SPINIDINIUM ECHINOIDEUM 543
SPINIDINIUM STYLONIFERUM 544
SPINIDINIUM SVERDRUPIANUM 545
SPINIDINIUM CF VESTITUM 546
SPINIFERITES MEMBRANACEUS 547
SPINIFERITES MIRABILIS 548
SPINIFERITES MONILIS 549
SPINIFERITES NODOSUS 550
SPINIFERITES POROSUS 551
SPINIFERITES PSEUDOFURCATUS 552
SPINIFERITES RAMOSUS MULTIBREVIS 553
SPINIFERITES SCABRATUS 554
SPINIFERITES SCABROSUS 555
SPINIFERITES TRIPODES 556
SPINIFERITES WETZELII 557
SPINIFERITES DA 558
SPINIFERITES DB 559
SPONGODINIUM DELITIENSE 560
STEPHODINIUM CORONATUM 561
SUBTILIDINIUM 562
SUBTILIDINIUM MINUTUM 563
SUBTILISPHAERA PERLUCIDA 564
SUMATRADINIUM 565
SURCULOSPHAERIDIUM LONGIFURCATUM 566
SURCULOSPHAERIDIUM LONGIFURCATUM A 567
SVALBARDELLA 568
SYSTEMATOPHORA ANCYREA 569
SYSTEMATOPHORA AREOLATA 570
SYSTEMATOPHORA PLACACANTHA 571
TANYOSPHAERIDIUM REGULARE 572
TANYOSPHAERIDIUM VARIECALAMUM 573
TANYOSPHAERIDIUM XANTHIOPYXIDES 574
TANYOSPHAERIDIUM DA 575
THALASSIPHORA DELICATA 576
THALASSIPHORA PATULA 577
THALASSIPHORA PELAGICA 578
TRIBLASTULA NUDA 579
TRICHODINIUM 580
TRICHODINIUM CASTANEUM 581
TRIGONOPYXIDIA 582
TRIGONOPYXIDIA GINELLA 583
TRINOVANTEDINIUM 584
TRITHYRODINIUM 585
TRITHYRODINIUM SUSPECTUM 586
TUBIDERMODINIUM SULCATUM 587
VOZZHENNIKOVIA EXTENSA 588
WALLODINIUM 589
WALLODINIUM LUNUM 590
WETZELIELLA ARTICULATA 591
WETZELIELLA LUNARIS 592
WETZELIELLA OVALIS 593
WETZELIELLA SYMMETRICA 594
WETZELIELLA SYMMETRICA B 595
WETZELIELLA DA 596
WETZELIELLA LV 597
WILSONIDIUM 598
WILSONIDIUM ECHINOSUTURATUM 599
WILSONIDIUM INTERMEDIUM 600

APPENDIX B

LISTING OF PROGRAMMES

```
100 '              MERGE PROGRAMME
110 '    PREPARED BY MARC D'IORIO, JULY 1984
120 ' REVISED SEPTEMBER 1984 AND DECEMBER 1987
130 '
140 '         THE PURPOSE OF THIS PROGRAMME
150 '     IS TO MERGE TWO DATA AND DEPTH FILES
160 ' TO PRODUCE INTEGRATED DATA AND DEPTH FILES
170 '
180 ' DEFINITION OF PARAMETERS:
190 '
200 ' A1$ : NAME OF FIRST DATA FILE
210 ' A2$ : NAME OF FIRST DEPTH FILE
220 ' A3$ : NAME OF SECOND DATA FILE
230 ' A4$ : NAME OF SECOND DEPTH FILE
240 ' A5$ : NAME OF INTEGRATED DATA FILE
250 ' A6$ : NAME OF INTEGRATED DEPTH FILE
260 ' NM$() : INTERIM WELL NAME ARRAY
270 ' S1(A,B,C) AND S2(A,B,C): INTERIM DATA MATRIX
280 '  WHERE : A IS THE WELL DIMENSION
290 '        : B REPRESENT THE LEVELS
300 '        : C REPRESENT THE EVENTS ON THE B LEVEL
310 '        : THE 14TH ELEMENT IS C THE DEPTH OF THAT LEVEL
320 '
330 KEY OFF
340 CLS
350 LOCATE 1,1,0
360 DIM S1(8,50,14), S2(8,50,14),NM$(8,3)
370 '
380 ' USER INPUT OF FILE NAMES AND SPECIFICATIONS
390 '
400 FOR OK=1 TO 9:PRINT "":NEXT OK
410 PRINT TAB(35) "**WARNING**":PRINT
420 PRINT TAB(16) "Your data files must follow the same sequence
     and"
430 PRINT TAB(20) "the well names must be exactly identical":PRINT
440 PRINT TAB(12) "On the last line of your dictionary, depth and
     data files"
450 PRINT TAB(28) "should be the word last !"
460 FOR OK=1 TO 6:PRINT "":NEXT OK:PRINT TAB(26) "hit any key when
     ready..."
470 OO$=INKEY$:IF OO$="" GOTO 470
480 CLS
490 PRINT ""
500 INPUT;"name of the first data file: ";A1$
510 PRINT "":PRINT ""
520 INPUT;"name of the first depth file: ";A2$
530 PRINT "":PRINT ""
540 INPUT;"name of the second data file: ";A3$
550 PRINT "":PRINT ""
560 INPUT;"name of the second depth file: ";A4$
570 PRINT "":PRINT ""
```

```
580 INPUT;"name of the integrated data file: ";A5$
590 PRINT "":PRINT ""
600 INPUT;"name of the integrated depth file: ";A6$
610 PRINT "":PRINT ""
620 INPUT;"number of data lines after water depth and rotary table
     height line? (5 or 7)";NL
630 PRINT "":PRINT ""
640 INPUT;"number of wells in file (max. 8)";NW
650 CLS
660 PRINT TAB(110) "Please wait..."
670 '
680 ' READING IN THE RASC DATA
690 '
700 PRINT
710 PRINT;"Reading in the first data file":PRINT
720 OPEN A1$ FOR INPUT AS #1:OPEN A3$ FOR INPUT AS #2
730 FOR X1=1 TO NW
740 LE=0:CO=1
750 LINE INPUT#1,Z$:IF Z$="" GOTO 750
760 IF Z$="last" GOTO 860
770 LINE INPUT#1,Y$:IF Y$="" GOTO 770
780 FOR AZ=1 TO 20:W=AZ*4-3
790 TB$=MID$(Y$,W,4):TB=VAL(TB$)
800 IF TB=-999 GOTO 850
810 IF TB<0 THEN CO=CO+1:S1(X1,LE,CO)=ABS(TB):GOTO 840
820 IF TB=0 GOTO 840
830 LE=LE+1:CO=1:S1(X1,LE,CO)=TB
840 NEXT AZ:GOTO 770
850 NEXT X1
860 PRINT;"Reading in the second data file":PRINT
870 FOR X1=1 TO NW
880 LE=0:CO=1
890 LINE INPUT#2,Z$:IF Z$="" GOTO 890
900 IF Z$="last" GOTO 1000
910 LINE INPUT#2,Y$:IF Y$="" GOTO 910
920 FOR AZ=1 TO 20:W=AZ*4-3
930 TB$=MID$(Y$,W,4):TB=VAL(TB$)
940 IF TB=-999 GOTO 990
950 IF TB<0 THEN CO=CO+1:S2(X1,LE,CO)=ABS(TB):GOTO 980
960 IF TB=0 GOTO 980
970 LE=LE+1:CO=1:S2(X1,LE,CO)=TB
980 NEXT AZ:GOTO 910
990 NEXT X1
1000 CLOSE#1:CLOSE#2
1010 '
1020 ' READING IN DEPTH FILES
1030 '
1040 OPEN A2$ FOR INPUT AS #1:OPEN A4$ FOR INPUT AS #2
1050 PRINT;"Reading in depth files":PRINT ""
1060 FOR X1=1 TO NW
1070 LINE INPUT#1,D$
```

```
1080 NM$(X1,1)=D$
1090 LINE INPUT#1,D$
1100 NM$(X1,2)=D$
1110 FOR T=1 TO NL
1120 LINE INPUT#1,KR$
1130 FOR W=1 TO 13
1140 N=W*6-5
1150 QF$=MID$(KR$,N,6)
1160 AJ=VAL(QF$)
1170 IF AJ=0 GOTO 1200
1180 HG=13*(T-1)+W
1190 S1(X1,HG,14)=AJ
1200 NEXT W
1210 NEXT T
1220 NEXT X1
1230 FOR X1=1 TO NW
1240 LINE INPUT#2,D$
1250 LINE INPUT#2,D$
1260 FOR T=1 TO NL
1270 INPUT#2,KR$
1280 FOR W=1 TO 13
1290 N=W*6-5
1300 QF$=MID$(KR$,N,6)
1310 AJ=VAL(QF$)
1320 IF AJ=0 GOTO 1350
1330 HG=13*(T-1)+W
1340 S2(X1,HG,14)=AJ
1350 NEXT W
1360 NEXT T
1370 NEXT X1
1380 CLOSE #1:CLOSE #2
1390 '
1400 ' COMPILING THE INTEGRATED OUTPUT FILE
1410 '
1420 PRINT;"Compiling integrated data and depth files"
1430 OPEN A5$ FOR OUTPUT AS #1:OPEN A6$ FOR OUTPUT AS #2
1440 FOR X1=1 TO NW
1450 PRINT#1,NM$(X1,1)
1460 PRINT#2,NM$(X1,1)
1470 PRINT#2,NM$(X1,2)
1480 V8=0:V9=0
1490 L1=1:L2=1
1500 D1=S1(X1,L1,14):D2=S2(X1,L2,14)
1510 IF D1=0 GOTO 1870
1520 IF D2=0 GOTO 1980
1530 IF D1>D2 GOTO 1690
1540 IF D1<D2 GOTO 1780
1550 PRINT#1,USING"####";S1(X1,L1,1);-S2(X1,L2,1);:V8=V8+2:IF V8=19
     OR V8=20 THEN PRINT#1,"":V8=0
1560 FOR UY=2 TO 13
1570 CO=S1(X1,L1,UY)
```

```
1580 IF CO=0 GOTO 1610
1590 PRINT#1,USING"####";-CO;:V8=V8+1:IF V8=20 THEN PRINT#1,"":V8=0
1600 NEXT UY
1610 FOR UY=2 TO 13
1620 CO=S2(X1,L2,UY)
1630 IF CO=0 GOTO 1660
1640 PRINT#1,USING"####";-CO;:V8=V8+1:IF V8=20 THEN PRINT#1,"":V8=0
1650 NEXT UY
1660 PRINT#2,USING"######";S1(X1,L1,14);:V9=V9+1:IF V9=13 THEN
     PRINT#2,"":V9=0
1670 L1=L1+1:L2=L2+1
1680 GOTO 1500
1690 PRINT#1,USING"####";S1(X1,L1,1);:V8=V8+1:IF V8=20 THEN
     PRINT#1,"":V8=0
1700 FOR UY=2 TO 13
1710 CO=S1(X1,L1,UY)
1720 IF CO=0 GOTO 1760
1730 PRINT#1,USING"####";-CO;:V8=V8+1:IF V8=20 THEN PRINT#1,"":V8=0
1740 NEXT UY
1750 PRINT#2,USING"######";S1(X1,L1,14);:V9=V9+1:IF V9=13 THEN
     PRINT#2,"":V9=0
1760 L1=L1+1
1770 GOTO 1500
1780 PRINT#1,USING"####";S2(X1,L2,1);:V8=V8+1:IF V8=20 THEN
     PRINT#1,"":V8=0
1790 FOR UY=2 TO 13
1800 CO=S2(X1,L2,UY)
1810 IF CO=0 GOTO 1850
1820 PRINT#1,USING"####";-CO;:V8=V8+1:IF V8=20 THEN PRINT#1,"":V8=0
1830 NEXT UY
1840 PRINT#2,USING"######";S2(X1,L2,14);:V9=V9+1:IF V9=13 THEN
     PRINT#2,"":V9=0
1850 L2=L2+1
1860 GOTO 1500
1870 PRINT#1,USING"####";S2(X1,L2,1);:V8=V8+1:IF V8=20 THEN
     PRINT#1,"":V8=0
1880 FOR UY=2 TO 13
1890 CO=S2(X1,L2,UY)
1900 IF CO=0 GOTO 1930
1910 PRINT#1,USING"####";-CO;:V8=V8+1:IF V8=20 THEN PRINT#1,"":V8=0
1920 NEXT UY
1930 PRINT#2,USING"######";S2(X1,L2,14);:V9=V9+1:IF V9=13 THEN
     PRINT#2,"":V9=0
1940 L2=L2+1
1950 D2=S2(X1,L2,14)
1960 IF D2=0 OR L2=51 GOTO 2090
1970 GOTO 1870
1980 PRINT#1,USING"####";S1(X1,L1,1);:V8=V8+1:IF V8=20 THEN
     PRINT#1,"":V8=0
1990 FOR UY=2 TO 13
2000 CO=S1(X1,L1,UY)
```

```
2010 IF CO=0 GOTO 2040
2020 PRINT#1,USING"####";-CO;:V8=V8+1:IF V8=20 THEN PRINT#1,"":V8=0
2030 NEXT UY
2040 PRINT#2,USING"######";S1(X1,L1,14);:V9=V9+1:IF V9=13 THEN
     PRINT#2,"":V9=0
2050 L1=L1+1
2060 D1=S1(X1,L1,14)
2070 IF D1=0 OR L1=51 GOTO 2090
2080 GOTO 1980
2090 PRINT#1,"":PRINT#1,-999
2100 PRINT#2,""
2110 NEXT X1
2120 CLOSE#1:CLOSE#2
2130 KEY ON
2140 CLS
2150 PRINT,"    ALL DONE..."
2160 BEEP:BEEP
```

```
100 '            DATALIST PROGRAMME
110 '    PREPARED BY MARC D'IORIO, DECEMBER 1986
120 '
130 '        THE PURPOSE OF THIS PROGRAMME
140 '    IS TO PRODUCE COMPREHENSIVE DATA FILES
150 ' USING RASC DATA, DEPTH AND DICTIONARY FILES
160 '
170 ' DEFINITION OF PARAMETERS:
180 '
190 ' A1$ : NAME OF DATA FILE
200 ' A2$ : NAME OF DICTIONARY FILE
210 ' A3$ : NAME OF DEPTH FILE
220 ' A4$ : NAME OF OUTPUT FILE
230 ' A$(). : DICTIONARY NAME MATRIX
240 ' DA$() : INTERIM DATA MATRIX
250 '
260 DIM T(20), DA$(13), A$(800)
270 KEY OFF
280 CLS
290 LOCATE 1,1,0
300 '
310 ' USER INPUT OF FILE NAMES AND SPECIFICATIONS
320 '
330 FOR OK=1 TO 11:PRINT "":NEXT OK
340 PRINT TAB(12) "On the last line of your dictionary, depth
    and data files"
350 PRINT TAB(28) "should be the word last !"
360 FOR OK=1 TO 9:PRINT "":NEXT OK:PRINT TAB(28) "hit any key
    when ready..."
370 OO$=INKEY$:IF OO$="" GOTO 370
380 CLS
390 PRINT ""
400 INPUT;"name of data file: ";A1$
410 PRINT "":PRINT ""
420 INPUT;"name of its dictionary: ";A2$
430 PRINT "":PRINT ""
440 INPUT;"name of its depth file: ";A3$
450 PRINT "":PRINT ""
460 INPUT;"name of output file: ";A4$
470 PRINT "":PRINT ""
480 INPUT;"number of data lines after water depth and rotary
    table height line? (5 or 7)";NL
490 CLS
500 PRINT TAB(110) "Please wait..."
510 '
520 ' READING IN THE DICTIONARY
530 '
540 OPEN A2$ FOR INPUT AS #1
550 FOR Q=1 TO 800
560 LINE INPUT#1,A$:IF A$="" GOTO 560
570 A$(Q)=A$
```

```
580 IF A$="last" OR A$="LAST" GOTO 600
590 NEXT Q
600 CLOSE#1
610 READING IN THE RASCDATA AND CHANGING THE 20I4 FORMAT TO
 20I5
620 OPEN A1$ FOR INPUT AS #1:OPEN A4$ FOR OUTPUT AS #3:OPEN
    "tempo" FOR OUTPUT AS #2
630 PRINT#3,""
640 LINE INPUT#1,Z$:IF Z$="" GOTO 640
650 PRINT#2,Z$
660 IF Z$="last" GOTO 750
670 LINE INPUT#1,Y$:IF Y$="" GOTO 670
680 FOR AZ=1 TO 20:W=AZ*4-3
690 TB$=MID$(Y$,W,4)+" "
700 IF TB$="-999 " THEN PRINT#2,TB$:KK=0:GOTO 640
710 KK=KK+1
720 IF KK=10 THEN PRINT#2,TB$:KK=0:GOTO 740
730 PRINT#2,TB$;
740 NEXT AZ:GOTO 670
750 CLOSE#1:CLOSE#2
760 '
770 ' COMPILATION OF COMPREHENSIVE FILE
780 '
790 OPEN "tempo" FOR INPUT AS #2:OPEN A3$ FOR INPUT AS #1
800 CLS:PRINT "Well sequence being compiled:":PRINT ""
810 LINE INPUT#2,B$:IF B$="" GOTO 810
820 LINE INPUT#1,D$:IF D$="" GOTO 820
830 CT=0
840 IF B$="last" OR B$="LAST" GOTO 1390
850 PRINT;B$
860 LINE INPUT#1,J$:IF J$="" GOTO 860
870 U1$=LEFT$(J$,1)
880 RT$=MID$(J$,2,5)
890 WD$=MID$(J$,7,7)
900 '
910 ' VERIFICATION OF WELL NAME MATCH
920 '
930 IF B$<>D$ THEN PRINT "The well names from the data and
    depth files do not match.":BEEP:BEEP:BEEP:END
940 PRINT#3,"":PRINT#3,""
950 PRINT#3,B$
960 PRINT#3,"Rotary table height: ";RT$;U1$
970 PRINT#3,"Water depth: ";WD$;U1$
980 PRINT#3,""
990 PRINT#3,"Depth","Number","   Fossil Name ":PRINT#3,""
1000 INPUT#2,T:IF T=0 GOTO 1000
1010 IF T=-999 GOTO 1120
1020 LINE INPUT#1,D$:IF D$="" GOTO 1020
1030 CT=CT+1
1040 FOR JA=1 TO 13:JB=JA*6-5
1050 DA$=MID$(D$,JB,6)
```

```
1060 DA$(JA)=DA$
1070 NEXT JA
1080 KD=1
1090 INPUT#2,T2:IF T2=0 GOTO 1090
1100 IF T2=-999 GOTO 1120
1110 IF T2<0 GOTO 1220
1120 PRINT #3,DA$(KD),T,A$(T)
1130 KD=KD+1
1140 IF T2<>-999 GOTO 1190
1150 IF CT=NL GOTO 810
1160 LINE INPUT #1,D$
1170 CT=CT+1
1180 GOTO 1150
1190 T=T2
1200 IF KD=14 GOTO 1020
1210 GOTO 1090
1220 T(1)=T:T(2)=-T2
1230 FOR N=3 TO 20
1240 INPUT#2,T2:IF T2=0 GOTO 1240
1250 IF T2>0 GOTO 1290
1260 IF T2=-999 GOTO 1290
1270 T(N)=-T2
1280 NEXT N
1290 PRINT#3,DA$(KD),T,A$(T)
1300 KD=KD+1
1310 FOR P=2 TO N-1
1320 X=T(P)
1330 PRINT#3,"",X,A$(X)
1340 NEXT P
1350 IF T2=-999 GOTO 1150
1360 T=T2
1370 IF KD=14 GOTO 1020
1380 GOTO 1090
1390 CLOSE#2
1400 CLOSE#3
1410 CLOSE#1
1420 BEEP:BEEP
1430 CLS
1440 KEY ON
1450 LOCATE 1,1,1
1460 END
```

```
100 ' ZONER PROGRAMME
110 ' PREPARED BY MARC D'IORIO, SEPTEMBER 1987.
120 '
130 ' THE PURPOSE OF THIS PROGRAMME IS TO USE A SLIGHTLY EDITED
140 ' VERSION OF THE DECORANA OUTPUT TO PRODUCE CORRESPONDENCE
150 ' ANALYSIS PLOTS FOR PREVIOUSLY DETERMINED RASC ZONES.
160 '
170 ' FILE NAMES:
180 ' J1$ : CORRESPONDENCE ANALYSIS ABBREVIATED OUTPUT
190 ' J2$ : CORRESPONDENCE ANALYSIS FIRST AXIS SCORES
200 ' A$ : ZONE FILE
210 ' B$ : ZONE OUTPUT FILE
220 '
230 ' DEFINITION OF MATRIX AND ARRAY:
240 ' MA() : EVENT NUMBER, FIRST AXIS SCORE AND RELATIVE ORDER
250 ' QQ$() : CORRESPONDENCE ANALYSIS OUTPUT
260 '
270 KEY OFF
280 CLS
290 DIM QQ$(350)
300 DIM MA(350,3)
310 '
320 ' INPUT FILE NAMES AND PARAMETERS AND
330 ' PREPARE COMPARISON AND SCORE MATRIX
340 '
350 INPUT "NUMBER OF EVENTS : ",NU
360 PRINT:PRINT
370  INPUT;"NAME OF  FILE  CONTAINING  CORRESPONDENCE  ANALYSIS
OUTPUT :      ";J1$
380 PRINT:PRINT
390 INPUT;"NAME OF FILE CONTAINING CORRESPONDENCE ANALYSIS
    SCORES :      ";J2$
400 PRINT:PRINT
410 INPUT;"NAME OF ZONE FILE : ";A$
420 IF A$="" GOTO 410
430 CLS
440 OPEN J2$ FOR INPUT AS #1
450 '
460 ' READ CORRESPONDENCE ANALYSIS SCORES
470 '
480 PRINT:PRINT:PRINT;"READING IN CORRESPONDENCE ANALYSIS
    SCORES..."
490 FOR CT=1 TO NU
500 INPUT#1,AA:IF AA=0 GOTO 500
510 INPUT#1,A2
520 MA(CT,1)=AA:MA(CT,2)=A2
530 NEXT CT
540 CLOSE#1
550 '
560 ' READ CORRESPONDENCE ANALYSIS OUTPUT
570 '
```

```
580 PRINT:PRINT:PRINT;"READING IN CORRESPONDENCE ANALYSIS
    OUTPUT..."
590 OPEN J1$ FOR INPUT AS #1
600 LINE INPUT#1,LA$:IF LA$="" GOTO 600
610 FOR CT=1 TO NU
620 LINE INPUT#1,Q$:IF Q$="" GOTO 620
630 QQ$(CT)=Q$
640 NEXT CT
650 CLOSE #1
660 '
670 ' READ ZONE FILE
680 '
690 B$=A$+".OUT"
700 OPEN A$ FOR INPUT AS #1
710 FOR QQ=1 TO 350
720 MA(QQ,3)=0
730 NEXT QQ
740 PRINT:PRINT:PRINT;"PROCESSING ZONE DATA":PRINT:PRINT
750 INPUT#1,P
760 PRINT;P;"EVENTS ARE IN THAT ZONE"
770 FOR TT=1 TO P
780 INPUT#1,AB
790 FOR YY=1 TO NU
800 QR=MA(YY,1)
810 IF QR=AB GOTO 830
820 NEXT YY
830 MA(YY,3)=1
840 NEXT TT
850 CLOSE#1
860 '
870 ' CREATE OUTPUT FILE
880 '
890 OPEN B$ FOR OUTPUT AS #1
900 PRINT#1,LA$
910 FOR PT=1 TO NU
920 WE=MA(PT,3)
930 IF WE=0 GOTO 960
940 RT$=QQ$(PT)
950 PRINT#1,RT$
960 NEXT PT
970 CLOSE #1
980 CLS
990 '
1000 ' OPTION TO PROCESS ANOTHER ZONE
1010 '
1020 PRINT:PRINT
1030 INPUT;"DO YOU WANT TO PROCESS ANOTHER ZONE? (Y/N): ";C$
1040 FOR HG=1 TO 3:PRINT:NEXT HG
1050 IF C$="" GOTO 1030
1060 IF C$="N" GOTO 1100
1070 INPUT;"NAME OF ZONE FILE? : ";A$
```

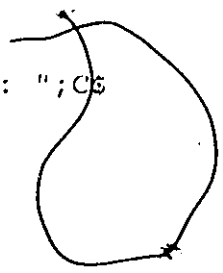

```
1080 IF A$="" GOTO 1080
1090 GOTO 670
1100 CLS
1110 PRINT:PRINT:PRINT:PRINT,"THANK YOU"
1120 KEY ON
1130 END
```

```
100 ' MODULES PROGRAMME
110 ' PREPARED BY MARC D'IORIO, JUNE 1987
120 '
130 ' THIS PROGRAMME WAS CREATED BY THE INTEGRATION OF
140 ' FOUR ROUTINES THAT FOLLOWED THE TSREG ANALYSIS OF
150 ' FREQUENCY DISTRIBUTION.
160 '
170 ' DEFINITION OF PARAMETERS:
180 ' M1$ : WELL NAME FILE
190 ' M2$ : EXTENTION OF WELL DATA FILE
200 ' M3$ : EXTENTION OF WELL OUTPUT FILE
210 ' M4$ : MASTER OUTPUT FILE (OUTPUT)
220 ' M5$ : EVENT ORDER FILE
230 ' M6$ : DIFFERENCE FILE (OUTPUT)
240 ' M7$ : STATISTICS FILE (OUTPUT)
250 ' M8$ : STANDARD DEVIATION WEIGHT FILE (OUTPUT)
260 ' M9$ : HISTOGRAM COMPRENSIVE DATA FILE (OUTPUT)
270 ' N0$ : HISTOGRAM RAW DATA FILE (OUTPUT)
280 ' DC$ : DICTIONARY FILE NAME
290 ' LD : LENGTH OF DICTIONARY
300 ' Y : NUMBER OF WELLS
310 ' M0 : NUMBER OF EVENTS IN THE OPTIMUM SEQUENCE
320 '
330 ' DEFINITION OF COMMON MATRICES:
340 ' A$() : WELL NAME ARRAY
350 ' AA() : EQUIVALENT OF MASTER OUTPUT FILE
360 ' DC$() : DICTIONARY NAME ARRAY
370 CLS
380 KEY OFF
390 DIM DC$(600), AA(1000,3), A$(40)
400 PRINT:PRINT
410 PRINT:PRINT
420 INPUT "Well name file ";M1$
430 PRINT:PRINT
440 INPUT "Filename extention of data files";M2$
450 PRINT:PRINT
460 INPUT "Filename extention of output files";M3$
470 PRINT:PRINT
480 INPUT "Order file";M5$
490 M5$=M5$+"."+M2$
500 PRINT:PRINT
510 INPUT "Name of dictionary";DC$
520 PRINT:PRINT
530 INPUT "Length of dictionary";LD
540 PRINT:PRINT
550 INPUT "Number of wells";Y
560 PRINT:PRINT
570 INPUT "Number of events";M0
580 CLS
590 '
600 ' READING IN THE DICTIONARY
```

```
610 '
620 PRINT:PRINT,"READING IN THE DICTIONARY"
630 OPEN DC$ FOR INPUT AS #1
640 FOR YI=1 TO LD
650 LINE INPUT#1,UV$:IF UV$="" GOTO 650
660 DC$(YI)=UV$
670 NEXT YI
680 CLOSE#1
690 '
700 ' COMPILING OUTPUT FILES
710 '
720 PRINT:PRINT,"COMPILING OUTPUT FILES..."
730 OPEN M1$ FOR INPUT AS #1
740 FOR C=1 TO Y
750 LINE INPUT #1,A$
760 A$(C)=A$
770 NEXT C
780 CLOSE #1
790 PRINT,"CALCULATING DIFFERENCES..."
800 '
810 ' DATA INPUT; ALL WELL DATA AND OUTPUT FILES ARE OPENED
820 '
830 M4$="MSTR01"+"."+M2$
840 OPEN M4$ FOR OUTPUT AS #3
850 KT=0
860 FOR CT=1 TO Y
870 AA$=A$(CT)
880 BB$=AA$+"."+M3$
890 AA$=AA$+"."+M2$
900 OPEN AA$ FOR INPUT AS #1:OPEN BB$ FOR INPUT AS #2
910 '
920 ' VALUES IN THE WELL INPUT FILES (#1) REPRESENT THE
930 ' OBSERVED VALUES; VALUES IN THE WELL OUTPUT FILES (#2)
940 ' REPRESENT THE EXPECTED VALUES.
950 ' OBSERVED MINUS EXPECTED VALUES CALCULATED
960 '
970 FOR T=1 TO 10
980 LINE INPUT #2,AS$
990 NEXT T
1000 LINE INPUT #1,LL$
1010 INPUT #1,AA
1020 FOR QQ=1 TO AA
1030 INPUT #2,Y1,Y2
1040 INPUT #1,X1,X2,X3,X4
1050 X1=ABS(X1)
1060 PRINT#3,X1,X3,Y2,CT
1070 KT=KT+1
1080 AA(KT,1)=X1
1090 AA(KT,2)=X3-Y2
1100 AA(KT,3)=CT
1110 NEXT QQ
```

```
1120 CLOSE #1
1130 CLOSE #2
1140 NEXT CT
1150 PRINT#3,"-999"
1160 CLOSE#3
1170 PRINT,"ORDERING DIFFERENCE FILE..."
1180 '
1190 ' DIFFERENCE FILE ORDERED USING RASC RANKING
1200 '
1210 M6$="DIFF01."+M2$
1220 OPEN M5$ FOR INPUT AS #2:OPEN M6$ FOR OUTPUT AS #3
1230 FOR MC=1 TO M0
1240 INPUT#2,RV:IF RV=0 GOTO 1230
1250 FOR Q=1 TO KT
1260 V=AA(Q,1)
1270 IF V<>RV GOTO 1280
1280 PRINT#3,RV,AA(Q,2),AA(Q,3)
1290 NEXT Q
1300 PRINT#3,-999
1310 NEXT MC
1320 PRINT#3,8888
1330 CLOSE#2
1340 CLOSE#3
1350 PRINT,"CALCULATING VARIANCES AND CREATING"
1360 PRINT,"THE STANDARD DEVIATION WEIGHTS FILES..."
1370 '
1380 ' CALCULATING THE MEAN, THE STANDARD DEVIATION, THE
1390 ' VARIANCE AND THE S2 VALUE OF THE DIFFERENCES IN OBSERVED
1400 ' AND EXPECTED POSITIONS.  A STANDARD DEVIATION WEIGHT
1410 ' FILE IS CREATED FOR USE IN THE STUDY OF FREQUENCY
1420 'DISTRIBUTION.
1430 '
1440 ' DEFINITION OF PARAMETERS :
1450 ' AV : MEAN
1460 ' N : NUMBER OF EVENTS
1470 ' VR : UNBIASED VARIANCE BASED ON CALCULATED MEAN
1480 ' VC : UNBIASED VARIANCE BASED ON ZERO MEAN
1490 ' FI : SUM OF DEGREES OF FREEDOM
1500 ' FS : SUM OF THE PRODUCT OF THE DEGREE OF FREEDOM TIMES
1510 '      VARIANCE (UNBIASED VARIANCE BASED ON ZERO MEAN)
1520 ' S2 : S SQUARED VALUE (FS/FI)
1530 '
1540 DIM VAR(30)
1550 N=0:D=0:FI=0:FS=0
1560 M7$="DATA01."+M2$
1570 M8$="SDW."+M2$
1580 OPEN M6$ FOR INPUT AS #1:OPEN M7$ FOR OUTPUT AS #2:OPEN
     M8$ FOR OUTPUT AS #3
1590 INPUT#1,A:IF A=0 GOTO 1570
1600 IF A=8888 THEN A=-999:PRINT #2,A;:PRINT#3,A;:GOTO 1870
1610 IF N=0 THEN PRINT #2,A;:PRINT#3,A;
```

```
1620 IF A=-999 GOTO 1660
1630 INPUT#1,B,Z9
1640 D=D+B
1650 N=N+1
1660 VAR(N)=B
1670 GOTO 1570
1680 AV=D/N
1690 PRINT#2,AV;
1700 D=0
1710 FOR A=1 TO N
1720 VR=VR+(VAR(A)*VAR(A)-AV*AV)
1730 VC=VC+(VAR(A)*VAR(A))
1740 NEXT A
1750 VR=VR/(N-1)
1760 VC=VC/(N-1)
1770 FI=FI+N-1
1780 FS=FS+((N-1)*VC)
1790 SD=SQR(VC)
1800 SD=SD*10000
1810 PRINT#2,N;
1820 PRINT#2,VR;
1830 PRINT#2,VC;
1840 PRINT#2,""
1850 PRINT#3,SD
1860 VR=O:VC=0
1870 N=0
1880 GOTO 1570
1890 S2=FS/FI
1900 CLOSE#1
1910 CLOSE#2
1920 CLOSE#3
1930 '
1940 ' PREPARING THE DATA FOR THE HISTOGRAM PROGRAMME
1950 '
1960 PRINT,"PREPARING THE HISTOGRAM DATA..."
1970 M9$="HIST01."+M2$
1980 N0$="HIST"+M2$+".RUN"
1990 OPEN M6$ FOR INPUT AS #1:OPEN M9$ FOR OUTPUT AS #2:OPEN
     N0$ FOR OUTPUT AS #3
2000 DIM A(33)
2010 FOR ZO=1 TO M0
2020 INPUT#1,A,B,C
2030 '
2040 ' EVENTS ARE PLACED IN THE APPROPRIATE RANGE
2050 '
2060 IF B<=-1.5 THEN A(2)=A(2)+1:GOTO 2360
2070 IF B<=-1.4 THEN A(3)=A(3)+1:GOTO 2360
2080 IF B<=-1.3 THEN A(4)=A(4)+1:GOTO 2360
2090 IF B<=-1.2 THEN A(5)=A(5)+1:GOTO 2360
2100 IF B<=-1.1 THEN A(6)=A(6)+1:GOTO 2360
2110 IF B<=-1 THEN A(7)=A(7)+1:GOTO 2360
```

```
2120 IF B<=-.9 THEN A(8)=A(8)+1:GOTO 2360
2130 IF B<=-.8 THEN A(9)=A(9)+1:GOTO 2360
2140 IF B<=-.7 THEN A(10)=A(10)+1:GOTO 2360
2150 IF B<=-.6 THEN A(11)=A(11)+1:GOTO 2360
2160 IF B<=-.5 THEN A(12)=A(12)+1:GOTO 2360
2170 IF B<=-.4 THEN A(13)=A(13)+1:GOTO 2360
2180 IF B<=-.3 THEN A(14)=A(14)+1:GOTO 2360
2190 IF B<=-.2 THEN A(15)=A(15)+1:GOTO 2360
2200 IF B<=-.1 THEN A(16)=A(16)+1:GOTO 2360
2210 IF B<=0 THEN A(17)=A(17)+1:GOTO 2360
2220 IF B<.1 THEN A(18)=A(18)+1:GOTO 2360
2230 IF B<.2 THEN A(19)=A(19)+1:GOTO 2360
2240 IF B<.3 THEN A(20)=A(20)+1:GOTO 2360
2250 IF B<.4 THEN A(21)=A(21)+1:GOTO 2360
2260 IF B<.5 THEN A(22)=A(22)+1:GOTO 2360
2270 IF B<.6 THEN A(23)=A(23)+1:GOTO 2360
2280 IF B<.7 THEN A(24)=A(24)+1:GOTO 2360
2290 IF B<.8 THEN A(25)=A(25)+1:GOTO 2360
2300 IF B<.9 THEN A(26)=A(26)+1:GOTO 2360
2310 IF B<1 THEN A(27)=A(27)+1:GOTO 2360
2320 IF B<1.1 THEN A(28)=A(28)+1:GOTO 2360
2330 IF B<1.2 THEN A(29)=A(29)+1:GOTO 2360
2340 IF B<1.3 THEN A(30)=A(30)+1:GOTO 2360
2350 IF B<1.4 THEN A(31)=A(31)+1:GOTO 2360
2360 IF B<1.5 THEN A(32)=A(32)+1:GOTO 2360
2370 A(33)=A(33)+1
2380 INPUT#1,C:IF C=0 GOTO 2360
2390 IF C=-999 GOTO 2420
2400 '
2410 ' COMPREHENSIVE AND RAW DATA FILES ARE PREPARED
2420 '
2430 INPUT #1,B,C2:GOTO 2040
2440 PRINT#2,DC$(A)
2450 PRINT#3,DC$(A)
2460 PRINT#2,""
2470 PRINT#2,"     < -1.5   ";A(2)
2480 PRINT#2,"-1.5 - -1.4   ";A(3)
2490 PRINT#2,"-1.4 - -1.3   ";A(4)
2500 PRINT#2,"-1.3 - -1.2   ";A(5)
2510 PRINT#2,"-1.2 - -1.1   ";A(6)
2520 PRINT#2,"-1.1 - -1.0   ";A(7)
2530 PRINT#2,"-1.0 - -0.9   ";A(8)
2540 PRINT#2,"-0.9 - -0.8   ";A(9)
2550 PRINT#2,"-0.8 - -0.7   ";A(10)
2560 PRINT#2,"-0.7 - -0.6   ";A(11)
2570 PRINT#2,"-0.6 - -0.5   ";A(12)
2580 PRINT#2,"-0.5 - -0.4   ";A(13)
2590 PRINT#2,"-0.4 - -0.3   ";A(14)
2600 PRINT#2,"-0.3 - -0.2   ";A(15)
2610 PRINT#2,"-0.2 - -0.1   ";A(16)
2620 PRINT#2,"-0.1 -  0.0   ";A(17)
```

```
2630 PRINT#2," 0.0 -  0.1  ";A(18)
2640 PRINT#2," 0.1 -  0.2  ";A(19)
2650 PRINT#2," 0.2 -  0.3  ";A(20)
2660 PRINT#2," 0.3 -  0.4  ";A(21)
2670 PRINT#2," 0.4 -  0.5  ";A(22)
2680 PRINT#2," 0.5 -  0.6  ";A(23)
2690 PRINT#2," 0.6 -  0.7  ";A(24)
2700 PRINT#2," 0.7 -  0.8  ";A(25)
2710 PRINT#2," 0.8 -  0.9  ";A(26)
2720 PRINT#2," 0.9 -  1.0  ";A(27)
2730 PRINT#2," 1.0 -  1.1  ";A(28)
2740 PRINT#2," 1.1 -  1.2  ";A(29)
2750 PRINT#2," 1.2 -  1.3  ";A(30)
2760 PRINT#2," 1.3 -  1.4  ";A(31)
2770 PRINT#2," 1.4 -  1.5  ";A(32)
2780 PRINT#2,"     >  1.5  ";A(33)
2790 PRINT#3,A(2)
2800 FOR PP=2 TO 16
2810 V=A(2*PP)+A(2*PP-1)
2820 PRINT#3,V
2830 NEXT PP
2840 PRINT#3,A(33)
2850 FOR QQ=1 TO 33
2860 A(QQ)=0
2870 NEXT QQ
2880 NEXT ZO
2890 CLOSE#1
2900 CLOSE#2
2910 '
2920 ' IN DEPTH, STATISTICAL ANALYSIS
2930 ' MANY ARRAYS AND MATRICES ARE REQUIRED BECAUSE OF THE
2940 ' MULTI-STEP PROCESSING REQUIRED FOR CALCULATING
2950 ' SKEWNESS, KURTOSIS, S2 AND CHI SQUARE
2960 '
2970 ' DEFINITION OF ARRAYS AND MATRICES:
2980 ' ST() : STATISTICS USING CALCULATED MEAN
2990 ' SI() : DEGREE OF FREEDOM
3000 ' FM() : VARIANCES DIVIDED BY S2
3010 ' FL() : DEGREE OF FREEDOM TIMES FM
3020 '
3030 DIM ST(99,5), FI(99), VC(99), SI(99), FL(99), FM(99),
     WAR(99)
3040 FJ=0:FK=0:HH=0:D=0:N=0
3050 N1$="STATTOT."+M2$
3060 OPEN M6$ FOR INPUT AS #1:OPEN N1$ FOR OUTPUT AS #2
3070 GB$="EVENT  MEAN   FREQ    VARIANCE   SKEWNESS
   KURTOSIS"
3080 PRINT#2,"STATISTICS BASED ON A MEAN OF ZERO":PRINT#2,""
3090 PRINT#2,GB$:PRINT#2,""
3100 HH=HH+1
3110 INPUT#1,A:IF A=0 GOTO 3090
```

```
3120 IF N=0 THEN PRINT #2,A;:ST(HH,1)=A
3130 IF A=8888 GOTO 3580
3140 IF A=-999 GOTO 3180
3150 INPUT#1,B,GQ
3160 D=D+B
3170 N=N+1
3180 WAR(N)=B
3190 GOTO 3090
3200 AV=D/N
3210 ST(HH,2)=AV
3220 PRINT#2,"0.00";
3230 D=0
3240 FOR A=1 TO N
3250 VC=VC+(WAR(A)*WAR(A))
3260 VZ=VZ+(WAR(A)*WAR(A)-(AV*AV))
3270 NEXT A
3280 VC=VC/(N-1)
3290 VZ=VZ/(N-1)
3300 ST(HH,3)=VZ
3310 SI(HH)=N-1
3320 XX=ABS(VC)
3330 XZ=ABS(VZ)
3340 SD=SQR(XX)
3350 SZ=SQR(XZ)
3360 FJ=FJ+((1/(N-1))-(1/FI))
3370 FM(HH)=VC/S2
3380 FL(HH)=(N-1)*(LOG(VC/S2))
3390 FK=FK+((N-1)*(LOG(VC/S2)))
3400 FOR A=1 TO N
3410 EM=EM+(WAR(A)^3)/(SD^3)
3420 EZ=EZ+((WAR(A)-AV)^3)/(SZ^3)
3430 KU=KU+(WAR(A)^4)/(SD^4)
3440 KZ=KZ+((WAR(A)-AV)^4)/(SZ^4)
3450 NEXT A
3460 F1=N/((N-1)*(N-2))
3470 F2=N*(N+1)/((N-1)*(N-2)*(N-3))
3480 F3=3*(N-1)*(N-1)/((N-2)*(N-3))
3490 SK=EM*F1
3500 SZ=EZ*F1
3510 KR=F2*KU-F3
3520 KZ=F2*KZ-F3
3530 ST(HH,4)=SZ
3540 ST(HH,5)=KZ
3550 PRINT#2,N;VC;SK;KR
3560 EM=0:KU=0:SK=0:KR=0:EZ=0:KZ=0:SZ=0
3570 VC=0:SD=0:VZ=0:SZ=0
3580 N=0
3590 GOTO 3080
3600 PRINT#2,"":PRINT#2,".PA"
3610 PRINT#2,"STATISTICS BASED ON THE CALCULATED
     MEAN":PRINT#2,""
```

```
3620 GC$="EVENT  MEAN   VARIANCE    SKEWNESS   KURTOSIS"
3630 PRINT#2,GC$
3640 FOR LK=1 TO M0
3650 PRINT#2,ST(LK,1);ST(LK,2);ST(LK,3);ST(LK,4);ST(LK,5)
3660 NEXT LK
3670 PRINT#2,"The value S2 (based on a mean of 0) is:";S2
3680 C=1+FJ/(3*(M0-1))
3690 KI=-FK/C
3700 PRINT#2,".pa"
3710 PRINT#2,"EVENT    DEGREES OF      "
3720 PRINT#2,"NUMBER     FREEDOM      "
3730 FOR ZX=1 TO M0
3740 QW=-FL(ZX)/C
3750 PRINT#2,ST(ZX,1),SI(ZX),FM(ZX),QW
3760 NEXT ZX
3770 PRINT#2,":?#2,""
3780 PRINT#2,"The value of C is: ";C
3790 PRINT#2,"The value of the sum of Fi*LN(Si2/S2) is: ";FK
3800 PRINT#2,"The chi squared value is: ";KI
3810 PRINT,"The value of C is: ";C
3820 PRINT,"The value of the sum of Fi*LN(Si2/S2) is: ";FK
3830 PRINT,"The chi squared value is: ";KI
3840 CLOSE#1
3850 CLOSE#2
3860 KEY ON
3870 CLS:BEEP:BEEP
3880 FOR HV=1 TO 3:PRINT:NEXT HV
3890 PRINT "ALL DONE"
3900 END
```

```
100 ' GRAPHTOT PROGRAMME
110 ' PREPARED BY MARC D'IORIO, JULY 1987
120 '
130 ' THIS PROGRAMME PLOTS THE FREQUENCY DISTRIBUTION OF EVENTS
140 ' FROM TSREG2 RESULTS.  THE MODULES OUTPUT FILES ARE USED AS
150 ' INPUT.
160 ' FILE NAMES AND SPECIFICATIONS:
170 ' H1$ : DICTIONARY FILE
180 ' H2$ : DIFFERENCE FILE
190 ' H3$ : STATISTICS FILE
200 ' H4$ : HISTOGRAM DATA FILE
210 ' H5 : LENGTH OF DICTIONARY
220 ' H6 : NUMBER OF EVENTS IN OPTIMUM SEQUENCE
230 '
240 ' INPUT PARAMATERS:
250 ' Y1$ : SAVING PICTURE FILE
260 ' Y2$ : PREFIX OF PICTURE FILE NAME
270 ' Y3$ : PRINTING PICTURE FILE
280 ' Y4$ : PAUSING BETWEEN PICTURES
290 ' Y5$ : STARRTING AT BEGINNING
300 ' Y6 : EVENT NUMBER AT WHICH TO START
310 '
320 ' DEFINITION OF COMMON MATRICES AND ARRAYS:
330 ' DC$() : DICTIONARY NAME ARRAY
340 ' LG$() : STATISTICS ARRAY
350 ' ST() : DIFFERENCES, EVENT AND WELL NUMBER MATRIX
360 ' HM() : HISTOGRAM DATA MATRIX
370 '
380 KEY OFF
390 CLS
400 PRINT,"Most of the files used by this programme are created
    by the MODULES programme"
410 PRINT,"                    these files must be unedited"
420 PRINT," except for DATA01 that must be in the standard
    legible format"
430 PRINT:PRINT:PRINT
440 '
450 ' USER FILENAME AND SPECIFICATION INPUT
460 '
470 INPUT "Name of dictionary file (e.g. fdsf2.dic):     ";H1$
480 INPUT "Name of difference file (e.g. diff01):        ";H2$
490 INPUT "Name of statistics file (e.g. data01):        ";H3$
500 INPUT "Name of histogram data file (e.g. hist.run): ";H4$
510 INPUT "Length of the dictionary: ";H5
520 INPUT "Number of events remaining: ";H6
530 CLS
540 PRINT,"Do you want to save the picture files? (Y/N)"
550 Y1$=INPUT$(1)
560 IF Y1$="n" OR Y1$="N" GOTO 590
570 IF Y1$<>"y" AND Y1$<>"Y" GOTO 540
580 INPUT "                Prefix of picture file name (5 char.
```

```
    max)";Y2$
590 PRINT,"Do you want the picture printed? (Y/N)"
600 Y3$=INPUT$(1)
610 IF Y3$="n" OR Y3$="N" GOTO 640
620 IF Y3$="y" OR Y3$="Y" GOTO 640
630 GOTO 590
640 PRINT,"Do you want to pause between each picture? (Y/N)"
650 Y4$=INPUT$(1)
660 IF Y4$="y" OR Y4$="Y" GOTO 680
670 IF Y4$="n" OR Y4$="N" GOTO 680
680 PRINT,"Do you want to start at the beginning? (Y/N)"
690 Y5$=INPUT$(1)
700 IF Y5$="y" OR Y5$="Y" GOTO 730
710 IF Y5$<>"n" AND Y5$<>"N" GOTO 680
720 INPUT "              Event number at which to start";Y6
730 CLS
740 LOCATE 1,1
750 PRINT,"Thank you.":PRINT:PRINT:PRINT
760 PRINT,"Reading in the dictionary"
770 '
780 ' READING IN THE DICTIONARY (EVENT NUMBER ABSENT)
790 '
800 DIM DC$(600), ST(2000,3), HM(H6,17), LG$(H6+3)
810 OPEN H1$ FOR INPUT AS #1
820 FOR YY=1 TO H5
830 INPUT #1,A$:IF A$="" GOTO 830
840 DC$(YY)=A$
850 NEXT YY
860 CLOSE #1
870 OPEN H3$ FOR INPUT AS #1
880 PRINT,"Reading in the statistics file"
890 '
900 ' READING IN THE STATISTICS FILE (FORMATTED MODULES OUTPUT)
910 '
920 FOR O9=1 TO H6+2
930 LINE INPUT#1,Q6$:IF Q6$="" GOTO 930
940 LG$(O9)=Q6$
950 NEXT O9
960 CLOSE#1
970 OPEN H2$ FOR INPUT AS #1:OPEN H4$ FOR INPUT AS #2
980 PRINT,"Reading in the histogram data"
990 '
1000 ' READING IN THE HISTOGRAM DATA (MODULES OUTPUT)
1010 '
1020 FOR H9=1 TO H6
1030 LINE INPUT #2,H9$:IF H9$="" GOTO 1030
1040 FOR H8=1 TO 17
1050 INPUT#2, L9
1060 HM(H9,H8)=L9*15
1070 NEXT H8
1080 NEXT H9
```

```
1090 CLOSE#2
1100 ST=1:TT=0
1110 PRINT,"Preparing the 'difference vs wells' data"
1120 '
1130 ' READING IN THE (OBSERVED MINUS EXPECTED) DIFFERENCES AND
1140 ' THE ASSOCIATED WELL NUMBERS
1150 '
1160 FOR C1=1 TO 2000
1170 INPUT#1,A:IF A=0 GOTO 1170
1180 IF A=-999 GOTO 1250
1190 IF A=8888 GOTO 1270
1200 INPUT#1,B,C
1210 B=INT(B*30)
1220 ST(C1+1,1)=A:ST(C1+1,2)=B:ST(C1+1,3)=C
1230 TT=TT+1
1240 GOTO 1260
1250 ST(ST,1)=TT:ST=C1+1:TT=0
1260 NEXT C1
1270 CT=1:BC=1
1280 SCREEN 100
1290 '
1300 ' GRAPHICS MODE INVOKED
1310 '
1320 FOR I=1 TO 43
1330 CLS
1340 '
1350 ' PLOTTING "DIFFERENCES VERSUS WELL NUMBERS"
1360 '
1370 LOCATE 2,4:PRINT 3
1380 LOCATE 2,12:PRINT "Difference between expected and
     observed event position"
1390 LOCATE 3,21:PRINT "for wells ordered from North to South"
1400 LOCATE 4,4:PRINT 2
1410 LOCATE 6,4:PRINT 1
1420 LOCATE 8,1:PRINT "North"
1430 LOCATE 8,67:PRINT "South"
1440 LOCATE 9,4:PRINT -1
1450 LOCATE 11,4:PRINT -2
1460 LOCATE 13,1:PRINT,LG$(1)
1470 PRINT,LG$(I+2)
1480 LOCATE 13,4:PRINT -3
1490 LINE (50,16)-(50,211)
1500 LINE (50,116)-(525,116)
1510 FOR S=1 TO 7
1520 Y=-4+30*S
1530 LINE (45,Y)-(55,Y)
1540 NEXT S
1550 FOR UU=1 TO 23
1560 X8=45+20*UU
1570 LINE (X8,114)-(X8,118)
1580 NEXT UU
```

```
1590 NM=ST(BC,1)
1600 FOR EE=1 TO NM
1610 VL=BC+EE
1620 A=ST(VL,1)
1630 IF EE>1 GOTO 1690
1640 LOCATE 1,15
1650 PRINT "EVENT NUMBER";A;":";DC$(A)
1660 '
1670 ' PLOTTING HISTOGRAM OF THE DISTRIBUTION OF DIFFERENCES
1680 '
1690 B=ST(VL,2):C=ST(VL,3)
1700 X1=37+20*C:X2=53+20*C:Y=116-B
1710 LINE (X1,116)-(X1,Y)
1720 LINE (X1,Y)-(X2,Y)
1730 LINE (X2,Y)-(X2,116)
1740 NEXT EE
1750 BC=BC+NM+1
1760 LOCATE 16,27:PRINT "Histogram of distribution"
1770 LOCATE 16,4:PRINT 8
1780 LOCATE 18,4:PRINT 6
1790 LOCATE 20,4:PRINT 4
1800 LOCATE 22,4:PRINT 2
1810 LOCATE 25,1:PRINT "       -1.5   -1.1   -.7    -.3   00
     .3          .7   1.1    1.5+  "
1820 LINE (50,232)-(50,372)
1830 LINE (50,372)-(570,372)
1840 FOR JA=1 TO 9
1850 Y=JA*15+222
1860 LINE (48,Y)-(52,Y)
1870 NEXT JA
1880 FOR R1=1 TO 16
1890 X=R1*27+50
1900 LINE (X,372)-(X,375)
1910 NEXT R1
1920 FOR S7=1 TO 17
1930 WQ=HM(I,S7)
1940 IF WQ=0 GOTO 2000
1950 Y=372-WQ
1960 X1=23+S7*27:X2=50+S7*27
1970 LINE (X1,372)-(X1,Y)
1980 LINE (X1,Y)-(X2,Y)
1990 LINE (X2,Y)-(X2,372)
2000 NEXT S7
2010 '
2020 ' SAVING AND/OR PLOTTING PICTURE FILE AS SPECIFIED BY USER
2030 '
2040 IF Y5$<>"n" AND Y5$<>"N" GOTO 2070
2050 IF Y6=A THEN Y5$="Y":GOTO 2070
2060 GOTO 2170
2070 IF Y1$<>"y" AND Y1$<>"Y" GOTO 2120
2080 Z$=STR$(I)
```

```
2090 XX$=Y2$+Z$+".pic"
2100 DEF SEG=&HB800
2110 BSAVE XX$,0,32767
2120 IF Y3$<>"y" AND Y3$<>"Y" GOTO 2150
2130 LCOPY
2140 FOR XS=1 TO 12:LPRINT,"":NEXT XS
2150 IF Y4$="N" OR Y4$="n" GOTO 2170
2160 Q$=INKEY$:IF Q$="" GOTO 2120
2170 NEXT I
2180 SCREEN 0
2190 END
```

THE FOLLOWING SUBROUTINES WERE MODIFIED FOR THE RASC OPEN FILE FOR THE FREQUENCY DISTRIBUTION STUDY AND STANDARD DEVIATION WEIGHTS ITERATIONS.

MAIN.FOR FORTRAN ROUTINE

```
      PROGRAM RASC
C
C
C
C     RRRR       A       SSS      CCC          PPPP      CCC
C     R   R     A A     S   S    C   C         P   P    C   C
C     R   R    A   A    S        C             P   P    C
C     RRRR     AAAAA     SSS     C      ===== PPPP     C
C     R R      A   A        S    C             P        C
C     R  R     A   A    S   S    C   C         P        C   C
C     R   R    A   A     SSS      CCC          P         CCC
C
```

F.P. AGTERBERG AND L.D. NEL
JANUARY 1981

WITH LATER REVISIONS BY
F.P. AGTERBERG, S.N. LEW, AND M. HELLER

FURTHER REVISIONS BY
GILLDAT: DATA ANALYSIS CONSULTING

REVISED MAY 1987 TO INCLUDE
STANDARD DEVIATION WEIGHTS DERIVED FROM TSREG

GEOLOGICAL SURVEY OF CANADA
601 BOOTH STREET
OTTAWA, ONTARIO
K1A 0E8

PROGRAM RASC IS A REVISED VERSION OF THE PROGRAMS SEQONE AND SEQTWO PRESENTED DURING THE IGCP PROJECT 148 WORKSHOPS IN DARTMOUTH, N.S., AUGUST 1979, AND OTTAWA, FEBRUARY 1980.

THE JANUARY 1981 RASC PROGRAM WAS PUBLISHED IN 1982 IN "COMPUTERS AND GEOSCIENCES", VOL.8 NO.1, PP.69-90, AND VOL.8, NO.1, PP.163-189.
A REVISED VERSION OF IT WAS PUBLISHED IN APRIL 1983 AS GEOLOGICAL SURVEY OF CANADA,

```
C            OPEN FILE NO. 922, WITH A 54-PAGE USER'S MANUAL
C            BY M. HELLER, W.S. GRADSTEIN, F.M. GRADSTEIN,
C            AND F.P. AGTERBERG.
C                THIS OPEN FILE RASC PROGRAM WAS AGAIN
C            MODIFIED BEFORE PRESENTATIONS DURING THE IGCP
C            PROJECT 148 SHORT COURSE IN DARTMOUTH, N.S.,
C            OCTOBER 1983.  IT SERVED AS A BASIS OF THE FORTRAN
C            IV PROGRAM RASC-C FOR PREPARATION OF CASC INPUT.
C            (SEE OPEN FILE NO. 1179, SEPTEMBER 1985)
C
C                THE PRESENT VERSION, WHICH ACCOMPANIES A NEW
C            RASC USER'S MANUAL, CONTAINS FURTHER REVISIONS
C            BY S.N. LEW AND COMPLIES WITH THE ANSI FORTRAN 77
C            STANDARD.
C
C            NOTE: THE FINAL OCCURANCE TABLE AND STEP MODEL
C                  TABLE (OUTPUT OPTION 9, SEE BELOW) DO NOT
C                  PROPERLY LIST DICTIONARY NAMES OF EVENTS.
C                  THIS IS PROBABLY DUE TO MEMORY CONFLICTS IN
C                  THE COMPILED CODE WHICH MAY RESULT FROM
C                  CONFLICTING ARRAY DIMENSIONS BETWEEN PROGRAM
C                  UNITS OR NON-STANDARD FORTRAN CODE.COPY
C
C
C
C              PROGRAM INPUTS
C              --------------
C
C
C
C     RECORD NO. 1      RUN PARAMETERS      (FREE FORMAT)
C     ------------      --------------
C
C  NS    - (INTEGER)  NUMBER OR SEQUENCES OR WELLS  (NS <= 24)
C  IOCR  - (INTEGER)  ELEMENTS OCCURRING FEWER THAN "IOCR" TIMES IN
C                     THE DATA SET WILL BE IGNORED
C  INIQ  - (INTEGER)  = 1, IF UNIQUE EVENTS OR MARKER HORIZONS ARE
C                     INCLUDED  (RECORDS 3 AND 4)
C  ITER - INTEGER)    MAXIMUM NUMBER OF CUMULATIVE ORDER MATRIX
C                     TRANSFORMATIONS ALLOWED  (EXAMPLE: 12000)
C  CRIT1 - (REAL)     TRANSPOSE ELEMENTS WITH SUM LESS THAN "CRIT1"
C                     IN THE ORDER MATRIX WILL BE ZEROED BEFORE
C                     THE RANKING SOLUTION.  (CRIT1 <= IOCR)
C   TOL    -  (REAL)       TOLERANCE:  S(I,J) MAY BE LOWER THAN
S(J,I)
C                     BY AS MUCH AS "TOL"
C  AAA    - (REAL)    FRACTILE FOR TRUNCATION POINT OF NORMAL
C                     DISTRIBUTION.  (EXAMPLE: AAA = 1.645)
C  CRIT2 - (REAL)     TRANSPOSE ELEMENTS WITH SUM LESS THAN "CRIT2"
C                     IN THE ORDER MATRIX WILL BE ZEROED BEFORE
C                     THE SCALING ANALYSIS.  (CRIT2 >= CRIT1)
```

```
C
C
C     RECORD NO. 2      PROCESSING CONTROL          (FREE FORMAT)
C     ------------      ------------------
C
C  ALL 12 PARAMETERS ON THIS RECORD ARE INTEGERS.
C  FOR SHORT VERSION OF RASC (RANKING ALGORITHMS ONLY), IALPHA=0
C
C
C   ITAPE     = 1    FOR DATA TO BE READ FROM "TAPE10"
C               ELSE,     DATA WILL BE READ FROM RECORDS IMMEDIATELY
C                         FOLLOWING RECORD NO. 4
C   IOMAT      = 1    FOR PRINTOUT OF ORDER AND FREQUENCY MATRICES
C                       AS WELL AS INTERMEDIATE TABLES;
C               ELSE,       THESE OUTPUTS WILL BE SUPPRESSED
C   ISRT    = 1,  DATA WILL BE PRE-SEQUENCED FOR OPTIMIZED STARTING
C                   SEQUENCE
C   IALPHA     = 0,  TERMINATION AFTER RANKING SOLUTION;
C              = 1,  SCALING ANALYSIS WILL BE DONE;
C               ELSE,       TERMINATION AFTER RANKING SOLUTION, BUT
C                           STEPWISE SEQUENCING PROGRESS WILL BE
C                           PRINTED BEFORE TERMINATION.
C   ITAB1   = 1, AN OCCURRENCE TABLE FOR THE WELLS IS TO BE PRINTED
C               ELSE,       NO TABLE.
C   ISCORE     = 1,  STEP MODEL COMPARISON OF INDIVIDUAL WELLS AND
C                       FOSSILS WITH OPTIMUM SEQUENCE IS PERFORMED
C   ICOMP      = 1    FOR NORMALITY TESTS ON INDIVIDUAL WELLS
C   ISKIP      = 1    IF CUMULATIVE ORDER MATRIX IS TO BE USED
C                      (RANKING SOLUTION WILL BE BASED ON PRESORTING
C                      ONLY)
C               ELSE,       RASC WILL GO AHEAD AND PERFORM MATRIX
C                           PERMUTATIONS.
C   IFIN       = 1    FOR APPLICATION OF FINAL RE-ORDERING
C   INOSC      = 0,  NO SCALING OUTPUT;
C              = 1,  WEIGHTED DISTANCE OUTPUT ONLY;
C               ELSE,       WEIGHTED AND UNWEIGHTED OUTPUT.
C   INEG = 1, LARGE DISTANCES FOR SMALL SAMPLES WILL BE SUPPRESSED
C               ELSE,       NO SUPPRESSION.
C   ISCAT      = 1,  SCATTERGRAMS ARE TO BE PRINTED FOR EACH WELL.
C               ELSE,       NO SCATTERGRAMS PRINTED
C
C     RECORD NO. 3      OUTPUT DIRECTION
C     ------------      ----------------
C
C THIS RECORD IS MADE UP OF 11 INTEGER VALUES (FREE FORMAT)
C WHICH DIRECT OUTPUT FROM THE 11 DIFFERENT PROGRAM SECTIONS.
C THESE VALUES ARE STORED IN THE PROGRAM IN THE ARRAY OUT().
C THE FIRST VALUE REFERS TO SECTION 1, THE SECOND TO SECTION
C 2 AND SO ON. IF SET TO 1, THE CORRESPONDING SECTION'S OUTPUT
C WILL BE DIRECTED TO THE MAIN OUTPUT FILE. OTHERWISE THE SECTIONS
C OUTPUT WILL GO TO THE EXTRA OUTPUT FILE.
```

```
C
C     OUT(1)  -  SEQUENCE DATA TABULATION OF EVENT OCCURANCES
C     OUT(2)  -  MODIFIED SEQUENCE DATA
C     OUT(3)  -  CYCLES
C     OUT(4)  -  DICTIONARIES
C     OUT(5)  -  OPTIMUM SEQUENCE
C     OUT(6)  -  SCATTERGRAMS USING OPTIMUM SEQUENCE
C     OUT(7)  -  SCALING UNWEIGHTED, WEIGHTED
C     OUT(8)  -  SCALING AFTER 5 ITERATIONS
C     OUT(9)  -  OCCURRENCE TABLE & STEP MODEL
C     OUT(10) -  NORMALITY TEST
C     OUT(11) -  SCALING & UE
C
C
C     RECORD NO. 4      UNIQUE EVENTS
C     ------------      -------------
C
C     IF INIQ = 1, UP TO 20 UNIQUE EVENTS WILL BE READ FROM THIS
C     RECORD IN 20I4 FORMAT.  IF NO UNIQUE EVENTS ARE REQUESTED,
C     THIS RECORD IS LEFT BLANK.  IF UNIQUE EVENTS ARE INCLUDED,
C     "ICOMP" MUST EQUAL 1.
C
C
C     RECORD NO. 5      MARKER HORIZONS
C     ------------      ---------------
C
C     IF INIQ = 1, UP TO 20 MARKER HORIZONS WILL BE READ FROM
C     THIS RECORD IN 20I4 FORMAT.  IF NO MARKER HORIZONS ARE
C     REQUESTED, THIS RECORD IS LEFT BLANK.
C
C
C
C     DATA SET                (SEMI-FREE FORMAT)
C     --------
C
C     OBSERVED EVENTS:        THE OBSERVED DATA ARE GIVEN AS "NS"
C                             SEQUENCES.  A "SEQUENCE" CONSISTS OF
C           A TITLE RECORD (IN 5A4 FORMAT) FOLLOWED BY ONE OR MORE
C           RECORDS OF SEQUENCE DATA (IN MULTIPLE I4 FORMAT).
C              EACH OF THESE DATA RECORDS IS PARTITIONED INTO 20
C           FIELDS, EACH FIELD HAVING I4 FORMAT.  THUS, THERE
C           MAY BE UP TO 20 EVENTS ON ONE RECORD.
C               NOTE:   FIELDS NEED NOT BE FILLED CONSECUTIVELY.
C                       EMPTY FIELDS ARE IGNORED.
C
C               A SEQUENCE IS DEEMED TO HAVE ENDED WHEN A FIELD
C           CONTAINING   -999   IS ENCOUNTERED.
C               THE SEQUENCES ARE READ EITHER FROM "TAPE10"
C           (IF ITAPE = 1) OR FROM RECORDS IMMEDIATELY FOLLOWING
C           RECORD NUMBER 4  (IF ITAPE = 0).
C
```

```
C
C     DICTIONARY:            THE DICTIONARY IS MERELY A LIST OF
C                            EVENT LABELS:  ONE LABEL PER RECORD,
C            10A4 FORMAT.  AN EXTRA RECORD WITH THE LABEL 'LAST'
C            IN THE FIRST 4 COLUMNS MUST BE PLACED AT THE END.
C            LIMIT:  605 RECORDS  (NOT COUNTING 'LAST' RECORD)
C            THE DICTIONARY IS ALWAYS READ FROM "TAPE99".
C
C
C    S.D. WEIGHTS:          THESE WEIGHTS ARE CALCULATED BY
C            USING THE STANDARD DEVIATIONS OF THE DIFFERENCES
C            BETWEEN OBSERVED AND EXPECTED VALUES OF THE EVENTS
C            IN THE R.A.S.C. SEQUENCE.  THE INPUT FILE MUST BE
C            IN A 2A6 FORMAT WITH -999 ON THE LAST LINE.  THE
C            VALUE IN THE FIRST COLUMN IS THE EVENT NUMBER WHILE
C            THE SECOND COLUMN REPRESENTS THE STANDARD DEVIATION
C            WEIGHTS.
C
C  ------------------------------------------------------------
C
      PARAMETER (KDIM1=24, KDIM3=120, KDIM4=605, KDIM5=10,
KDIM6=145)
      PARAMETER (MAXCYC=300, MAXUQ=20)
C
      COMMON N, NS, MMAX, IX(KDIM1,KDIM3), ICODE(KDIM4),
IRCODE(KDIM4),
     +        C(KDIM6,KDIM6)
      COMMON  /BETA/ IUNIQ(KDIM4,2), NUNIQ(KDIM1),
MUNIQ(KDIM1,MAXUQ*2)
      COMMON  /DELTA/ IOCR, INIQ, CRIT1, TOL, AAA, CRIT2, MAX, ITER,
     +        IOMAT, ISRT, IALPHA, ITAB1, ISCORE, ICOMP, ISKIP,
IFIN,
     +        INOSC, INEG, ISCAT, TMAT(KDIM1,KDIM3)
      COMMON  /TEXT/ NAME(KDIM1,10), ITITLE(KDIM4,10)
      COMMON  /PESEE/ SDW(KDIM4), IWEIT(KDIM4,2)
      INTEGER AA, AID, COUNT, T, TEST, IPOS(KDIM6), IQD(KDIM3),
     +        IRANGE(KDIM6,2), JIRCOD(KDIM6), IPAIR(2,KDIM6+MAXUQ),
     +        MPAIR(KDIM6+MAXUQ), TMAT, OUT(11)
      REAL    A(300), B(300), CC(600), QDAR(KDIM6+MAXUQ),
WVEC(KDIM5),
     +        XLEV(KDIM6+MAXUQ)
      CHARACTER*4   NAME, ITITLE
      CHARACTER*50
INPFIL,DATFIL,SDWFIL,DICFIL,OUTFIL1,OUTFIL2,T7FILE
C
C  EXPLANATION OF CONSTANTS IN THE PARAMETER LIST
C
C  KDIM1   - MAXIMUM NUMBER OF WELLS (SECTIONS)
C  KDIM3   - MAXIMUM LENGTH OF ANY ONE WELL
C  KDIM4   - MAXIMUM NUMBER OF EVENT LABELS IN THE DICTIONARY
C  KDIM5   - MAXIMUM NUMBER OF FOSSILS PERMITTED TO BE IMPLICATED IN
```

```
C                ONE CYCLE
C  KDIM6   - MAXIMUM NUMBER OF EVENTS REMAINING AFTER FILTERING
C  MAXCYC - MAXIMUM NUMBER OF CYCLES ALLOWED
C  MAXUQ   - MAXIMUM NUMBER OF UNIQUE EVENTS
C
      WRITE (*,*) 'Enter filename for run parameters: '
      READ (*,900) INPFIL
  900 FORMAT (A50)
      WRITE (*,*) 'Enter filename for well data: '
      READ (*,900) DATFIL
      WRITE (*,*) 'Enter filename for S.D. weights: '
      READ (*,900) SDWFIL
      WRITE (*,*) 'Enter filename for dictionary: '
      READ (*,900) DICFIL
      WRITE (*,*) '  '
      WRITE (*,*) 'Enter filename for main output (results): '
      READ (*,900) OUTFIL1
      WRITE (*,*) 'Enter filename for extra output (results): '
      READ (*,900) OUTFIL2
      WRITE (*,*) 'Enter filename for "TAPE7" output: '
      READ (*,900) T7FILE
      WRITE (*,*) 'Thank you.  Please wait   (or Ctrl-Break to
abort)'
C
      OPEN (5,FILE=INPFIL,BLANK='ZERO')
      OPEN (10,FILE=DATFIL,STATUS='OLD',BLANK='ZERO')
      OPEN (51,FILE=SDWFIL,STATUS='OLD',BLANK='ZERO')
      OPEN (99,FILE=DICFIL,STATUS='OLD',ACCESS='SEQUENTIAL')
      OPEN (61,FILE=OUTFIL1,STATUS='UNKNOWN')
      OPEN (62,FILE=OUTFIL2,STATUS='UNKNOWN')
      OPEN (7,FILE=T7FILE,ACCESS='SEQUENTIAL',STATUS='UNKNOWN')
C
C  READS IN:  INPUT (RUN PARAMETERS), TAPE10 (WELL DATA),
C             TAPE99 (DICTIONARY)
C  CREATES:   OUTPUT (THE PRINT FILE OF RESULTS)
C             TAPE7 (INPUT TO 'DENO' PROGRAMME FOR DISSPLA PLOTS OF
C                    OPTIMUM FOSSIL SEQUENCE AND DENDROGRAMS)
C
C  THIS IS RASC, VERSION 19851212,  BLANK='ZERO', STATUS.NE.'NEW'
C
      WRITE (61,*) CHAR(15)
      WRITE (62,*) CHAR(15)
      WRITE (61,1000)
      WRITE (61,1001)
      WRITE (61,1002)
      WRITE (61,1003)
 1000 FORMAT (/////4X, 'RESULTS OBTAINED BY MEANS OF PROGRAM RASC')
 1001 FORMAT (/5X, 'PREPARED BY F.P. AGTERBERG AND L.D. NEL',
     +   /5X, 'JANUARY 1981')
 1002 FORMAT (/5X, 'REVISED BY F.P. AGTERBERG AND S.N. LEW',
     +  /5X, 'SEPTEMBER 1985')
```

```
 1003 FORMAT (/5X, 'GEOLOGICAL SURVEY OF CANADA'/5X,
     + '601 BOOTH STREET'/5X, 'OTTAWA, ONTARIO'/5X, 'K1A 0E8')
C
C     READ INPUTS
C     -----------
      WRITE (*,*) 'READING IN THE DATA'
C
      CALL READIN (OUT)
C
C
C     PREPROCESSING
C     -------------
C
C
      WRITE (OUT(1),2000)
      WRITE (OUT(1),2001)
 2000 FORMAT (/////5X,'PREPROCESSING INITIATED')
 2001 FORMAT (5X,'-----------------------')
C
C  CONSTRUCT  NUNIQ(KDIM1)  - MAP SHOWING WHICH SEQUENCES HAVE
C                                 UNIQUE EVENTS
C  IRCODE(KDIM4)  - BEING USED HERE AS A TABLE TO BE SENT TO
C                   OCCTAB().  (REALLY ONLY NEED KDIM6 OF THE
C                   KDIM4 AVAILABLE.)
C
      DO 205 I = 1,NS
          DO 200 J = 1,KDIM3
             ID = TMAT(I,J)
             AID = IABS (ID)
             IF (AID.EQ.0) GO TO 205
             IF (INIQ.EQ.1 .AND. IUNIQ(AID,1).EQ.1) NUNIQ(I) = 1
             IRCODE(AID) = IRCODE(AID) + 1
  200     CONTINUE
  205 CONTINUE
C
C  PRINT A TABLE SHOWING FOR EACH DICTIONARY EVENT THE NUMBER
C  OF WELLS IN WHICH THIS EVENT APPEARS
C
      CALL OCCTAB (OUT(1))
C
C
C  LOW OCCURRENCE FILTERING AND RECODING OF DATA
C
C  ALL EVENTS IN THE DATA SET WHICH DO NOT OCCUR IN AT LEAST
C  "IOCR" SEQUENCES ARE ELIMINATED, AND THE DATA ARE RE-CODED SUCH
C  THAT IF "MMAX" EVENTS ARE RETAINED, THE NEW CODE NUMBERS WILL
C  RUN FROM 1 TO "MMAX".
C  "TMAT" WILL BECOME THE FILTERED (BUT NOT RE-CODED) DATA SET.
C
      WRITE (*,*) 'FILTERING THE DATA'
C
```

```
      CALL HPFILT (TMAT,IOCR,INIQ,IOMAT,OUT(2))
C
C
C  PRESORT OPTION:  A PRELIMINARY SEQUENCE IS DERIVED FROM THE SORT-
C  ING OF EVENT 'SCORES' BASED ON THE FREQUENCIES OF ALL EVENTS,
C  COMPARED WITH ALL OTHER EVENTS IN AN ORDER RELATION MATRIX.
C
      WRITE (*,*) 'RANKING ANALYSIS'
      IF (ISRT.EQ.1) CALL PRESRT (IOMAT,OUT(2))
C
C
C
C     RANKING SOLUTION
C     ----------------
C
C
C  CREATION OF CUMULATIVE ORDER MATRIX
C
C  CUMULATIVE ORDER MATRIX C(I,J) IS CONSTRUCTED SUCH THAT
C  ELEMENTS C(I,J) CONTAIN THE NUMBER OF TIMES EVENT I
C  OCCURRED ABOVE (BEFORE) EVENT J.
C
      WRITE (OUT(3),3000)
      WRITE (OUT(3),3001)
 3000 FORMAT ('////4X,'RANKING SOLUTION')
 3001 FORMAT (5X,'----------------')
      DO 305 I = 1,KDIM6
          DO 300 J = 1,KDIM6
              C(I,J) = 0.0
  300     CONTINUE
  305 CONTINUE
      WRITE (OUT(3),3010) IOCR, INT (CRIT1)
 3010 FORMAT ('////'  RUN FOR', I2, ' OR MORE OCCURRENCES AND', I2,
     + ' OR MORE PAIRS')
C
C  PRODUCES A NEW C.O. MATRIX BASED ON THE CURRENT STATE OF THE
C  WELL DATA.  (THAT IS,  PRESORTED OR ...)
C
C  IX  - THE RECODED DATASET
C
      DO 325 L = 1,NS
          J = 1
  307     IF (J.GT.KDIM3)  GO TO 325
          MM = IX(L,J)
          IF (MM.EQ.0)  GO TO 325
              TEST = 0
              K = J
              I = IABS (MM)
  310         K = K + 1
              IF (K.GT.KDIM3)  GO TO 320
              AA = IX(L,K)
```

```
            IF (AA.EQ.0) GO TO 320
                KK = IABS (AA)
                IF (AA.LT.0 .AND. TEST.LE.0) GO TO 315
                    TEST = TEST + 1
                    C(I,KK) = C(I,KK) + 1.0
                    GO TO 310
  315           C(I,KK) = C(I,KK) + 0.5
                    C(KK,I) = C(KK,I) + 0.5
                    GO TO 310
  320       J = J + 1
            GO TO 307
  325 CONTINUE
      IF (IOMAT.NE.1) GO TO 335
          WRITE (OUT(3),3020)
 3020     FORMAT (/////,24H CUMULATIVE ORDER MATRIX/)
          DO 330 I = 1,MMAX
              WRITE (OUT(3),3030)
 3030         FORMAT (//)
              WRITE (OUT(3),3040) (C(I,J), J = 1,MMAX)
  330     CONTINUE
 3040     FORMAT (1X, 20F6.1)
C
C  MODIFICATION OF CUMULATIVE ORDER MATRIX
C
C  THE TRANSPOSE ELEMENT PAIRS C(I,J) AND C(J,I)
C  WHOSE SUM IS LESS THAN CRIT1 ARE ZEROED
C
      WRITE (*,*) 'RANKING'
C
  335 IKNT = 0
      IMAX = MMAX - 1
      DO 345 I = 1,IMAX
          L = I + 1
          DO 340 J = L,MMAX
              IF ((C(I,J)+C(J,I)) .GE. CRIT1) GO TO 340
              C(I,J) = 0.0
              C(J,I) = 0.0
              IKNT = IKNT + 1
  340     CONTINUE
  345 CONTINUE
      MMSQ = (MMAX * MMAX - MMAX) * 0.5
      WRITE (OUT(3),3050)
 3050 FORMAT (//'  MODIFICATION OF ORDER MATRIX')
          WRITE (OUT(3),3060) CRIT1, IKNT, MMSQ
 3060 FORMAT (/' BASED ON CRIT1 =',F5.1,',',I5,' PAIRS OUT OF',I6,
     + ' HAVE BEEN ZEROED')
      IF (IOMAT.NE.1) GO TO 400
          WRITE (OUT(3),3070)
 3070     FORMAT (/////24X,'MODIFIED RELATION MATRIX'/)
          DO 350 I = 1,MMAX
              WRITE (OUT(3),3030)
```

```
            WRITE (OUT(3),3080) (C(I,J), J = 1,MMAX)
  350       CONTINUE
 3080       FORMAT (/20F6.1)
C
C  OPTIMUM SEQUENCE DETERMINED BY MATRIX TRANSFORMATION (RANKING)
C
C  AN OPTIMUM SEQUENCE IS DETERMINED BY EXAMINING THE ORDER MATRIX.
C  FREQUENCIES (TRANSPOSE ELEMENTS C(I,J) AND C(J,I) ) ARE
C  COMPARED AND ROWS AND COLUMNS I AND J ARE INTERCHANGED SUCH THAT
C  ALL LARGER ELEMENTS APPEAR IN THE UPPER TRIANGLE OF THE MATRIX
C
C  IA      - NUMBER OF CYCLES              COUNT  - # OF ITERATIONS
C  ICORT   - (A SWITCH;  SENT TO CYCLE SUBRTN.)
C  ICYC    - # FOSSILS IN THE CYCLE;  SENT TO CYCLE SUBRTN.
C
  400 IA = 1
      DO 405 I = 1,KDIM6
          IPOS(I) = I
  405 CONTINUE
      IF (ISKIP.EQ.1) GO TO 480
      COUNT = 0
      ICORT = 0
      DO 470 I = 1,MMAX
  410     IF (IA.LE.MAXCYC) GO TO 415
              WRITE (OUT(3),4000) MAXCYC
 4000         FORMAT (/1X, '*** NUMBER OF CYCLES HAS EXCEEDED THE',
     +          ' ALLOWED MAXIMUM OF', I5, '.',
     +          //1X, '**** EXECUTION TERMINATED.'/)
              GO TO 9999
  415     ICYC = 0
          ISUP = 0
          DO 420 J = 1,KDIM5
              WVEC(J) = 0.0
  420     CONTINUE
  425     K = I + 1
          IF (K.GT.MMAX) GO TO 470
          DO 465 J = K,MMAX
              IF (C(I,J).GE.(C(J,I)-TOL)) GO TO 465
              DO 430 T = 1,MMAX
                  TEMP = C(I,T)
                  C(I,T) = C(J,T)
                  C(J,T) = TEMP
  430         CONTINUE
              DO 435 T = 1,MMAX
                  TEMP = C(T,I)
                  C(T,I) = C(T,J)
                  C(T,J) = TEMP
  435         CONTINUE
              ITEMP = IPOS(I)
              IPOS(I) = IPOS(J)
              IPOS(J) = ITEMP
```

```
                LIMT = KDIM5 - 1
                DO 440 T = 1,LIMT
                    WVEC(T) = WVEC(T+1)
  440           CONTINUE
                WVEC(KDIM5) = FLOAT (IPOS(I))
                COUNT = COUNT + 1
                IF (COUNT.LT.ITER) GO TO 445
                    WRITE (OUT(3),4020) ITER
 4020               FORMAT (/1X, '*** NUMBER OF ALLOWED MATRIX TRANS',
     +                'FORMATIONS (ITER =', I6, ') EXCEEDED.',
     +                //1X, '**** EXECUTION TERMINATED IN M/PROG.'/)
                    GO TO 9999
  445           IF (IALPHA.EQ.0 .OR. IALPHA.EQ.1)  GO TO 450
                    WRITE (OUT(3),4050)
 4050               FORMAT (//20H SEQUENCING PROGRESS)
                    WRITE (OUT(3),4060) (IPOS(L), L = 1,MMAX)
 4060               FORMAT (1X, 20I5)
  450           CONTINUE
C
C           TEST AND CORRECT FOR CYCLICITY
C
                ISUP = ISUP + 1
                IF (ISUP.LE.100 .OR. WVEC(1).LE.0.0) GO TO 425
                DO 455 T = 4,KDIM5
                    IF (WVEC(T).EQ.WVEC(1)) GO TO 460
  455           CONTINUE
                GO TO 425
  460           ICYC = T - 1
                CALL CYCLE (ICORT,ICYC,WVEC,IA,A,B,CC,IPOS,OUT(3))
                GO TO 410
  465       CONTINUE
  470 CONTINUE
C
C  REPLACE ELEMENTS ZEROED IN CORRECTION OF CYCLICITY
C
      ICORT = 1
      CALL CYCLE (ICORT,ICYC,WVEC,IA,A,B,CC,IPOS,OUT(3))
C
C
C  OUTPUT FINAL ORDER RELATION MATRIX, OPTIMUM SEQUENCE
C  AND RUN CONDITIONS
C
C
      IF (IOMAT.NE.1) GO TO 480
          WRITE (OUT(3),4070)
 4070     FORMAT (///1X, 'FINAL ORDER RELATION MATRIX')
          DO 475 I = 1,MMAX
              WRITE (OUT(3),4080) I
 4080         FORMAT (//2X,I3)
              WRITE (OUT(3),3080) (C(I,J), J = 1,MMAX)
  475     CONTINUE
```

```
C
  480 WRITE (OUT(3),4090)
 4090 FORMAT (///// ' OPTIMUM SEQUENCE OBTAINED VIA RANKING'/)
      WRITE (OUT(3),4060) (IPQS(L), L = 1,MMAX)
      DO 485 I = 1,MMAX
          IRCODE(I) = ICODE(IPOS(I))
  485 CONTINUE
C
C  IPOS    - HOLDS THE OPT. SEQ.  (ENCODED RASC INDEX-NUMBERS)
C  IRCODE - HOLDS THE OPT. SEQ.  (ORIGINAL CODE NUMBERS)
C
      WRITE (OUT(3),4100)
 4100 FORMAT (///// ' OPTIMUM SEQUENCE USING ORIGINAL CODE NUMBERS')
      WRITE (OUT(3),4110) (IRCODE(I), I = 1,MMAX)
 4110 FORMAT (1X, 20I5)
      WRITE (OUT(3),4130) COUNT, ITER
 4130 FORMAT (///// ' RANKING SOLUTION OBTAINED WITH:' //10X, I5,
     +   ' ITERATIONS OUT OF MAXIMUM',I7)
      WRITE (OUT(3),4150) CRIT1, TOL
 4150 FORMAT (//10X, 'CRITICAL TRANSPOSE ELEMENT SUM OF', F6.1,
     +  //10X, 'TOLERANCE OF', F6.1)
C
C
C     EVENT RANGES
C     ------------
C
C  PRINT SEQUENCE WITH NAMES (EVENT LABELS) AND RANGES
C  (WE MAKE USE OF THE CUM.ORDER MATRIX AND THE CORRESPONDING
C    POSITION MATRIX)
C
C
      DO 520 I = 1,MMAX
          K = I
  500     K = K - 1
              IF (K.EQ.0) GO TO 505
              ARG = C(K,I) - C(I,K)
              IF (ARG.LE.0.0) GO TO 500
  505     INK = K
          K = I
  510     K = K + 1
              IF (K.EQ.(MMAX+1)) GO TO 515
              ARG = C(I,K) - C(K,I)
              IF (ARG.LE.0.0) GO TO 510
  515     JNK = K
          IRANGE(I,1) = INK
          IRANGE(I,2) = JNK
  520 CONTINUE
      WRITE (OUT(4),7040)
 7040 FORMAT (////10X,'NUMERICAL LISTING'//)
      DO 525 I = 1,N
          WRITE (OUT(4),7050) I, (ITITLE(I,J), J = 1,10)
```

```
 7050     FORMAT (1X, I5, 2X, 10A4)
  525 CONTINUE
      NCOLS = 10
      CALL ASORT (NCOLS,OUT(4))
C
      WRITE (OUT(5),5010)
      WRITE (OUT(5),5020)
      WRITE (OUT(5),5030)
      WRITE (OUT(5),5040)
 5010 FORMAT (/////'OPTIMUM SEQUENCE TABULATED WITH EVENT RANGES
AND',
     +   ' LABELS:'///)
 5020 FORMAT (7X, 'SEQUENCE  FOSSIL  RANGE   FOSSIL    - RANGES',
     + ' DEFINE OUTER LIMITS IN THE POSITION SEQUENCE.  EVENTS CAN',
     + ' OCCUR ANYWHERE')
 5030 FORMAT (7X, 'POSITION  NUMBER', 10X, 'NAME', 8X, 'WITHIN
THESE',
     + ' LIMITS.  (NOTE: THIS RANGE IS NOT STRATIGRAPHIC)')
 5040 FORMAT (//)
      DO 530 I = 1,MMAX
          ID = IRCODE(I)
          JIRCOD(I) = ID
          WRITE (OUT(5),5050) I, ID, IRANGE(I,1), IRANGE(I,2),
     +      (ITITLE(ID,J), J = 1,10)
          WRITE (7,5047) I, ID, IRANGE(I,1), IRANGE(I,2),
     +      (ITITLE(ID,J), J = 1,10)
 5047     FORMAT (1X, I8, I9, I8, I4, 3X, 10A4)
 5050     FORMAT (1X, I8, I9, I8, '-', I3, 3X, 10A4)
  530 CONTINUE
C
C  JIRCOD  - A COPY OF THE OPTIMUM SEQUENCE OBTAINED BY RANKING.
C            (ORIGINAL FOSSIL NUMBERS).  TO BE USED AS INPUT TO
WDIST().
C
      IF (ISCAT.NE.1)  GO TO 534
          WRITE (OUT(6),5055)
 5055     FORMAT (/////'CORRELATION OF WELL SEQUENCE DATA TO
OPTIMUM',
     +      ' SEQUENCE'/)
          DO 533 IS = 1,NS
              DO 531 I = 1,KDIM3
                  IQD(I) = TMAT(IS,I)
                  IF (IQD(I).EQ.0) GO TO 532
                  NED = I
  531         CONTINUE
  532         WRITE (OUT(6),5060) (NAME(IS,J), J = 1,10)
 5060         FORMAT (///2X,10A4/)
              CALL SCATTR (IQD,NED,IS,OUT(6))
  533     CONTINUE
  534 IF (IALPHA.EQ.1) GO TO 535
C
```

```
C       ---- SMALL MISS-PLACED OUTPUT 9 GROUP ------
C
          IF (ITAB1.EQ.1) CALL TAB1 (OUT(9))
          IF (ISCORE.EQ.1) CALL SCORE (OUT(9))
          GO TO 9999
C       ------------------------------------------
C
C     SCALING ANALYSIS
C     ----------------
C
C  SECOND MODIFICATION OF CUMULATIVE ORDER MATRIX
C
C
  535 IF (CRIT2.LE.CRIT1) GO TO 590
      WRITE (*,*) 'SCALING ANALYSIS'
          IKNT = 0
          DO 560 I = 1,IMAX
              L = I + 1
              DO 550 J = L,MMAX
                  IF (C(I,J)+C(J,I).GE.CRIT2) GO TO 550
                  C(I,J) = 0.0
                  C(J,I) = 0.0
                  IKNT = IKNT + 1
  550         CONTINUE
  560     CONTINUE
          WRITE (OUT(3),5070) CRIT2, IKNT, MMSQ
 5070     FORMAT (//1X, 'SECOND MODIFICATION OF ORDER MATRIX:',
     +       /6X, 'BASED ON CRIT2 = ', F5.1, ', A TOTAL OF', I5,
     +       ' PAIRS (OUT OF', I5, ') HAVE BEEN ZEROED.')
          IF (IOMAT.NE.1) GO TO 590
          WRITE (OUT(3),3070)
          DO 570 I = 1,MMAX
              WRITE (OUT(3),3030)
              WRITE (OUT(3),3080) (C(I,J), J = 1,MMAX)
  570     CONTINUE
C
C     (IF LLL = 1,  THEN RESULTS OF SCALING WILL NOT BE PRINTED)
  590 LLL = INOSC
      IF (INOSC.EQ.1) LLL = 0
      WRITE (OUT(7),6000)
      WRITE (OUT(7),6010)
 6000 FORMAT (////4X,'SCALING ANALYSIS')
 6010 FORMAT (5X,'----------------')
C
C  EVALUATION OF OPTIMUM SEQUENCE BASED ON UNWEIGHTED AND WEIGHTED
C       DISTANCE ANALYSIS
C
      WRITE (OUT(7),6020)
 6020 FORMAT (//'  EVALUATION BASED ON UNWEIGHTED AND WEIGHTED',
     + ' DISTANCE ANALYSIS')
C
```

```
C  COMPUTE NORMAL Z VALUES OF FREQUENCIES CALCULATED FROM ORDER
MATRIX
C
      CALL NORMZ (AAA,LLL,IOMAT,OUT(7))
C
C  COMPUTE 'DISTANCES' BETWEEN EVENTS AND CONSTRUCT DENDROGRAM
C
C
      CALL DIST (QDAR,MPAIR,AAA,LLL,OUT(7))
      LOUT = 0
      CALL ORDER (QDAR,IPAIR,XLEV,LLL,LOUT,OUT(7))
      IF (LLL.NE.0) WRITE (OUT(7),7010)
 7010 FORMAT (//5X,'DENDROGRAM OF UNWEIGHTED INTERFOSSIL
DISTANCES'//)
      IF (LLL.NE.0) CALL DENDRO (IPAIR,XLEV,OUT(7))
C
C  REPEAT DISTANCE ANALYSIS WITH WEIGHTED DIFFERENCES
C
      LLL = INOSC
      CALL WDIST (JIRCOD,QDAR,MPAIR,AAA,LLL,INEG,CRIT2,OUT(7))
      LOUT = 1
      CALL ORDER (QDAR,IPAIR,XLEV,LLL,LOUT,OUT(7))
      IF (LLL.NE.0) WRITE (OUT(7),7020)
 7020 FORMAT (//5X,'DENDROGRAM OF WEIGTHED INTERFOSSIL DISTANCES'//)
      IF (LLL.NE.0) CALL DENDRO (IPAIR,XLEV,OUT(7))
C
C  REORDER FINAL RELATION MATRIX AND REPEAT CLUSTER ANALYSIS
C     FOR UNWEIGHTED AND WEIGHTED DIFFERENCES
C
      IF (IFIN.NE.1) GO TO 700
      DO 625 KKK = 1,5
          IRET  = 1
          DO 600 I = 1,MMAX
              IF (JIRCOD(I).NE.IRCODE(I)) IRET = 0
  600     CONTINUE
          IF (KKK.EQ.5) IRET = 1
          LLL = IRET
          IF (IRET.NE.1) GO TO 610
          WRITE (OUT(7),6030)
 6030     FORMAT (///)
          WRITE (OUT(7),6040)
 6040     FORMAT (/'  APPLICATION OF FINAL REORDERING'//)
          WRITE (OUT(7),6050)
 6050     FORMAT ('  DISTANCES ESTIMATED FROM SUCCESSIVE EVENTS'///)
          WRITE (OUT(7),6051)
 6051     FORMAT (/4X, 'TO RECALCULATE STANDARD DEVIATIONS,
DISTANCE),
     +     ' VALUES HAVE TO BE RECALCULATED STARTING WITH THE NEW',
     +     ' SEQUENCE'//)
          IF (IOMAT.NE.1) GO TO 620
              WRITE (OUT(7),6060)
```

```
 6060          FORMAT (////'  UPPER TRIANGLE OF NORMAL Z VALUES')
               DO 605 I = 1,MMAX
                   WRITE (OUT(7),6070)
 6070              FORMAT (///)
                   WRITE (OUT(7),6080) (C(I,J), J = 1,MMAX)
 6080              FORMAT (1X,15F8.3)
  605          CONTINUE
               GO TO 620
  610      CALL REORD (AAA,IPOS)
               DO 615 I = 1,MMAX
                   JIRCOD(I) = IRCODE(I)
  615          CONTINUE
               LLL = 0
               IF (INOSC.GT.1 .AND. IRET.EQ.1) LLL = 1
C
C              COMPUTE NORMAL Z VALUES
C
               CALL NORMZ (AAA,LLL,IOMAT,OUT(7))
C
C              COMPUTE DISTANCES BETWEEN FOSSIL EVENTS
C
  620      LLL = 0
           IF (INOSC.GT.1 .AND. IRET.EQ.1) LLL = 1
           CALL DIST (QDAR,MPAIR,AAA,LLL,OUT(7))
           LOUT = 0
           CALL ORDER (QDAR,IPAIR,XLEV,LLL,LOUT,OUT(7))
           IF (LLL.NE.0) WRITE (OUT(7),7010)
           IF (LLL.NE.0) CALL DENDRO (IPAIR,XLEV,OUT(7))
C
C      REPEAT DISTANCE CALCULATION WITH WEIGHTED DIFFERENCES
C
           LLL = 0
           IF (INOSC.GE.1 .AND. IRET.EQ.1) LLL = 1
           CALL WDIST (JIRCOD,QDAR,MPAIR,AAA,LLL,INEG,CRIT2,OUT(8))
           LOUT = 1
           CALL ORDER (QDAR,IPAIR,XLEV,LLL,LOUT,OUT(8))
           IF (LLL.NE.0) WRITE (OUT(8),7020)
           IF (LLL.NE.0) CALL DENDRO (IPAIR,XLEV,OUT(8))
           IF (IRET.EQ.1) GO TO 630
  625 CONTINUE
  630 WRITE (OUT(8),6090) KKK
 6090 FORMAT ('///' SOLUTION AFTER ',I3,' ITERATIONS'///)
C
C
C
C      FINAL PROCESSING OPTIONS
C      ------------------------
C
       WRITE (*,*) 'NORMALITY TESTS'
C
C  CONSTRUCT OCCURRENCE TABLE FOR WELLS
```

```
C
  700 IF (ITAB1.EQ.1) CALL TAB1 (OUT(9))
C
C  STEP MODEL FOR INDIVIDUAL WELLS
C
      IF (ISCORE.EQ.1) CALL SCORE (OUT(9))
C
      IF (ISCAT.NE.1) GO TO 850
      WRITE (OUT(10),5055)
      DO 800 I = 1,NS
        DO 790 J = 1,KDIM3
              IQD(J) = TMAT(I,J)
              IF (IQD(J).EQ.0) GO TO 795
              NED = J
  790      CONTINUE
  795      WRITE (OUT(10),5060) (NAME(I,J), J = 1,10)
           CALL SCATTR (IQD,NED,I,OUT(10))
  800 CONTINUE
C
C  PERFORM NORMALITY TEST ON INDIVIDUAL WELLS
C
  850 IF (ICOMP.EQ.1) CALL COMP (QDAR,INIQ,OUT(10))
C
C  ENTER UNIQUE EVENTS INTO SEQUENCE AND PRINT FINAL DENDROGRAM
C
      IF (INIQ.NE.1 .OR. ICOMP.NE.1) GO TO 9999
          WRITE (OUT(11),7000)
 7000     FORMAT (///, 'POSITIONING OF UNIQUE EVENTS IN FINAL
SEQUENCE')
          CALL ORDER (QDAR,IPAIR,XLEV,LLL,0,OUT(11))
          CALL DENDRO (IPAIR,XLEV,OUT(11))
C
 9999 CLOSE (61)
      CLOSE (62)
      CLOSE (5)
      CLOSE (10)
      CLOSE (51)
      CLOSE (99)
      CLOSE (7)
      STOP
      END
```

```
      SUBROUTINE READIN (OUT)
C
C ... SUBROUTINE TO READ IN ALL THE INPUT PARAMETERS, SEQUENCE
C  DATA, AND DICTIONARY.
C  EXECUTION IS TERMINATED IF ANY ERRORS ARE DISCOVERED.
C
C  CALLED IN MAIN PROGRAMME
C
      PARAMETER (KDIM1=24, KDIM3=120, KDIM4=605, KDIM5=10,
     KDIM6=145)
      PARAMETER (MAXCYC=300, MAXUQ=20)
      COMMON  N, NS, MMAX, IX(KDIM1,KDIM3), ICODE(KDIM4),
     IRCODE(KDIM4),
     +        C(KDIM6,KDIM6)
      COMMON  /BETA/ IUNIQ(KDIM4,2), NUNIQ(KDIM1),
     MUNIQ(KDIM1,MAXUQ*2)
      COMMON  /DELTA/ IOCR, INIQ, CRIT1, TOL, AAA, CRIT2, MAX, ITER,
     +        IOMAT, ISRT, IALPHA, ITAB1, ISCORE, ICOMP, ISKIP,
     IFIN,
     +        INOSC, INEG, ISCAT, TMAT(KDIM1,KDIM3)
      COMMON  /TEXT/ NAME(KDIM1,10), ITITLE(KDIM4,10)
      COMMON  /PESEE/ SDW(KDIM4), IWEIT(KDIM4,2)
      INTEGER ITEM(MAXUQ), TMAT, ITALLY(KDIM4), OUT(11)
      CHARACTER*4 NAME, ITITLE, ITEMP
C
C RETURNS THE OBSERVED DATA IN TMAT(*,*) VIA COMMON /DELTA/,
C         AND IN IX(*,*) VIA BLANK COMMON.
C  IUNIQ(KDIM4, 2)  IS A MAP SHOWING THE UNIQUE EVENTS IN COLUMN 1
C         AND THE MARKER HORIZONS IN COLUMN 2
C  NUNIQ(KDIM1) IS A MAP SHOWING WHICH SEQUENCES HAVE UNIQUE EVENTS
C
C  READ THE RUN-PARAMETERS AND THE PROCESSING OPTIONS
C
      READ (5,*) NS, IOCR, INIQ, ITER, CRIT1, TOL, AAA, CRIT2
      READ (5,*) ITAPE, IOMAT, ISRT, IALPHA, ITAB1, ISCORE, ICOMP,
     +    ISKIP, IFIN, INOSC, INEG, ISCAT
      READ (5,*) (OUT(I),I=1,11)
C
C----- SET UP OUTPUT --------------------
C
      DO 101 I=1,11
        IF (OUT(I).EQ.1) THEN
          OUT(I)=61
        ELSE
          OUT(I)=62
        ENDIF
 101  CONTINUE
C
C ---------------------------------------
C
      WRITE (OUT(1),1040)
```

```
      WRITE (OUT(1),1041)
      WRITE (OUT(1),1042) NS, IOCR, INIQ, ITER, CRIT1, TOL, AAA,
CRIT2
      WRITE (OUT(1),1045)
      WRITE (OUT(1),1046) ITAPE, IOMAT, ISRT, IALPHA, ITAB1, ISCORE,
ICOMP,
     +      ISKIP, IFIN, INOSC, INEG, ISCAT
 1040 FORMAT (///5X, 'VALUES OF INPUT PARAMETERS'//)
 1041 FORMAT (1X, 'RUN PARAMETERS:    NS IOCR INIQ  ITER  CRIT1
TOL',
     +  6X, 'AAA', 5X, 'CRIT2')
 1042 FORMAT (17X, I5, I5, I5, I6, F7.1, F7.1, F11.5, F7.1)
 1045 FORMAT (/1X, 'PROCESSING OP:  ITAPE IOMAT ISRT IALPHA ITAB1'
     +  ' ISCORE ICOMP ISKIP IFIN INOSC INEG ISCAT')
 1046 FORMAT (18X, I4, I6, I5, I7, I6, I7, I6, I6, I5, I6, I5, I6)
      DO 100 I = 1,KDIM4
          IRCODE(I) = 0
          IUNIQ(I,1) = 0
          IUNIQ(I,2) = 0
  100 CONTINUE
C
C  READ UNIQUE EVENTS AND MARKER HORIZONS
C
      READ 1050, (ITEM(J), J = 1,20)
 1050 FORMAT (20I4)
      IF (ITEM(1).EQ.0 .OR. INIQ.EQ.1)  GO TO 1055
          WRITE (OUT(1),1051)
 1051     FORMAT (///1X, '** WARNING:  UNIQUE EVENTS FOUND ON RECORD
3'
     +      /15X, '"INIQ" SET EQUAL TO 1')
          INIQ = 1
 1055 IF (INIQ.EQ.1) WRITE (OUT(1),1060)
 1060 FORMAT (///' THE FOLLOWING UNIQUE EVENTS HAVE BEEN
SELECTED:'/)
      DO 105 I = 1,20
          ID = ITEM(I)
          IF (ID.EQ.0) GO TO 110
          IUNIQ(ID,1) = 1
          WRITE (OUT(1),1070) ID
 1070     FORMAT (5X,I4)
  105 CONTINUE
  110 READ 1050, (ITEM(J), J = 1,20)
      IF (ITEM(1).EQ.0 .OR. INIQ.EQ.1)  GO TO 112
          WRITE (OUT(1),1075)
 1075     FORMAT (///1X, '** WARNING:  MARKER HORIZONS FOUND ON
RECORD',
     +      ' 4'/ 15X, '"INIQ" SET EQUAL TO 1')
          INIQ = 1
  112 IF (INIQ.EQ.1) WRITE (OUT(1),1080)
 1080 FORMAT (///' THE FOLLOWING MARKER HORIZONS HAVE BEEN
SELECTED:'/)
```

```
      DO 115 I = 1,20
          ID = ITEM(I)
          IF (ID.EQ.0) GO TO 120
          IUNIQ(ID,2) = 1
          WRITE (OUT(1),1070) ID
  115 CONTINUE
C
C  PERFORM DATA VALIDATION ON INPUT PARAMETERS
C
  120 CALL CHECK (NS,CRIT1,CRIT2,IOCR,IER)
      IF (IER.NE.0)  STOP
C
C  READ IN THE WELL DATA
C
      DO 129 I = 1,NS
          NUNIQ(I) = 0
          DO 125 J = 1,KDIM3
              TMAT(I,J) = 0
              IX(I,J) = 0
  125     CONTINUE
  129 CONTINUE
      DO 130 I = 1,KDIM4
          SDW (I) = 0
          IWEIT (I,1) = 0
          IWEIT (I,2) = 0
  130 CONTINUE
      IODATA = 5
      IF (ITAPE.EQ.1) IODATA = 10
      DO 135 I = 1,NS
          READ (IODATA,1090) (NAME(I,J), J = 1,10)
 1090     FORMAT (10A4)
          K = 0
  131     READ (IODATA,1100) (ITEM(J), J = 1,20)
 1100         FORMAT (20I4)
              DO 133 J = 1,20
                  ITEMJ = ITEM(J)
                  IF (ITEMJ.EQ.-999)  GO TO 134
                  IF (ITEMJ.EQ.0)  GO TO 133
                      K = K + 1
                      IF (K.LE.KDIM3)  GO TO 132
                          WRITE (OUT(1),1105)
 1105                     FORMAT (//1X, '*** ERROR:  SEQUENCE TOO
LONG',
     +                        /12X, 'POSSIBLE CAUSE:  MISSING -999',
     +                        /12X, 'OTHERWISE:  USE A LARGER
VERSION',
     +                        ' OF RASC'//' **** EXECUTION
TERMINATED'/)
                          STOP
  132                 TMAT(I,K) = ITEMJ
  133         CONTINUE
```

```
                GO TO 131
  134       IF (K.LT.KDIM3)  TMAT(I,K+1) = 0
  135 CONTINUE
C
C  READ IN THE S.D. WEIGHTS
C
        I = 1
  140 READ (51,2000) (IWEIT(I,J), J = 1,2)
 2000 FORMAT (2I6)
            L = IWEIT(I,1)
            IF (L.EQ.-999)  GO TO 141
            SDW (L) = IWEIT (I,2)
            I = I + 1
            IF (I.EQ.86)  GO TO 141
        GO TO 140
C
C  READ IN THE DICTIONARY
C
  141 I = 1
        READ (99,5000) (ITITLE(I,J), J = 1,10)
 5000 FORMAT (10A4)
 5500 IF (ITITLE(I,1).EQ.'LAST' .OR. I.EQ.KDIM4)  GO TO 6000
            I = I + 1
            READ (99,5000) (ITITLE(I,J), J = 1,10)
            GO TO 5500
 6000 IF (ITITLE(I,1).EQ.'LAST')  GO TO 7000
            I = I + 1
            READ (99,5000) ITEMP
            IF (ITEMP.EQ.'LAST')  GO TO 7000
                WRITE (OUT(1),6200) KDIM4, KDIM4
 6200           FORMAT (///1X, '*** ERROR:  MORE THAN',I5,' EVENT',
     +,           ' LABELS FOUND IN DICTIONARY'/16X, 'FOR
DICTIONARIES',
     +           ' WITH MORE THAN',I5, ' NAMES,',/16X, 'PLEASE USE',
     +           ' A LARGER VERSION OF RASC')
                WRITE (OUT(1),6250)
 6250           FORMAT (///' **** EXECUTION TERMINATED IN',
     +             '   SUBROUTINE READIN')
                STOP
 7000 N = I - 1
        WRITE (OUT(1),7500) N
 7500 FORMAT (/1X, 'DICTIONARY:', I5, ' NAMES WERE READ IN.')
C
C  CHECK THE WELL DATA
C
        IERR = 0
        IERR2 = 0
        DO 9000 I = 1,NS
            DO 8300 J = 1,N
                ITALLY(J) = 0
 8300       CONTINUE
```

```
          DO 8500 J = 1,KDIM3
              ID = IABS (TMAT(I,J))
              IF (ID.EQ.0)  GO TO 9000
              IF (ID.GT.N)  GO TO 8370
              IF (ITALLY(ID).EQ.0)  GO TO 8400
                  WRITE (OUT(1),8340) (NAME(I,K), K = 1,5), ID
 8340             FORMAT (/' IN ',10A4,' FOSSIL',I5,' OCCURS MORE
THAN',
     +               ' ONCE')
                  IERR = IERR + 1
                  GO TO 8500
 8370         WRITE (OUT(1),8380) (NAME(I,K), K = 1,5), ID
 8380             FORMAT (/' IN ',10A4,' FOSSIL',I5,
     +               '  -  EXCEEDS LIMIT OF YOUR DICTIONARY')
                  IERR2 = IERR2 + 1
                  GO TO 8500
 8400         ITALLY(ID) = 1
 8500     CONTINUE
 9000 CONTINUE
      IF (IERR.EQ.0)  GO TO 9200
          WRITE (OUT(1),9100) IERR
 9100     FORMAT (//' *** ERROR -  ON',I6,' OCCASION(S), AN EVENT',
     +      ' OCCURRED MORE THAN ONCE IN THE SAME WELL.'/15X, 'YOU',
     +      ' MAY NOT REPORT MORE THAN ONE OCCURRENCE OF ANY
FOSSIL',
     +      ' IN ANY WELL.')
 9200 IF (IERR2 .EQ. 0) GO TO 9300
          WRITE (OUT(1),9220) IERR2, N
 9220     FORMAT (//' *** ERROR - ON',I6,' OCCASION(S), THERE',
     +      ' WAS A FOSSIL NUMBER GREATER THAN THE LARGEST',
     +      ' DICTIONARY NUMBER:',I5)
C
C  PRINT ORIGINAL SEQUENCE DATA
 9300 DO 9340 I = 1,NS
          DO 9320 J = 1,KDIM3
              IX(I,J) = TMAT(I,J)
 9320     CONTINUE
 9340 CONTINUE
      WRITE (OUT(1),9390)
 9390 FORMAT (///'   ORIGINAL SEQUENCE DATA')
      CALL ECHO (OUT(1))
C
      IF (IERR.EQ.0 .AND. IERR2.EQ.0)  GO TO 9400
          WRITE (OUT(1),6250)
          STOP
C
 9400 RETURN
      END
```

```
      SUBROUTINE HPFILT (IC,IOCR,INIQ,IOMAT,UNIT)
C
C ... SUBROUTINE HPFILT REMOVES FROM THE DATA SET ALL EVENTS WHICH
DO
C  DO NOT OCCUR AT LEAST "IOCR" TIMES AND RECODES THE MODIFIED DATA
C  WITH CODE NUMBERS RUNNING FROM 1 TO MMAX
C
C  ACCEPTS:  IC     - ORIGINAL SEQUENCE DATA
C            M      - THE OCCURRENCE TABULATION
C
C  RETURNS:  IC     - NOW, THE FILTERED SEQUENCE DATA.
C            ICC    - THE FILTERED, RECODED SEQUENCE DATA
C            MMAX   - NUMBER OF DIFFERENT FOSSILS REMAINING
C
C  CALLED IN MAIN PROGRAMME
C
      PARAMETER (KDIM1=24, KDIM3=120, KDIM4=605, KDIM5=10,
KDIM6=145)
      PARAMETER (MAXCYC=300, MAXUQ=20)
      COMMON  N, NS, MMAX, ICC(KDIM1,KDIM3), MM(KDIM4), M(KDIM4),
     +        RMAT(KDIM6,KDIM6)
      COMMON /BETA/ IUNIQ(KDIM4,2), NUNIQ(KDIM1),
MUNIQ(KDIM1,MAXUQ*2)
      COMMON /TEXT/ NAME(KDIM1,10), ITITLE(KDIM4,10)
      COMMON /PESEE/ SDW(KDIM4), IWEIT(KDIM4,2)
      INTEGER IC(KDIM1,KDIM3), UNIT
      CHARACTER*4  NAME, ITITLE
C
      DO 30 I = 1,NS
          DO 10 J = 1,KDIM3
              ICC(I,J) = 0
   10     CONTINUE
          IF (INIQ.NE.1) GO TO 30
          DO 20 J = 1,40
              MUNIQ(I,J) = 0
   20     CONTINUE
   30 CONTINUE
C
C  ELIMINATE EVENTS WHICH OCCUR FEWER THAN "IOCR" TIMES
C
      DO 60 I = 1,NS
          INDIC = 0
          K = 1
          DO 50 J = 1,KDIM3
              ID = IC(I,J)
              IF (ID.EQ.0) GO TO 60
              IDA = IABS (ID)
              IF (INIQ.EQ.1 .AND. IUNIQ(IDA,1).EQ.1) M(IDA) = 0
              IF (M(IDA).LT.IOCR) GO TO 40
              IF (INDIC.EQ.1 .AND. ID.LT.0) ID = ID * (-1)
              ICC(I,K) = ID
```

```
                K = K + 1
                INDIC = 0
                GO TO 50
   40           IF (ID.GT.0 .AND. INDIC.EQ.0) INDIC = 1
   50        CONTINUE
   60   CONTINUE
        WRITE (UNIT,1000)
 1000   FORMAT (//////'   SEQUENCE DATA MODIFIED TO INCLUDE ONLY')
        WRITE (UNIT,1010) IOCR
 1010   FORMAT ('   THOSE EVENTS WHICH OCCUR AT LEAST',I3,' TIMES')
        CALL ECHO (UNIT)
C  SEND ICC TO ECHO() VIA BLANK COMMON
C
C  PREPARE TABLES TO BE USED IN RECODING
C
        DO 70 I = 1,N
            M(I) = 0
            MM(I) = 0
   70   CONTINUE
        DO 90 I = 1,NS
            DO 80 J = 1,KDIM3
                ID = ICC(I,J)
                IF (ID.EQ.0) GO TO 90
                IDA = IABS (ID)
                M(IDA) = M(IDA) + 1
   80       CONTINUE
   90   CONTINUE
        IF (IOMAT.EQ.1) WRITE (UNIT,1020)
 1020   FORMAT (////'   RECODE REFERENCE TABLE, OLD CODE VS. NEW
CODE')
C  "M" IS USED AS WORK-AREA FOR THE RECODING TABLE
        K = 1
        DO 100 I = 1,N
            ID = M(I)
            IF (ID.EQ.0) GO TO 100
            M(I) = K
            IF (IOMAT.EQ.1) WRITE (UNIT,1030) I, K
 1030       FORMAT (2I6)
            MM(K) = I
            K = K + 1
  100   CONTINUE
        IF (INIQ.NE.1) GO TO 120
        DO 110 I = 1,NS
            IF (NUNIQ(I).EQ.1) CALL XUNIQ1 (I,IC)
  110   CONTINUE
C
C       MAKE A COPY OF THE FILTERED DATA SET BEFORE RECODING.
C            (DESTROY THE UN-FILTERED DATA SET)
C
  120   DO 128 I = 1,NS
            DO 125 J = 1,KDIM3
```

```
            IC(I,J) = ICC(I,J)
  125     CONTINUE
  128 CONTINUE
C
C  PERFORM RECODING
C
      MMAX = K - 1
      DO 140 I = 1,NS
          DO 130 J = 1,KDIM3
              ID = ICC(I,J)
              IF (ID.EQ.0) GO TO 140
              IDA = IABS (ID)
              IDD = M(IDA)
              IF (ID.LT.0) IDD = IDD * (-1)
              ICC(I,J) = IDD
  130     CONTINUE
  140 CONTINUE
      WRITE (UNIT,1040)
 1040 FORMAT (////'   RECODED SEQUENCE DATA')
C  RECODE STANDARD DEVIATION WEIGHT FILE
      DO 150 I = 1,KDIM4
          V = SDW (I)
          IF (V.EQ.0) GOTO 150
          IDD = M (I)
          SDW (IDD) = V
          SDW (I) = 0
  150 CONTINUE
C  AGAIN, SEND ICC TO ECHO()
      CALL ECHO (UNIT)
      IF (IOMAT.NE.1)  GO TO 170
          WRITE (UNIT,1050)
 1050     FORMAT (///'   CROSS REFERENCE TABLE, NEW CODE VS. OLD
CODE')
C  "MM" IS A SERIAL LIST OF OLD CODE NUMBERS
          DO 160 I = 1,MMAX
              WRITE (UNIT,1060) I, MM(I)
 1060         FORMAT (2I6)
  160     CONTINUE
  170 WRITE (UNIT,1070) MMAX
 1070 FORMAT (////'    NUMBER OF FOSSILS RETAINED:',I5)
      WRITE (7,1071) MMAX
 1071 FORMAT (I10)
C
      IF (MMAX.GT.1 .AND. MMAX.LT.KDIM6)  GO TO 999
      IF (MMAX.GT.KDIM6)  GO TO 220
          WRITE (UNIT,1075)
 1075     FORMAT (///1X, '*** ERROR:  TOO MUCH FILTERING DONE --',
     +       ' NO DATA LEFT'/16X, 'RECOMMENDED ACTION: DECREASE',
     +       ' VALUE OF "IOCR"')
          WRITE (UNIT,1090)
          STOP
```

```
  220 WRITE (UNIT,1080) KDIM6
 1080     FORMAT (///1X,'*** ERROR:   TOO MANY EVENTS REMAINING
(>',I4,
     +       ')', /16X, 'CAUSE:  NOT ENOUGH FILTERING DONE',
     +       /16X, 'RECOMMENDED ACTION:  INCREASE VALUE OF "IOCR"
OR',
     +       /36X, 'USE A BIGGER VERSION OF RASC')
          WRITE (UNIT,1090)
 1090     FORMAT (///' *** EXECUTION TERMINATED IN   SUBROUTINE
HPFILT')
          STOP
C
  999 RETURN
      END
```

```
      SUBROUTINE NORMZ (AAA,LLL,IOMAT,UNIT)
C
C ... SUBROUTINE TO COMPUTE 'Z' (NORMAL) VALUES OF FREQUENCIES
C
C       C(I,J)
C  ---------------      FROM CUMULATIVE ORDER MATRIX.
C  C(I,J) + C(J,I)
C
C  ACCEPTS:  C  - CUMULATIVE ORDER MATRIX
C  RETURNS:  UPPER TRIANGLE OF "C", EXCLUDING THE MAIN DIAGONAL
C
C  CALLED IN MAIN PROGRAMME.
C
      PARAMETER (KDIM1=24, KDIM3=120, KDIM4=605, KDIM5=10,
     KDIM6=145)
      COMMON N, NS, MMAX, IX(KDIM1,KDIM3), ICODE(KDIM4),
     IRCODE(KDIM4),
     +       C(KDIM6,KDIM6)
      COMMON  /PESEE/ SDW(KDIM4), IWEIT(KDIM4,2)
      INTEGER UNIT
      DATA  CONST/9.0/, TAILL/0.05/, TAILR/0.95/
C
      DO 40 I = 1,MMAX
          K = I + 1
          DO 30 J = K,MMAX
              RCL1 = C(I,J)
              RCL2 = C(J,I)
              S1 = SDW(I) / 10000
              S2 = SDW(J) / 10000
              S3 = S1 * S1
              S4 = S2 * S2
              S5 = S3 + S4
              SRCL = RCL1 + RCL2
              S6 = SQRT (S5)
              IF (SRCL.EQ.0.0) GO TO 20
              QRCL = RCL1 / SRCL
              IF (QRCL.LE.0.0 .OR. QRCL.GE.1.0)  GO TO 10
              CALL FTOZ (QRCL,S6,QX)
              C(I,J) = QX
              GO TO 30
   10         IF (QRCL.EQ.1.0) C(I,J) = AAA
              IF (QRCL.EQ.1.0) C(J,I) = TAILL * SRCL
              IF (QRCL.EQ.0.0) C(I,J) = -AAA
              IF (QRCL.EQ.0.0) C(J,I) = TAILR * SRCL
              GO TO 30
   20         C(I,J) = CONST
   30     CONTINUE
   40 CONTINUE
      IF (LLL.EQ.0 .OR. IOMAT.NE.1)  GO TO 60
      WRITE (UNIT,1000)
 1000 FORMAT ('1///'  UPPER TRIANGLE OF NORMAL Z VALUES')
```

```
      DO 50 I = 1,MMAX
          WRITE (UNIT,1001)
1001      FORMAT (///)
          WRITE (UNIT,1002) (C(I,J), J = 1,MMAX)
1002      FORMAT (1X,.15F8.3)
  50  CONTINUE
  60  RETURN
      END
```

```
      SUBROUTINE FTOZ (P,S6,ZP)
C
C ... SUBROUTINE TO COMPUTE Z FROM FREQUENCY.   EQ. 26.2.23   IN
C
C      ABRAMOWITZ, M. AND STEGUN, I.A.     (EDITORS)
C      "HANDBOOK OF MATHEMATICAL FUNCTIONS
C         WITH FORMULAS, GRAPHS, AND MATHEMATICAL TABLES"
C      PUB. BY NATIONAL BUREAU OF STANDARDS OF THE
C         U.S. DEPARTMENT OF COMMERCE,   1964.
C
C  CALLED BY SUBROUTINE NORMZ
C
      DATA  C0/2.515517/, C1/0.802853/, C2/0.010328/,
     +      D1/1.432788/, D2/0.189269/, D3/0.001308/
C
      Q = P
      IF (P.GT.0.5)  Q = 1.0 - P
      TT = ALOG (1.0 / (Q * Q))
      T = SQRT (TT)
      UP = C0 + (C1 * T) + (C2 * T * T)
      DN = 1.0 + (D1 * T) + (D2 * T * T) + (D3 * T**3)
      ZP = T - (UP / DN)
      ZP = ZP * S6
      IF (P.LE.0.5)  ZP = -ZP
      RETURN
      END
```

APPENDIX C

FREQUENCY DISTRIBUTION PLOTS

OF THE EVENTS OF THE SCALED OPTIMUM SEQUENCE

EVENT NUMBER 17 :ASTERIGERINA GURICHI

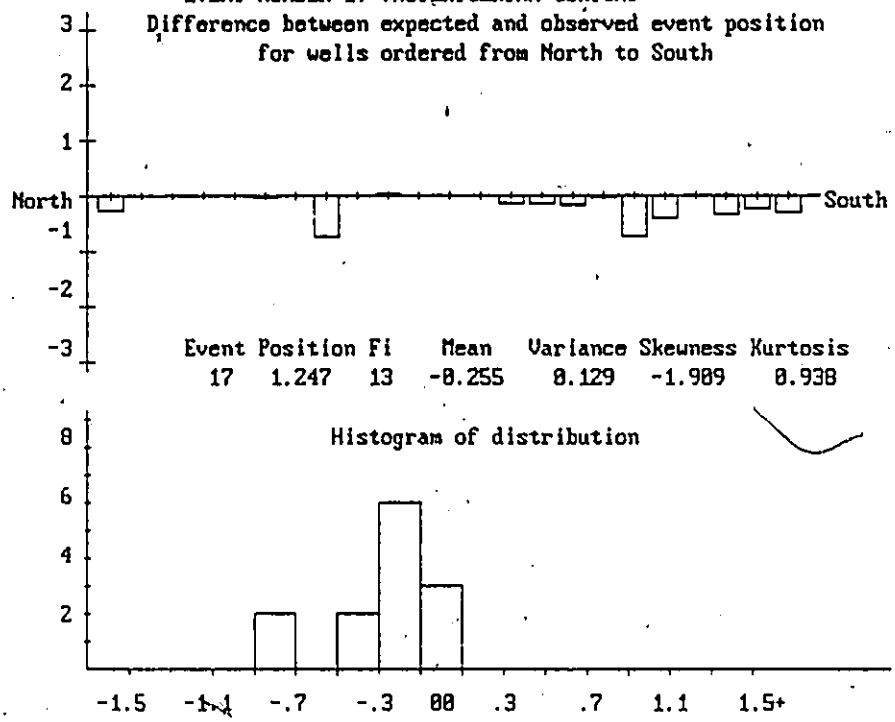

Event	Position	Fi	Mean	Variance	Skewness	Kurtosis
17	1.247	13	-0.255	0.129	-1.989	0.938

EVENT NUMBER 569 :SYSTEMATOPHORA ANCYREA

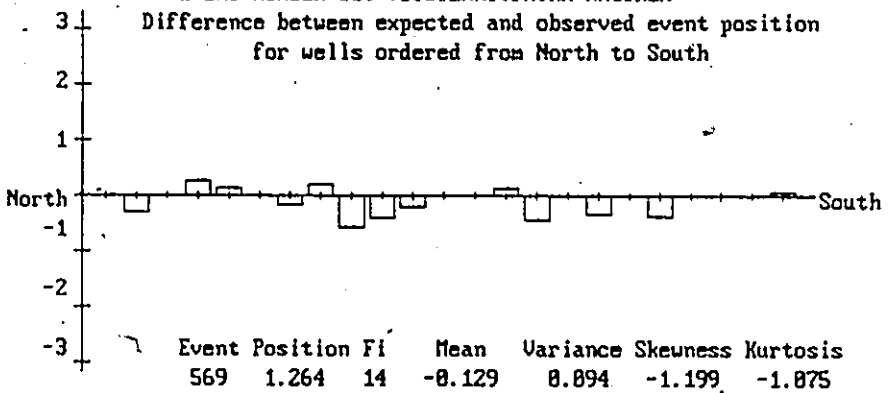

Event	Position	Fi	Mean	Variance	Skewness	Kurtosis
569	1.264	14	-0.129	0.094	-1.199	-1.075

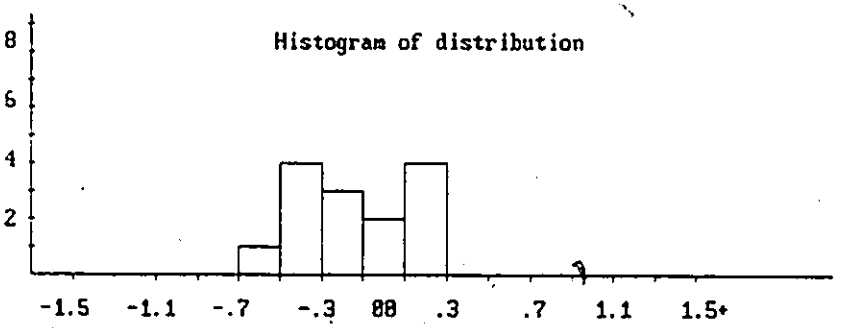

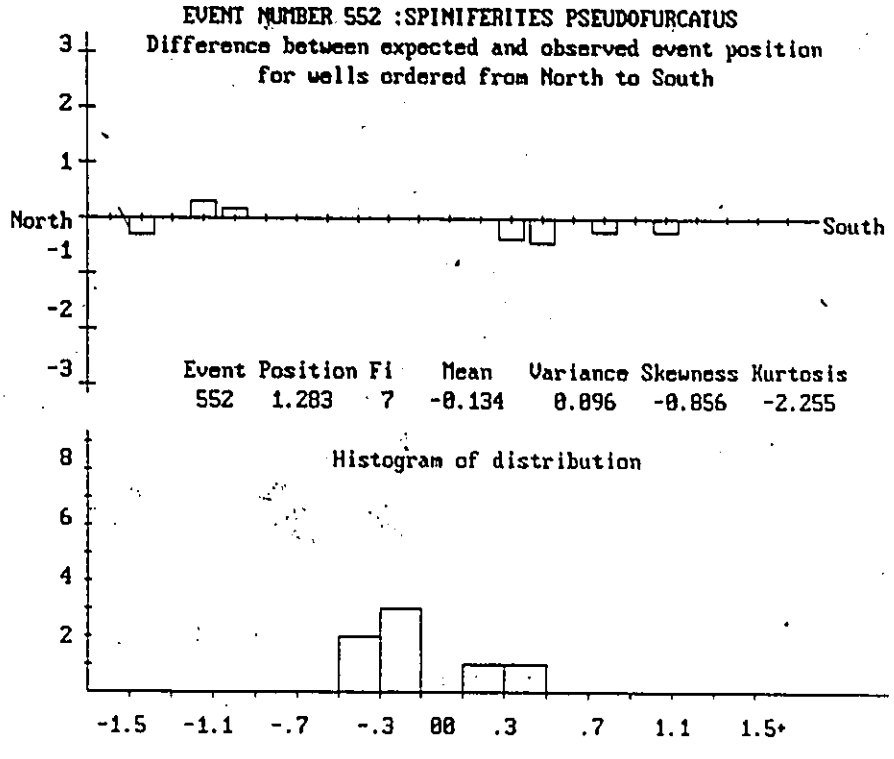
EVENT NUMBER 552 :SPINIFERITES PSEUDOFURCATUS
Difference between expected and observed event position
for wells ordered from North to South
3
2
1
North
-1
-2
-3
South
Event Position Fi Mean Variance Skewness Kurtosis
552 1.283 7 -0.134 0.096 -0.856 -2.255
Histogram of distribution
8
6
4
2
-1.5 -1.1 -.7 -.3 00 .3 .7 1.1 1.5+

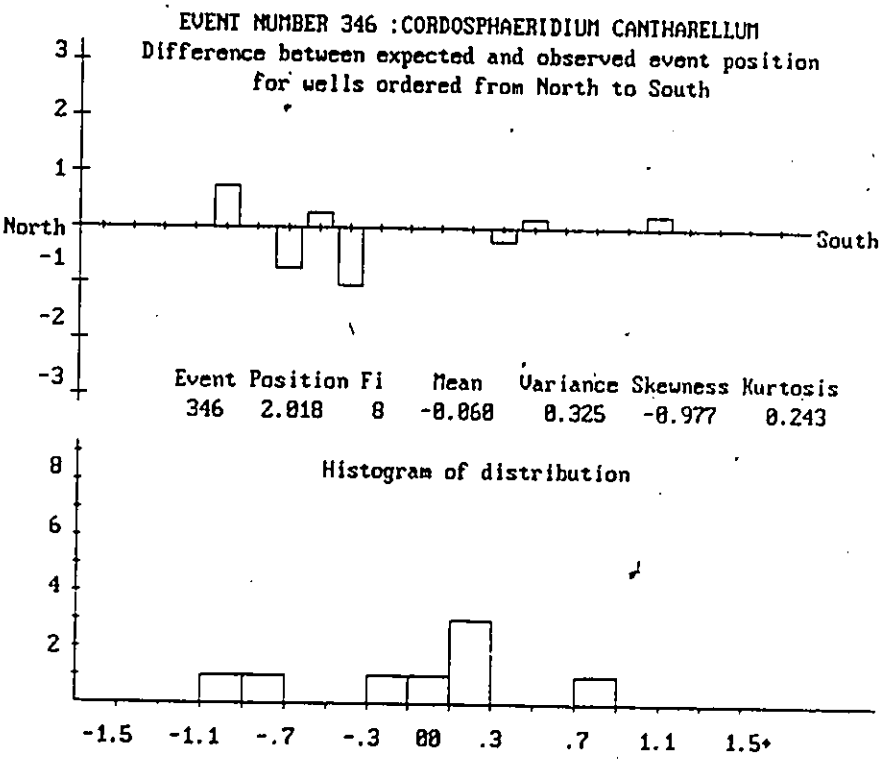
EVENT NUMBER 346 :CORDOSPHAERIDIUM CANTHARELLUM
Difference between expected and observed event position
for wells ordered from North to South
3
2
1
North
-1
-2
-3
South
Event Position Fi Mean Variance Skewness Kurtosis
346 2.018 8 -0.060 0.325 -0.977 0.243
Histogram of distribution
8
6
4
2
-1.5 -1.1 -.7 -.3 00 .3 .7 1.1 1.5+

EVENT NUMBER 15 :GLOBIGERINA PRAEBULLOIDES
Difference between expected and observed event position
for wells ordered from North to South

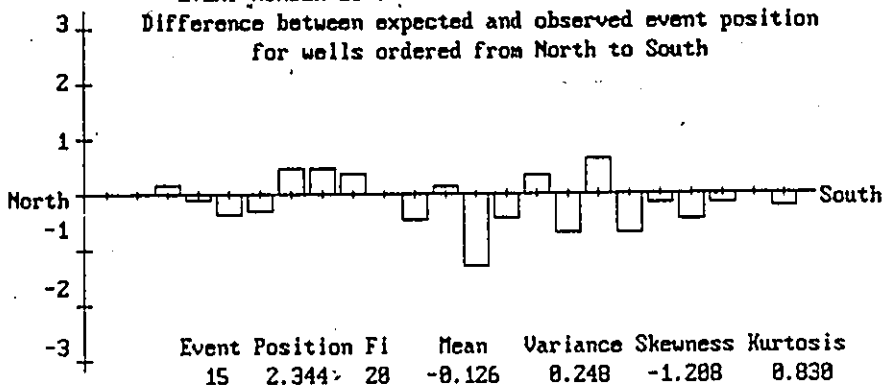

Event	Position	Fi	Mean	Variance	Skewness	Kurtosis
15	2.344	28	-0.126	0.248	-1.288	0.830

Histogram of distribution

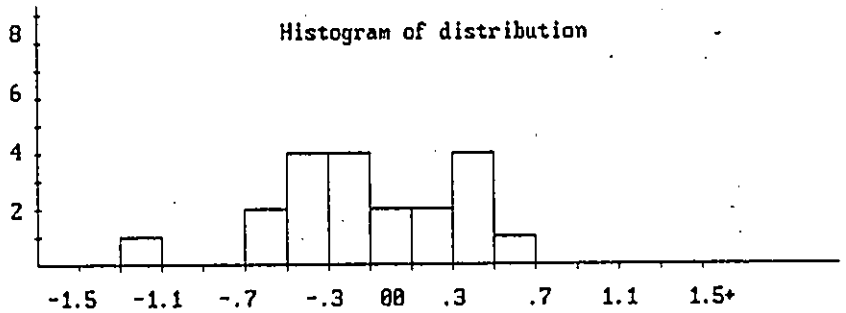

EVENT NUMBER 26 :UVIGERINA EX.GR.MIOZEA-NUTTALI
Difference between expected and observed event position
for wells ordered from North to South

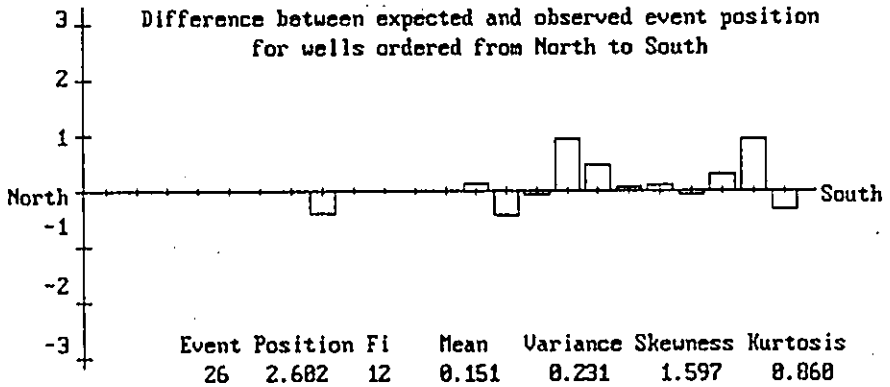

Event	Position	Fi	Mean	Variance	Skewness	Kurtosis
26	2.682	12	0.151	0.231	1.597	0.860

Histogram of distribution

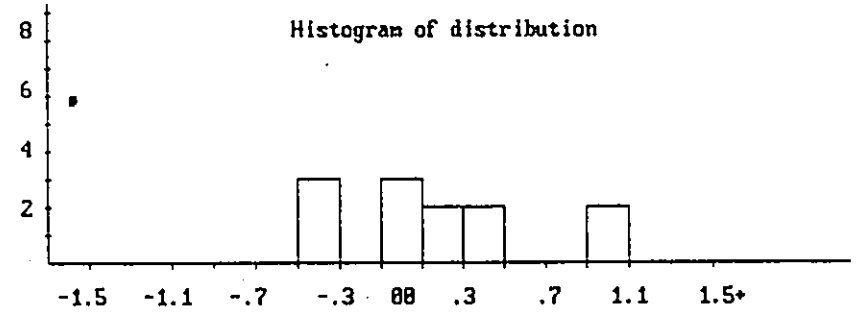

EVENT NUMBER 377 :DEFLANDREA PHOSPHORITICA

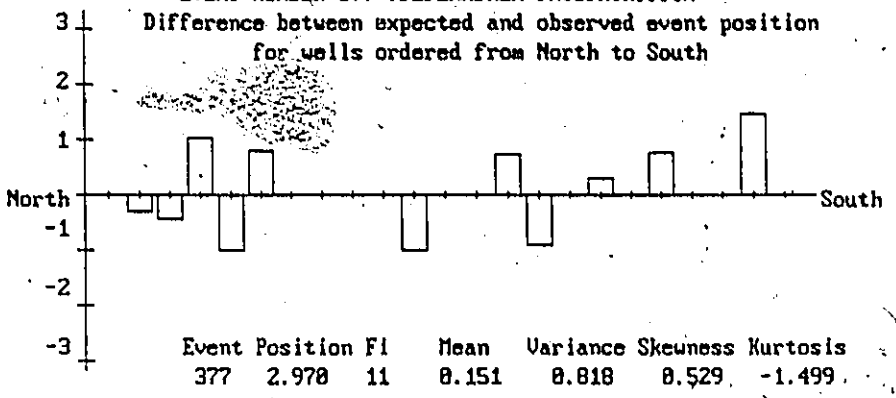

Event	Position	Fi	Mean	Variance	Skewness	Kurtosis
377	2.970	11	0.151	0.818	0.529	-1.499

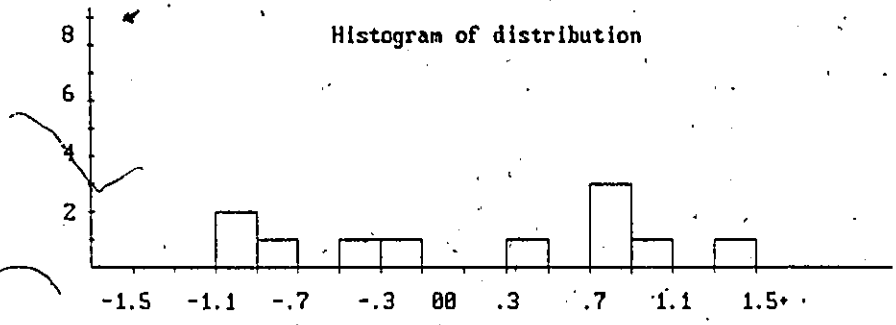

EVENT NUMBER 24 :TURRILINA ALSATICA

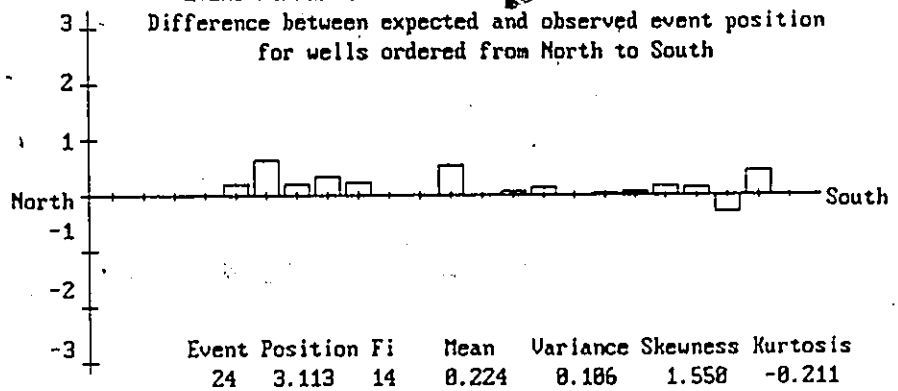

Event	Position	Fi	Mean	Variance	Skewness	Kurtosis
24	3.113	14	0.224	0.186	1.558	-0.211

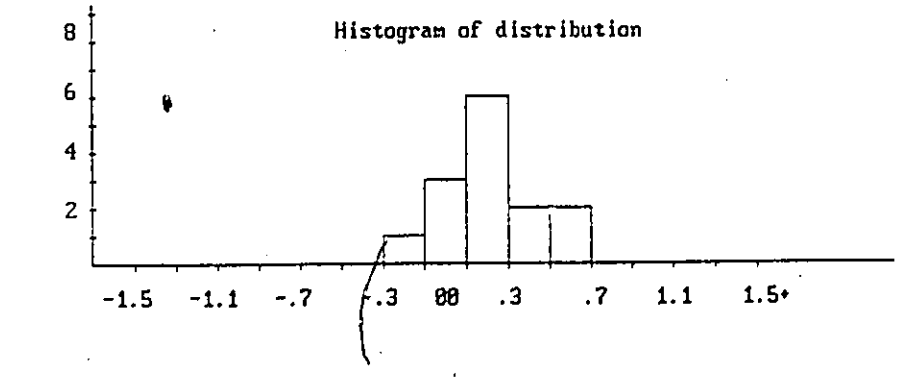

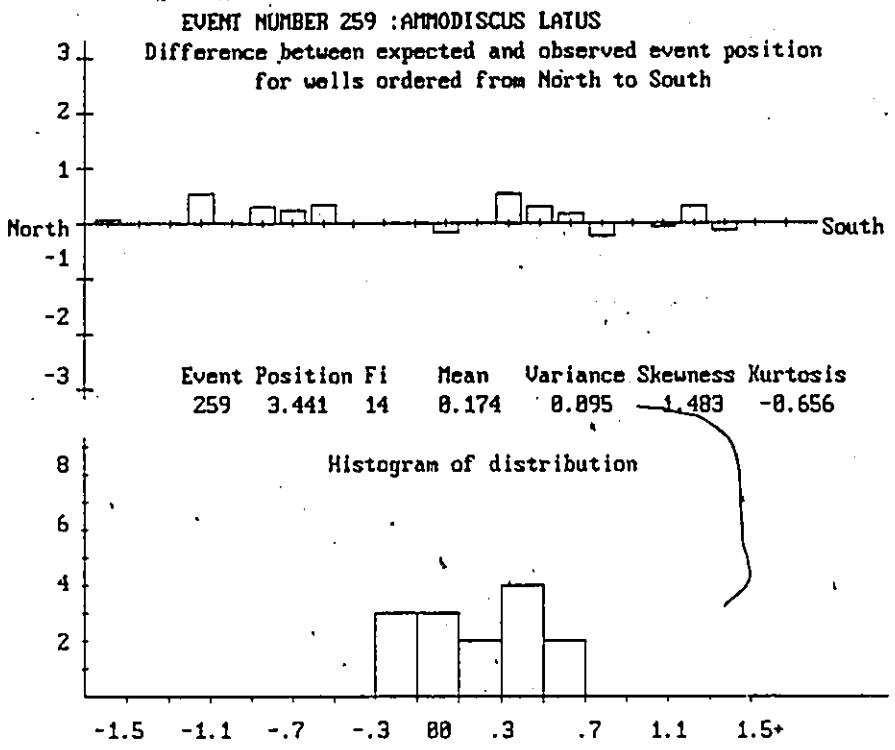
EVENT NUMBER 259 :AMMODISCUS LATUS
Difference between expected and observed event position
for wells ordered from North to South
3
2
1
North
-1
-2
-3
South
Event Position Fi Mean Variance Skewness Kurtosis
259 3.441 14 0.174 0.895 -1.483 -0.656
Histogram of distribution
8
6
4
2
-1.5 -1.1 -.7 -.3 00 .3 .7 1.1 1.5+

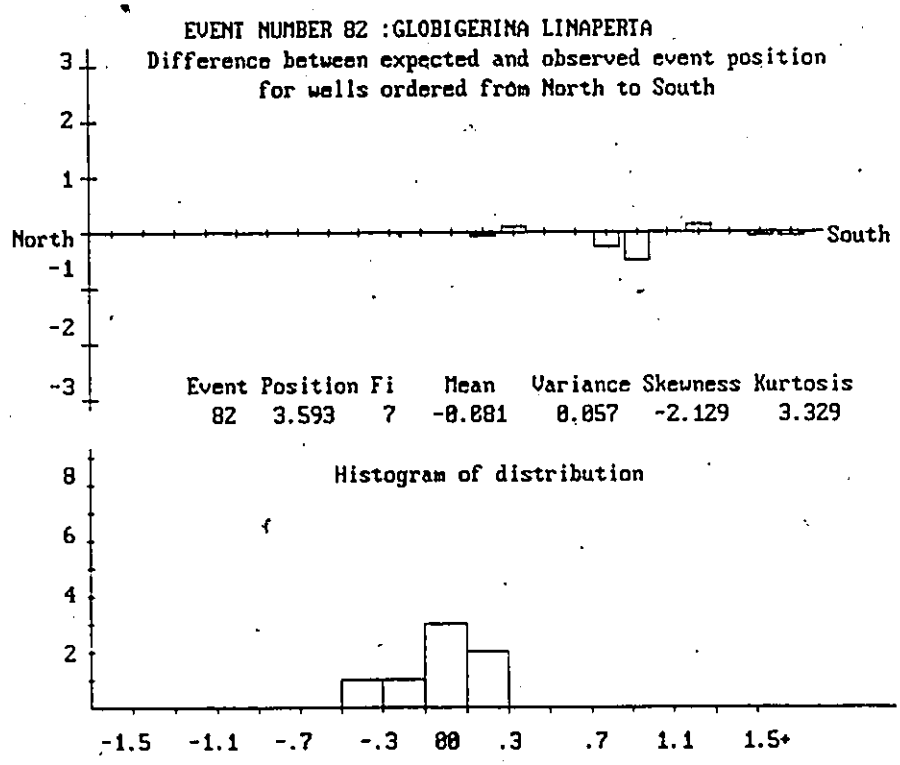
EVENT NUMBER 82 :GLOBIGERINA LINAPERTA
Difference between expected and observed event position
for wells ordered from North to South
3
2
1
North
-1
-2
-3
South
Event Position Fi Mean Variance Skewness Kurtosis
82 3.593 7 -0.881 0.857 -2.129 3.329
Histogram of distribution
8
6
4
2
-1.5 -1.1 -.7 -.3 00 .3 .7 1.1 1.5+

EVENT NUMBER 487 :CRIBROPERIDINIUM GIUSEPPEI

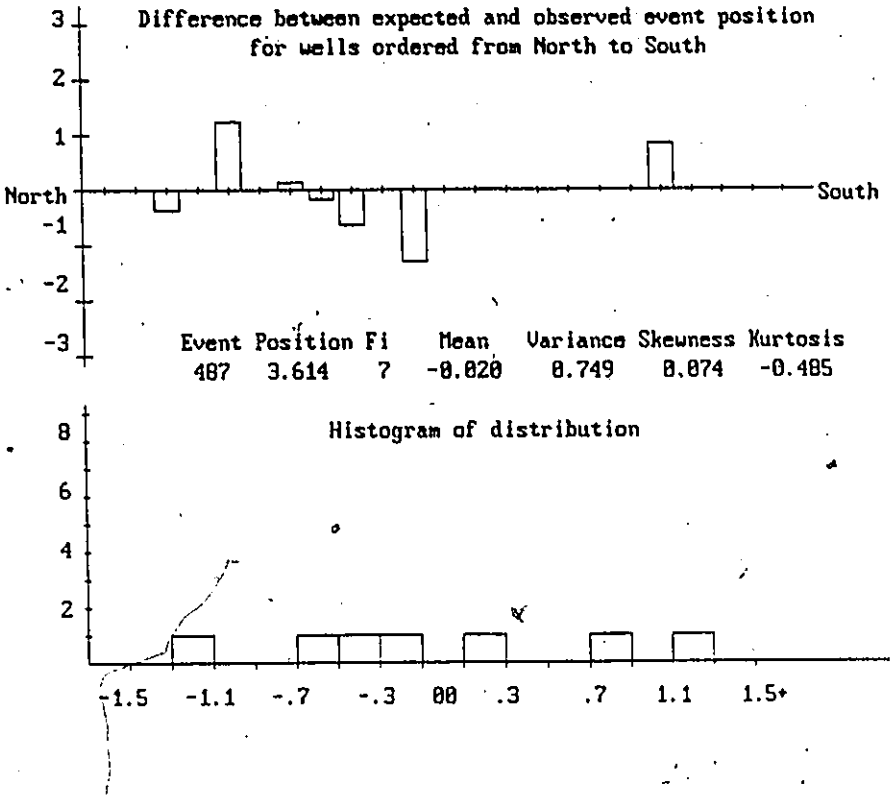

EVENT NUMBER 591 :WETZELIELLA ARTICULATA

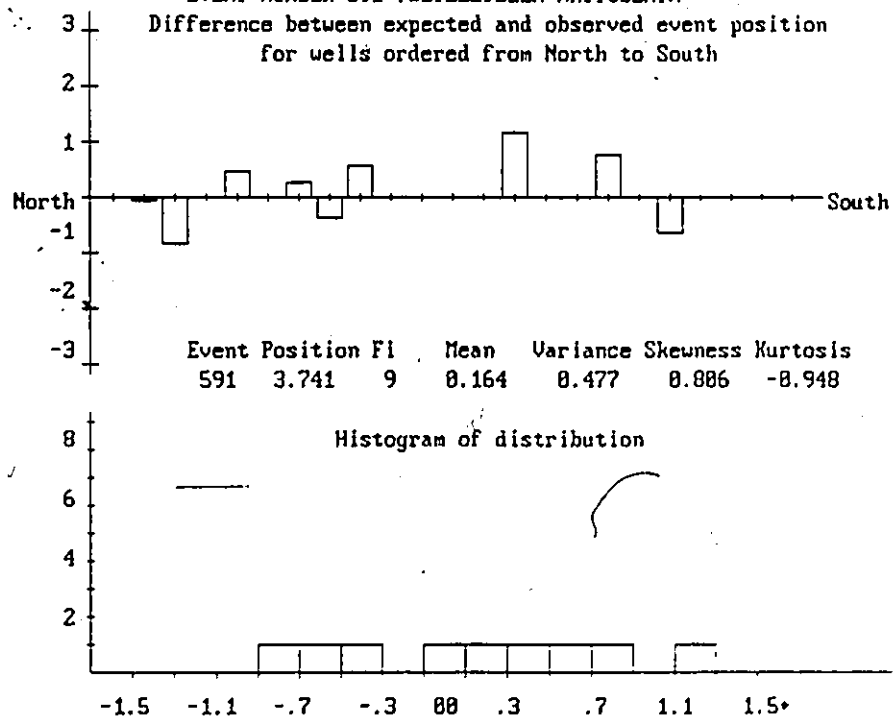

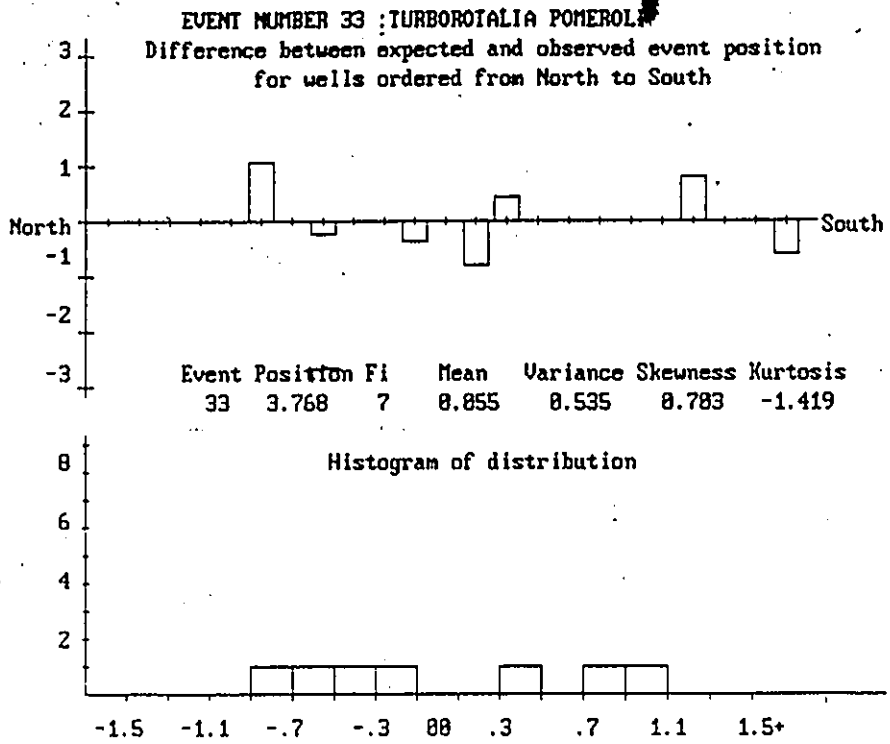
EVENT NUMBER 33 :TURBOROTALIA POMEROL
Difference between expected and observed event position
for wells ordered from North to South
3
2
1
North
-1
-2
-3
South
Event Position Fi Mean Variance Skewness Kurtosis
33 3.768 7 0.855 0.535 0.783 -1.419
Histogram of distribution
8
6
4
2
-1.5 -1.1 -.7 -.3 00 .3 .7 1.1 1.5+

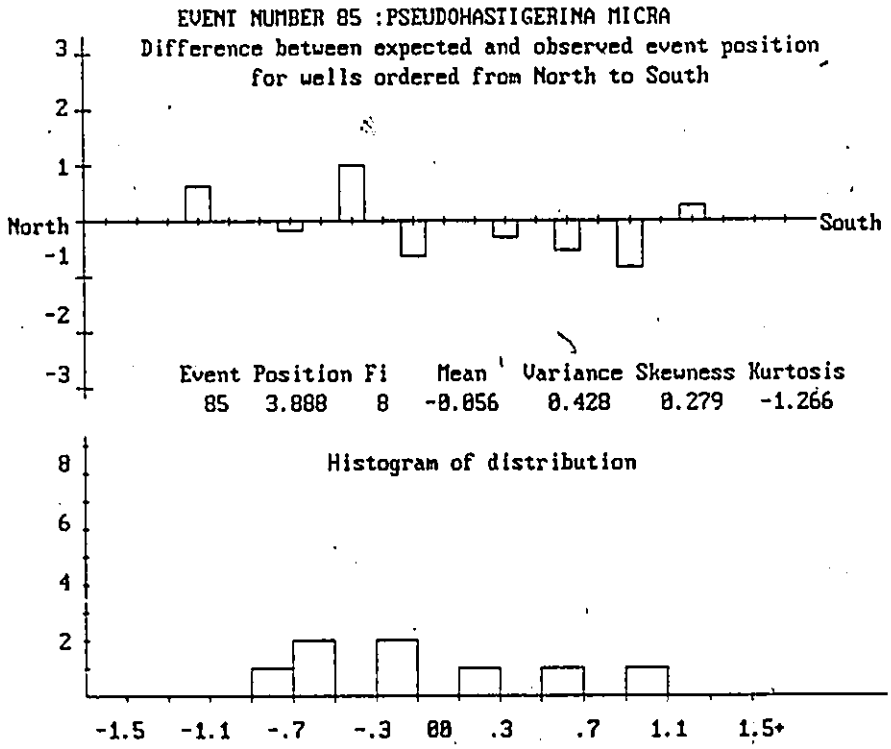
EVENT NUMBER 85 :PSEUDOHASTIGERINA MICRA
Difference between expected and observed event position
for wells ordered from North to South
3
2
1
North
-1
-2
-3
South
Event Position Fi Mean Variance Skewness Kurtosis
85 3.888 8 -0.056 0.428 0.279 -1.266
Histogram of distribution
8
6
4
2
-1.5 -1.1 -.7 -.3 00 .3 .7 1.1 1.5+

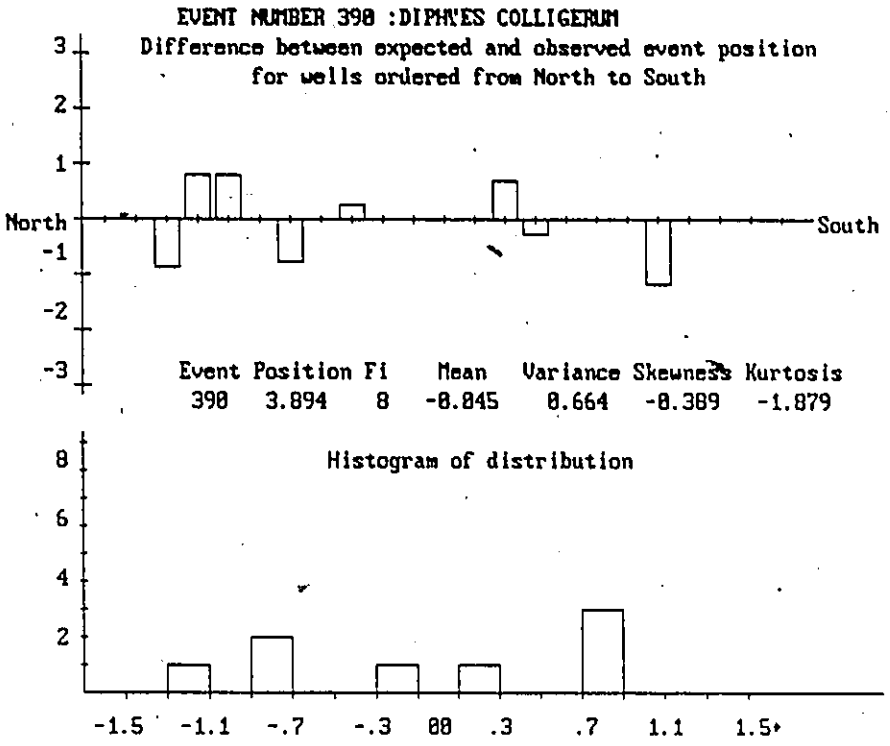
EVENT NUMBER 398 :DIPHYES COLLIGERUM
Difference between expected and observed event position
for wells ordered from North to South
3
2
1
North
-1
-2
-3
South
Event Position Fi Mean Variance Skewness Kurtosis
398 3.894 8 -0.845 0.664 -0.389 -1.879
Histogram of distribution
8
6
4
2
-1.5 -1.1 -.7 -.3 00 .3 .7 1.1 1.5+

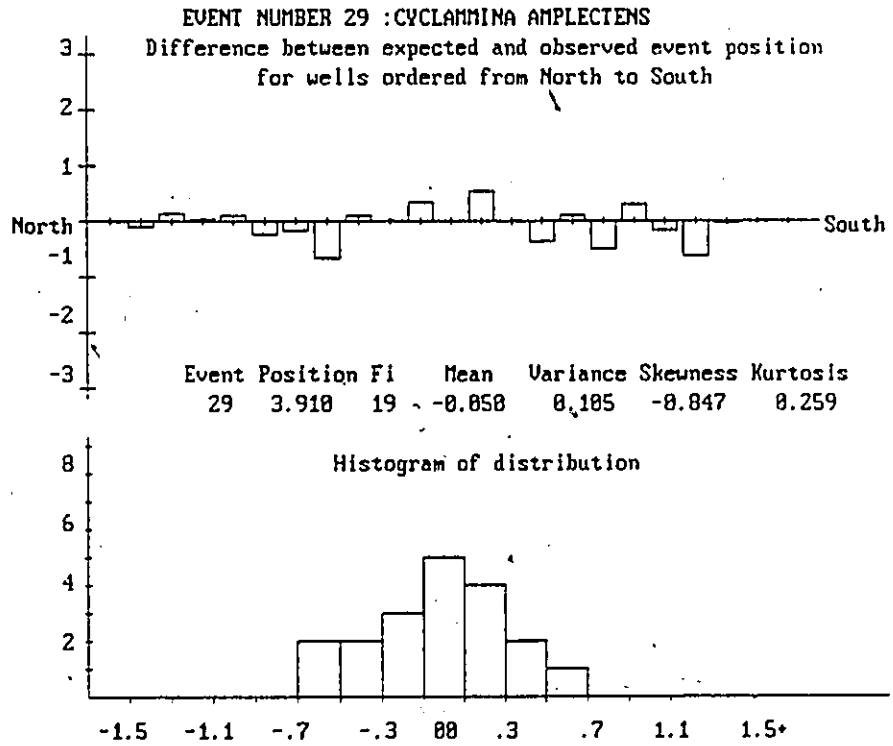
EVENT NUMBER 29 :CYCLAMMINA AMPLECTENS
Difference between expected and observed event position
for wells ordered from North to South
3
2
1
North
-1
-2
-3
South
Event Position Fi Mean Variance Skewness Kurtosis
29 3.910 19 -0.050 0.105 -0.847 0.259
Histogram of distribution
8
6
4
2
-1.5 -1.1 -.7 -.3 00 .3 .7 1.1 1.5+

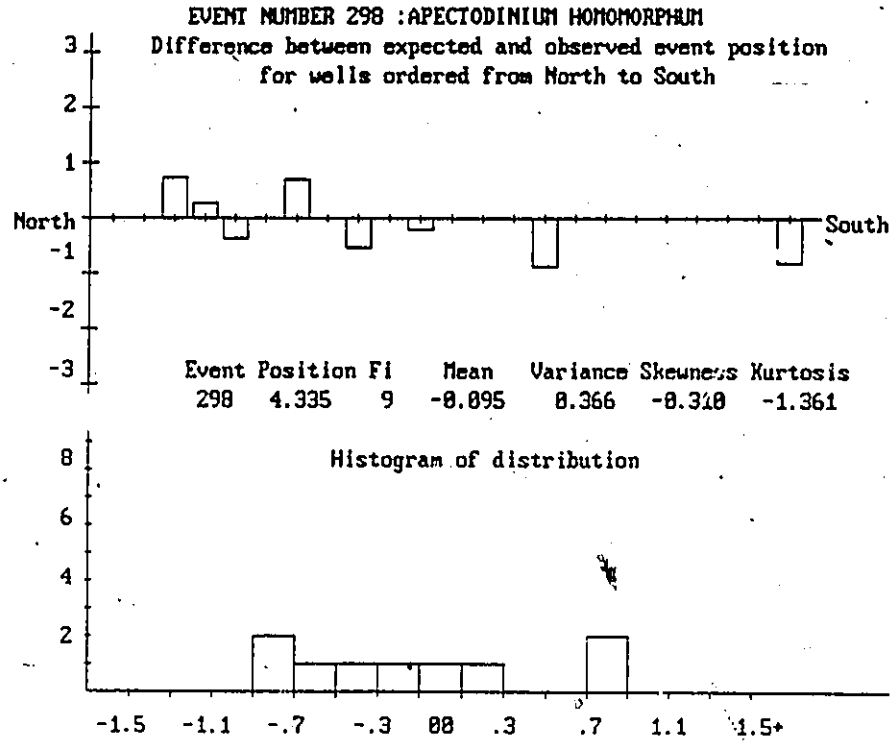
EVENT NUMBER 298 :APECTODINIUM HOMOMORPHUM
Difference between expected and observed event position
for wells ordered from North to South
3
2
1
North
-1
-2
-3
South
Event Position Fi Mean Variance Skewness Kurtosis
298 4.335 9 -0.095 0.366 -0.310 -1.361
Histogram of distribution
8
6
4
2
-1.5 -1.1 -.7 -.3 00 .3 .7 1.1 1.5+

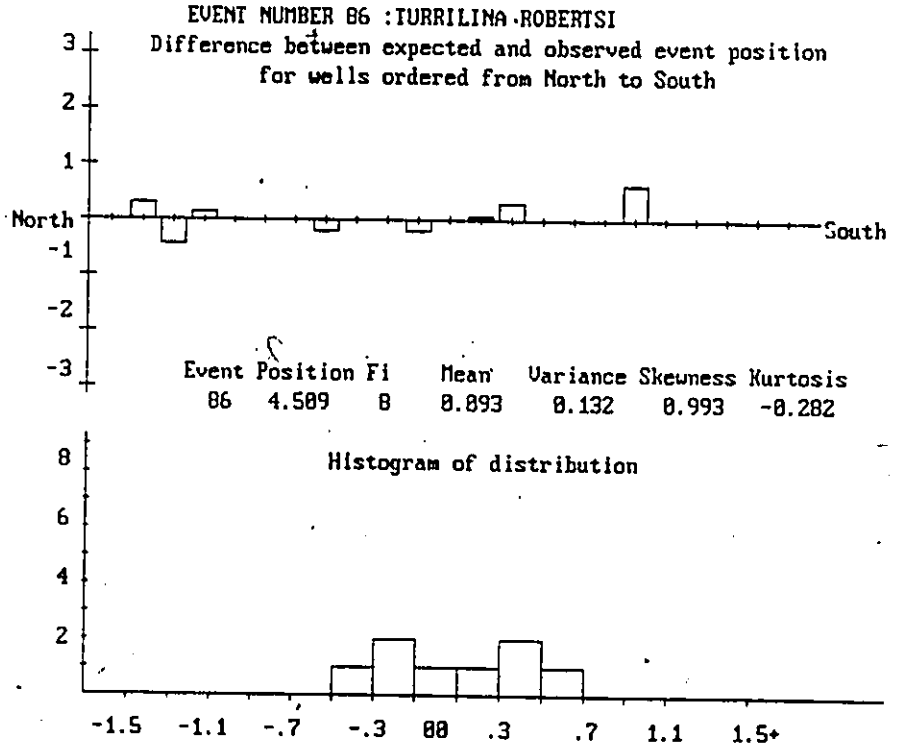
EVENT NUMBER 86 :TURRILINA ROBERTSI
Difference between expected and observed event position
for wells ordered from North to South
3
2
1
North
-1
-2
-3
South
Event Position Fi Mean Variance Skewness Kurtosis
86 4.509 8 0.893 0.132 0.993 -0.282
Histogram of distribution
8
6
4
2
-1.5 -1.1 -.7 -.3 00 .3 .7 1.1 1.5+

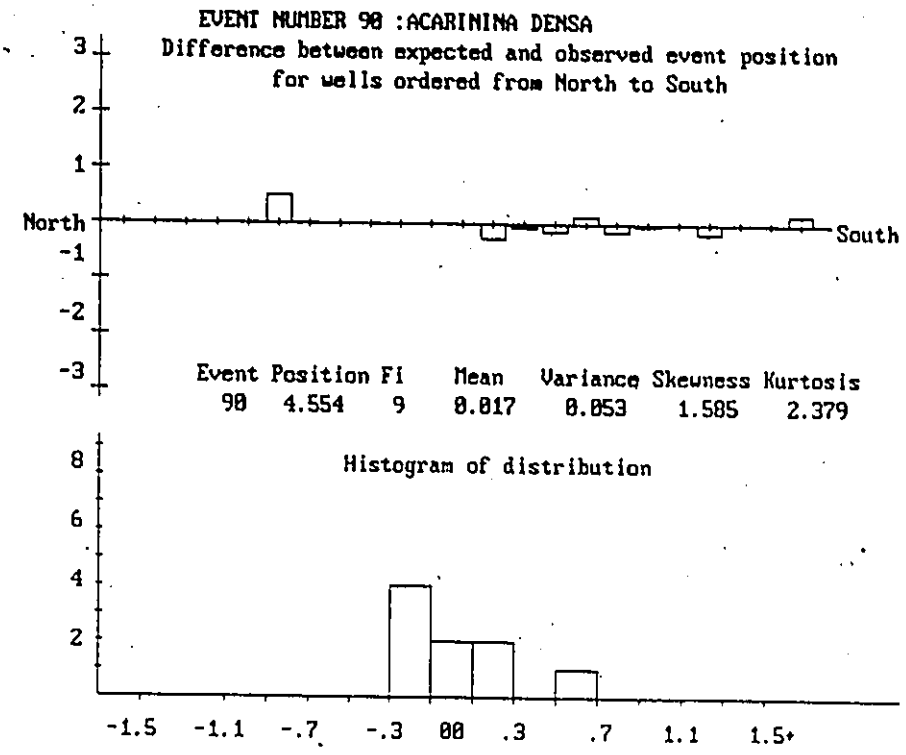
EVENT NUMBER 90 :ACARININA DENSA
Difference between expected and observed event position
for wells ordered from North to South
3
2
1
North
-1
-2
-3
South
Event Position Fi Mean Variance Skewness Kurtosis
90 4.554 9 0.017 0.053 1.585 2.379
Histogram of distribution
8
6
4
2
-1.5 -1.1 -.7 -.3 00 .3 .7 1.1 1.5+

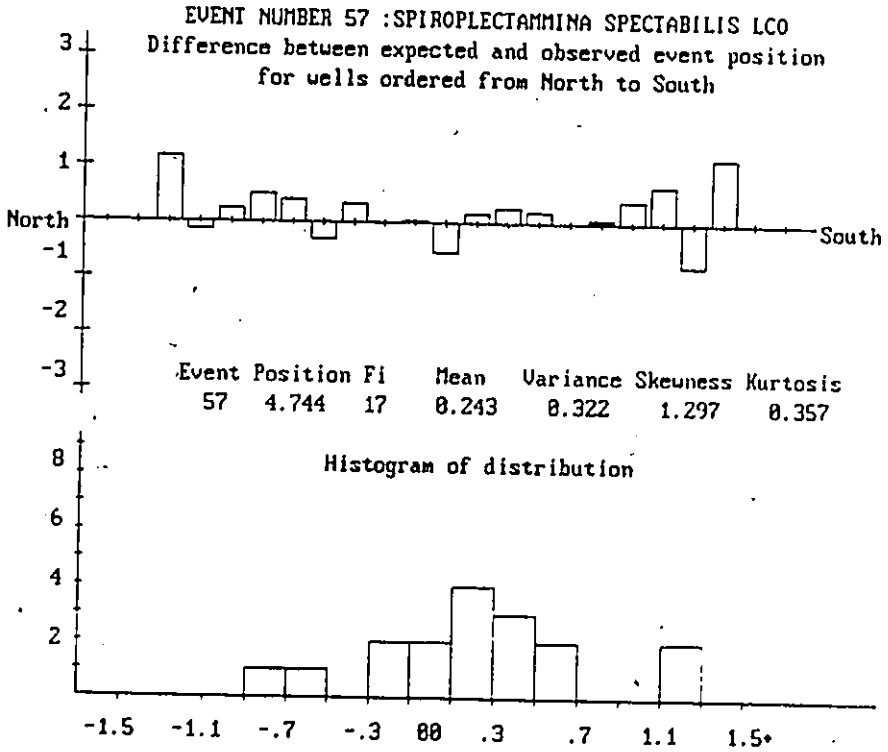
EVENT NUMBER 57 :SPIROPLECTAMMINA SPECTABILIS LCO
Difference between expected and observed event position
for wells ordered from North to South
3
2
1
North
-1
-2
-3
South
Event Position Fi Mean Variance Skewness Kurtosis
57 4.744 17 0.243 0.322 1.297 0.357
Histogram of distribution
8
6
4
2
-1.5 -1.1 -.7 -.3 00 .3 .7 1.1 1.5+

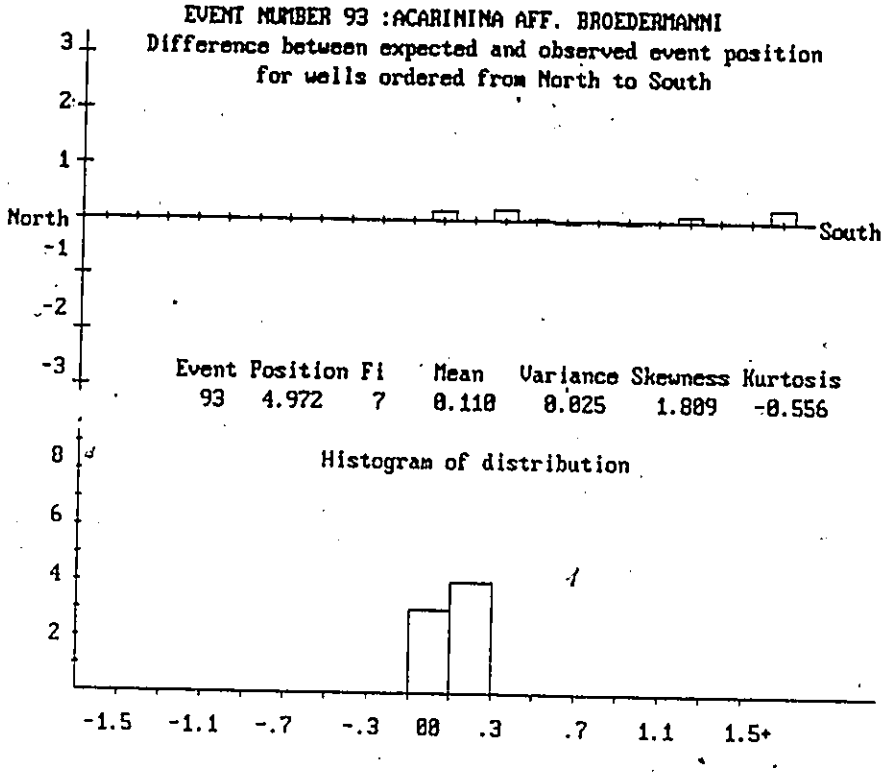
EVENT NUMBER 93 :ACARININA AFF. BROEDERMANNI
Difference between expected and observed event position
for wells ordered from North to South
3
2
1
North
-1
-2
-3
South
Event Position Fi Mean Variance Skewness Kurtosis
93 4.972 7 0.110 0.025 1.809 -0.556
Histogram of distribution
8
6
4
2
-1.5 -1.1 -.7 -.3 00 .3 .7 1.1 1.5+

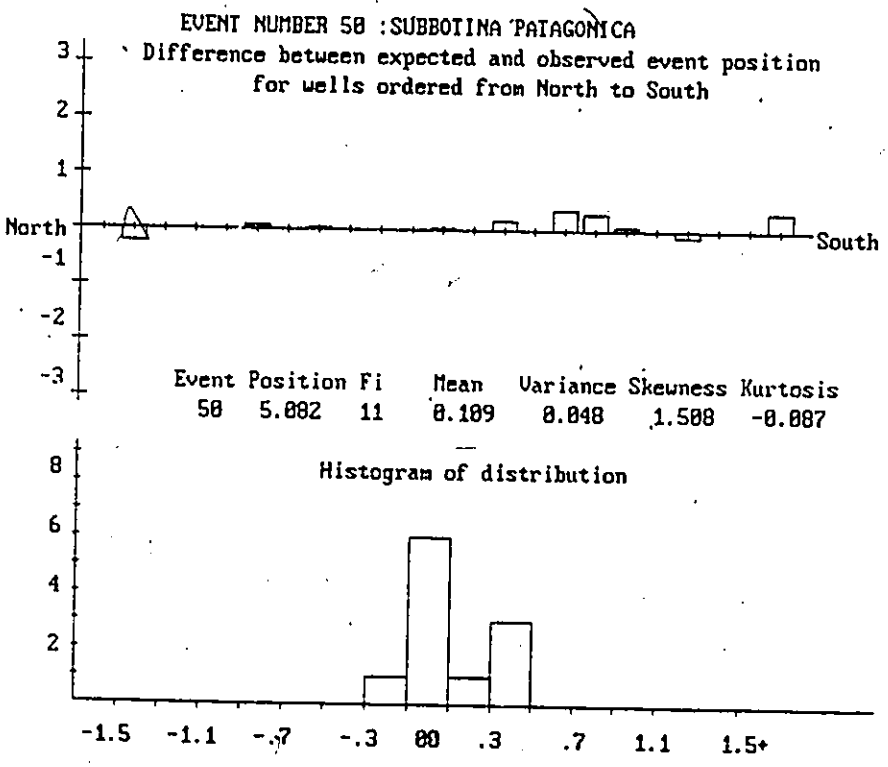
EVENT NUMBER 58 :SUBBOTINA PATAGONICA
Difference between expected and observed event position
for wells ordered from North to South
3
2
1
North
-1
-2
-3
South
Event Position Fi Mean Variance Skewness Kurtosis
58 5.082 11 0.109 0.048 1.508 -0.087
Histogram of distribution
8
6
4
2
-1.5 -1.1 -.7 -.3 00 .3 .7 1.1 1.5+

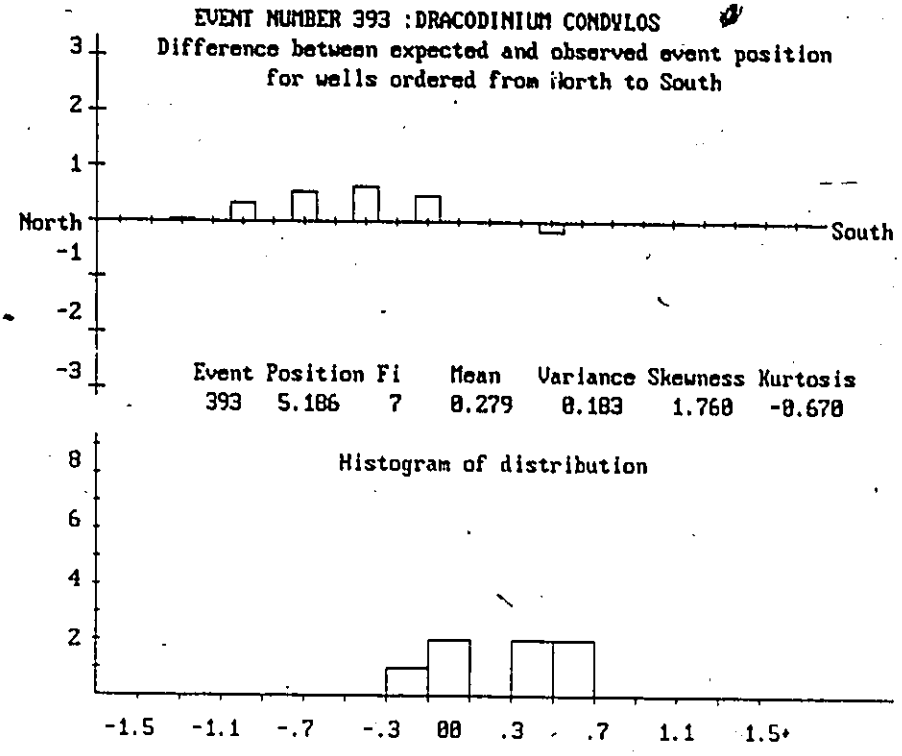
EVENT NUMBER 393 :DRACODINIUM CONDYLOS
Difference between expected and observed event position
for wells ordered from North to South
3
2
1
North
-1
-2
-3
South
Event Position Fi Mean Variance Skewness Kurtosis
393 5.186 7 0.279 0.183 1.760 -0.670
Histogram of distribution
8
6
4
2
-1.5 -1.1 -.7 -.3 00 .3 .7 1.1 1.5+

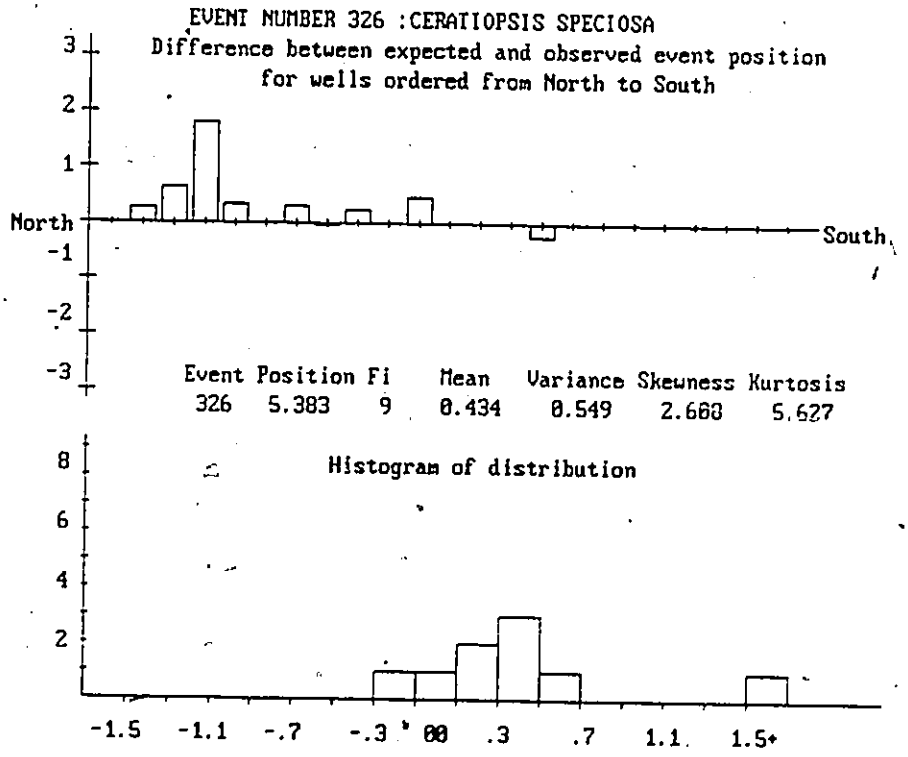
EVENT NUMBER 326 :CERATIOPSIS SPECIOSA
Difference between expected and observed event position
for wells ordered from North to South
3
2
1
North
-1
-2
-3
South
Event Position Fi Mean Variance Skewness Kurtosis
326 5.383 9 0.434 0.549 2.668 5.627
Histogram of distribution
8
6
4
2
-1.5 -1.1 -.7 -.3 00 .3 .7 1.1 1.5+

EVENT NUMBER 56 :GLOMOSPIRA CORONA

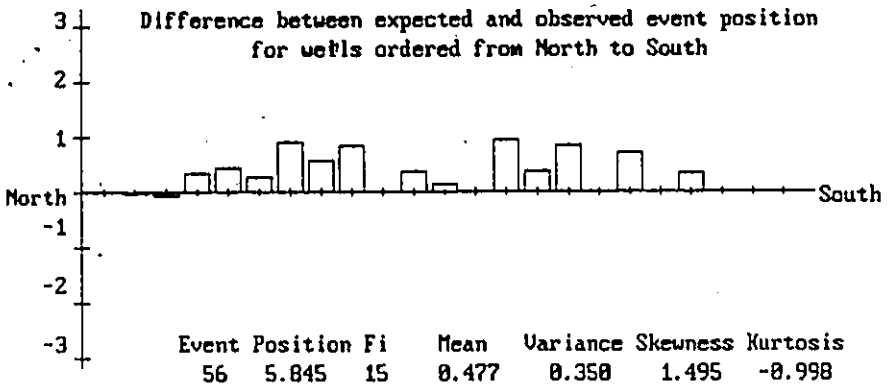

Event	Position	Fi	Mean	Variance	Skewness	Kurtosis
56	5.845	15	0.477	0.350	1.495	-0.998

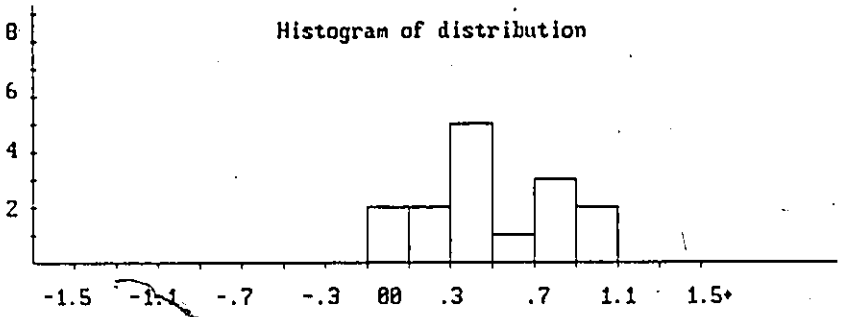

EVENT NUMBER 512 :PALAEOPERIDINIUM PYROPHORUM

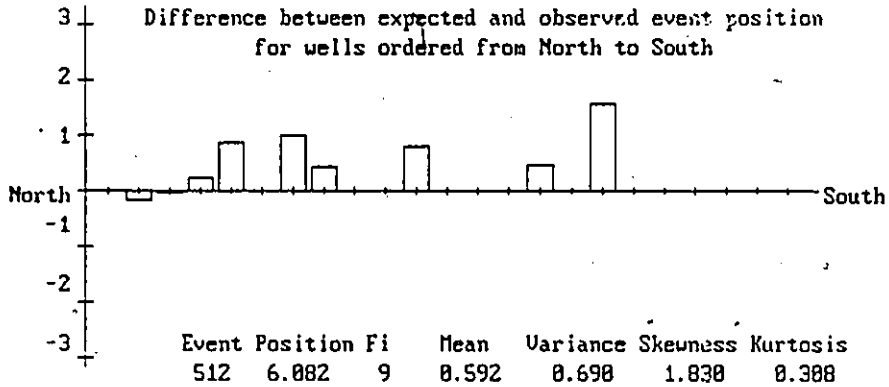

Event	Position	Fi	Mean	Variance	Skewness	Kurtosis
512	6.082	9	0.592	0.690	1.830	0.388

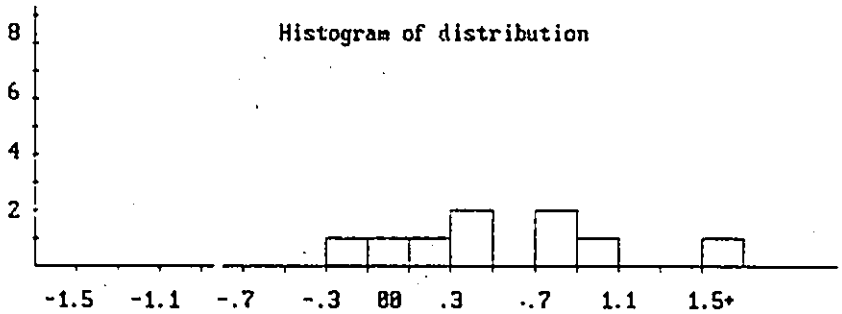

EVENT NUMBER 55 :GAVELINELLA BECCARIIFORMIS
Difference between expected and observed event position
for wells ordered from North to South

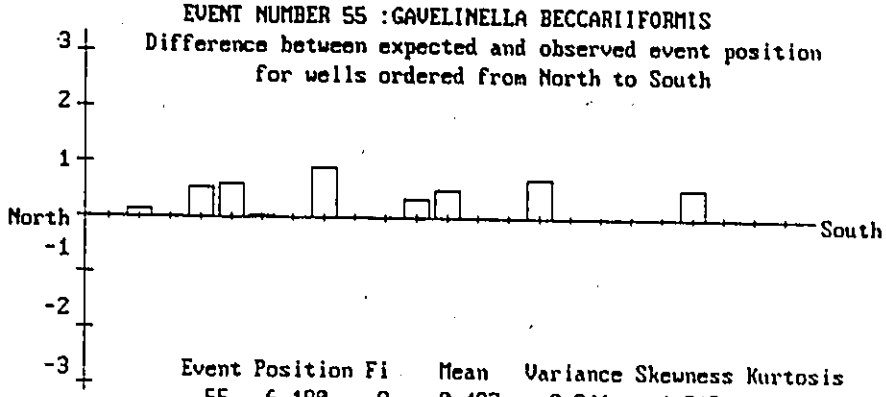

Event	Position	Fi	Mean	Variance	Skewness	Kurtosis
55	6.190	9	0.487	0.341	1.515	-1.394

Histogram of distribution

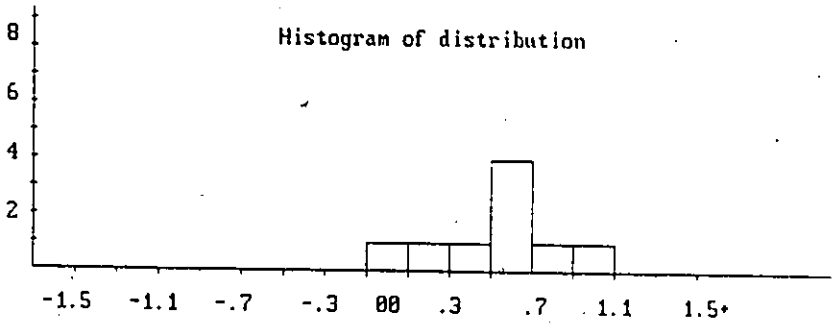

EVENT NUMBER 283 :PINUS
Difference between expected and observed event position
for wells ordered from North to South

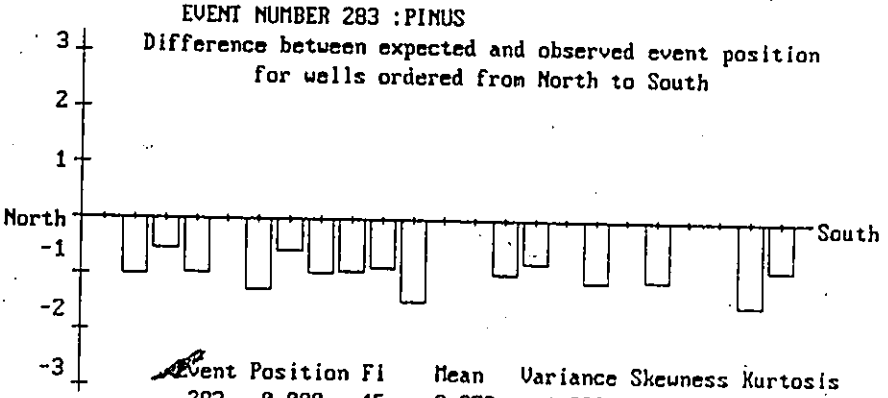

Event	Position	Fi	Mean	Variance	Skewness	Kurtosis
283	0.000	15	-0.970	1.086	-1.233	-1.911

Histogram of distribution

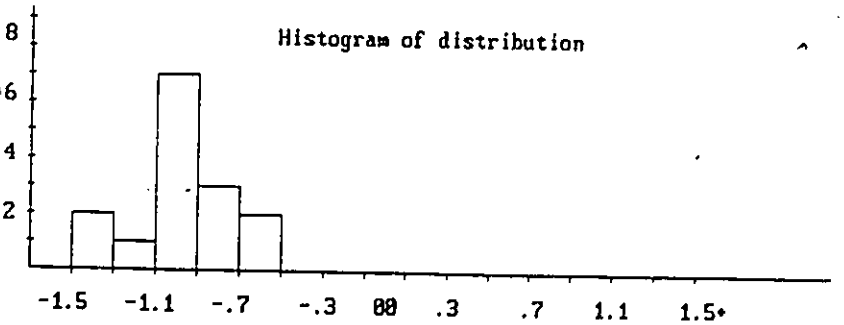

EVENT NUMBER 77 :ELPHIDIUM SPP.
Difference between expected and observed event position
for wells ordered from North to South

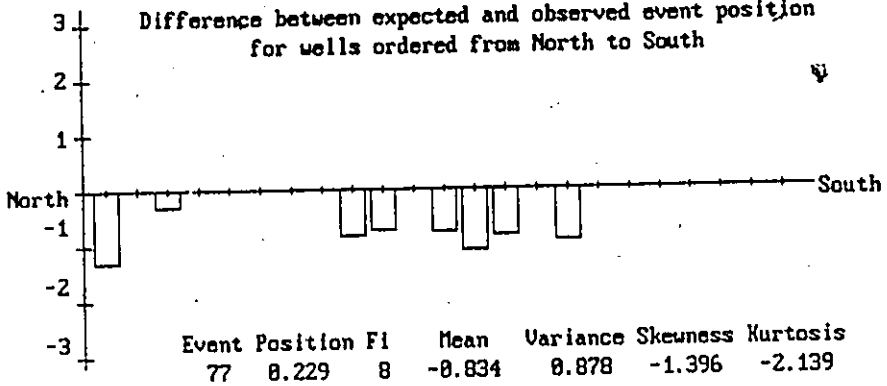

Event	Position	Fi	Mean	Variance	Skewness	Kurtosis
77	0.229	8	-0.834	0.878	-1.396	-2.139

Histogram of distribution

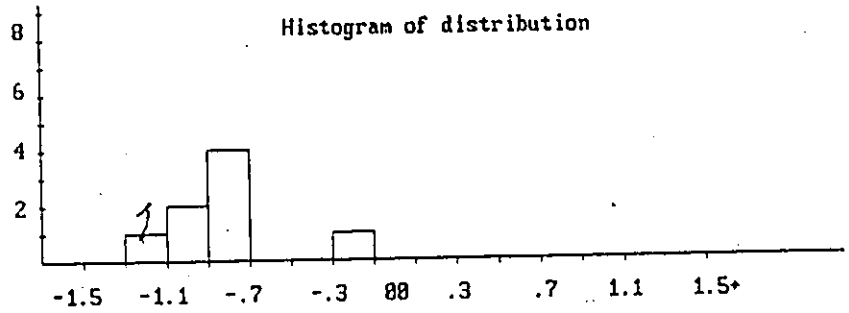

EVENT NUMBER 293 :TSUGAEPOLLENITES INGNICULUS
Difference between expected and observed event position
for wells ordered from North to South

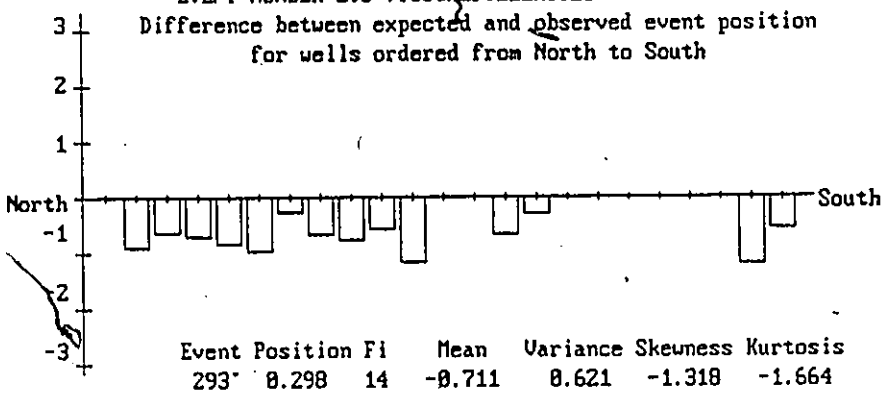

Event	Position	Fi	Mean	Variance	Skewness	Kurtosis
293	0.298	14	-0.711	0.621	-1.318	-1.664

Histogram of distribution

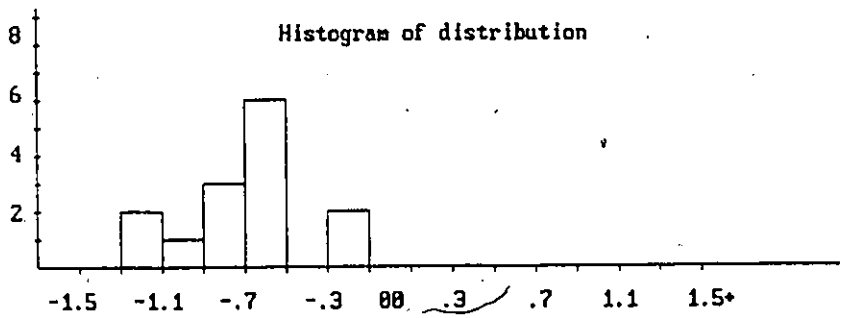

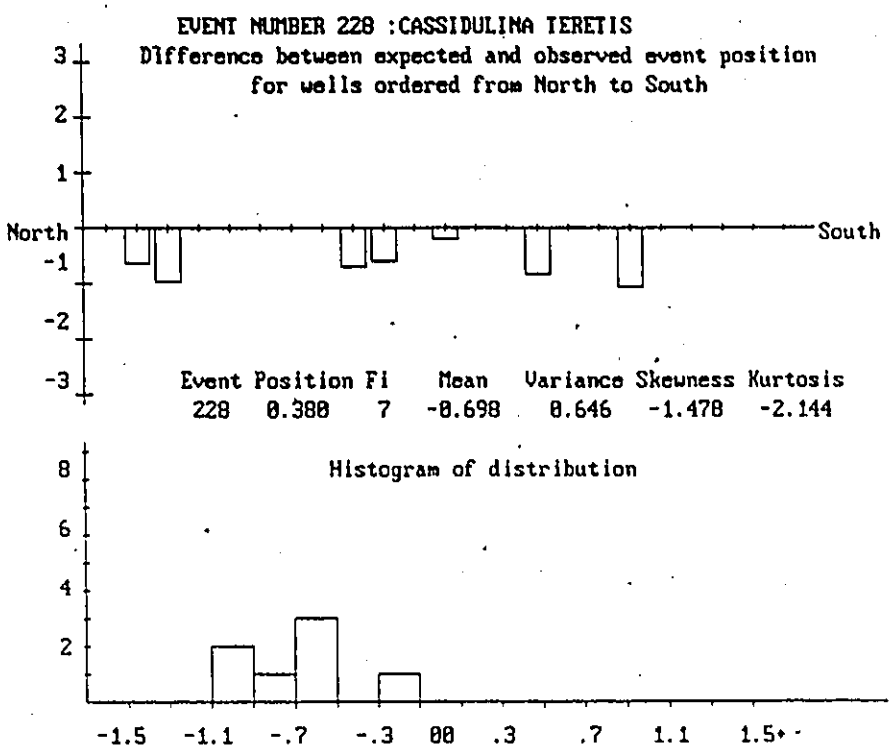
EVENT NUMBER 228 :CASSIDULINA TERETIS
Difference between expected and observed event position
for wells ordered from North to South
3
2
1
North
-1
-2
-3
South
Event Position Fi Mean Variance Skewness Kurtosis
228 0.388 7 -0.698 0.646 -1.478 -2.144
Histogram of distribution
8
6
4
2
-1.5 -1.1 -.7 -.3 00 .3 .7 1.1 1.5+

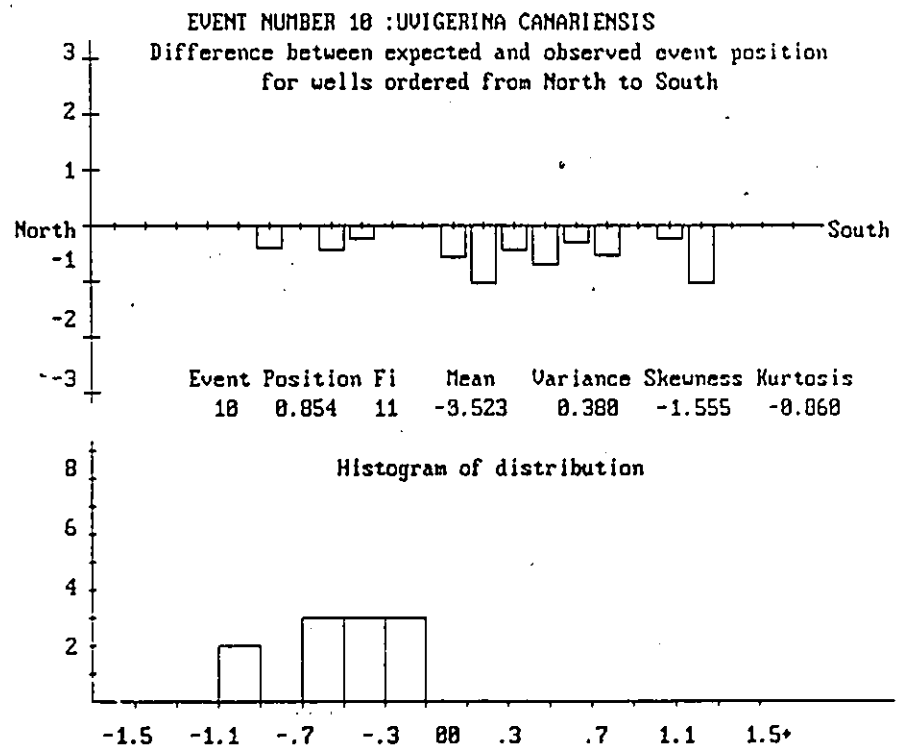
EVENT NUMBER 10 :UVIGERINA CANARIENSIS
Difference between expected and observed event position
for wells ordered from North to South
3
2
1
North
-1
-2
-3
South
Event Position Fi Mean Variance Skewness Kurtosis
10 0.854 11 -3.523 0.388 -1.555 -0.060
Histogram of distribution
8
6
4
2
-1.5 -1.1 -.7 -.3 00 .3 .7 1.1 1.5+

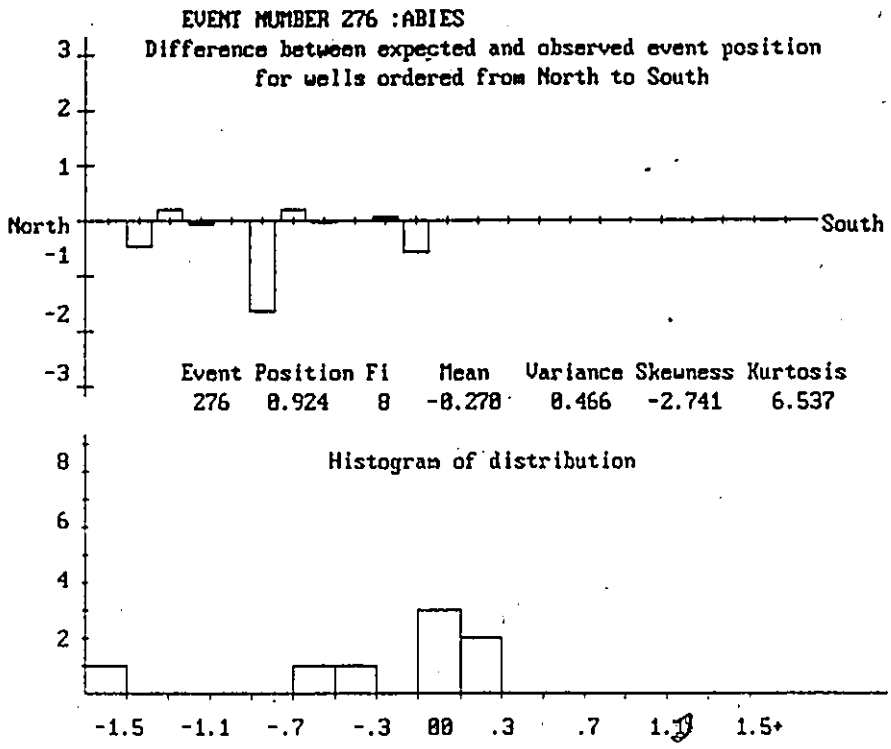
EVENT NUMBER 276 :ABIES
Difference between expected and observed event position
for wells ordered from North to South
3
2
1
North
-1
-2
-3
South
Event Position Fi Mean Variance Skewness Kurtosis
276 0.924 8 -0.278 0.466 -2.741 6.537
Histogram of distribution
8
6
4
2
-1.5 -1.1 -.7 -.3 00 .3 .7 1.1 1.5+

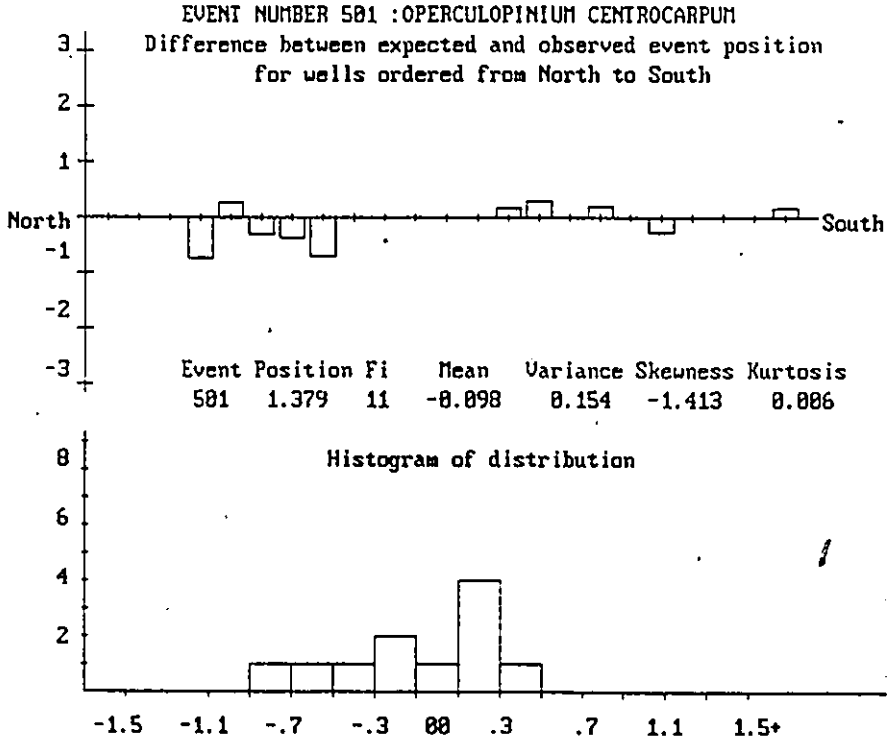
EVENT NUMBER 501 :OPERCULOPINIUM CENTROCARPUM
Difference between expected and observed event position
for wells ordered from North to South
3
2
1
North
-1
-2
-3
South
Event Position Fi Mean Variance Skewness Kurtosis
501 1.379 11 -0.098 0.154 -1.413 0.006
Histogram of distribution
8
6
4
2
-1.5 -1.1 -.7 -.3 00 .3 .7 1.1 1.5+

EVENT NUMBER 282 :OSMUNDACIDITES DA
Difference between expected and observed event position
for wells ordered from North to South

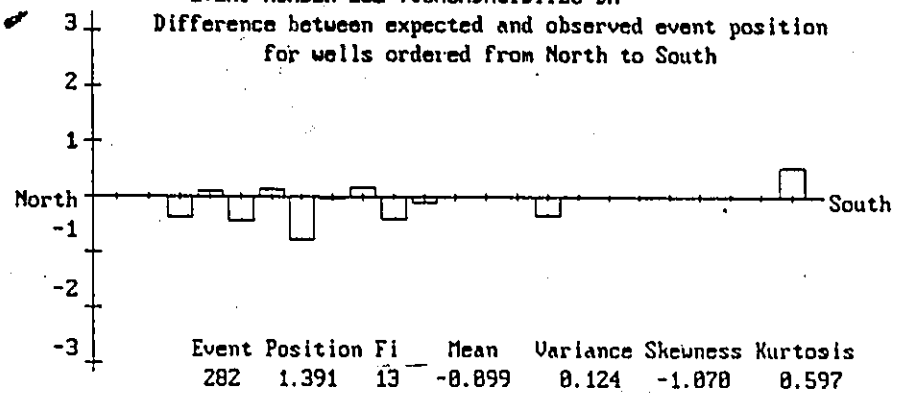

Event	Position	Fi	Mean	Variance	Skewness	Kurtosis
282	1.391	13	-0.899	0.124	-1.878	0.597

Histogram of distribution

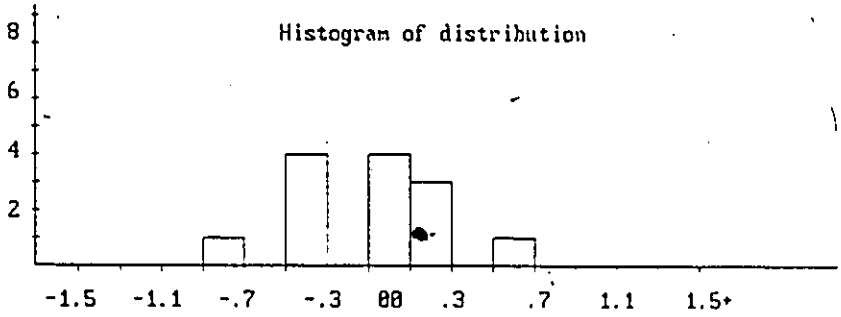

EVENT NUMBER 316 :XENIKOON DA
Difference between expected and observed event position
for wells ordered from North to South

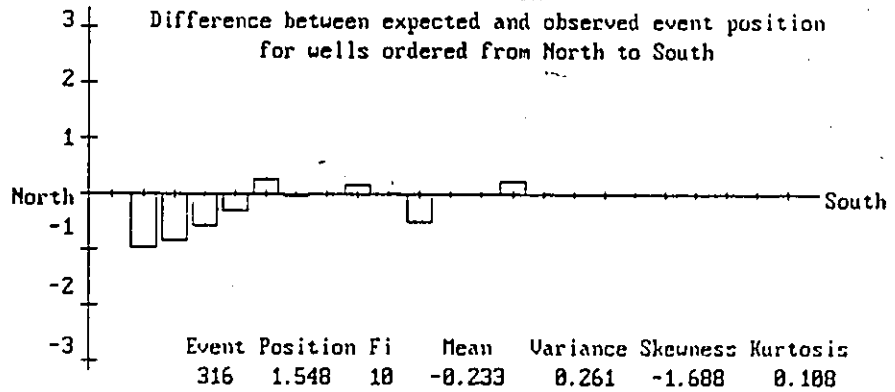

Event	Position	Fi	Mean	Variance	Skewness	Kurtosis
316	1.548	10	-0.233	0.261	-1.688	0.108

Histogram of distribution

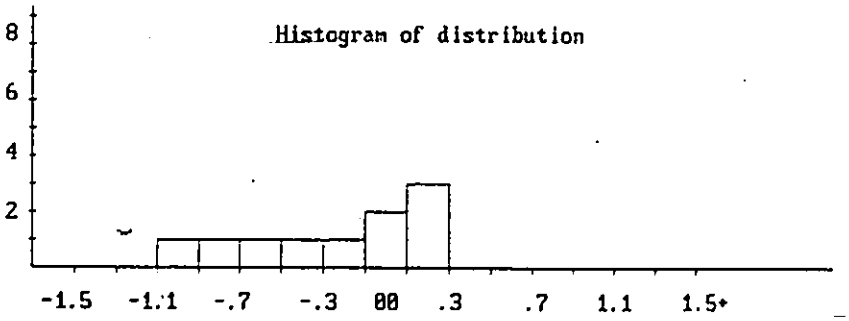

EVENT NUMBER 433 :HYSTRICHOKOLPOMA RIGAUDIAE

Difference between expected and observed event position
for wells ordered from North to South

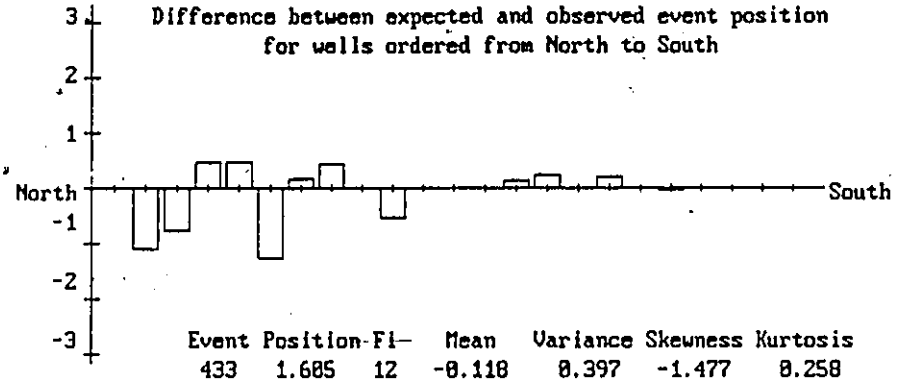

Event	Position	Fi	Mean	Variance	Skewness	Kurtosis
433	1.685	12	-0.118	0.397	-1.477	0.258

Histogram of distribution

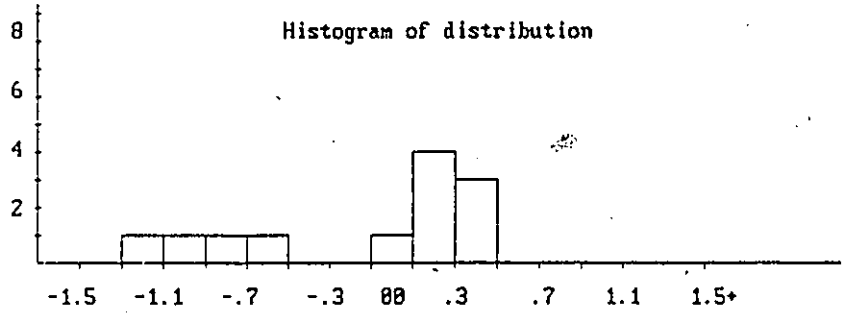

EVENT NUMBER 16 :CERATOBULIMINA CONTRARIA

Difference between expected and observed event position
for wells ordered from North to South

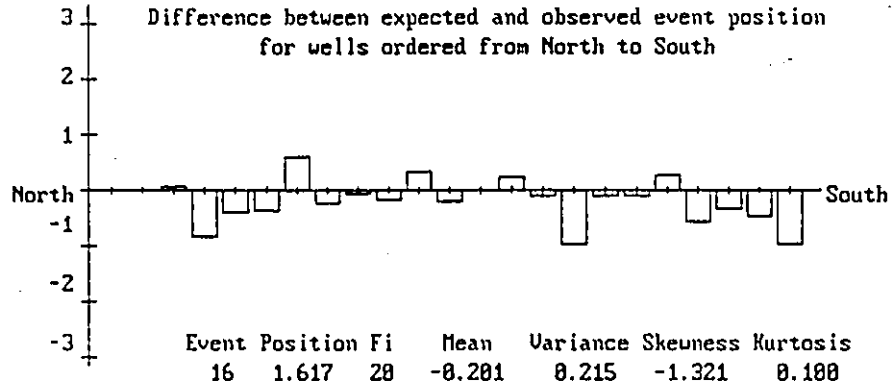

Event	Position	Fi	Mean	Variance	Skewness	Kurtosis
16	1.617	20	-0.201	0.215	-1.321	0.100

Histogram of distribution

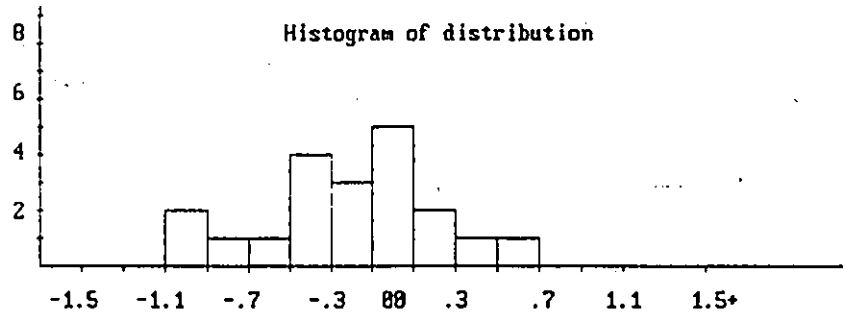

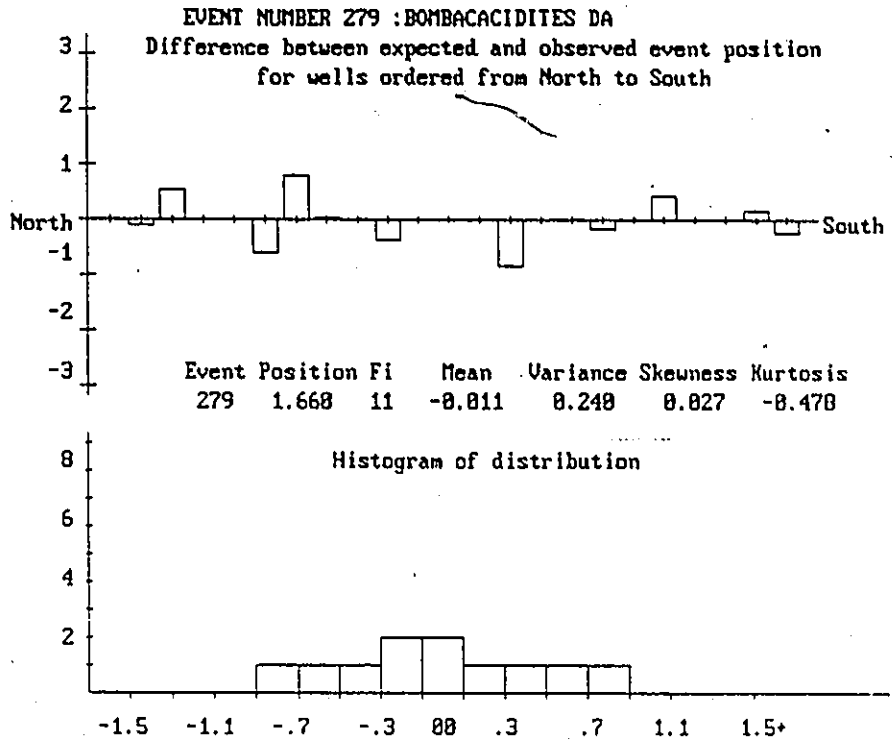
EVENT NUMBER 279 :BOMBACACIDITES DA
Difference between expected and observed event position
for wells ordered from North to South
3
2
1
North
-1
-2
-3
South
Event Position Fi Mean Variance Skewness Kurtosis
279 1.668 11 -0.011 0.248 0.027 -0.470
Histogram of distribution
8
6
4
2
-1.5 -1.1 -.7 -.3 00 .3 .7 1.1 1.5+

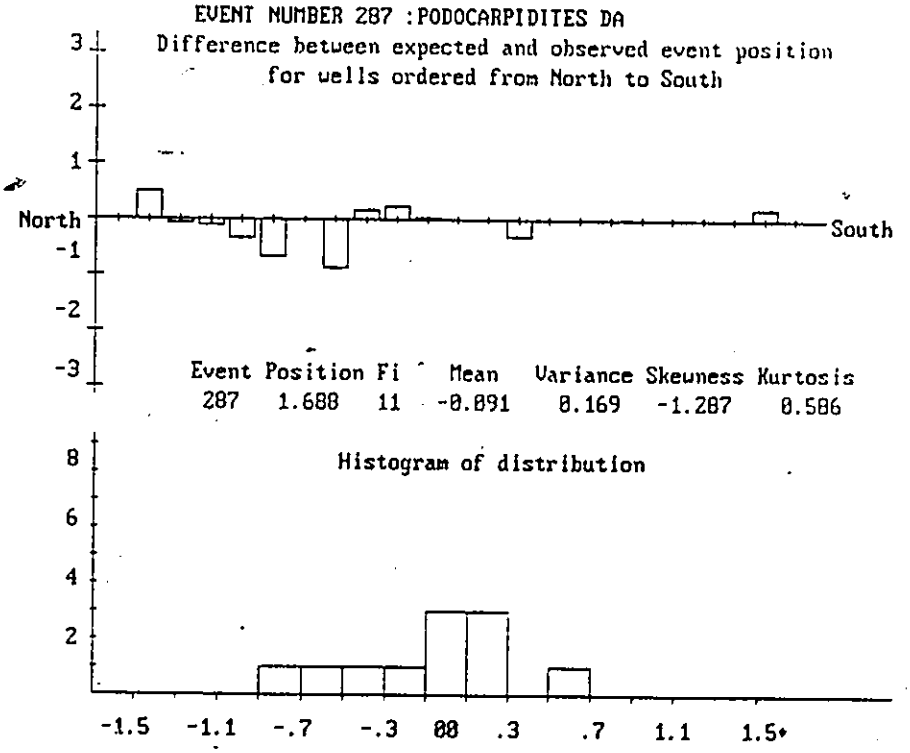
EVENT NUMBER 287 :PODOCARPIDITES DA
Difference between expected and observed event position
for wells ordered from North to South
3
2
1
North
-1
-2
-3
South
Event Position Fi Mean Variance Skewness Kurtosis
287 1.688 11 -0.091 0.169 -1.287 0.586
Histogram of distribution
8
6
4
2
-1.5 -1.1 -.7 -.3 00 .3 .7 1.1 1.5+

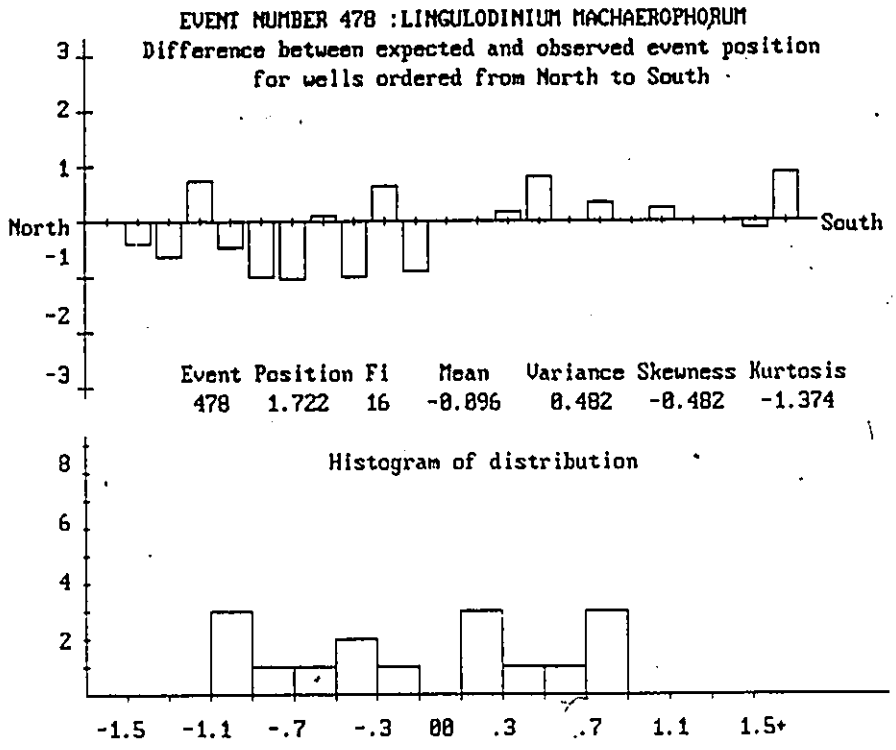
EVENT NUMBER 478 :LINGULODINIUM MACHAEROPHORUM
Difference between expected and observed event position
for wells ordered from North to South
3
2
1
North
-1
-2
-3
South
Event Position Fi Mean Variance Skewness Kurtosis
478 1.722 16 -0.896 0.482 -0.482 -1.374
Histogram of distribution
8
6
4
2
-1.5 -1.1 -.7 -.3 00 .3 .7 1.1 1.5+

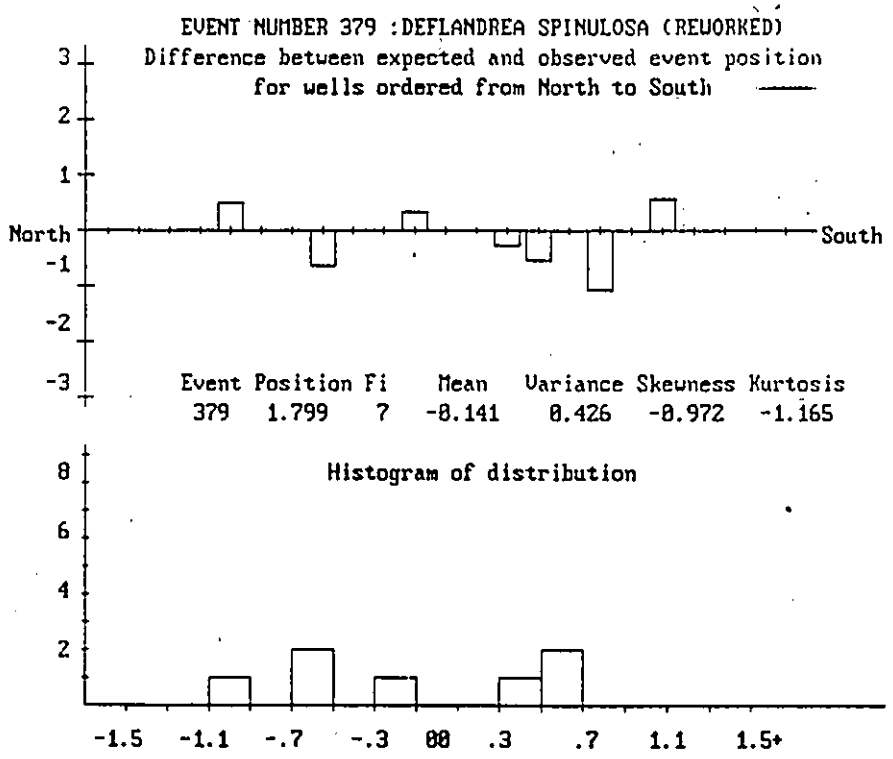
EVENT NUMBER 379 :DEFLANDREA SPINULOSA (REVORKED)
Difference between expected and observed event position
for wells ordered from North to South
3
2
1
North
-1
-2
-3
South
Event Position Fi Mean Variance Skewness Kurtosis
379 1.799 7 -0.141 0.426 -0.972 -1.165
Histogram of distribution
8
6
4
2
-1.5 -1.1 -.7 -.3 00 .3 .7 1.1 1.5+

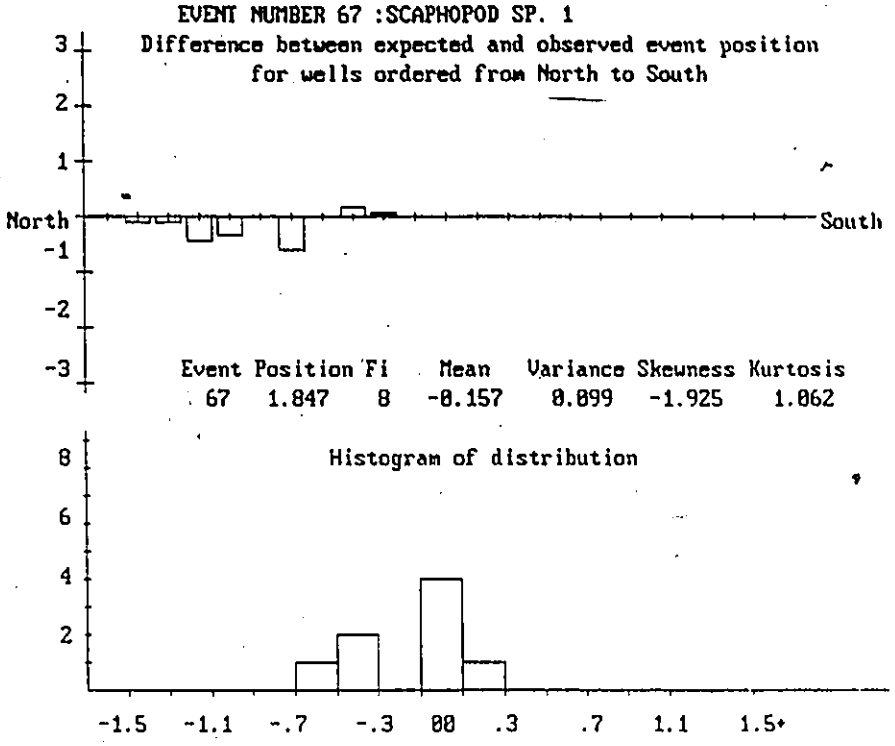
EVENT NUMBER 67 :SCAPHOPOD SP. 1
Difference between expected and observed event position
for wells ordered from North to South
3
2
1
North
-1
-2
-3
South
Event Position Fi Mean Variance Skewness Kurtosis
67 1.847 8 -0.157 0.899 -1.925 1.062
Histogram of distribution
8
6
4
2
-1.5 -1.1 -.7 -.3 00 .3 .7 1.1 1.5+

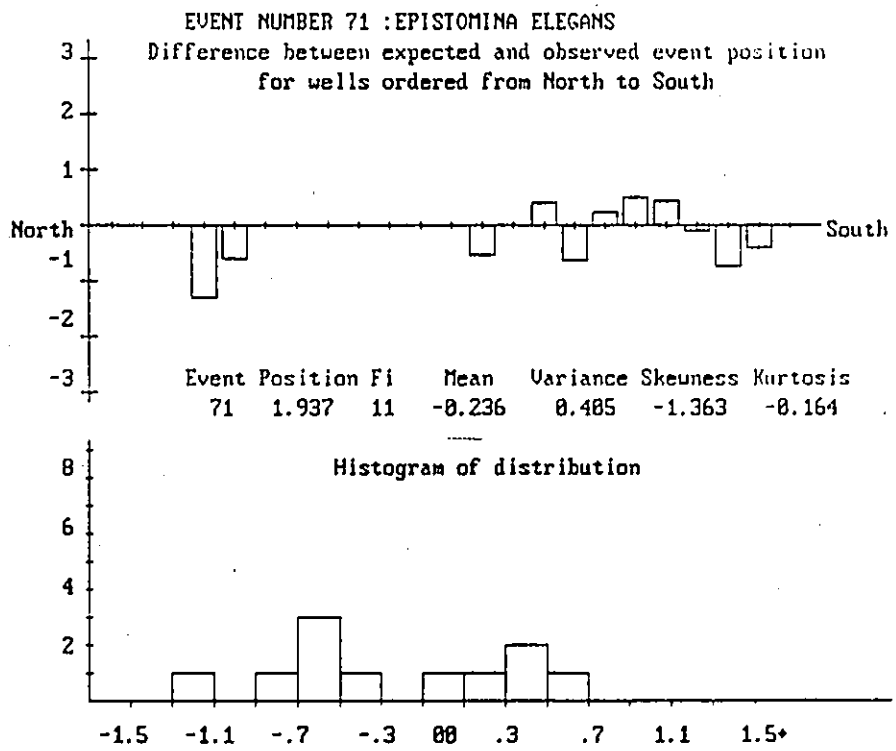
EVENT NUMBER 71 :EPISTOMINA ELEGANS
Difference between expected and observed event position
for wells ordered from North to South
3
2
1
North
-1
-2
-3
South
Event Position Fi Mean Variance Skewness Kurtosis
71 1.937 11 -0.236 0.485 -1.363 -0.164
Histogram of distribution
8
6
4
2
-1.5 -1.1 -.7 -.3 00 .3 .7 1.1 1.5+

EVENT NUMBER 18 :SPIROPLECTAMMINA CARINATA
Difference between expected and observed event position
for wells ordered from North to South

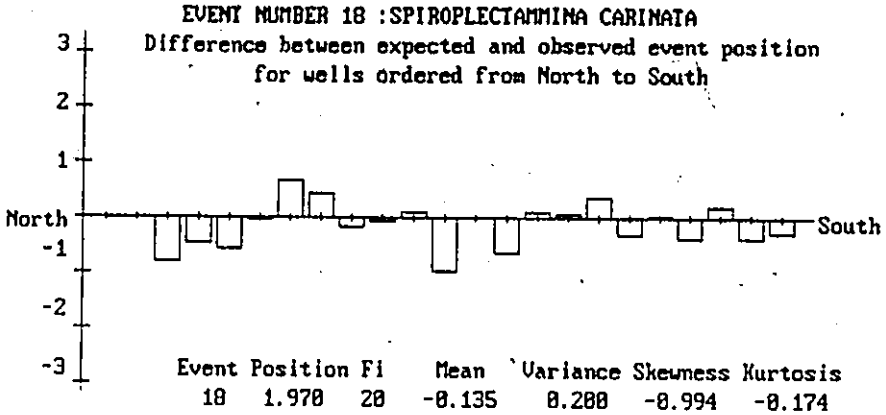

Event	Position	Fi	Mean	Variance	Skewness	Kurtosis
18	1.970	20	-0.135	0.288	-0.994	-0.174

Histogram of distribution

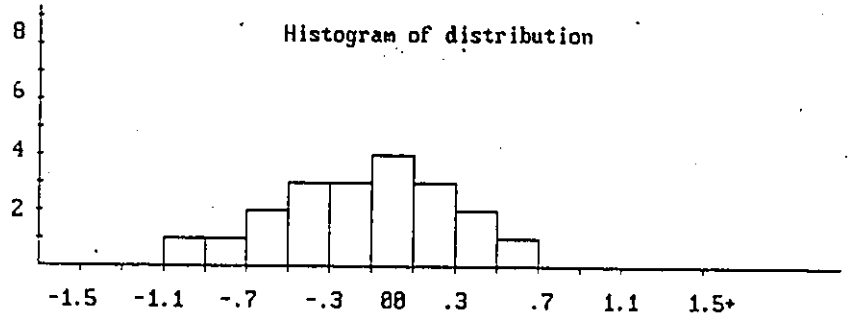

EVENT NUMBER 338 :CHIROPTERIDIUM MESPILANUM
Difference between expected and observed event position
for wells ordered from North to South

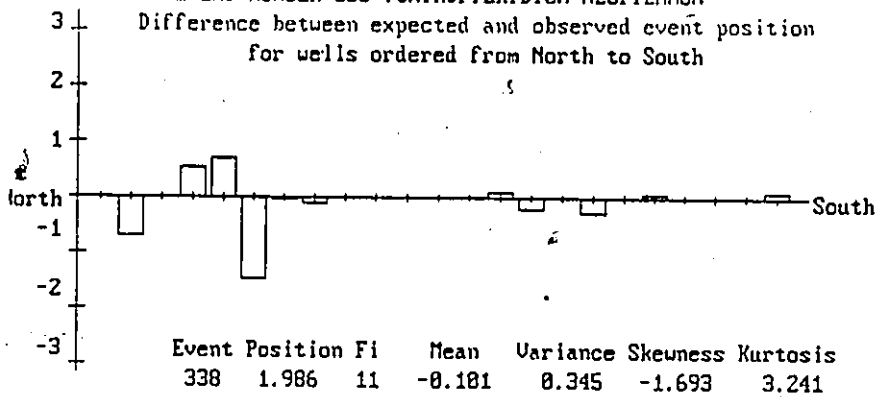

Event	Position	Fi	Mean	Variance	Skewness	Kurtosis
338	1.986	11	-0.181	0.345	-1.693	3.241

Histogram of distribution

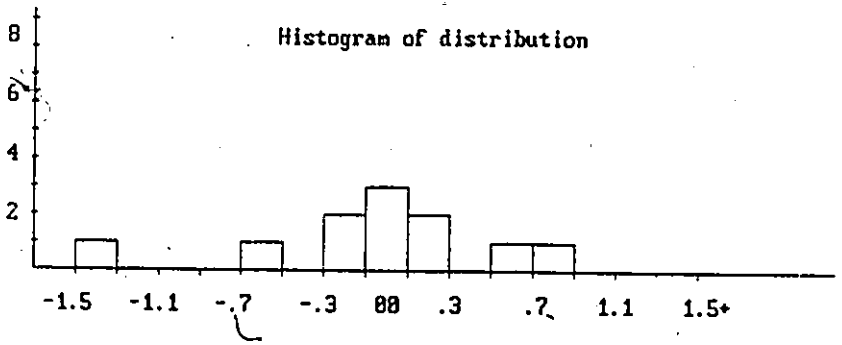

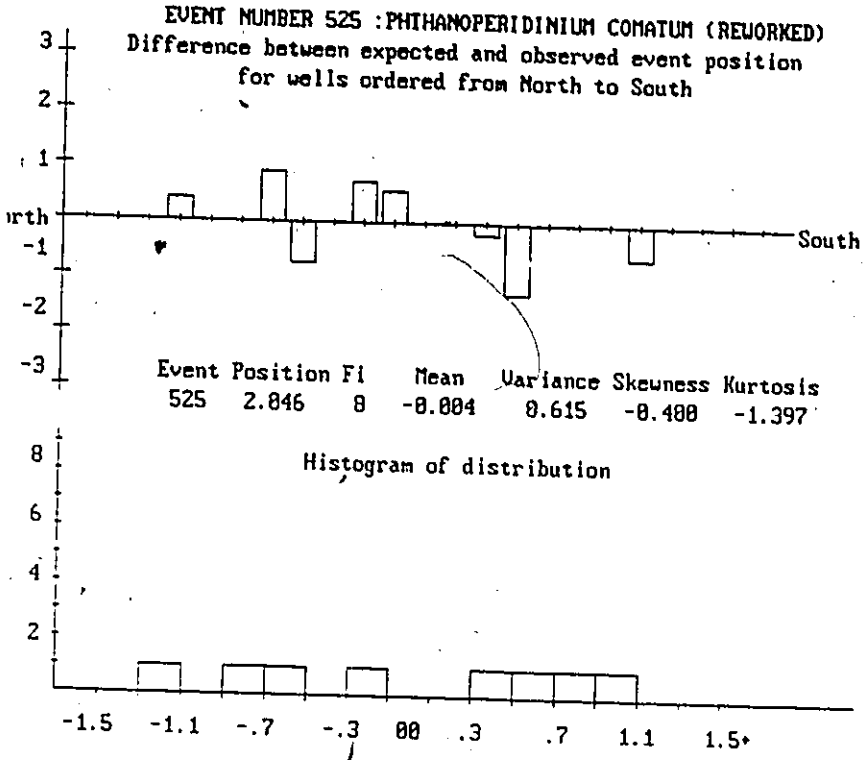
EVENT NUMBER 525 :PHTHANOPERIDINIUM COMATUM (REWORKED)
Difference between expected and observed event position
for wells ordered from North to South
3
2
1
-1
-2
-3
South
Event Position Fi Mean Variance Skewness Kurtosis
525 2.846 8 -0.004 0.615 -0.488 -1.397
Histogram of distribution
8
6
4
2
-1.5 -1.1 -.7 -.3 00 .3 .7 1.1 1.5+

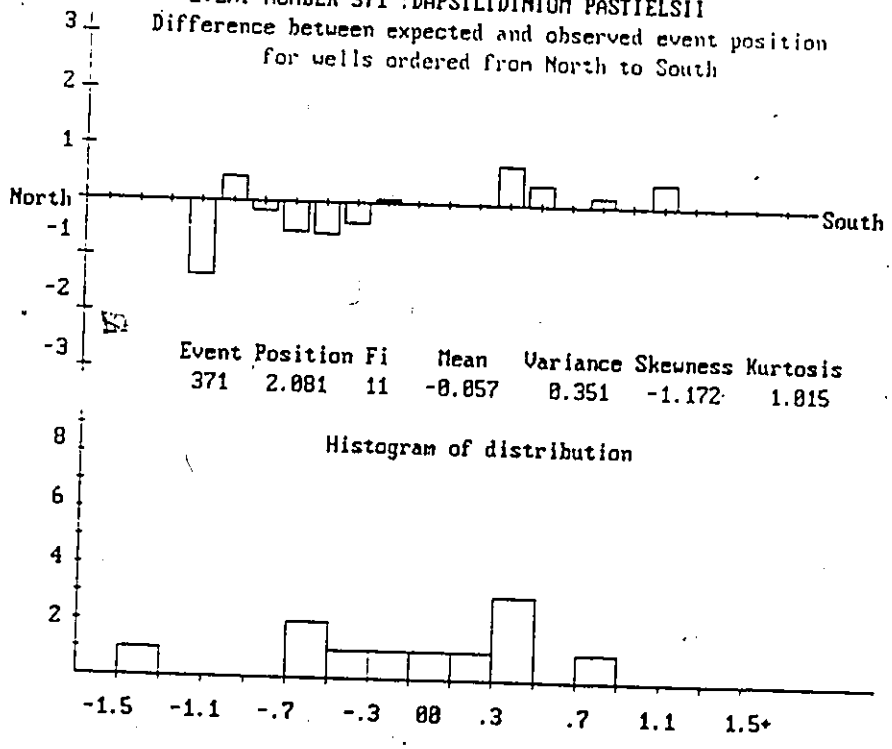
EVENT NUMBER 371 :DAPSILIDINIUM PASTIELSII
Difference between expected and observed event position
for wells ordered from North to South
3
2
1
North
-1
-2
-3
South
Event Position Fi Mean Variance Skewness Kurtosis
371 2.081 11 -0.057 0.351 -1.172 1.815
Histogram of distribution
8
6
4
2
-1.5 -1.1 -.7 -.3 00 .3 .7 1.1 1.5+

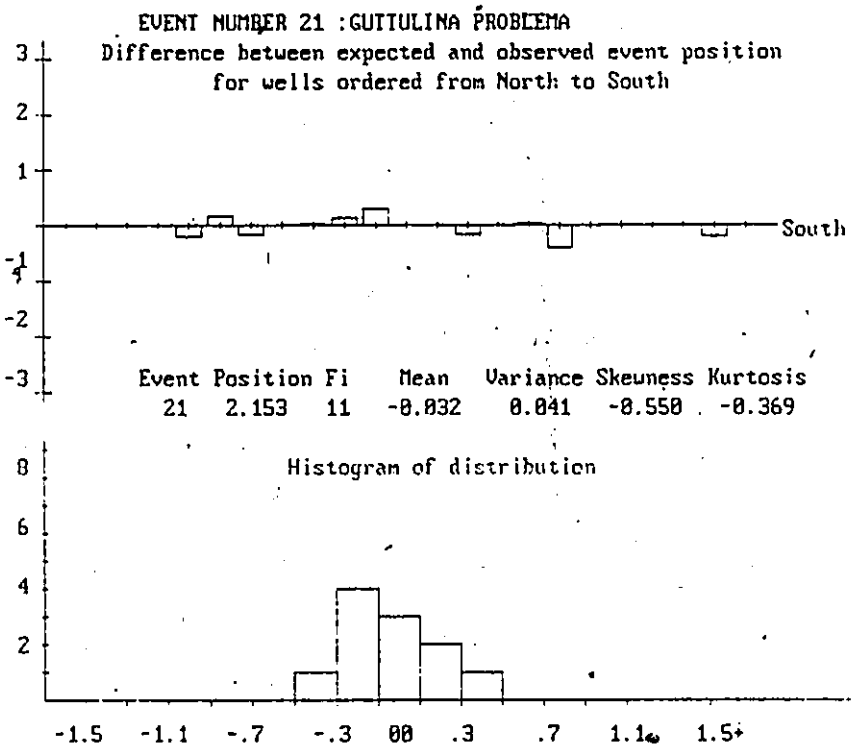
EVENT NUMBER 21 :GUTTULINA PROBLEMA
Difference between expected and observed event position
for wells ordered from North to South
3
2
1
-1
-2
-3
South
Event Position Fi Mean Variance Skewness Kurtosis
21 2.153 11 -0.032 0.041 -0.550 -0.369
Histogram of distribution
8
6
4
2
-1.5 -1.1 -.7 -.3 00 .3 .7 1.1 1.5+

EVENT NUMBER 28 :GYROIDINA GIRARDANA

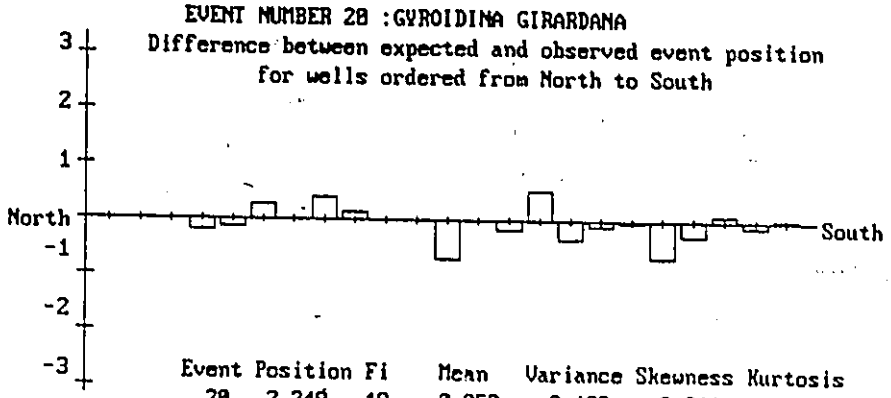

Event	Position	Fi	Mean	Variance	Skewness	Kurtosis
28	2.249	18	-0.050	0.100	-0.811	0.922

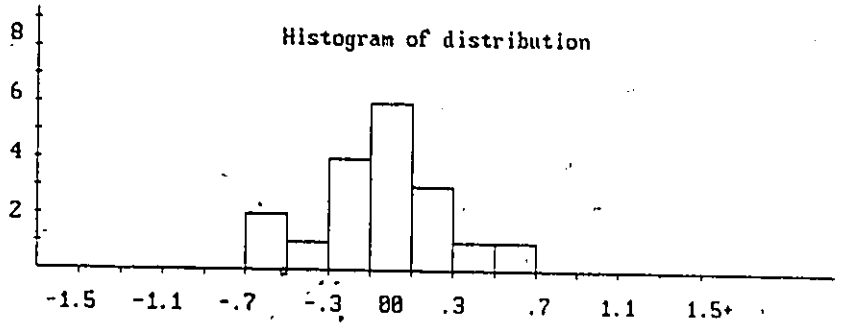

EVENT NUMBER 522 :PHTHANOPERIDINIUM

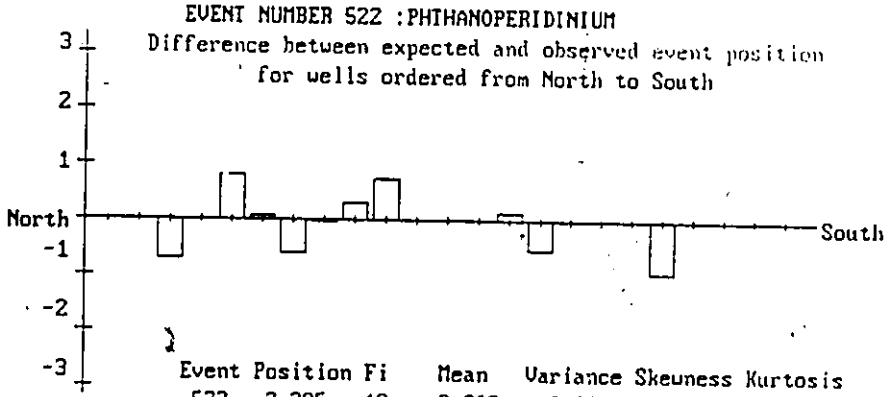

Event	Position	Fi	Mean	Variance	Skewness	Kurtosis
522	2.285	10	-0.062	0.366	-0.279	-1.251

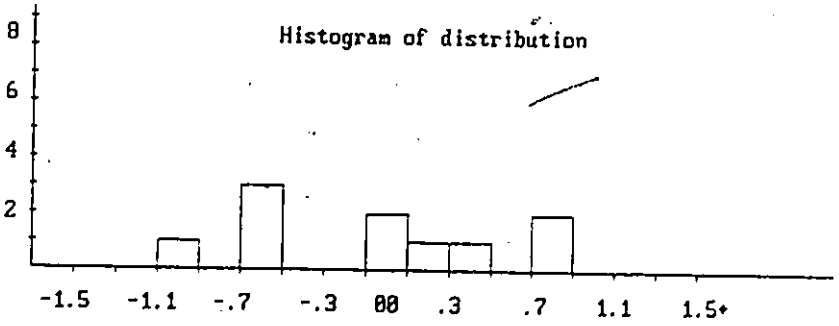

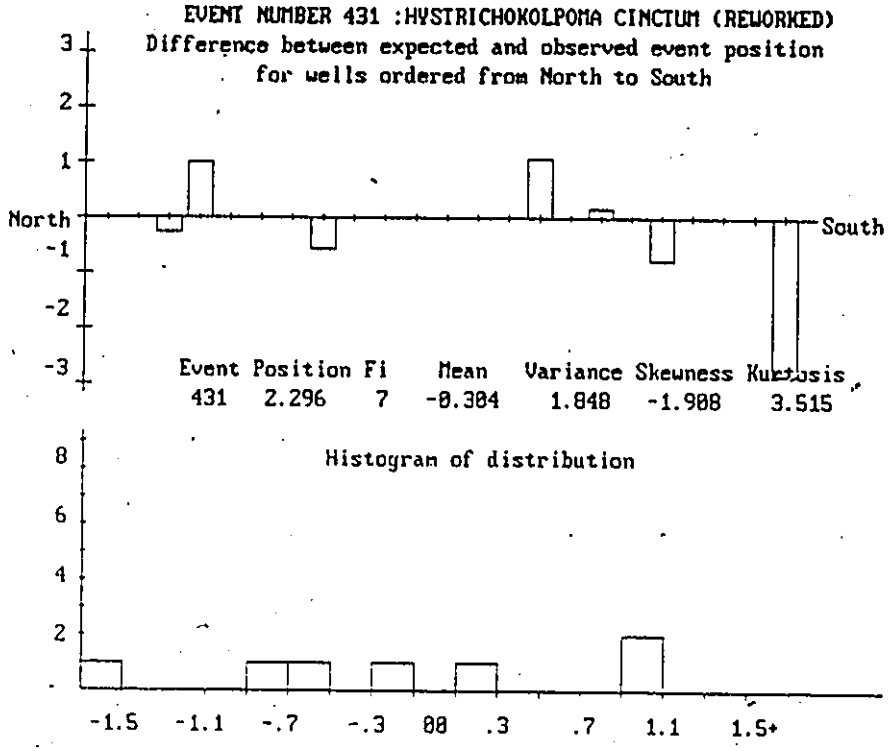
EVENT NUMBER 431 :HYSTRICHOKOLPOMA CINCTUM (REWORKED)
Difference between expected and observed event position
for wells ordered from North to South
3
2
1
North
-1
-2
-3
South
Event Position Fi Mean Variance Skewness Kurtosis
431 2.296 7 -0.384 1.848 -1.908 3.515
Histogram of distribution
8
6
4
2
-1.5 -1.1 -.7 -.3 00 .3 .7 1.1 1.5+

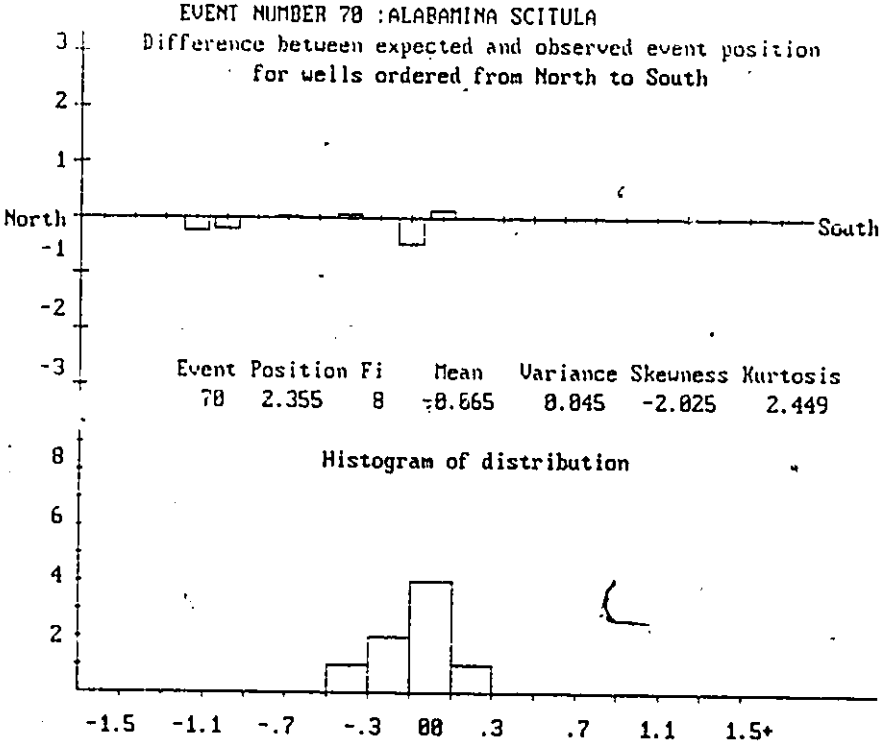
EVENT NUMBER 70 :ALABAMINA SCITULA
Difference between expected and observed event position
for wells ordered from North to South
3
2
1
North
-1
-2
-3
South
Event Position Fi Mean Variance Skewness Kurtosis
70 2.355 8 -0.665 0.845 -2.025 2.449
Histogram of distribution
8
6
4
2
-1.5 -1.1 -.7 -.3 00 .3 .7 1.1 1.5+

EVENT NUMBER 448 :IMPLETOSPHAERIDIUM TRANSFODUM
Difference between expected and observed event position
for wells ordered from North to South

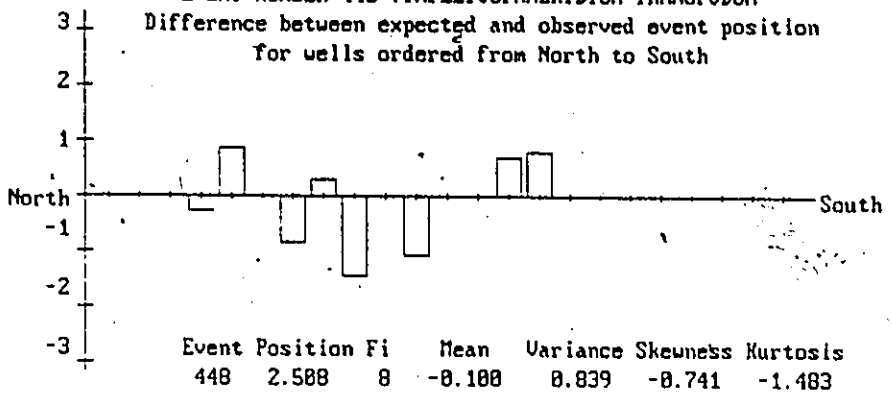

Event	Position	Fi	Mean	Variance	Skewness	Kurtosis
448	2.508	8	-0.100	0.839	-0.741	-1.483

Histogram of distribution

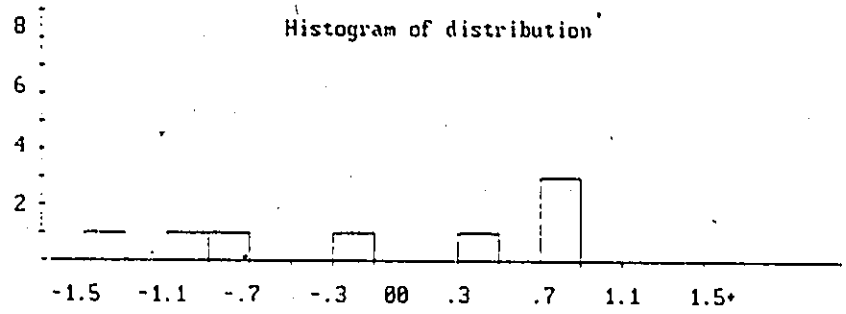

EVENT NUMBER 312 :AREOSPHAERIDIUM PECTINIFORME (REWORKED)
Difference between expected and observed event position
for wells ordered from North to South

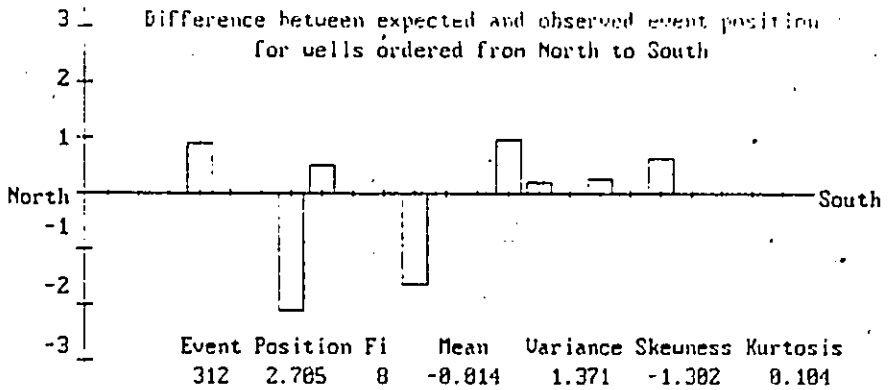

Event	Position	Fi	Mean	Variance	Skewness	Kurtosis
312	2.705	8	-0.814	1.371	-1.302	0.104

Histogram of distribution

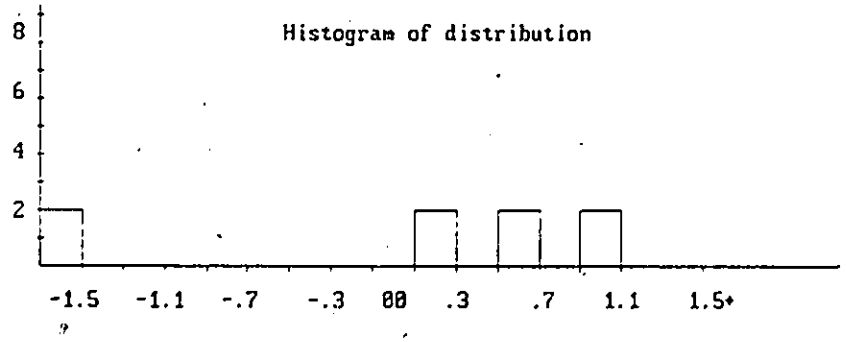

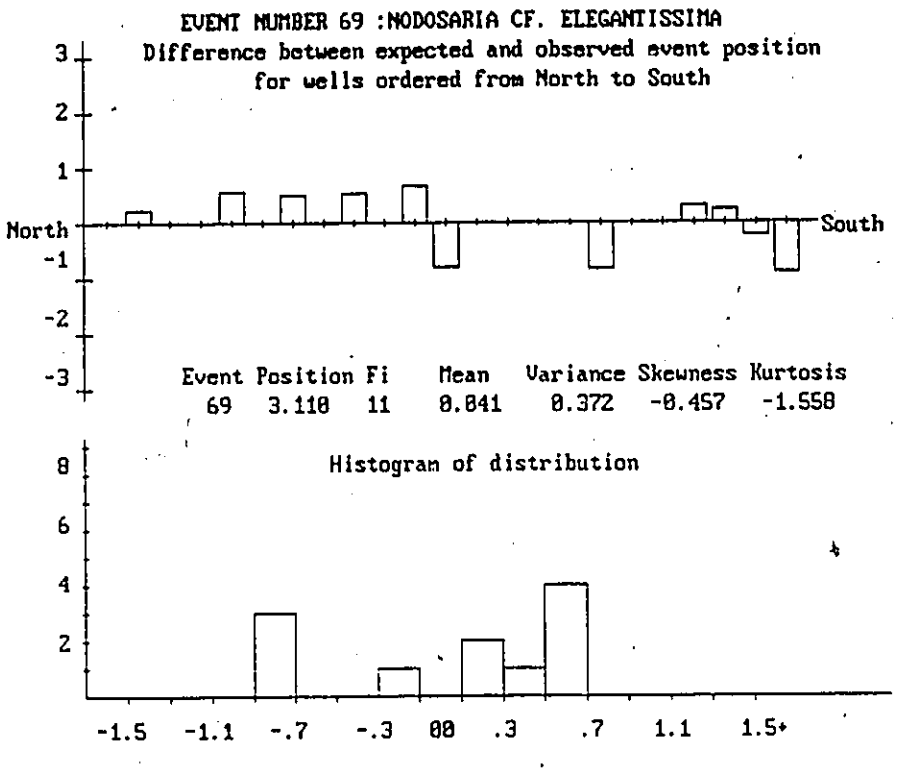
EVENT NUMBER 69 :NODOSARIA CF. ELEGANTISSIMA
Difference between expected and observed event position
for wells ordered from North to South
3
2
1
North
-1
-2
-3
South
Event Position Fi Mean Variance Skewness Kurtosis
69 3.118 11 0.041 0.372 -0.457 -1.558
Histogram of distribution
8
6
4
2
-1.5 -1.1 -.7 -.3 00 .3 .7 1.1 1.5+

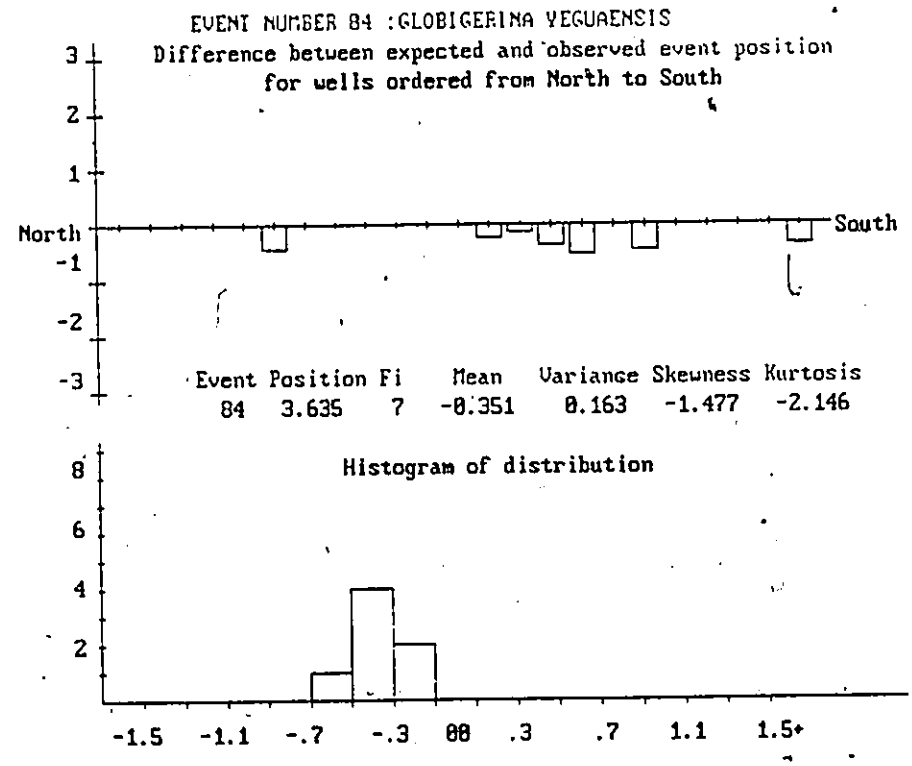
EVENT NUMBER 84 :GLOBIGERINA VEGUAENSIS
Difference between expected and observed event position
for wells ordered from North to South
3
2
1
North
-1
-2
-3
South
Event Position Fi Mean Variance Skewness Kurtosis
84 3.635 7 -0.351 0.163 -1.477 -2.146
Histogram of distribution
8
6
4
2
-1.5 -1.1 -.7 -.3 00 .3 .7 1.1 1.5+

EVENT NUMBER 25 :COARSE ARENACEOUS SPP.

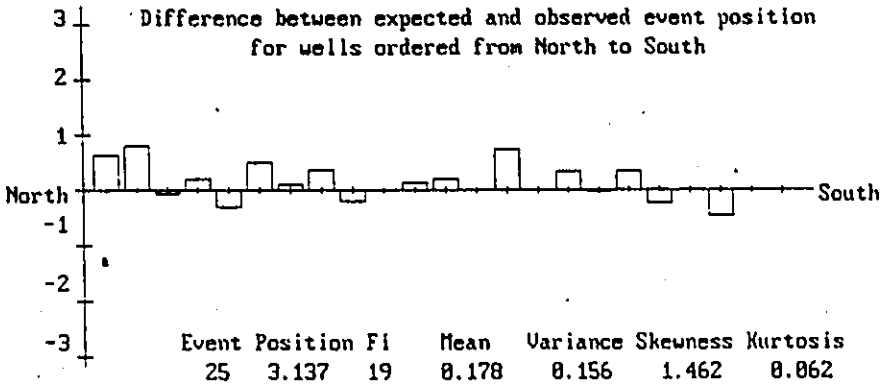

Event	Position	Fi	Mean	Variance	Skewness	Kurtosis
25	3.137	19	0.178	0.156	1.462	0.062

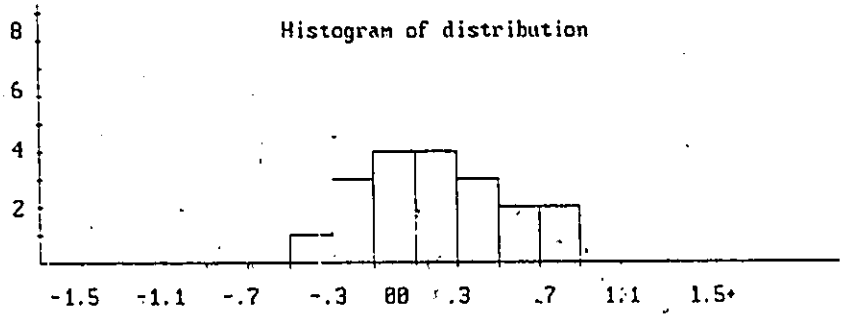

EVENT NUMBER 27 :EPONIDES UMBONATUS

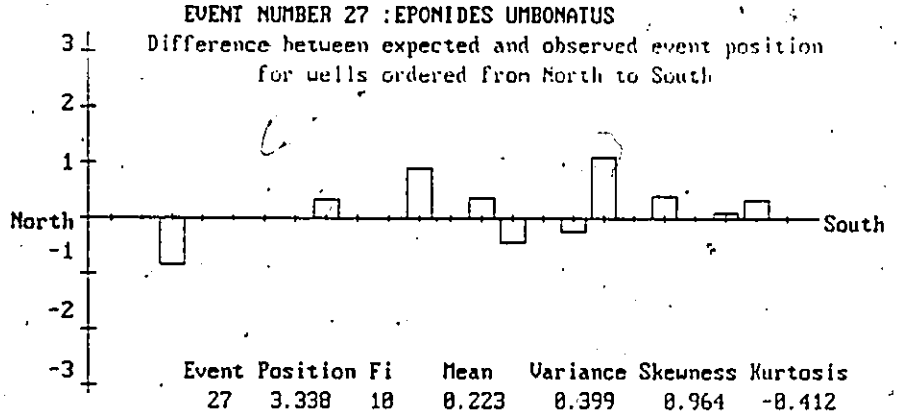

Event	Position	Fi	Mean	Variance	Skewness	Kurtosis
27	3.338	18	0.223	0.399	0.964	-0.412

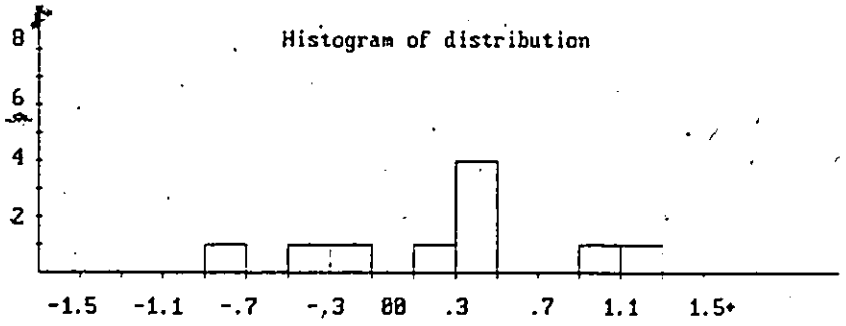

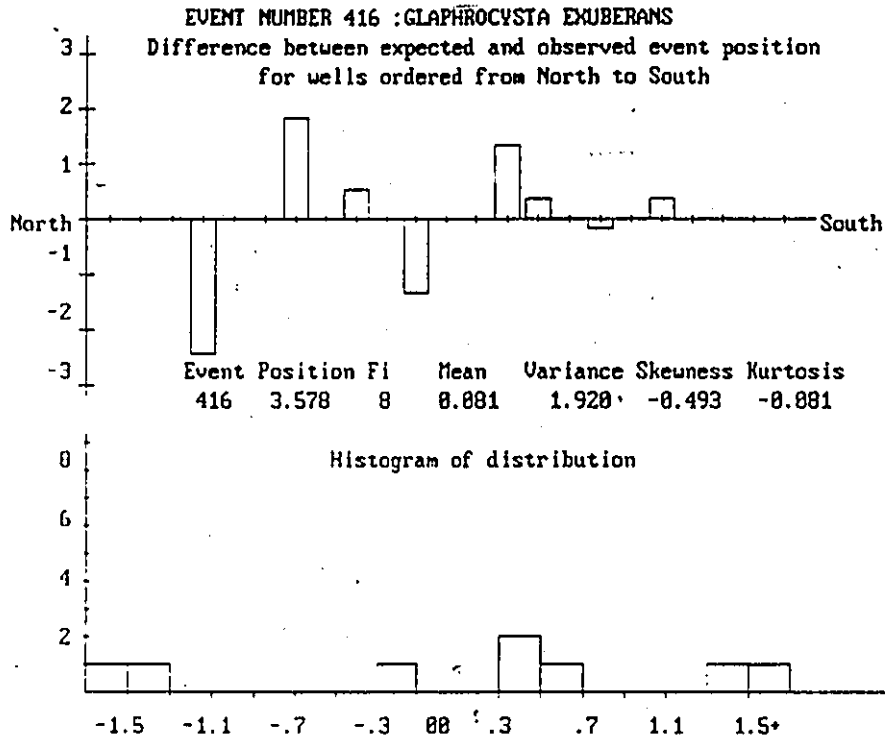
EVENT NUMBER 416 :GLAPHROCYSTA EXUBERANS
Difference between expected and observed event position
for wells ordered from North to South
3
2
1
North
-1
-2
-3
South
Event Position Fi Mean Variance Skewness Kurtosis
416 3.578 8 0.081 1.920 -0.493 -0.081
Histogram of distribution
8
6
4
2
-1.5 -1.1 -.7 -.3 00 .3 .7 1.1 1.5+

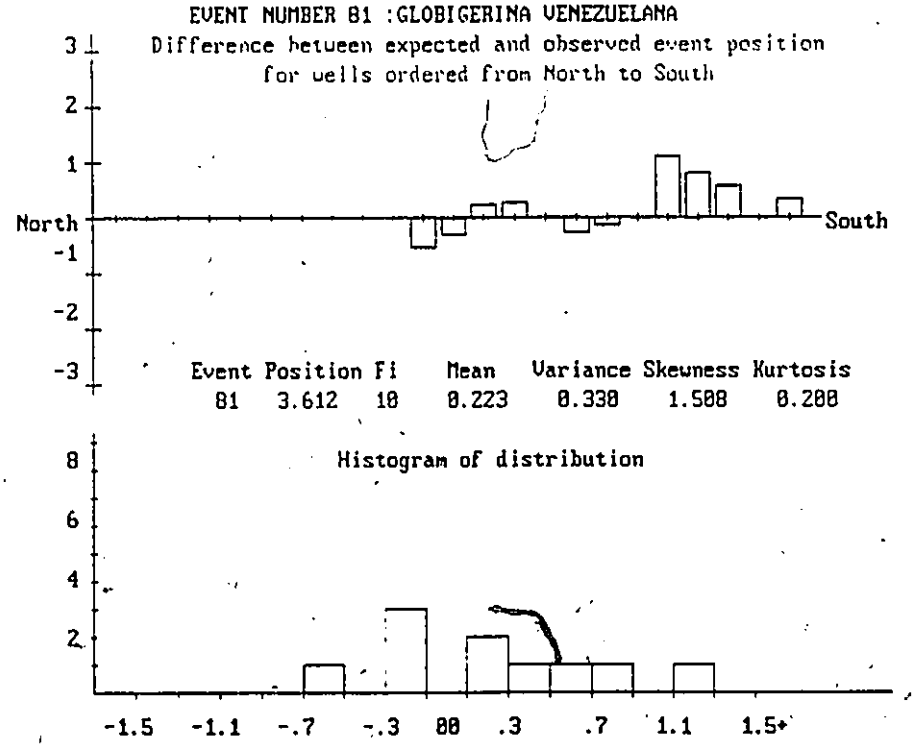
EVENT NUMBER 81 :GLOBIGERINA VENEZUELANA
Difference between expected and observed event position
for wells ordered from North to South
3
2
1
North
-1
-2
-3
South
Event Position Fi Mean Variance Skewness Kurtosis
81 3.612 10 0.223 0.330 1.500 0.200
Histogram of distribution
8
6
4
2
-1.5 -1.1 -.7 -.3 00 .3 .7 1.1 1.5+

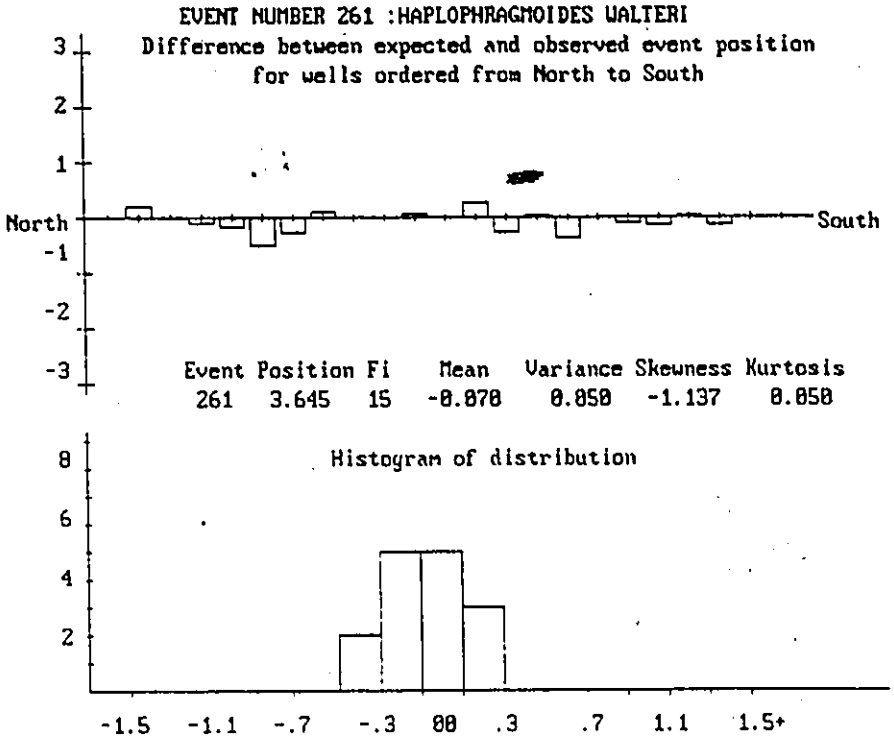
EVENT NUMBER 261 :HAPLOPHRAGMOIDES WALTERI
Difference between expected and observed event position
for wells ordered from North to South
3
2
1
North
-1
-2
-3
South
Event Position Fi Mean Variance Skewness Kurtosis
261 3.645 15 -0.070 0.050 -1.137 0.050
Histogram of distribution
8
6
4
2
-1.5 -1.1 -.7 -.3 00 .3 .7 1.1 1.5+

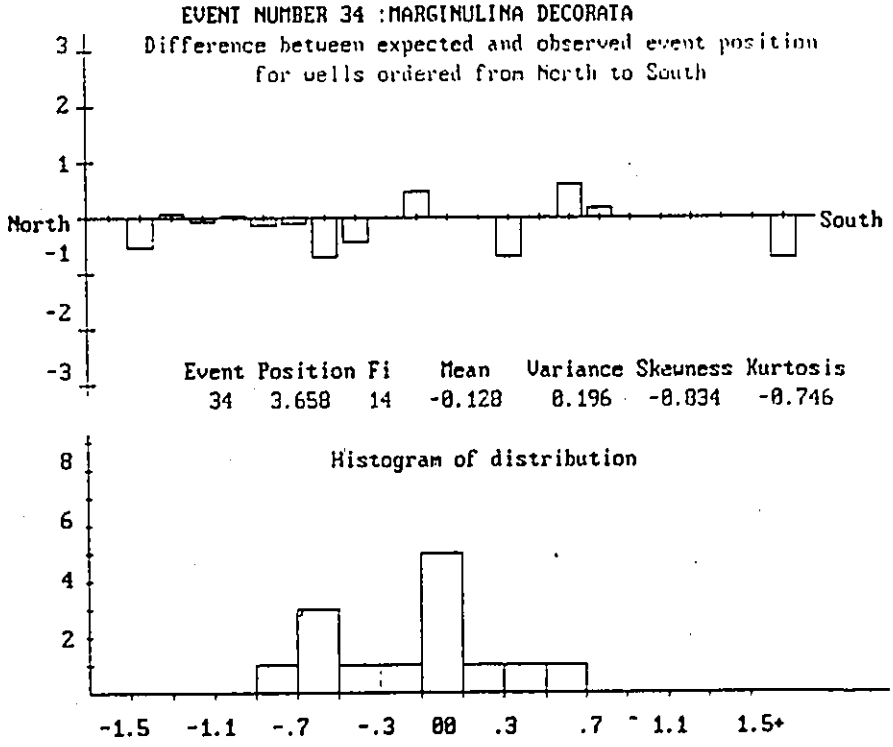
EVENT NUMBER 34 :MARGINULINA DECORATA
Difference between expected and observed event position
for wells ordered from North to South
3
2
1
North
-1
-2
-3
South
Event Position Fi Mean Variance Skewness Kurtosis
34 3.658 14 -0.128 0.196 -0.034 -0.746
Histogram of distribution
8
6
4
2
-1.5 -1.1 -.7 -.3 00 .3 .7 1.1 1.5+

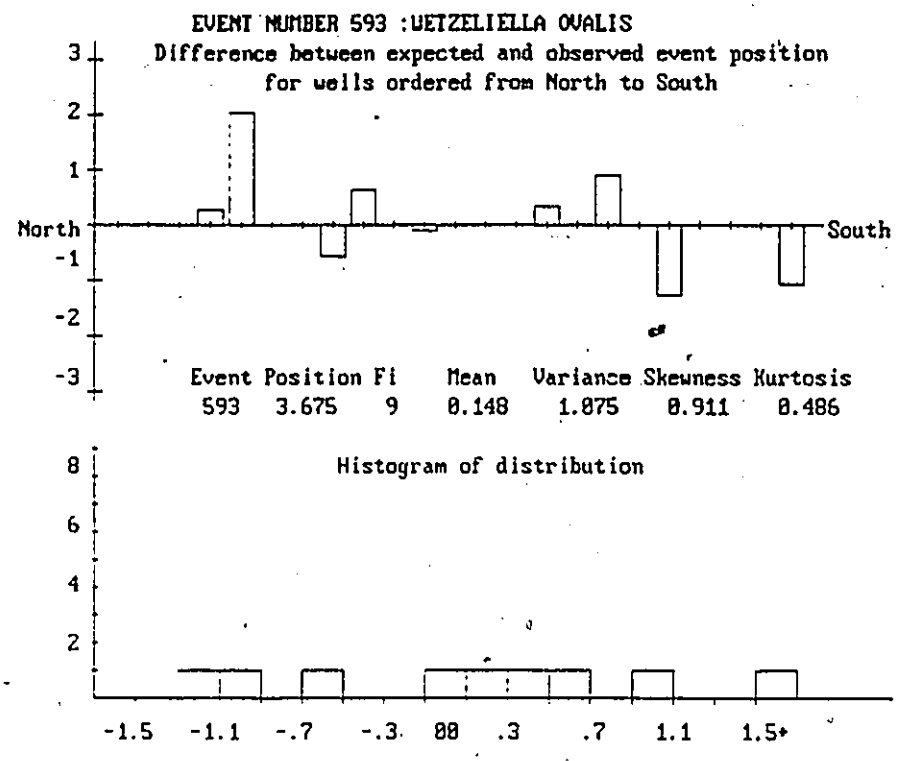
EVENT NUMBER 593 :UETZELIELLA OVALIS
Difference between expected and observed event position
for wells ordered from North to South
3
2
1
North
-1
-2
-3
South
Event Position Fi Mean Variance Skewness Kurtosis
593 3.675 9 0.148 1.875 0.911 0.486
Histogram of distribution
8
6
4
2
-1.5 -1.1 -.7 -.3 00 .3 .7 1.1 1.5+

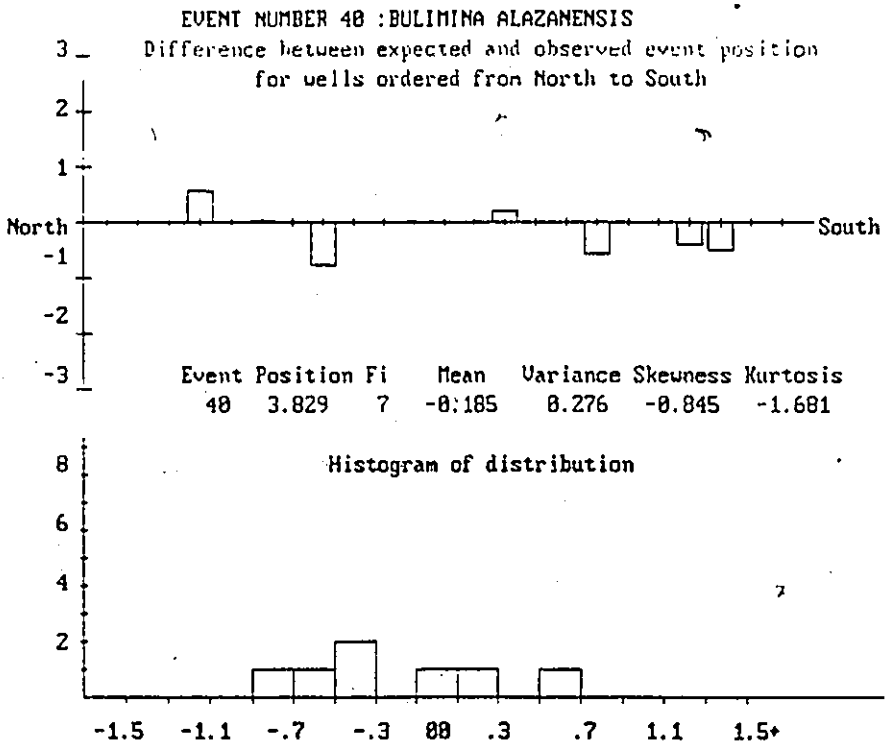
EVENT NUMBER 40 :BULIMINA ALAZANENSIS
Difference between expected and observed event position
for wells ordered from North to South
3
2
1
North
-1
-2
-3
South
Event Position Fi Mean Variance Skewness Kurtosis
40 3.829 7 -0.185 0.276 -0.845 -1.681
Histogram of distribution
8
6
4
2
-1.5 -1.1 -.7 -.3 00 .3 .7 1.1 1.5+

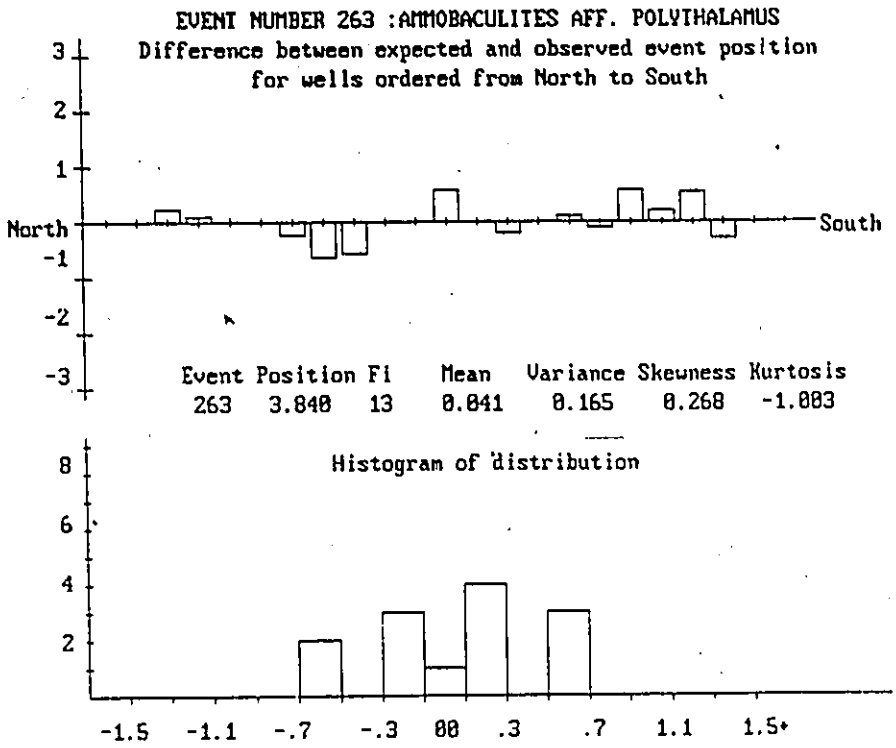
EVENT NUMBER 263 :AMMOBACULITES AFF. POLYTHALAMUS
Difference between expected and observed event position
for wells ordered from North to South
3
2
1
North
-1
-2
-3
South
Event Position Fi Mean Variance Skewness Kurtosis
263 3.840 13 0.041 0.165 0.268 -1.083
Histogram of distribution
8
6
4
2
-1.5 -1.1 -.7 -.3 00 .3 .7 1.1 1.5+

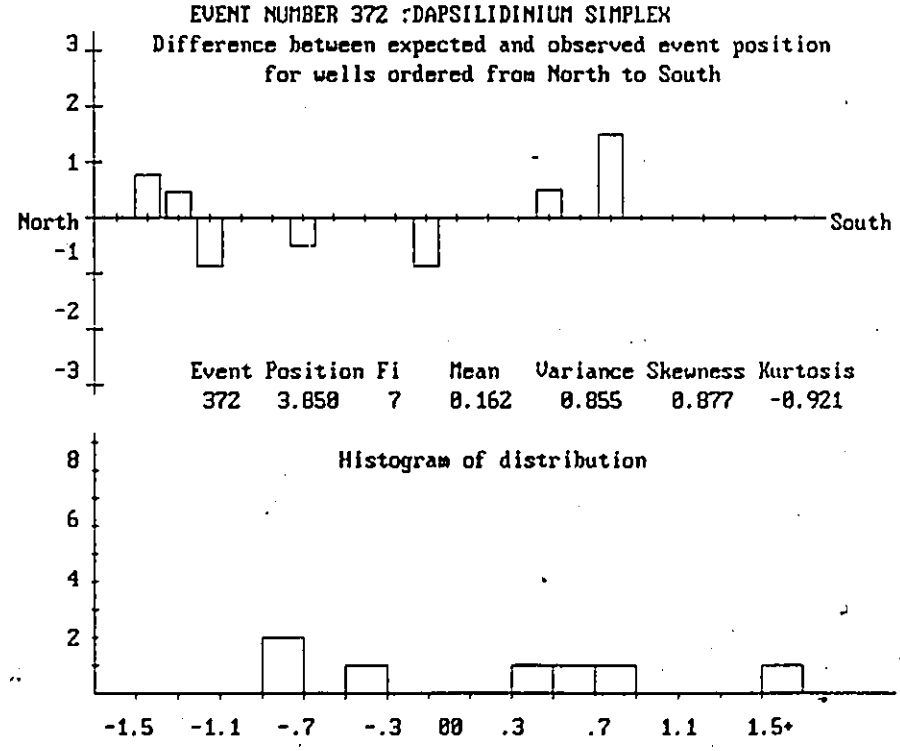
EVENT NUMBER 372 :DAPSILIDINIUM SIMPLEX
Difference between expected and observed event position
for wells ordered from North to South
3
2
1
North
-1
-2
-3
South
Event Position Fi Mean Variance Skewness Kurtosis
372 3.850 7 0.162 0.855 0.877 -0.921
Histogram of distribution
8
6
4
2
-1.5 -1.1 -.7 -.3 00 .3 .7 1.1 1.5+

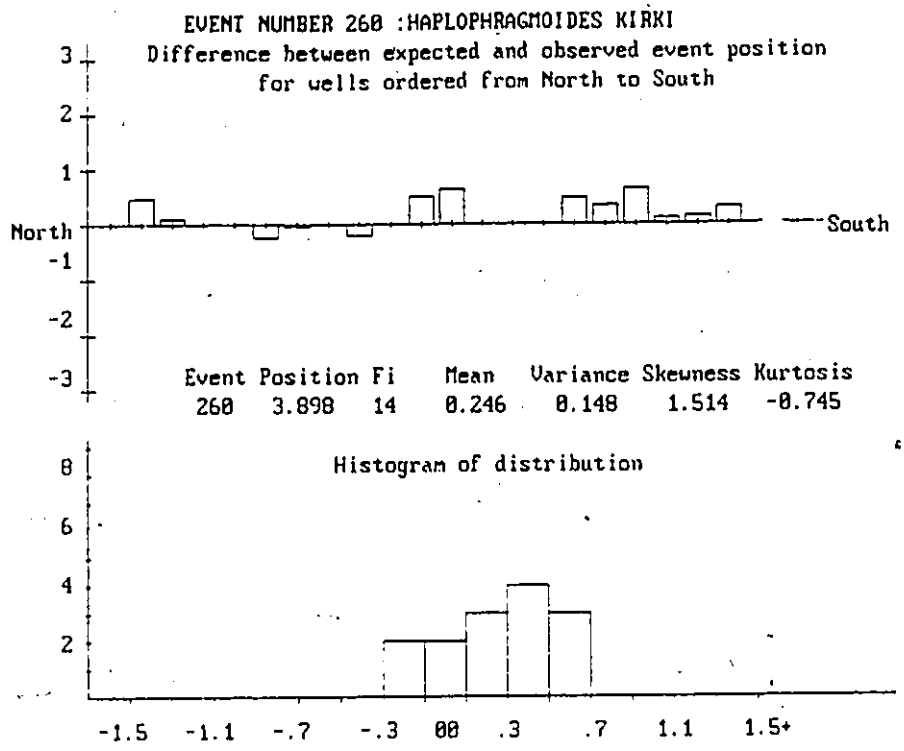
EVENT NUMBER 260 :HAPLOPHRAGMOIDES KIRKI
Difference between expected and observed event position
for wells ordered from North to South
3
2
1
North
-1
-2
-3
South
Event Position Fi Mean Variance Skewness Kurtosis
260 3.898 14 0.246 0.148 1.514 -0.745
Histogram of distribution
8
6
4
2
-1.5 -1.1 -.7 -.3 00 .3 .7 1.1 1.5+

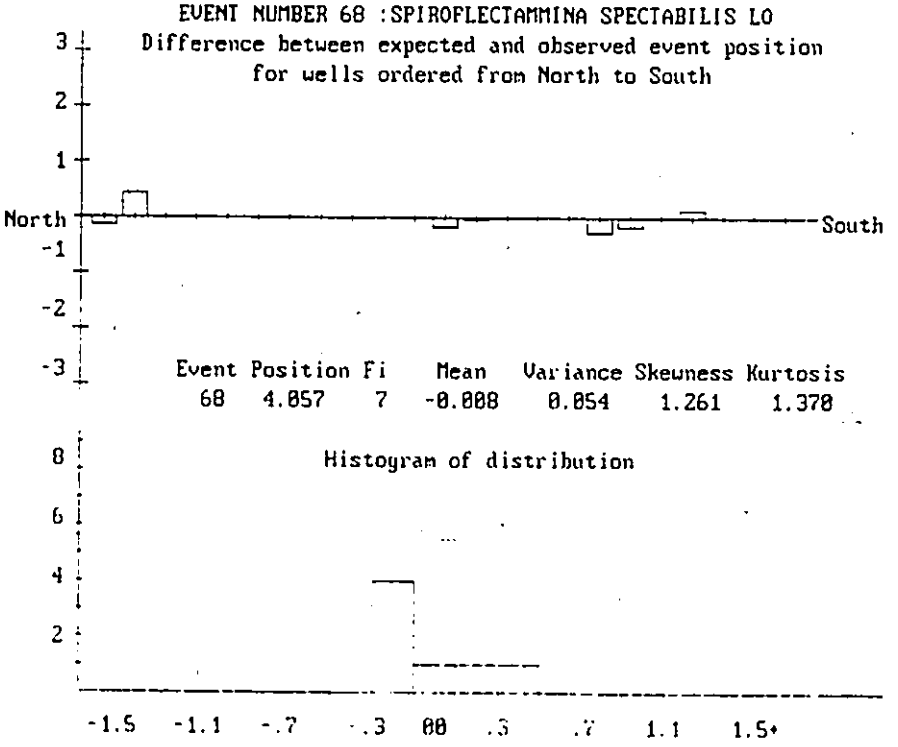
EVENT NUMBER 68 :SPIROPLECTAMMINA SPECTABILIS LO
Difference between expected and observed event position
for wells ordered from North to South
3
2
1
North
-1
-2
-3
South
Event Position Fi Mean Variance Skewness Kurtosis
68 4.857 7 -0.008 0.054 1.261 1.378
Histogram of distribution
8
6
4
2
-1.5 -1.1 -.7 -.3 00 .3 .7 1.1 1.5+

EVENT NUMBER 32 :AMMOSPHAEROIDINA SP. 1
Difference between expected and observed event position
for wells ordered from North to South

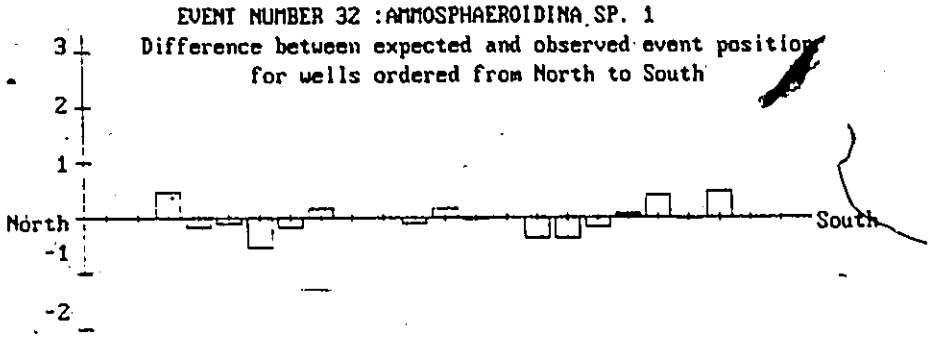

Event	Position	Fi	Mean	Variance	Skewness	Kurtosis
32	4.863	17	0.000	0.881	0.345	-0.256

Histogram of distribution

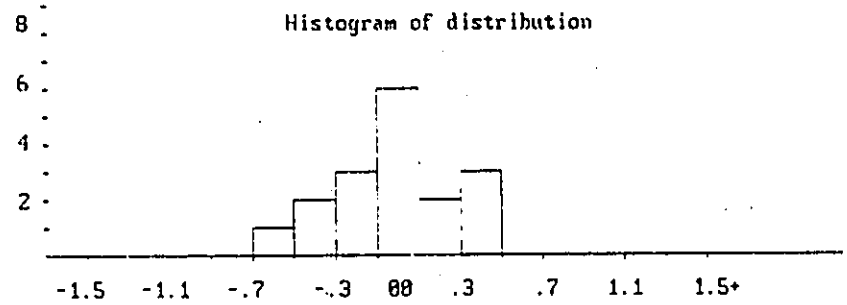

EVENT NUMBER 264 :KARRERIELLA CONVERSA
Difference between expected and observed event position
for wells ordered from North to South

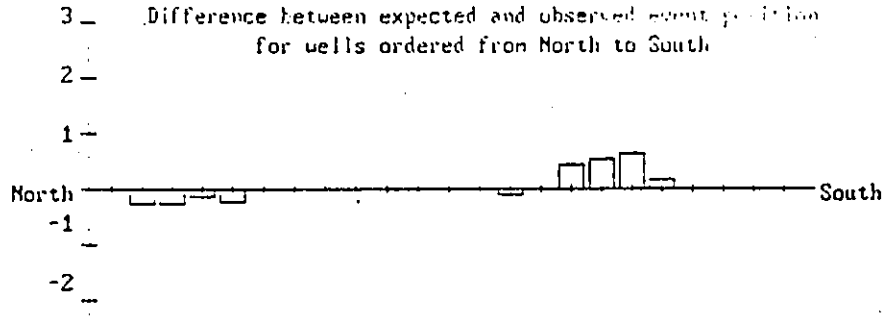

Event	Position	Fi	Mean	Variance	Skewness	Kurtosis
264	4.897	9	0.099	0.145	1.414	-0.448

Histogram of distribution

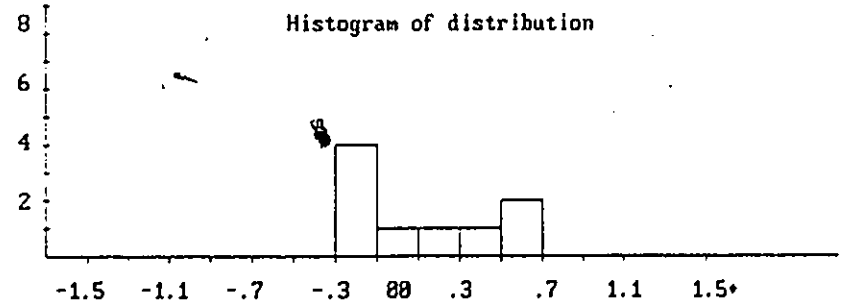

EVENT NUMBER 42 :CIBICIDOIDES ALLENI

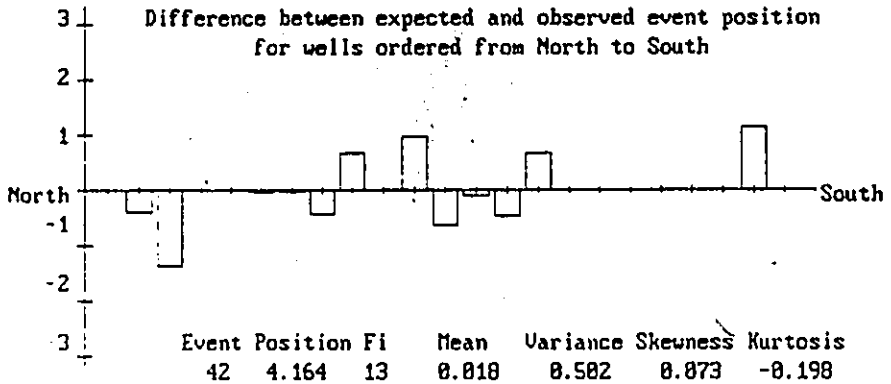

Event	Position	Fi	Mean	Variance	Skewness	Kurtosis
42	4.164	13	0.010	0.502	0.073	-0.198

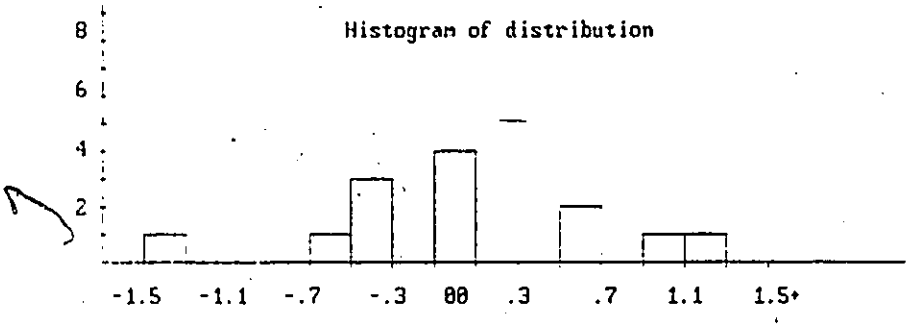

EVENT NUMBER 30 :CIBICIDOIDES BLANPIEDI

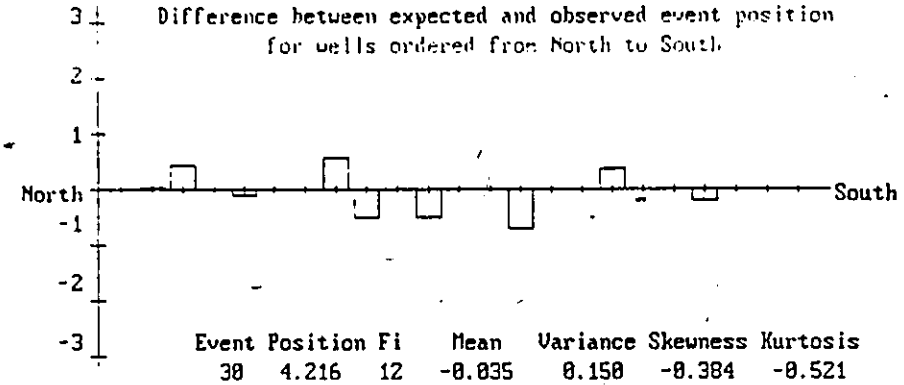

Event	Position	Fi	Mean	Variance	Skewness	Kurtosis
30	4.216	12	-0.035	0.150	-0.384	-0.521

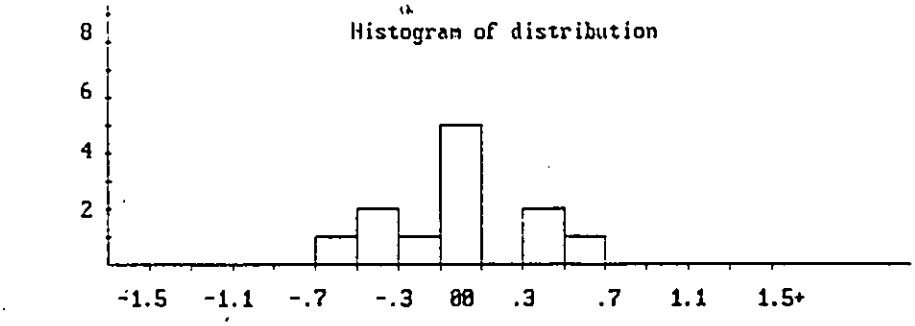

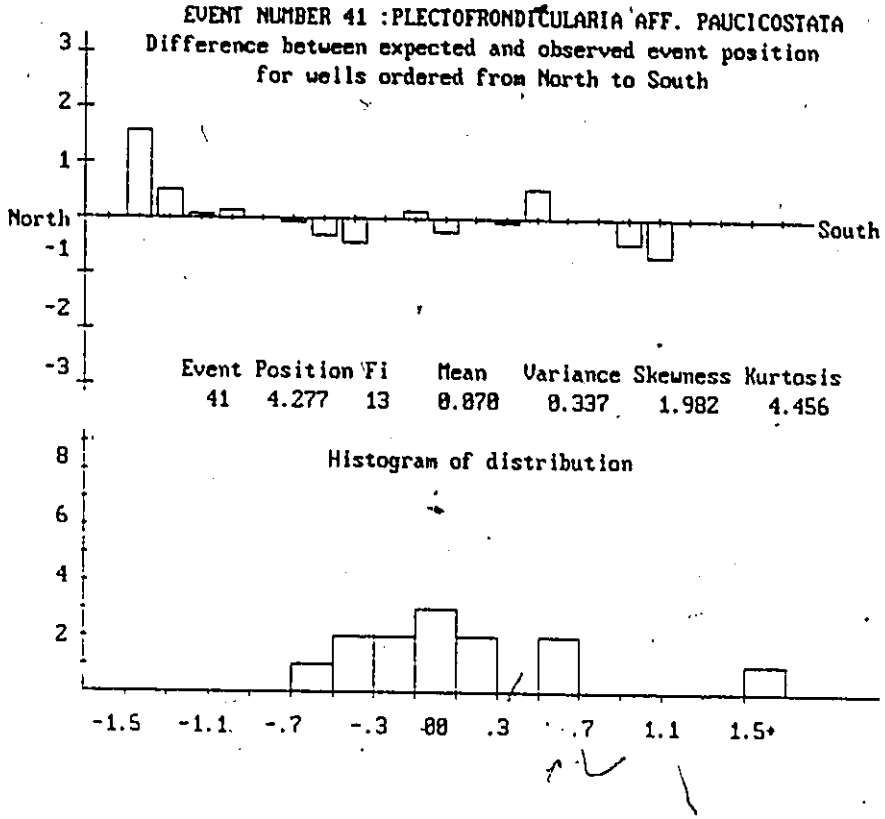
EVENT NUMBER 41 :PLECTOFRONDICULARIA AFF. PAUCICOSTATA
Difference between expected and observed event position
for wells ordered from North to South
3
2
1
North
-1
-2
-3
South
Event Position Fi Mean Variance Skewness Kurtosis
41 4.277 13 0.870 0.337 1.982 4.456
Histogram of distribution
8
6
4
2
-1.5 -1.1 -.7 -.3 00 .3 .7 1.1 1.5+

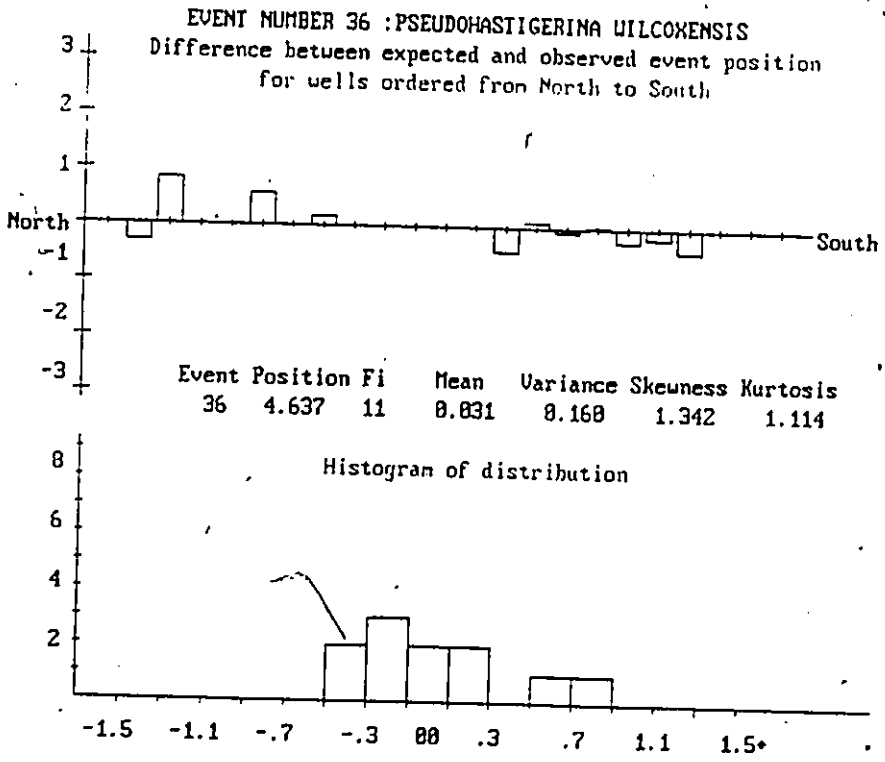
EVENT NUMBER 36 :PSEUDOHASTIGERINA WILCOXENSIS
Difference between expected and observed event position
for wells ordered from North to South
3
2
1
North
-1
-2
-3
South
Event Position Fi Mean Variance Skewness Kurtosis
36 4.637 11 0.831 0.168 1.342 1.114
Histogram of distribution
8
6
4
2
-1.5 -1.1 -.7 -.3 00 .3 .7 1.1 1.5+

EVENT NUMBER 384 :AREOLIGERA CORONATA

Difference between expected and observed event position for wells ordered from North to South

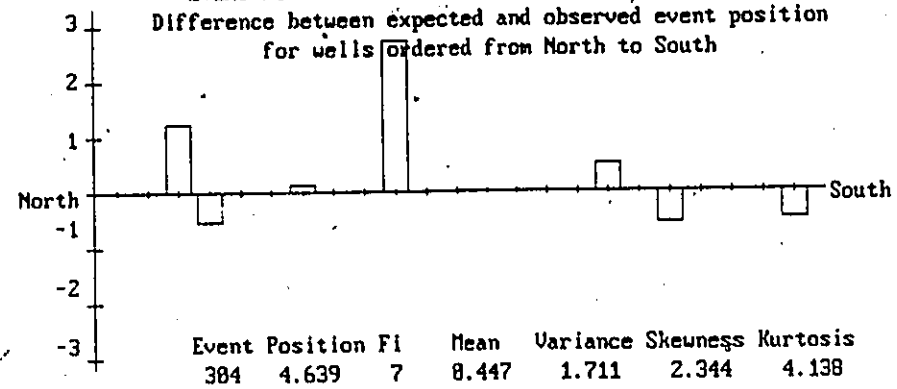

Event	Position	Fi	Mean	Variance	Skewness	Kurtosis
384	4.639	7	0.447	1.711	2.344	4.138

Histogram of distribution

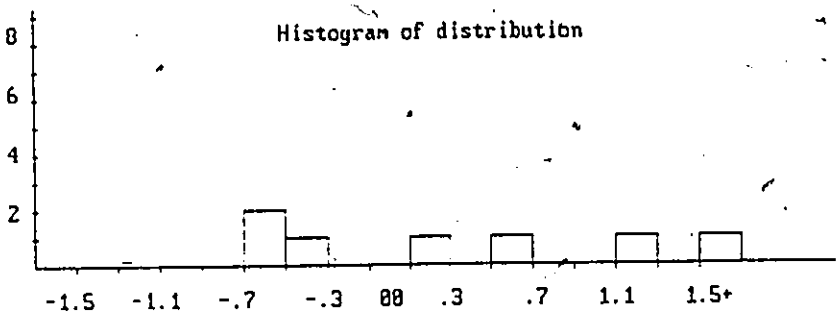

EVENT NUMBER 45 :BULIMINA TRIGONALIS

Difference between expected and observed event position for wells ordered from North to South

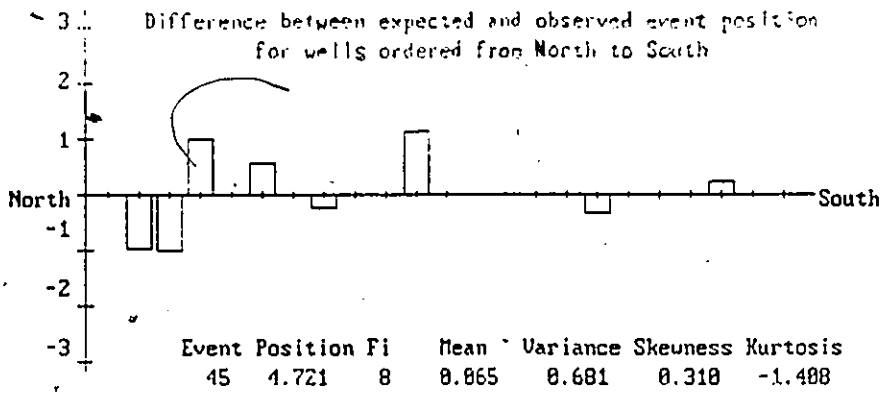

Event	Position	Fi	Mean	Variance	Skewness	Kurtosis
45	4.721	8	0.865	0.681	0.310	-1.408

Histogram of distribution

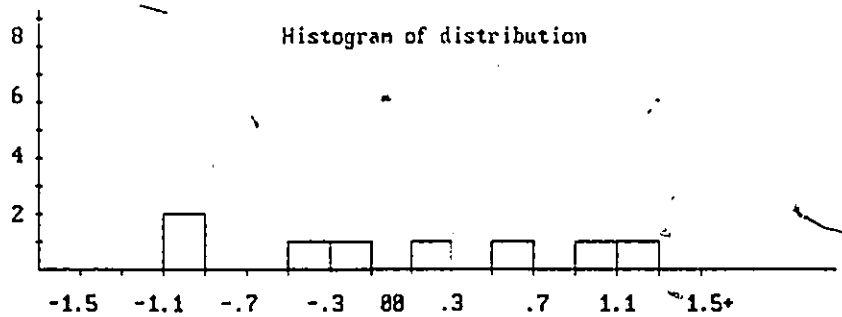

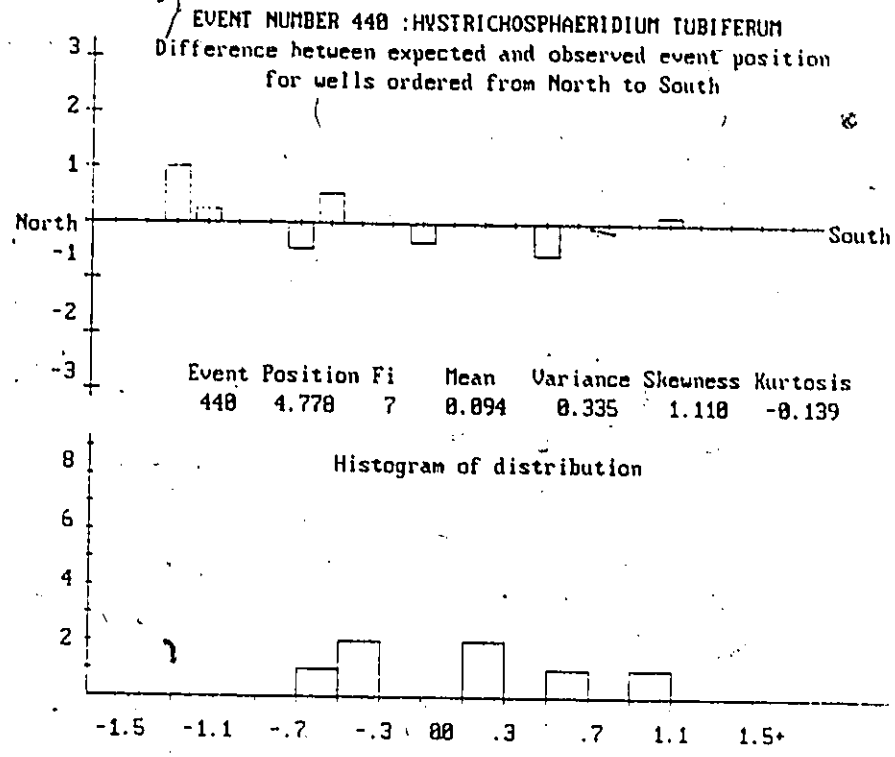
EVENT NUMBER 440 :HYSTRICHOSPHAERIDIUM TUBIFERUM
Difference hetween expected and observed event position
for wells ordered from North to South
3
2
1
North
-1
-2
-3
South
Event Position Fi Mean Variance Skewness Kurtosis
440 4.778 7 0.094 0.335 1.110 -0.139
Histogram of distribution
8
6
4
2
-1.5 -1.1 -.7 -.3 00 .3 .7 1.1 1.5+

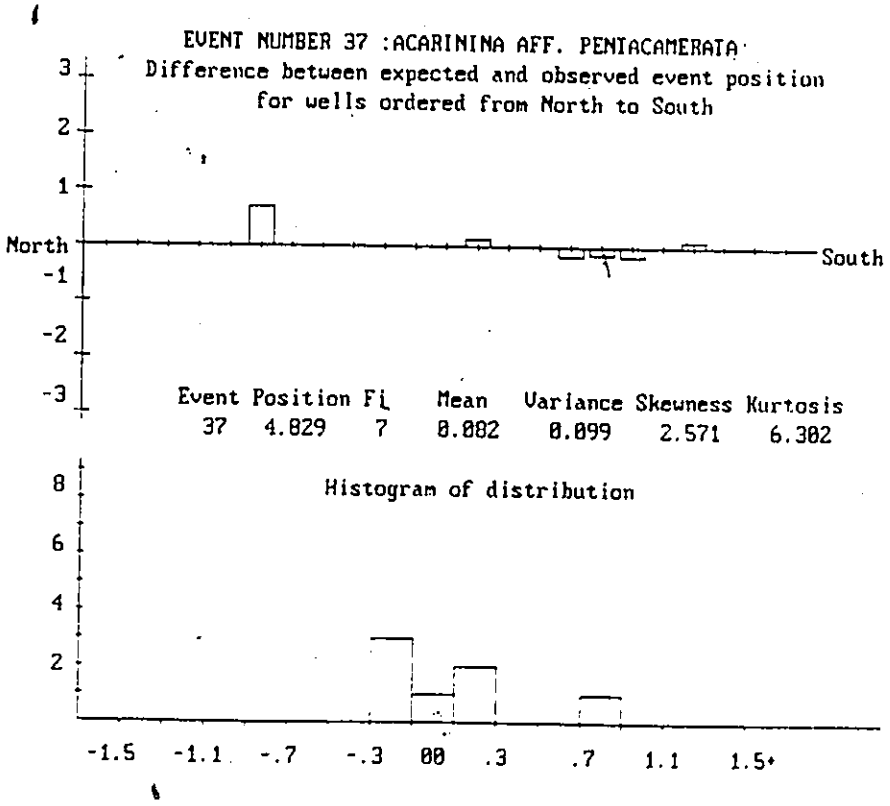
EVENT NUMBER 37 :ACARININA AFF. PENTACAMERATA
Difference between expected and observed event position
for wells ordered from North to South
3
2
1
North
-1
-2
-3
South
Event Position Fi Mean Variance Skewness Kurtosis
37 4.829 7 0.082 0.099 2.571 6.302
Histogram of distribution
8
6
4
2
-1.5 -1.1 -.7 -.3 00 .3 .7 1.1 1.5+

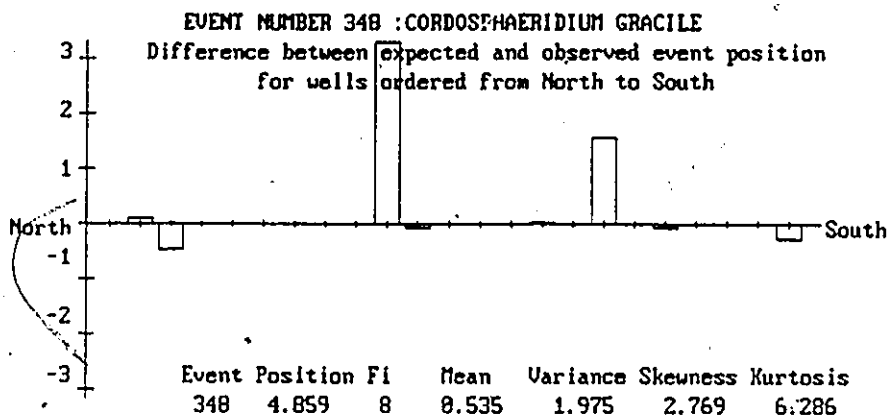

Event	Position	Fi	Mean	Variance	Skewness	Kurtosis
348	4.859	8	0.535	1.975	2.769	6.286

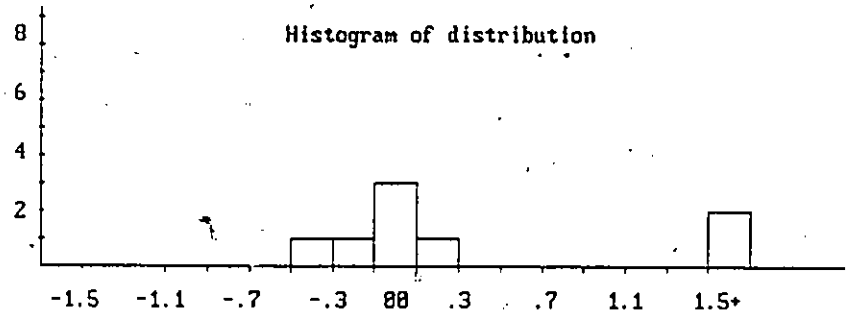

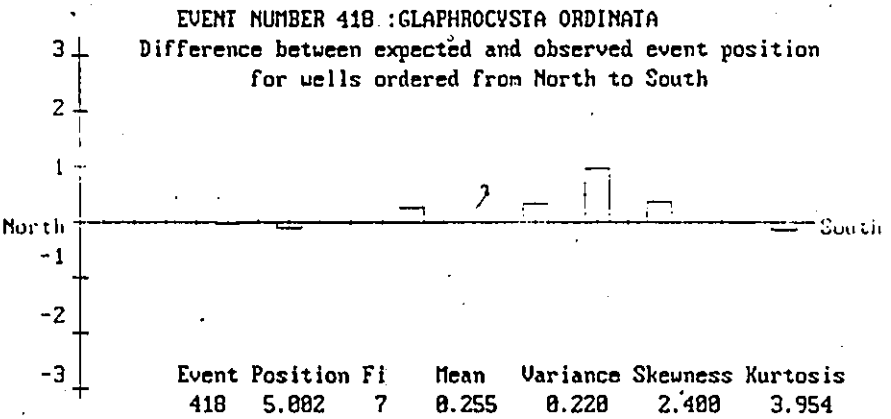

Event	Position	Fi	Mean	Variance	Skewness	Kurtosis
418	5.082	7	0.255	0.220	2.400	3.954

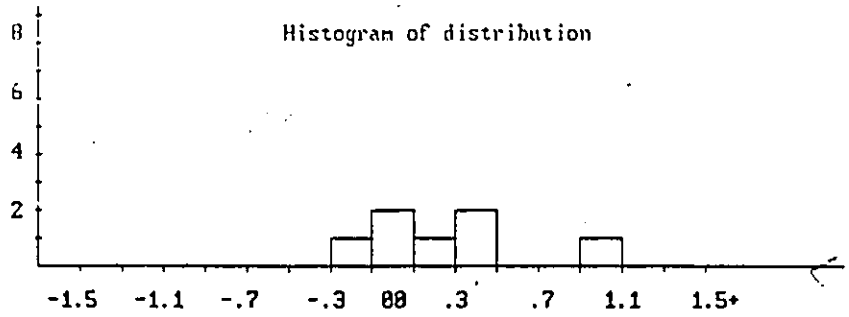

EVENT NUMBER 297 :MEGASPORE SP. 1

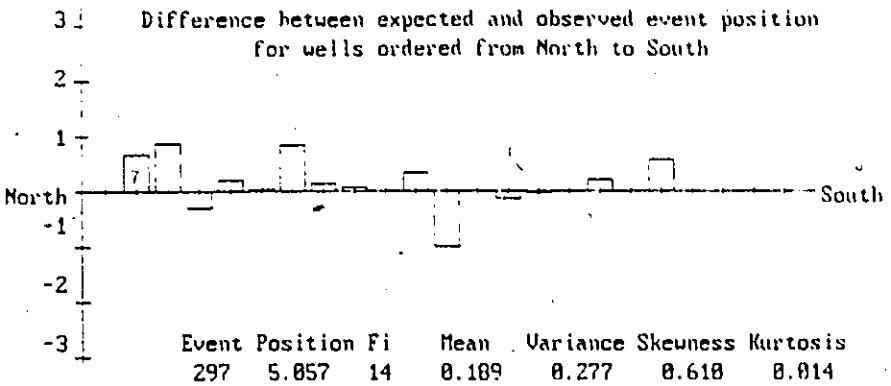

Event	Position	Fi	Mean	Variance	Skewness	Kurtosis
297	5.857	14	0.189	0.277	0.618	0.014

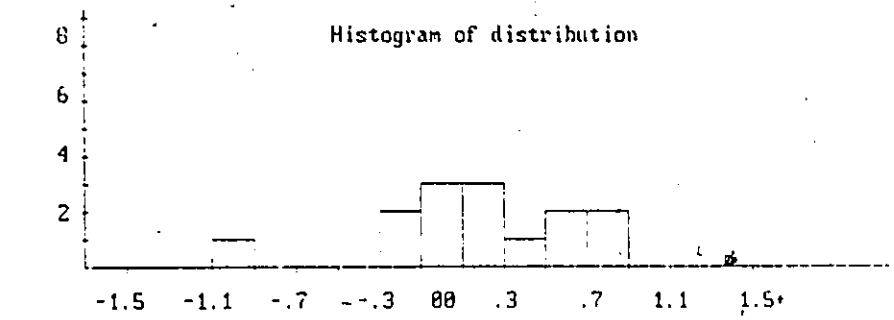

EVENT NUMBER 52 :ACARININA SOLDADOENSIS

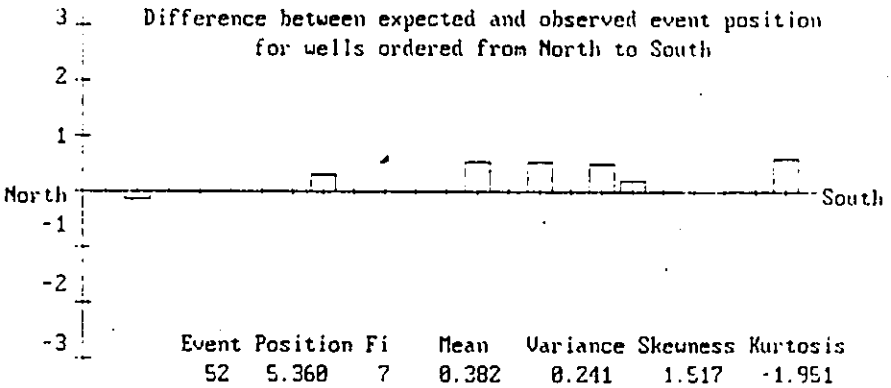

Event	Position	Fi	Mean	Variance	Skewness	Kurtosis
52	5.360	7	0.382	0.241	1.517	-1.951

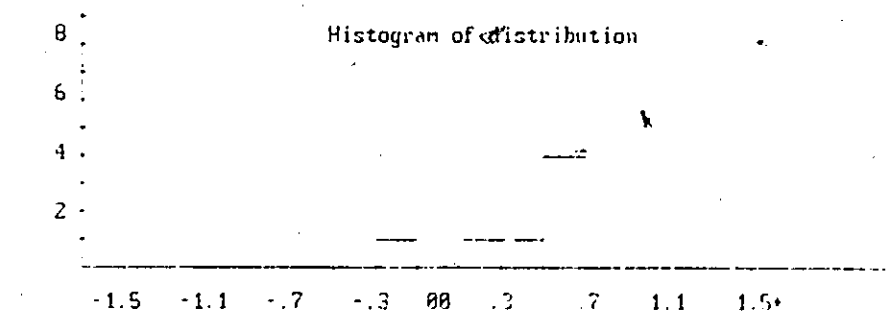

EVENT NUMBER 54 :SPIROPLECTAMMINA NAVARROANA
Difference between expected and observed event position
for wells ordered from North to South

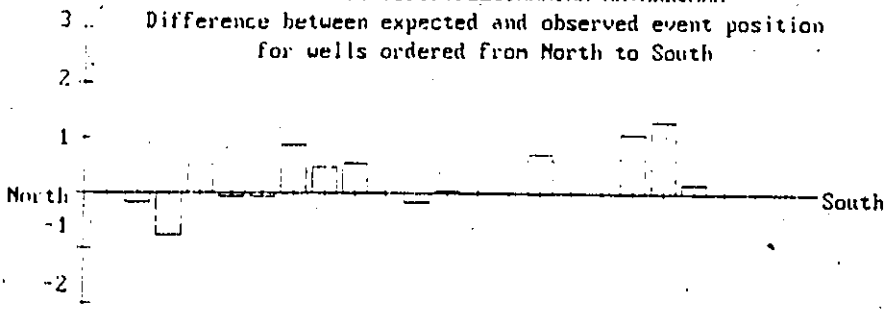

Event	Position	Fi	Mean	Variance	Skewness	Kurtosis
54	5.526	14	0.335	0.439	1.445	-0.875

Histogram of distribution

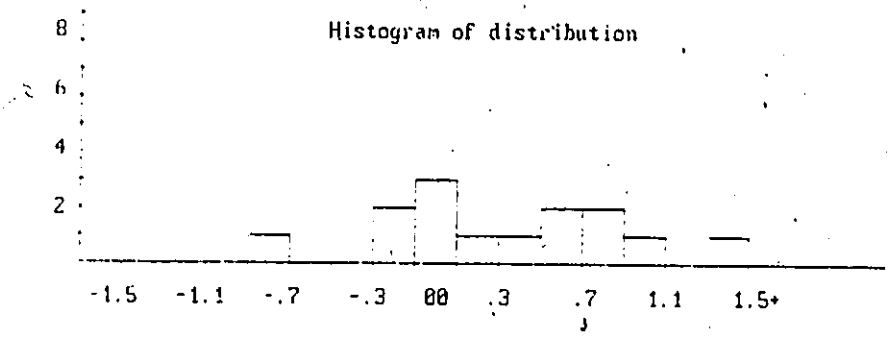

EVENT NUMBER 59 :RZEHAKINA EPIGONA
Difference between expected and observed event position
for wells ordered from North to South

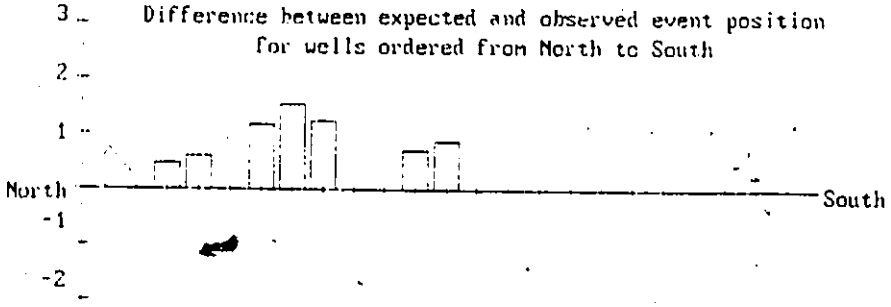

Event	Position	Fi	Mean	Variance	Skewness	Kurtosis
59	6.753	7	0.950	1.201	1.526	-1.841

Histogram of distribution